Declaration of Authorship

I, Luca Dellantonio, declare that this thesis, titled 'Entanglement criteria for Spin Squeezing' and the work presented in it are my own. I confirm that:

- This work was done wholly or mainly while in candidature for a research degree at this University.
- Where any part of this thesis has previously been submitted for a degree or any other qualification at this University or any other institution, this has been clearly stated.
- Where I have consulted the published work of others, this is always clearly attributed.
- Where I have quoted from the work of others, the source is always given. With the exception of such quotations, this thesis is entirely my own work.
- I have acknowledged all main sources of help.
- Where the thesis is based on work done by myself jointly with others, I have made clear exactly what was done by others and what I have contributed myself.

Signed: _____

Date: _____

"Non tutti i fisici son proprio da buttare."

Anonimo

UNIVERSITY OF COPENHAGEN

Abstract

Faculty of Physics
Niels Bohr Institute

Master in Physics

Entanglement criteria for Spin Squeezing

by Luca Dellantonio

Spin squeezing is a fundamental instrument for beating the standard quantum limit in measurement precision [1–3]. Experimentally, it has already been achieved and tested, proving its advantage with respect to classical systems [4–17]. From an elementary point of view, there are two key features of these experiments: the *creation* and the *detection* of entanglement. For the latter, the squeezing parameter [18] is the most used criterion: it consists of a simple inequality that can be easily verified. It represents a powerful, sufficient criterion for proving the existence of quantum correlation in an ensemble of atoms. Moreover, in terms of measurement, it involves only the mean and variance of the collective spin operator in the z and x direction respectively. However, in a typical experiment atoms are generally *not* equally illuminated by the probing beam, and thus we can suppose they do *not* contribute equally to the measurement. It is thus important to understand the effect of this on the squeezing parameter, to make the entanglement measures suitable to realistic situations. In this thesis, we first point out the necessity of the creation of a new entanglement criterion, showing the failure of the squeezing parameter in experiments involving ensembles of particles. Later on, we introduce this new criterion and generalize it for the detection of multi-partite entanglement. Finally, we apply the theory we developed to analyse experimental data, establishing more than 2-particle entanglement in an atomic ensemble.

The thesis is arranged as follows: in chapter 1 we will introduce some definitions and the notation we will use afterwards. In its last section 1.4 we are going to generalize the collective spin operator $\vec{J}$ to a new observable $\vec{S}$, that we believe resembles better the real-life case. Later on, in chapter 2, we will prove that the spin squeezing inequality does not hold any more using $\vec{S}$, pointing out the necessity of the creation of a new entanglement criterion. This will be found in chapter 3, and later on generalized in 4 for multi-partite entanglement. In chapter 5, using the experimental results obtained by Appel et al. in the article "Mesoscopic atomic entanglement for precision measurements beyond the standard quantum limit" [19], we will determine the quantum correlation of a collection of $\gtrsim 10^5$ particles. We will compare our criterion with the old one, and give a stronger proof of spin squeezing for the considered experimental setup. In chapter 6 we will list the main results and give the conclusions about this work.

Contents

List of Figures

List of Tables

Alla mia Nonna e ai miei genitori.

Chapter 1

Introduction

Ensemble of atoms with significant statistical behavior have already been successfully trapped and probed in experiments [5, 19–21]. Quantum correlations in these samples are of fundamental importance, as they open the doors of many interesting applications, ranging from quantum memories [22–28] to gates for quantum computers [29–31]. A particular example is given by spin squeezed states with which, for instance, it is possible to beat the standard quantum limit and achieve higher resolution in the experimental measurements [4–17]. The spin squeezing inequality is a fundamental instrument that allows us to determine if the state describing the system is squeezed, and therefore entangled. The success of this criterion is found in its simplicity; only the mean and variance of the collective spin operator along different axes need to be known. However, if these observables are not accessible to us, we need to revise the spin squeezing inequality and eventually propose a new criterion for entanglement detection.

In the next few chapters we will build a theoretical framework for defining a multi-particle entanglement criteria. Our criteria will be based on an inequality which is generic and can be applied for detection of any two, three and multi-partite entanglement. To begin with, here we give some of the definitions that will be useful for the rest of this thesis. In the conclusion of this chapter, we will introduce the new operator $\vec{S}$, that generalizes the collective spin $\vec{J}$. According to qualitative observation, we will see how this new operator is, indeed, appropriate to describe experimental measurements. Furthermore, we will understand how the framework at our disposition - the squeezing parameter ξ^2, for instance - changes once we look at it using $\vec{S}$ instead of $\vec{J}$.

1.1 The beginning. Separable... or entangled?

Quantum systems are broadly divided into two categories, namely the separable states, that satisfy the principle of local reality, and the correlated ones which have non-local features. This behaviour of non-locality was quite disturbing to Einstein who described it as a "spooky action at a distance", which we now call entanglement - an intriguing quantum phenomenon that was pointed out as a critic of quantum mechanics [32]. In recent years, it has been a resource in many applications, from optics to quantum information. With the advent of new experiments and technology it can now be utilized in practical applications like quantum cryptography and precision measurements beyond the standard quantum limit. Measurement of entanglement provides knowledge about the fundamental nature of correlation between quantum systems. As such, even though quite challenging, it has attracted immense attention [33]. In fact, several different measures had been introduced for problems or systems with small dimensions [34]. However, finding a useful and justified measure of entanglement for a system of many particles remains yet an open question. A possible solution is to use the squeezing parameter in terms of an inequality, similar to Bell's [35].

1.1.1 Two particles entanglement

Let us first consider the simplest possible case: two two-level atoms. The composite system can then be described by the tensor product of the bases for each particle, and therefore a generic wave vector describing the system will be

$$|\psi\rangle = C_{\uparrow\uparrow}|\uparrow\rangle_1 \otimes |\uparrow\rangle_2 + C_{\uparrow\downarrow}|\uparrow\rangle_1 \otimes |\downarrow\rangle_2 + C_{\downarrow\uparrow}|\downarrow\rangle_1 \otimes |\uparrow\rangle_2 + C_{\downarrow\downarrow}|\downarrow\rangle_1 \otimes |\downarrow\rangle_2, \tag{1.1}$$

where the appendices "$_1$" and "$_2$" refer to the first and second particle respectively. In the future the tensor product $|\uparrow\rangle_1 \otimes |\downarrow\rangle_2$, for simplicity of notation, will be denoted with $|\uparrow\downarrow\rangle$.
Now we are able to give the first definition of an entangled pure state (see [36]). The adjective "pure" refers to the fact that we are considering vectors $|\psi\rangle$ inside the Hilbert space of the whole system; the more general notion of "mixed" states will be given later, using the concept of density matrix.

Definition 1. Let us suppose the composite system $\mathcal{H} = \mathcal{H}_1 \otimes \mathcal{H}_2$ is given. A pure state $|\psi\rangle \in \mathcal{H}$ is called *product state* or *separable* if we can find $|\phi_1\rangle \in \mathcal{H}_1$ and $|\phi_2\rangle \in \mathcal{H}_2$ such that

$$|\psi\rangle = |\phi_1\rangle \otimes |\phi_2\rangle. \tag{1.2}$$

Otherwise $|\psi\rangle$ is entangled.

In many kind of situations a description of the system through its state vector is not convenient, or even hard to access. if $|\psi_i\rangle$ are states referring to the whole system, each one with a probability p_i to happen, then we can express the general wave vector using the density matrix ρ:

$$\rho = \sum_i p_i |\psi_i\rangle\langle\psi_i|, \tag{1.3}$$

where the p_i, being probabilities, have to respect $\sum_i p_i = 1$ and $p_i > 0$. A state written in the form of eq.1.3 is called *mixed*. The density matrix is a well known instrument in quantum mechanics, and therefore we will not focus our attention on its properties. However we will use it extensively in the next chapters, mostly because of the following definition of entanglement and separability for mixed states (always from [36]).

Definition 2. Let ρ be a density matrix for a two particles system. We say that ρ is a

- *Product state* if there exist states ρ_1 and ρ_2 for the first and second particle respectively, such that
$$\rho = \rho_1 \otimes \rho_2 \tag{1.4}$$
- *Separable state* if there are probabilities p_i and product states $\rho_{i_1} \otimes \rho_{i_2}$ such that
$$\rho = \sum_i p_i \rho_{i_1} \otimes \rho_{i_2} \tag{1.5}$$
- *Entangled state* otherwise.

As already pointed out in [36], this definition distinguish three possible cases. The less interesting one is the product state, where the two particles are completely uncorrelated. *Classical* correlations are given, whenever the state is not a product, but is separable. Previously and later on in this work we will use the word "correlated" as a synonym of "entangled". What we are meaning here with the adjective "classical" is well explained by the following example. Andrea and Samantha, working in Copenhagen and Calcutta respectively, decide that, depending on the shared random number "i", they will prepare their two particles in the state $\rho_{i_1} \otimes \rho_{i_2}$. If, later on, they forget i, then the system would be described by the separable state $\rho = \sum_i p_i \rho_{i_1} \otimes \rho_{i_2}$, that clearly is correlated, but classically. The last and more interesting case, that requires interaction between the two particles, is the entangled one. The correlation is here non-classical, and non local operations are necessary to be performed on the whole system in order to achieve it.

In the following, we will extend the definitions 1 and 2 to N particles and many-particles entanglement. Later on, we will briefly recall one of the work that brought entanglement to be one of the most important and interesting topic in physics: we will introduce the

definition of spin squeezing as in [18] and we will understand how to beat the standard quantum limit. This will be our launch pad for introducing the main argument of this work, that can be summarized saying that it is the generalization of the spin squeezing inequality to a more generic and realistic situation. Here we used words and expressions - standard quantum limit, spin squeezing inequality, many-particles entanglement - we still do not know properly. These will be discovered soon; let us start with order, so that everything will be clear shortly.

1.1.2 Many-particles entanglement

Always following the excellent work of [36], we will here give the definition of entanglement for a general system made of N particles:

Definition 3. Let us suppose to have a system made of N particles, and described by the state $|\psi\rangle$ and the density matrix ρ. We will call it:

- *Pure, fully separable*, if it can be written as the product state of every single particle

$$|\psi\rangle = \bigotimes_{i=1}^{N} |\phi_i\rangle \tag{1.6}$$

- *Mixed, fully separable*, if it is a convex combination of pure, fully separable states

$$\rho = \sum_l p_l \rho_{l_1} \otimes ... \otimes \rho_{l_N}. \tag{1.7}$$

  Here, the ρ_{l_i}, for $i = 1, ..., N$, are the density matrices of a single-particle state: $\rho_{l_i} = |\phi_{l_i}\rangle\langle\phi_{l_i}|$.

- *Pure, k-particle entangled*, with $1 < k < N$, if it cannot be split better than the product of k particles for the remaining ones collected in less-than-k state vectors. For instance,

$$|\psi\rangle = |\phi_{1,...,k}\rangle \otimes |\phi_{k+1}\rangle \otimes |\phi_{k+2}\rangle \otimes ... \otimes |\phi_N\rangle \tag{1.8}$$

  is a pure, k-particle entangled state, *if* it is not possible to further reduce $|\phi_{1,...,k}\rangle$ to a product of states with less particles each

- *Mixed, k-particle entangled*, if it is a convex combination of pure, k-particle entangled states. An example that will be useful later is the 2-particle entangled mixed state made by an even number N of particles with the form

$$\rho = \sum_k p_k \rho_{k_1,k_2} \otimes ... \otimes \rho_{k_{N-1},k_N}. \tag{1.9}$$

Here, for each k, $k_1, ..., k_N$ is a permutation of the numbers $1, ..., N$ and, for instance, the density matrix ρ_{k_1,k_2} describes the entangled couple made by particles k_1 and k_2.

- *Pure, N-particle entangled*, if the vector describing the system cannot be factorized in two states of any subsystems:

$$|\psi\rangle = |\phi_{1,...,N}\rangle \tag{1.10}$$

- *Mixed, N-particle entangled*, if it is a convex combination of Pure, N-particle entangled states.

In order to be less heavy with the notation, in the following chapters we will only distinguish between (fully) separable and k-particle entangled state. We will not explicitly say if the system is pure or mixed; this will be clear by the context.

Now that we have introduced the relevant kind of states, we can take a step further and introduce one of the main topics in quantum metrology: the spin squeezing.

1.2 Squeezed atomic states

One of the most important works regarding squeezed atomic states is, without doubts, the article of D.J.Wineland, J.J.Bollinger and W.M.Itano [18], the goal of which was to achieve a high resolution in Ramsey method metrology. These authors introduced first the so-called squeezing parameter ξ^2 that, defined as the ratio between the statistical uncertainty of entangled versus separable states, quantifies the sensitivity of the experimental apparatus. In particular, they proved that, for some systems with $\xi^2 < 1$, a resolution higher than the one achieved with separable states could be obtained. In literature, this result is known as "beating the standard quantum limit".

The experimental setup consisted of N identical two-level atoms, whose proper frequency ω_0 was measured, through spectroscopy. All particles had a spin $j = \frac{1}{2}$, and the distance separating them is supposed to be big enough to not have any atom-atom interaction. The collective spin operator is defined $\vec{J} = \sum_{i=1}^{N} \vec{j}_i$. The method used for measuring ω_0 was the Ramsey one, consisting of a first $\frac{\pi}{2}$ pulse, a free evolution and another $\frac{\pi}{2}$ pulse. For separable states, the best resolution $|\Delta\omega|_{CSS}$ measuring ω_0 is given by:

$$|\Delta\omega|_{CSS} = \frac{1}{T(N)^{\frac{1}{2}}}, \tag{1.11}$$

where T is the time of the free evolution in the Ramsey sequence. The appendix "$_{CSS}$" refers to the coherent spin state $|CSS\rangle$, defined as

$$|CSS\rangle = \bigotimes_{i=1}^{N} |\uparrow\rangle_i, \tag{1.12}$$

and is the state in which the system should be prepared at the beginning of the experiment.

After having proved that $|\Delta\omega|_{CSS}$ is the best possible resolution achievable with separable states, the authors in [18] introduced the squeezing parameter, that indicates the level of improvement achieved using some other particular states instead of $|CSS\rangle$:

$$\xi_R^2 = \frac{|\Delta\omega|^2}{|\Delta\omega|_{CSS}^2} = N\frac{(\Delta J_x)^2}{\langle J_z\rangle^2}. \tag{1.13}$$

We will use the appendix "$_R$" for this particular definition of the squeezing parameter. In our case, it is useful to give another completely equivalent form of the parameter ξ_R^2,

$$\xi_R^2 = \frac{\langle J_z\rangle_{CSS}^2}{(\Delta J_x)_{CSS}^2}\frac{(\Delta J_x)^2}{\langle J_z\rangle^2}, \tag{1.14}$$

where $\langle J_z\rangle_{CSS}$ and $(\Delta J_x)_{CSS}^2$ are the average spin and variance of the collective spin operator $\vec{J}$ for the coherent spin state. They are clearly given by

$$\langle J_z\rangle_{CSS} = \langle CSS|J_z|CSS\rangle = \frac{N}{2} \tag{1.15a}$$

$$(\Delta J_x)_{CSS}^2 = \langle CSS|J_x^2|CSS\rangle - \langle CSS|J_x|CSS\rangle^2 = \frac{N}{4}, \tag{1.15b}$$

and the reason for which we rewrote ξ_R^2 as in eq.1.14, is that it gives a clear meaning of the squeezing parameter, as ratio between the noises of the considered and the coherent systems.

The conclusion the authors took in [18], is that the signal-to-noise ratio can be improved over the case of initially uncorrelated atoms if the particles are prepared in some particular "squeezed states". These are defined to be the states for which the squeezing parameter is less than unit, and can reduce significantly - for instance - the time needed for achieving a particular resolution on the proper frequency ω_0.

In the next section we will introduce another fundamental article that definitively relates the squeezing parameter with the concept of entanglement, and proceeds further identifying several criteria for discriminating the quality of the entanglement of the system.

1.3 Entanglement and extreme spin squeezing

In the article "Entanglement and extreme spin squeezing" [37], Anders Sørensen and Klaus Mølmer identify several curves - each one for a different value of J - that define a limit for squeezed spin states described by the associated J. More in details, the Fig.1.1 present the minimum achievable variances $\frac{(\Delta J_x)^2}{2(\Delta J_x)^2_{CSS}}$ with respect to the spin $\frac{\langle J_z\rangle}{\langle J_z\rangle_{CSS}}$, for different two-level systems made by $N = 2J$ atoms.

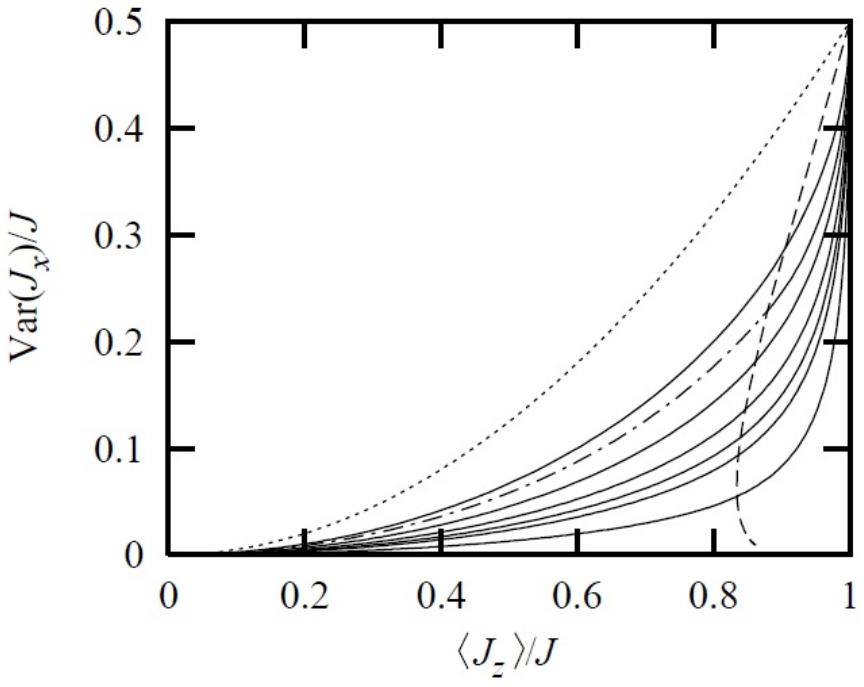

FIGURE 1.1: Maximal squeezing for different values of J. From above, the curves refer to $J = \frac{1}{2}, 1, \frac{3}{2}, 2, 3, 4, 5$ and 10. The *dotted* curve, characterized by $J = \frac{1}{2}$ and therefore referring to the separable case, is the quadratic function that can be found by setting $\xi_R^2 = 1$ in eq.1.14. The *dashed* curve represents the position of a bifurcation in the solution of half-integer spin. To its left the minimum is found by a variational calculation (*dash dotted* curve for $J = \frac{3}{2}$), to its right diagonalization of the operator $\mu J_z + J_x^2$ can be applied. For details, see [37], from which this figure has been taken

For drawing the figure, the facts $\langle J_z\rangle_{CSS} = J$ and $(\Delta J_x)^2_{CSS} = \frac{J}{2}$ have been used. All the curves are determined numerically. In particular, diagonalization of the operator $\mu J_z + J_x^2$ and variational calculations were used. Skipping some details, the different methods are needed, because for odd values of J the average of J_x is not always null, and the diagonalization cannot be used. Analytical equations for the curves related to $J = \frac{1}{2}$ and $J = 1$ are known. The first one is just a quadratic curve, as it is possible to deduce from the definition 1.14 of the squeezing parameter, by setting $\xi_R^2 = 1$. This constraint force us to always saturate the minimum for the separable case (i.e.: only one

particle, no entanglement), and we get:

$$1 = \xi_R^2 = \frac{\langle J_z \rangle_{CSS}^2}{(\Delta J_x)_{CSS}^2} \frac{(\Delta J_x)^2}{\langle J_z \rangle^2} \Longrightarrow \frac{(\Delta J_x)^2}{(\Delta J_x)_{CSS}^2} = \left(\frac{\langle J_z \rangle}{\langle J_z \rangle_{CSS}} \right)^2 . \tag{1.16}$$

For $J = 1$ the analytical form of the relative curve in Fig.1.1 is determined in [37], and is given by

$$\frac{(\Delta J_x)^2}{(\Delta J_x)_{CSS}^2} = 1 - \sqrt{1 - \left(\frac{\langle J_z \rangle}{\langle J_z \rangle_{CSS}} \right)^2} . \tag{1.17}$$

The important conclusion taken in [37] is that exactly the same limit can be taken for systems made by $M > N$ particles, of which only N can be entangled. Let us be more clear about this statement. Suppose we have $M > N$ two-level atoms, and that, for some reason, we cannot find more than N of these particles entangled. Then, if we measure the normalized variance $\frac{(\Delta J_x)^2}{2(\Delta J_x)_{CSS}^2}$ and the normalized spin $\frac{\langle J_z \rangle}{\langle J_z \rangle_{CSS}}$, any experimental point having these coordinates cannot lie below the curve of Fig.1.1 characterized by $J = \frac{N}{2}$. The reader should not be worried if what said here is not completely clear. These "multipartite" or "multi-particle" entanglement criteria - which goal is clearly to prove stronger and more advantageous entanglement - will be the main argument of this work.

In the next and last section of this introduction we will say where the assertion stated here may fail. Or, better, where it is not possible to use the criteria represented by the curves of Fig.1.1. In fact, their derivation is sound. However, the problem is that - we believe - in many experimental situations the environment is not the one to which these criteria refer. A generalization is therefore needed, and such generalization will be done in the following chapters 3 and 4.

1.4 The operator $\vec{S}$ and the generalization of the squeezing parameter

Let us start this section by describing, very qualitatively, a standard experiment involving atoms shined by light. A more detailed discussion will be given later, in chapter 5; for the moment we are interested in pointing out the possible problem of the squeezing parameter as entanglement criteria.

In a standard quantum optic experiment, the measurements on the atoms, previously cooled and loaded inside the probing chamber, is performed using a Gaussian laser beam. This beam, because of the interaction with the particles, is shifted, and detecting this

phase difference it is possible to determine the average values of important atomic observables - the collective spin components, for instance. Except a billion of other very important details, this is the very essence of many experimental applications, from spectroscopy to metrology, and also in quantum computation. Let us now zoom inside the probing box, and look at two particular particles inside it. The first one is at the exact middle of the chamber, in the precise spot where the probe is focused; the other is flying around, far away from the main axis of the laser beam. The interaction between the (classical) light and the atoms is well described by the scalar product of the electrical field $\vec{E}(\vec{r})$ of the probe with the dipole moment $\vec{d}$ of the particles, being this latter one an operator, the first a vector field. Now, remembering our two identical atoms, we need to consider that the electric field to which they are subject is fairly different. In fact, away from the main axis of the probe, the electric field decays, and therefore the atom-light interaction of our second particle is (much) weaker than the first. Our hypothesis is very simple: since any atom contributes differently to the phase shift of the probe, we could have no access to the collective spin operator $\vec{J} = \sum_{i=1}^{N} \vec{j}_i$. It is more reliable to say that what we are measuring is the "weighted" spin operator $\vec{S}$, where

$$\vec{S} = \sum_{i=1}^{N} \eta_i \vec{j}_i. \tag{1.18}$$

Here and previously we used $\vec{j}_i$, for $i = 1, ..., N$, to indicate the spin of the i-th particle. What are the coefficients $\{\eta_i\}_{i=1}^{N}$ then? At first, let us make a naive comment. *If* all of them are unitary, the operator $\vec{S}$ becomes the collective spin: $\vec{S} \to \vec{J}$. Therefore, we can always recover the results given by the previous interpretation - the one saying that $\vec{J}$ was the observed operator - by defining the weights $\{\eta_i\}_{i=1}^{N}$ in a proper way. On the other hand, if there are reasons for which $\vec{S}$ is truly the measured observable instead of $\vec{J}$, we will point out some new characteristics of the system they were to us precluded considering $\vec{J}$ only.
What are the coefficients $\{\eta_i\}_{i=1}^{N}$? In general, they can be everything: varying in time, in space, because of the atomic speed... The only condition we put so far is that they have to be scalar. However, since we are not mathematicians (with all respect!), we need to put our hands in the real, dirty world and give some interpretation to them. Let us start recalling what is going on in our experiment:

- A Gaussian laser beam, the probe, enters the box loaded with atoms, shining them
- The probe, because of the interaction with the particles, subject a phase shift that can be determined

- As said above, such interaction is different from atom to atom, depending on "how" they are shined
- From the phase shift - and here resides the difference from the old model - we are not really measuring the collective spin operator, but $\vec{S}$

We deduce that the $\{\eta_i\}_{i=1}^N$ have something to do with "how" the atoms are shined by the probe, that means which is its intensity in the position occupied by the particles. This will be the interpretation we will use in the following; it is not necessarily the best one or the most complete, but we believe it is reliable.
As a final comment, let us give the squeezing parameter in the case in which the measured observable is $\vec{S}$. We can substitute it to $\vec{J}$ in eq.1.14, and obtain:

$$\xi_N^2 = \frac{\langle S_z\rangle_{CSS}^2}{(\Delta S_x)_{CSS}^2}\frac{(\Delta S_x)^2}{\langle S_z\rangle^2} = \frac{\left(\sum_{i=1}^N \eta_i\right)^2}{\sum_{i=1}^N \eta_i^2}\frac{(\Delta S_x)^2}{\langle S_z\rangle^2}. \tag{1.19}$$

We changed the appendix of ξ^2 from "$_R$" to "$_N$", in order to make clear to which operator, $\vec{J}$ or $\vec{S}$, we are referring. In eq.1.19 we substituted $\langle S_z\rangle_{CSS}$ and $(\Delta S_x)_{CSS}^2$ with their values:

$$\langle S_z\rangle_{CSS} = \langle CSS|S_z|CSS\rangle = \frac{1}{2}\sum_{i=1}^N \eta_i \tag{1.20a}$$

$$(\Delta S_x)_{CSS}^2 = \langle CSS|S_x^2|CSS\rangle - \langle CSS|S_x|CSS\rangle^2 = \frac{1}{4}\sum_{i=1}^N \eta_i^2. \tag{1.20b}$$

It is important to note that what we did in eq.1.19 is not formal. We just said: "Well, given that in the experiment we measure $\vec{S}$ at the place of $\vec{J}$, if we calculate from the data the squeezing parameter, than we would obtain ξ^2 as in eq.1.19, not 1.14". The point here is that, having modified ξ^2, we lost its property as an entanglement detector. The inequality stating that, for all separable states, $\xi_R^2 \geq 1$, it is not valid any more for ξ_N^2. Or it is? Proving that ξ_N^2, as in eq.1.19, is not a useful entanglement criterion will be the main argument of the next Chapter 2. Different ways for determining if the system is correlated or not will be discussed later.

Chapter 2

ξ^2 as entanglement criterion

2.1 Counterexample

We have discussed how it is possible to use the parameter ξ_R^2 for detecting spin squeezing (and thus entanglement), in the case where the measurement is performed by the collective operator $\vec{J} = \sum_{i=1}^{N} \vec{j}_i$, and we pointed out the difficulty, in the experiment, to have such operator. In fact, taking into account the laser dispersion, a more realistic one is

$$\vec{S} = \sum_{i=1}^{N} \eta_i \vec{j}_i, \tag{2.1}$$

where the coefficient η_i are supposed to carry information about "how" the atoms are hit by the detecting laser.

As we discussed previously in section 1.4, we can generalize the parameter ξ^2 in the following way:

$$\xi_R^2 = N\frac{(\Delta J_x)^2}{\langle J_z\rangle^2} \xrightarrow[\vec{J}\to\vec{S}]{} \xi_N^2 = \frac{\left(\sum_{i=1}^{N}\eta_i\right)^2}{\sum_{i=1}^{N}\eta_i^2}\frac{(\Delta S_x)^2}{\langle S_z\rangle^2} \tag{2.2}$$

Intuitively the substitution of $\vec{J}$ with $\vec{S}$ is clear. The reason for which we introduce the two sums in place of N can be understood looking at eq.1.19. It is important to point out that if one particle is not detected at all we have $\eta_i \to 0$, and that if $\eta_i = 1$ for all $i = 1, ..., N$

$$\frac{\left(\sum_{i=1}^{N}\eta_i\right)^2}{\sum_{i=1}^{N}\eta_i^2} \to N, \tag{2.3}$$

as we expected.

One of the most interesting purposes for which the squeezing parameter is utilized is to detect entanglement. In fact, it is possible to prove that, whenever ξ_R^2 takes values strictly smaller then one, the system over which is evaluated is entangled. A natural question now arises: "Can we infer something similar about ξ_N^2?"
In the following we are going to give a first elementary example for which this parameter takes some value less than one *for a separable states*, and subsequently we will introduce a slightly more complex model that will prove that ξ^2 becomes almost useless if evaluated with our new weighted spin operator $\vec{S}$.

2.1.1 Four uncorrelated atoms

Here we are going to prove that $\xi_N^2 < 1$ for a separable state made of four particles.
Let us suppose we have a state $|\psi\rangle = |\uparrow\rangle_1|\uparrow\rangle_2|\theta\rangle_3|-\theta\rangle_4$, where $|\vartheta\rangle = e^{-i\frac{\vartheta}{2}j_y}|\uparrow\rangle$. The atomic indices will be omitted, where it will not be necessary. We want to determine the possible values ξ_N^2 can take varying parameters $\theta \in [0, \pi]$ and $\eta_i \in (0, 1]$. It is clear why η_i cannot be negative, while we decide to limit them to a range between zero and the unity. This is because we are always able to rescale them by dividing both numerator and denominator with the square of the biggest possible value of η_i.
For such a state we thus have:

- $\langle S_x\rangle = \langle\psi|S_x|\psi\rangle = \eta_3\langle\theta|j_{x_3}|\theta\rangle + \eta_4\langle-\theta|j_{x_4}|-\theta\rangle = \frac{\eta_3}{2}\sin\theta - \frac{\eta_4}{2}\sin\theta$
  Now, for simplicity, let us suppose $\eta_3 = \eta_4 = \lambda$, that in practice means that the third and the fourth atoms $|\theta\rangle_3|-\theta\rangle_4$ lies at the same distance with respect to the main direction of the laser (see Fig.2.1). With this assumption we can conclude that $\langle S_x\rangle = 0$

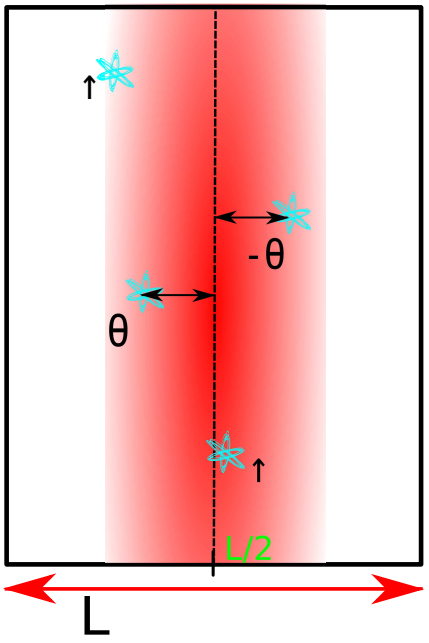

FIGURE 2.1: Standard experimental setup; a laser shines particles in a box. In the specific example, there are four atoms: two of them described by the state $|\uparrow\rangle$, they can be everywhere, and two by $|\pm\theta\rangle$, they find themselves at the same distance from the laser symmetry axis

- $\langle S_z\rangle = \langle\psi|S_z|\psi\rangle = \eta_1\langle\uparrow |j_{z_1}| \uparrow\rangle + \eta_2\langle\uparrow |j_{z_2}| \uparrow\rangle + \lambda(\langle\theta|j_{z_3}|\theta\rangle + \langle-\theta|j_{z_4}|-\theta\rangle) = \frac{\eta_1}{2} + \frac{\eta_2}{2} + \lambda\cos\theta$
- $\langle S_x^2\rangle = \frac{1}{4}\left(\eta_1^2 + \eta_2^2 + 2\lambda^2\cos^2\theta\right)$
  Let us briefly explain this result. We have that

$$S_x^2 = \left(\sum_{i=1}^{4}\eta_i j_{x_i}\right)^2 = \sum_{i=1}^{4}\eta_i^2 j_{x_i}^2 + 2\sum_{i>j}\eta_i\eta_j j_{x_i} j_{x_j} \tag{2.4}$$

  Now, since calculation of $\langle j_{x_i}^2\rangle$ is straightforward, let us focus on the mixed terms $\langle j_{x_i} j_{x_j}\rangle$, for $i \neq j$. Obviously these terms are null when computed over at least one of the first two particles $|\uparrow\rangle_1$ and $|\uparrow\rangle_2$, but we cannot take the same conclusion for the remaining two particles. In fact for $|\theta\rangle_3$ and $|\theta\rangle_4$ we get:

$$\langle j_{x_3} j_{x_4}\rangle = \langle\theta|j_{x_3}|\theta\rangle\langle-\theta|j_{x_4}|-\theta\rangle = -\frac{1}{4}\sin^2\theta \tag{2.5}$$

  At this point is straightforward to obtain the result for $\langle S_x^2\rangle$ we reported before, since $\lambda^2\langle j_{x_3}^2 + j_{x_4}^2 + 2j_{x_3}j_{x_4}\rangle = \lambda^2\left(\frac{1}{2} - \frac{1}{2}\sin^2\theta\right) = \frac{\lambda^2}{2}\cos^2\theta$.

We can now collect the results obtained so far:

$$\langle S_z \rangle = \frac{\eta_1}{2} + \frac{\eta_2}{2} + \lambda \cos\theta \tag{2.6a}$$

$$(\Delta S_x)^2 = \langle S_x^2 \rangle - \langle S_x \rangle^2 = \frac{1}{4}\left(\eta_1^2 + \eta_2^2 + 2\lambda^2 \cos^2\theta\right) \tag{2.6b}$$

so that we can conclude

$$\xi_N^2 = \frac{(\eta_1 + \eta_2 + 2\lambda)^2}{\eta_1^2 + \eta_2^2 + 2\lambda^2} \frac{(\Delta S_x)^2}{\langle S_z \rangle^2} = \frac{(\mu + \lambda)^2}{\mu^2 + \lambda^2} \frac{\mu^2 + \lambda^2 \cos^2\theta}{(\mu + \lambda\cos\theta)^2} \tag{2.7}$$

In the last equality we also supposed there exists a symmetry between the first couple of particles $|\uparrow\rangle_1|\uparrow\rangle_2$, in such a way that $\eta_1 = \eta_2 = \mu$. This will slightly simplify the next calculations.

In the following we will just study the function $\xi_N^2(\theta, \mu, \lambda)$, and in particular find its minima in our domain.
First notice that such a function is always positive, and is singular for $\mu + \lambda\cos\theta = 0$, where it goes to infinity. Thus the global minima must lie in between of zero and infinity. Let us derive $\xi_N^2(\theta, \mu, \lambda)$ with respect to θ:

$$\frac{\partial \xi_N^2(\theta, \mu, \lambda)}{\partial \theta} = \frac{2\lambda\mu \sin\theta(\mu - \lambda\cos\theta)}{(\mu + \lambda\cos\theta)^3} \tag{2.8}$$

Now we want to study the sign of the derivative in the two following cases:

1. $\mu > \lambda$:
   Here the denominator is always positive and bigger than zero, as well as $\mu - \lambda\cos\theta$. Thus we have:
   $$\frac{\partial \xi_N^2}{\partial \theta} \geq 0 \Leftrightarrow \sin\theta \geq 0 \tag{2.9}$$
   This means that for $\theta = 0$ and $\theta = \pm\pi$ we have stationary points, respectively a local minimum and two local maxima (as it is easy to check).
   For $\theta = 0$ our squeezing parameter takes the value $\xi_N^2(\theta = 0) = 1$, not depending on parameters μ and λ. Since on the boundary $\theta = \pm\pi$ the function always takes maximum values (always bigger than one), we can conclude that $\theta = 0$ is a global minimum.

   So far, it seems that the constraints $\xi_N^2 \geq 1$ for all separable states is still valid.

2. $\mu \leq \lambda$:
   This case is slightly more complicated, but for sure more interesting. In fact, studying the sign of the derivative $\frac{\partial \xi_N^2}{\partial \theta} \geq 0$ it is possible to find three local minima:

$$\theta = 0 \tag{2.10a}$$

$$\theta = \pm \arccos \frac{\mu}{\lambda} \tag{2.10b}$$

The first one is the same as before, and we already know how our parameter ξ_N^2 behaves in such point, while for the others we obtain:

$$\xi_N^2(\lambda, \mu, \theta = \pm \arccos \frac{\mu}{\lambda}) = \frac{1}{2} \frac{(\mu + \lambda)^2}{\mu^2 + \lambda^2} \tag{2.11}$$

We can now study $\xi_N^2(\mu, \lambda)$ with respect to the two remaining parameters; it suffices to note that, since

$$\frac{1}{2} \frac{(\mu + \lambda)^2}{\mu^2 + \lambda^2} \leq 1 \quad \forall \lambda, \mu \in (0, 1], \tag{2.12}$$

we get that $\xi_N^2(\mu, \lambda) < 1$ for almost all choices of μ and λ.
More precisely, it is easy to see that $\xi_N^2(\mu, \lambda) = 1$ if and only if $\mu = \lambda$, while $\xi_N^2(\mu, \lambda) \to \frac{1}{2}$ for $\mu \to 0$ and $\lambda \gg \mu$ (or vice versa). It is important to note that when both parameters λ and μ approach zero, $\xi_N^2(\mu, \lambda)$ is still bounded from below by $\frac{1}{2}$. In conclusion we can say that

$$\frac{1}{2} < \xi_N^2(\theta = \pm \arccos \frac{\mu}{\lambda}) \leq 1, \tag{2.13}$$

and thus, due to the periodicity of $\xi_N^2(\mu, \lambda, \theta)$ with respect to its last variable, we can say that our squeezing parameter doesn't have a global minimum, but it is bounded from below by the constant function $\frac{1}{2}$.

In other words, the constraint $\xi_N^2 \geq 1$ is not valid any more when we are dealing with some measurements apparatus that does not affect all particles in the same way.
In subsection 2.1.2 we are going to find some straighter lower bound for our squeezing parameter, using a more general model with many atoms respecting similar symmetries as the ones we had here. We will see how this new lower bound depends on the number of atoms, and thus we need to admit that experimentally evaluating ξ_N^2 can become a hard task to accomplish, for example with atomic clock setups, for which we have to deal with systems made of approximately 10^6 particles. Before that we will slightly generalize our previous result to an intermediate level, in order to introduce the proceeding we will use later.

2.1.1.1 A more formal proof

Let us suppose we are dealing with four atoms described by $|\psi\rangle = |\theta\rangle_1|-\theta\rangle_2|\phi\rangle_3|-\phi\rangle_4$, disposed in such a symmetric way for which $\eta_1 = \eta_2 = \mu$ and $\eta_3 = \eta_4 = \lambda$. Here θ and ϕ vary inside $[0, \pi]$, while λ and μ in $(0, 1]$.
If now we define the function $h(x, y)$ as:

$$h(x, y) = \frac{(x + y)^2}{x^2 + y^2} \tag{2.14}$$

with a very little effort we can show that our parameter ξ^2_N takes the form

$$\xi^2_N(\mu, \lambda, \theta, \phi) = \frac{h(\mu, \lambda)}{h(\mu \cos\theta, \lambda \cos\phi)} \tag{2.15}$$

In this way, noticing that $h(x, y)$ is always positive, we can reduce the problem of minimizing ξ^2_N to find maxima and minima of the new function $h(x, y)$. Of course we need to be careful, cause numerator and denominator in ξ^2_N are *not* independent, but correlated. In fact we will show that the conditions for approaching the minimum in $h(\mu, \lambda)$ can be obtained simultaneously with the ones for having maximum in $h(\mu \cos\theta, \lambda \cos\phi)$.

The **upper bound** of $h(x, y)$ is obtainable easily using Jensen's inequality, that in its simplest form states that:

Lemma 1. *Let us suppose that are given:*

1. *A real, convex function ϕ, with domain $\mathbb{D}$ inside the real line $\mathbb{R}$*
2. *A discrete set of points $\{x_1, ..., x_N\}$ inside $\mathbb{D}$*
3. *Positive weights $a_1, ..., a_N$.*

Then the inequality

$$\phi\left(\frac{\sum_{i=1}^{N} a_i x_i}{\sum_{i=1}^{N} a_i}\right) \leq \frac{\sum_{i=1}^{N} a_i \phi(x_i)}{\sum_{i=1}^{N} a_i} \tag{2.16}$$

holds. Equality holds if and only if $x_i = x_j$ for all possible i, j between 1 and N.
As a particular case, if the weights $a_1, ..., a_N$ are all equal, then eq.2.16 becomes

$$\phi\left(\frac{1}{N}\sum_{i=1}^{N} x_i\right) \leq \frac{1}{N}\sum_{i=1}^{N} \phi(x_i). \tag{2.17}$$

The inequalities 2.16 and 2.17 are reversed if ϕ is concave.

Using lemma 1 it is now simple to obtain an upper bound for $h(x,y)$. In fact we have that

$$\frac{h(x,y)}{2} = \frac{(\frac{x+y}{2})^2}{\frac{x^2+y^2}{2}} \leq \frac{(\frac{|x|+|y|}{2})^2}{\frac{x^2+y^2}{2}} \leq 1, \tag{2.18}$$

so that $h(x,y) \leq 2$, i.e.: 2 is the upper bound for our function, and it is reached for $\mu\cos\theta = \lambda\cos\phi$. Notice that this condition is equivalent to equation 2.10b, with $\cos\phi = 1$.

The **lower bound** of $h(x,y)$ is actually straightforward to determine when both x and y are positive (as in our case!). Suppose $x \geq y$, so that:

$$h(x,y) = \frac{(x+y)^2}{x^2+y^2} = 1 + \frac{\overbrace{2xy}^{\geq 0}}{x^2+y^2} \geq 1; \tag{2.19}$$

it is clearly possible to approach the limit $h(x,y) = 1$ when $y \to 0$ and $x \gg y$.

In conclusion, the requirements they have both to be verified for minimizing $\xi_N^2(\mu,\lambda,\theta,\phi)$ are exactly the ones we found previously and they obviously can be true at the same time.
The sketch of this proof will be followed again in the next section, when we are dealing with a potentially bigger number of particles.

2.1.2 Many uncorrelated atoms

Here we will try to generalize the previous section with an arbitrary number of atoms $N = 2\mathcal{N}$. The generalized wave function describing the system is defined to be:

$$|\psi\rangle = |\theta_1\rangle_1|-\theta_1\rangle_2...|\theta_{\mathcal{N}}\rangle_{N-1}|-\theta_{\mathcal{N}}\rangle_N, \tag{2.20}$$

with $\theta_i \in [0,\pi]$ for all $i = 1,...,\mathcal{N}$.
Moreover we will consider the same symmetry we used before, so that each couple of atoms $|\theta_j\rangle_{2j-1}|-\theta_j\rangle_{2j}$ will be described by the same weight $\tilde{\eta}_{2j-1} = \tilde{\eta}_{2j} = \eta_i$, for $j = 1,...,N$ and consequently $i = 1,...,\mathcal{N}$. Again, the range in which we will allow the η_i to vary is $(0,1]$, for the same reason we mentioned in section 2.1.1.
The spin measurement operator is thus expressed by the following equation:

$$\vec{S} = \sum_{j=1}^{N} \tilde{\eta}_j \vec{j}_i = \sum_{i=1}^{\mathcal{N}} \eta_i \left(\vec{j}_{2i-1} + \vec{j}_{2i}\right) \tag{2.21}$$

For determining the squeezing parameter ξ_N^2 we have now to compute the various terms in its definition:

- The average spin along z:

$$\begin{aligned}\langle S_z\rangle = \langle\sum_{i=1}^{\mathcal{N}} \eta_i \left(j_{z_{2i-1}} + j_{z_{2i}}\right)\rangle = \sum_{i=1}^{\mathcal{N}} \eta_i \left(\langle j_{z_{2i-1}}\rangle + \langle j_{z_{2i}}\rangle\right) = \\ = \sum_{i=1}^{\mathcal{N}} \eta_i \left(\frac{\cos\theta_i}{2} + \frac{\cos\left(-\theta_i\right)}{2}\right) = \sum_{i=1}^{\mathcal{N}} \eta_i \cos\theta_i\end{aligned} \tag{2.22}$$

- The average spin along x:

$$\begin{aligned}\langle S_x\rangle = \langle\sum_{i=1}^{\mathcal{N}} \eta_i \left(j_{x_{2i-1}} + j_{x_{2i}}\right)\rangle = \sum_{i=1}^{\mathcal{N}} \eta_i \left(\langle j_{x_{2i-1}}\rangle + \langle j_{x_{2i}}\rangle\right) = \\ = \sum_{i=1}^{\mathcal{N}} \eta_i \left(\frac{\sin\theta_i}{2} + \frac{\sin\left(-\theta_i\right)}{2}\right) = 0\end{aligned} \tag{2.23}$$

- The average of the squared component of the spin along x:

$$\langle S_x^2\rangle = \sum_{i=1}^{\mathcal{N}} \frac{\eta_i^2}{2} \cos^2\theta_i \tag{2.24}$$

  This result, as before, is less obvious than the others. Let us derive it starting from the definition of S_x^2:

$$\begin{aligned}S_x^2 = \left(\sum_{i=1}^{\mathcal{N}} \eta_i \left(j_{x_{2i-1}} + j_{x_{2i}}\right)^2\right)^2 = \sum_{i=1}^{\mathcal{N}} \eta_i^2 \left(j_{x_{2i-1}} + j_{x_{2i}}\right)^2 + \\ + \sum_{i\neq j} \eta_i\eta_j \left(j_{x_{2i-1}} j_{x_{2j-1}} + j_{x_{2i-1}} j_{x_{2j}} + j_{x_{2i}} j_{x_{2j-1}} + j_{x_{2i}} j_{x_{2j}}\right)\end{aligned} \tag{2.25}$$

  Now consider the second term in the right hand side of eq. (2.25); Since $\langle j_{x_{2k}}\rangle = \frac{\sin(-\theta_k)}{2} = -\frac{\sin(\theta_k)}{2} = -\langle j_{x_{2k-1}}\rangle$, for $i \neq j$ we get:

$$\langle j_{x_{2i-1}} j_{x_{2j-1}}\rangle = \langle j_{x_{2i-1}}\rangle\langle j_{x_{2j-1}}\rangle = -\langle j_{x_{2i-1}}\rangle\langle j_{x_{2j}}\rangle = -\langle j_{x_{2i-1}} j_{x_{2j}}\rangle \tag{2.26a}$$

$$\langle j_{x_{2i}} j_{x_{2j-1}}\rangle = \langle j_{x_{2i}}\rangle\langle j_{x_{2j-1}}\rangle = -\langle j_{x_{2i}}\rangle\langle j_{x_{2j}}\rangle = -\langle j_{x_{2i}} j_{x_{2j}}\rangle \tag{2.26b}$$

  So that we can conclude that, when averaging, the four terms in the considered sum are neglecting themselves in couples. In other words, $\langle\sum_{i\neq j} \eta_i\eta_j \big(j_{x_{2i-1}} j_{x_{2j-1}} +$

$j_{x_{2i-1}}j_{x_{2j}} + j_{x_{2i}}j_{x_{2j-1}} + j_{x_{2i}}j_{x_{2j}}\big)\rangle = 0$ and

$$\langle S_x^2\rangle = \langle\sum_{i=1}^{\mathcal{N}} \eta_i^2 \left(j_{x_{2i-1}} + j_{x_{2i}}\right)^2\rangle = \sum_{i=1}^{\mathcal{N}} \eta_i^2 \left(\langle j_{x_{2i-1}}^2\rangle + \langle j_{x_{2i}}^2\rangle + 2\langle j_{x_{2i-1}}j_{x_{2i}}\rangle\right) \quad (2.27)$$

At this point it is straightforward to compute $\langle S_x^2\rangle$; in fact:

$$\begin{aligned}
\langle S_x^2\rangle &= \langle\sum_{i=1}^{\mathcal{N}} \eta_i^2 \left(j_{x_{2i-1}}^2 + j_{x_{2i}}^2 + 2j_{x_{2i-1}}j_{x_{2i}}\right)\rangle = \\
&= \sum_{i=1}^{\mathcal{N}} \eta_i^2 \left(\langle j_{x_{2i-1}}^2\rangle + \langle j_{x_{2i}}^2\rangle + 2\langle j_{x_{2i-1}}j_{x_{2i}}\rangle\right) = \\
&= \sum_{i=1}^{\mathcal{N}} \eta_i^2 \left(\frac{1}{4} + \frac{1}{4} + 2\langle j_{x_{2i-1}}\rangle\langle j_{x_{2i}}\rangle\right) = \\
&= \sum_{i=1}^{\mathcal{N}} \eta_i^2 \left(\frac{1}{2} - \frac{2\sin^2\theta_i}{4}\right) = \sum_{i=1}^{\mathcal{N}} \left(\frac{\eta_i^2}{2}\cos^2\theta_i\right),
\end{aligned} \quad (2.28)$$

that exactly is the result reported before.

We can now collect what we got in order to proceed with determining ξ_N^2:

$$\langle S_z\rangle = \sum_{i=1}^{\mathcal{N}} \eta_i \cos\theta_i \quad (2.29a)$$

$$(\Delta S_x)^2 = \langle S_x^2\rangle - \langle S_x\rangle^2 = \frac{1}{2}\sum_{i=1}^{\mathcal{N}} \eta_i^2 \cos^2\theta_i, \quad (2.29b)$$

so that it is straightforward to get

$$\xi_N^2\left(\eta_1, ..., \eta_{\mathcal{N}}; \theta_1, ..., \theta_{\mathcal{N}}\right) = \frac{\left(\sum_{i=1}^{N}\eta_i\right)^2}{\sum_{i=1}^{N}\eta_i^2}\frac{(\Delta S_x)^2}{\langle S_z\rangle^2} = \frac{\left(\sum_{i=1}^{\mathcal{N}}\eta_i\right)^2}{\sum_{i=1}^{\mathcal{N}}\eta_i^2}\frac{\sum_{i=1}^{\mathcal{N}}\eta_i^2\cos^2\theta_i}{\left(\sum_{i=1}^{\mathcal{N}}\eta_i\cos\theta_i\right)^2} \quad (2.30)$$

From now on it is just a matter of generalizing what we did in section 2.1.1.1; in fact extending the definition of $h(x, y)$ to more variables,

$$h(\vec{x}) = h\left(x_1, ..., x_{\mathcal{N}}\right) = \frac{\left(\sum_{i=1}^{\mathcal{N}} x_i\right)^2}{\sum_{i=1}^{\mathcal{N}} x_i^2}, \quad (2.31)$$

it is obvious we can express ξ_N^2 in terms of $h(\vec{x})$ as:

$$\xi_N^2\left(\vec{\eta},\vec{\theta}\right)=\frac{h\left(\eta_1,...,\eta_{\mathcal{N}}\right)}{h\left(\eta_1\cos\theta_1,...,\eta_{\mathcal{N}}\cos\theta_{\mathcal{N}}\right)} \tag{2.32}$$

Here we used the notation $\vec{x}=(x_1,...,x_{\mathcal{N}})$ for one $\mathcal{N}$-dimensional vector.
Now, following the same steps of before, we will search again a lower and an upper bounds for the function $h(\vec{x})$, in order to get some constraints to apply to our squeezing parameter ξ_N^2 and thus determine its minimum.

The **upper bound** of $h(\vec{x})$ is derived, without any conceptual difference from section 2.1.1.1, using Jensen's inequality (lemma 1):

$$\frac{h(\vec{x})}{\mathcal{N}}=\frac{\left(\frac{1}{\mathcal{N}}\sum\limits_{i=1}^{\mathcal{N}}x_i\right)^2}{\frac{1}{\mathcal{N}}\sum\limits_{i=1}^{\mathcal{N}}x_i^2}\leq\frac{\left(\frac{1}{\mathcal{N}}\sum\limits_{i=1}^{\mathcal{N}}|x_i|\right)^2}{\frac{1}{\mathcal{N}}\sum\limits_{i=1}^{\mathcal{N}}x_i^2}\leq 1, \tag{2.33}$$

In other words $h(\vec{x})\leq\mathcal{N}=\frac{N}{2}$, where N represents the number of the particles. Moreover we know, always from lemma 1, that the inequality is saturated if and only if $x_i=x_j$ for all $i,j=1,...,\mathcal{N}$.

The **lower bound** of $h(\vec{x})$, in the special case in which $x_1\geq x_i>0$ for all $i=2,...,\mathcal{N}$, is again very simple to obtain. In fact

$$h(\vec{x})=\frac{\left(\sum\limits_{i=1}^{\mathcal{N}}x_i\right)^2}{\sum\limits_{i=1}^{\mathcal{N}}x_i^2}=\frac{\sum\limits_{i=1}^{\mathcal{N}}x_i^2+2\sum\limits_{i>j}x_ix_j}{\sum\limits_{i=1}^{\mathcal{N}}x_i^2}=1+2\frac{\sum\limits_{i>j}\overbrace{x_ix_j}^{\geq 0}}{\sum\limits_{i=1}^{\mathcal{N}}x_i^2}\geq 1; \tag{2.34}$$

in particular $h(\vec{x})\to 1$ for $x_1\gg x_i$ and $x_i\to 0$ for all $i=2,...,\mathcal{N}$.
Notice that in the critical case in which $\|\vec{x}\|\to 0$, the corresponding limit for $h(\vec{x})$ is not well defined (it depends on how $\vec{x}$ is approaching the null vector), but still it is bigger than one.

At this point we have all the conditions they have to be satisfied for finding the minimum of $\xi_N^2(\vec{\eta},\vec{\theta})=h\left(\eta_1,...,\eta_{\mathcal{N}}\right)h^{-1}\left(\eta_1\cos\theta_1,...,\eta_{\mathcal{N}}\cos\theta_{\mathcal{N}}\right)$:

$$\eta_i\cos\theta_i=\eta_j\cos\theta_j \qquad \forall\ i,j=1,...,\mathcal{N} \tag{2.35a}$$

$$\eta_1\gg\eta_i \qquad \forall\ i=1,...,\mathcal{N} \tag{2.35b}$$

$$\eta_i\to 0 \qquad \forall\ i=2,...,\mathcal{N} \tag{2.35c}$$

Here eq.2.35a is referred to maximize $h\left(\eta_1 \cos\theta_1, ..., \eta_{\mathcal{N}} \cos\theta_{\mathcal{N}}\right)$, while equations 2.35b and 2.35c to minimize $h\left(\eta_1, ..., \eta_{\mathcal{N}}\right)$. The values these functions assume with these constraints are, putting $\alpha = \eta_i \cos\theta_i$ for all $i = 1, ..., \mathcal{N}$:

$$h^{-1}(\alpha) = \frac{\sum_{i=1}^{\mathcal{N}} \alpha^2}{\left(\sum_{i=1}^{\mathcal{N}} \alpha\right)^2} = \frac{1}{\mathcal{N}} \tag{2.36a}$$

$$h(\vec{\eta}) = \frac{\left(\sum_{i=1}^{\mathcal{N}} \eta_i\right)^2}{\sum_{i=1}^{\mathcal{N}} \eta_i^2} \simeq h(\eta_1) = 1 \tag{2.36b}$$

At this point it is just a matter of multiplying $h^{-1}(\alpha)$ and $h(\eta_1)$ together in order to obtain the lowest bound our squeezing parameter can approach:

$$\xi_N^2(\vec{\eta}, \vec{\theta}) \geq \min\{\xi_N^2\} \equiv \frac{h(\eta_1)}{h(\alpha)} = \frac{1}{\mathcal{N}} = \frac{2}{N} \tag{2.37}$$

As anticipated, when we suppose the operator representing the measure is $\vec{S}$, it is not true any more that the squeezing parameter ξ_N^2 is bounded from below by one. We have shown that there exists at least one example in which it can approach the value $\xi_N^2 \to \frac{2}{N}$, so that with a big number of atoms it is a hard task to determine if the system is really entangled or not. We can now interpret the conditions 2.35a, 2.35b and 2.35c, in order to understand what happens to the particles when the lowest bound is saturated. Such limit is reached when our apparatus detects only the first couple of atoms $|\theta_1\rangle_1|-\theta_1\rangle_2$ in the particular state $|\rightarrow\rangle_1|\leftarrow\rangle_2$, all other particles being at the board of the detecting laser beam (see the next Fig.2.2).

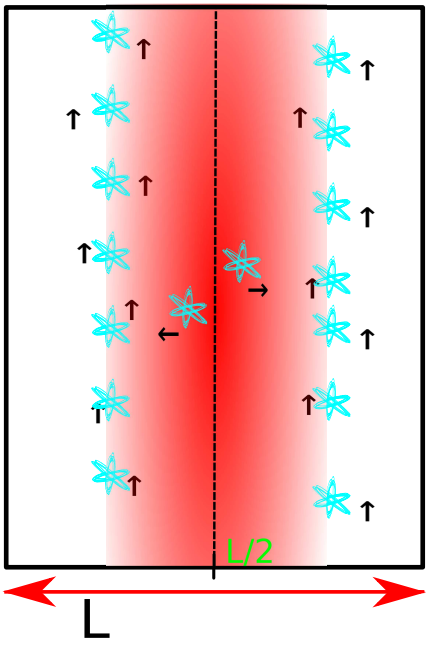

FIGURE 2.2: Situation, described in the text, for which the minimum possible squeezing parameter is reached. There are two particles, well shined by the laser, in the states $|\rightarrow\rangle$ and $|\leftarrow\rangle$; all the others are barely hit by the beam

It is useless to explain how absurd this behaviour is in the reality; and the model used for deriving this result is already very unlikely: the symmetries we supposed are easily broken during the experiment, and the situation described in this section will never be realized in the laboratory. However, supposing the bound $\xi_N^2 \geq \frac{1}{N}$ being true for a generic separable state (otherwise it can only be lower!), we must admit that it is impossible to speak about entanglement without measuring a lower value. Thus, we would like to find some different kind of squeezing parameter, which bound does not depend on the number of particles constituting the system, easy to measure and practical experimentally. An attempt will be made in the next section.

2.2 The new parameter ξ_U^2

We can try to think why the lower bound of ξ_N^2 moves from 1 to $\frac{2}{N}$ when using the new collective spin operator $\vec{S}$. As it has been possible to see during Section 2.1.2, this is intuitively a consequence of the fact that we can loose the presence of all the atoms but the first couple in the first product term of ξ_N^2 (see eq.2.36b):

$$h(\vec{\eta}) = \frac{\left(\sum_{i=1}^{\mathcal{N}} \eta_i\right)^2}{\sum_{i=1}^{\mathcal{N}} \eta_i^2} \rightarrow h(\eta_1) = \frac{\eta_1^2}{\eta_1^2} = 1, \tag{2.38}$$

while their presence is well kept in the second product term $h(\eta_1 \cos\theta_1, ..., \eta_{\mathcal{N}} \cos\theta_{\mathcal{N}})$. In fact, in the situation where $|\theta_1\rangle_1|-\theta_1\rangle_2 = |\rightarrow\rangle_1|\leftarrow\rangle_2$, we have that even if the coefficient η_1 of the first couple is much bigger than all the others ($\eta_1 \gg \eta_i$ for all $i = 1, ..., \mathcal{N}$), its contribution can be the same to the ones of all other couples in both $(\Delta S_x)^2$ and $\langle S_z\rangle$ (see eq: 2.36a):

$$h^{-1}(\eta_1 \cos\theta_1, ..., \eta_{\mathcal{N}} \cos\theta_{\mathcal{N}}) \rightarrow h^{-1}(\alpha) = \frac{1}{\mathcal{N}} \tag{2.39}$$

Consequently, we would like to multiply our squeezing parameter ξ_N^2 to some coefficient able to avoid this undesirable behaviour. A possibility could be to generalize ξ_N^2 in the following way:

$$\xi_U^2 \equiv \xi_N^2 \frac{\langle S_z^2\rangle}{\langle S_z\rangle^2} = \frac{\left(\sum_{i=1}^{N} \eta_i\right)^2}{\sum_{i=1}^{N} \eta_i^2} \frac{(\Delta S_x)^2 \langle S_z^2\rangle}{\langle S_z\rangle^4}, \tag{2.40}$$

so that in the critical situation described above, the new factor goes to infinity, keeping ξ_U^2 safely bigger than one (as it is easily deduced from section 2.1.2).

Let us think about to the multiplicative factor

$$\frac{\langle S_z^2\rangle}{\langle S_z\rangle^2}. \tag{2.41}$$

In the following sections we will largely discuss if it solves the problem we pointed out previously; now let us describe it more qualitatively:

- How it behaves in the pure, separable state minimizing

$$\xi_R^2 = N \frac{\Delta J_x^2}{\langle J_z\rangle^2} = N \frac{\sum_{i=1}^{N} (\Delta j_{x_i})^2}{\left(\sum_{i=1}^{N} \langle j_{z_i}\rangle\right)^2}, \tag{2.42}$$

  i.e.: our squeezing parameter with "classical" collective spin operator? Such state clearly is

$$|CSS\rangle = |\uparrow\rangle_1|\uparrow\rangle_2 ... |\uparrow\rangle_{N-1}|\uparrow\rangle_N; \tag{2.43}$$

  in fact, for such wave vector,

$$(\Delta j_{x_i})^2 = \frac{1}{4} \tag{2.44a}$$

$$\langle j_{z_i}\rangle = \frac{1}{2} \tag{2.44b}$$

and ξ_R^2 reaches the lower bound

$$\xi_R^2 = \frac{N}{N} = 1. \tag{2.45}$$

What about ξ_N^2 and ξ_U^2? Supposing the symmetries used in section 2.1.2 valid, and using the results obtained in the same section (in particular eq.2.29a and 2.29b), we automatically obtain

$$(\Delta S_x)^2 = \frac{1}{2}\sum_{i=1}^{\mathcal{N}} \eta_i^2 \tag{2.46a}$$

$$\langle S_z \rangle = \sum_{i=1}^{\mathcal{N}} \eta_i \tag{2.46b}$$

and thus $\xi_N^2 = 1$.
For ξ_U^2 the only missing piece is $\langle S_z^2 \rangle$, that is given by:

$$\langle S_z^2 \rangle = \langle \left(\sum_{i=1}^{N} \tilde{\eta}_i j_{z_i} \right)^2 \rangle = 4 \left[\sum_{i=1}^{\mathcal{N}} \eta_i^2 \langle j_{z_i}^2 \rangle + 2 \sum_{i>j} \eta_i \eta_j \langle j_{z_i} j_{z_j} \rangle \right] = \left(\sum_{i=1}^{\mathcal{N}} \eta_i \right)^2 \tag{2.47}$$

Putting all these results together we finally get $\xi_U^2 = 1$; i.e.:

$$\xi_R^2 = \xi_N^2 = \xi_U^2 = 1 \tag{2.48}$$

In particular the factor

$$\frac{\langle S_z^2 \rangle}{\langle S_z \rangle^2} = \frac{\left(\sum_{i=1}^{\mathcal{N}} \eta_i \right)^2}{\left(\sum_{i=1}^{\mathcal{N}} \eta_i \right)^2} = 1, \tag{2.49}$$

that means that this factor is *not* correcting the wave vector of eq. 2.43, namely the one for which the old squeezing parameter is minimized.

- Which is the lower bound for $\frac{\langle S_z^2 \rangle}{\langle S_z \rangle^2}$? It is easy to prove that

$$\frac{\langle S_z^2 \rangle}{\langle S_z \rangle^2} = \frac{\langle S_z^2 \rangle - \langle S_z \rangle^2 + \langle S_z \rangle^2}{\langle S_z \rangle^2} = 1 + \frac{\overbrace{(\Delta S_z)^2}^{\geq 0}}{\langle S_z \rangle^2} \geq 1 \tag{2.50}$$

In particular, we already know a state for which this last inequality is saturated: namely the one described by eq.2.43. Due to eq.2.50, we automatically get that

$$\xi_U^2 = \xi_N^2 \frac{\langle S_z^2 \rangle}{\langle S_z \rangle^2} \geq \xi_N^2, \tag{2.51}$$

that means that ξ_U^2 cannot take smaller values then ξ_N^2.

In the following section we will study ξ^2_U, trying to obtain a useful inequality satisfied by all separable states. First, we will get an expression for ξ^2_U considering the same model introduced above. Later, we will generalize this result for a generic separable state, and in conclusion we will prove that under some constraints this parameter is allowed to be smaller than unity.

2.2.1 ξ^2_U in the many atoms model

In this section we will refer to the same situation described in 2.1.2. Thus we can use the results we obtained there, that means equations 2.29a and 2.29b, and only derive a comfortable expression for $\langle S_z^2 \rangle$:

$$\langle S_z^2 \rangle = \langle \left(\sum_{i=1}^{N} \tilde{\eta}_i j_{z_i} \right)^2 \rangle = \sum_{i,j=1}^{N} \tilde{\eta}_i \tilde{\eta}_j \langle j_{z_i} j_{z_j} \rangle \tag{2.52}$$

According to the indices we can distinguish the next three kind of terms in the sum:

1. If $i = j$ they are:
$$\{i = j\} \Rightarrow \tilde{\eta}_i \tilde{\eta}_j \langle j_{z_i} j_{z_j} \rangle = \tilde{\eta}_i^2 \langle j_{z_i}^2 \rangle = \frac{\tilde{\eta}_i^2}{4} \tag{2.53}$$

2. If $i = 2k-1$ and $j = 2k$ with $k = 1, ..., \mathcal{N} = \frac{N}{2}$ they are:
$$\begin{aligned} \{i = 2k-1, j = 2k\} \Rightarrow \tilde{\eta}_i \tilde{\eta}_j \langle j_{z_i} j_{z_j} \rangle = \\ = \tilde{\eta}_{2k-1} \tilde{\eta}_{2k} \langle j_{z_{2k-1}} \rangle \langle j_{z_{2k}} \rangle = \\ = \eta_k^2 \langle \theta_k | J_z | \theta_k \rangle \langle -\theta_k | J_z | -\theta_k \rangle = \\ = \frac{\eta_k^2 \cos^2 \theta_k}{4} \end{aligned} \tag{2.54}$$

   Here we remember that, due to the symmetry of the problem, we have done the substitution $\tilde{\eta}_{2k-1} = \tilde{\eta}_{2k} = \eta_k$.

3. In all other cases we have that the terms of the sum are given by:
$$\{i \neq j\} \Rightarrow \tilde{\eta}_i \tilde{\eta}_j \langle j_{z_i} j_{z_j} \rangle = \tilde{\eta}_i \langle j_{z_i} \rangle \tilde{\eta}_j \langle j_{z_j} \rangle = \frac{\tilde{\eta}_i \cos\theta_i \tilde{\eta}_j \cos\theta_j}{4} \tag{2.55}$$

   Where θ_l and $\tilde{\eta}_l$ refers respectfully to the particle and the coefficient associated to the index l.

Now we are able to split the sum in the three corresponding parts. Helped by the following table,

Index ***(i\j)***	***1***	***2***	***3***	***4***	***...***	***2$\mathcal{N}$-1***	***2$\mathcal{N}$***
1	**11**	**12**	13	14	...	1(2$\mathcal{N}$-1)	1(2$\mathcal{N}$)
2	**21**	**22**	23	24	...	2(2$\mathcal{N}$-1)	2(2$\mathcal{N}$)
3	31	32	**33**	**34**	...	3(2$\mathcal{N}$-1)	3(2$\mathcal{N}$)
4	41	42	**43**	**44**	...	4(2$\mathcal{N}$-1)	4(2$\mathcal{N}$)
...	...	...	...	...	...	...	...
2$\mathcal{N}$-1	(2$\mathcal{N}$-1)1	(2$\mathcal{N}$-1)2	(2$\mathcal{N}$-1)3	(2$\mathcal{N}$-1)4	...	**(2$\mathcal{N}$-1)(2$\mathcal{N}$-1)**	**(2$\mathcal{N}$-1)(2$\mathcal{N}$)**
2$\mathcal{N}$	(2$\mathcal{N}$)1	(2$\mathcal{N}$)2	(2$\mathcal{N}$)3	(2$\mathcal{N}$)4	...	**(2$\mathcal{N}$)(2$\mathcal{N}$-1)**	**(2$\mathcal{N}$)(2$\mathcal{N}$)**

TABLE 2.1: The table represents all possible indices we have in the various sums. We used different colours and boxes for making evident some contributions of interest, as explained in the text below. Remember that $2\mathcal{N} = N$

we can recognize:

1. **The diagonal terms** (*red* in Table 2.1); i.e.: the terms for which $i = j$:

$$\sum_{j=1}^{N} \frac{\tilde{\eta}_j^2}{4} = \sum_{i=1}^{\mathcal{N}} \frac{\eta_i^2}{2} \tag{2.56}$$

2. **The "jumping" near-diagonal terms** (*blue* in Table 2.1), so defined because they are all the terms adjacent to the diagonal with $i + j = 4k - 1$ (with $k = 1, ..., \mathcal{N}$), thus leaving uncounted their "brothers" with $i + j = 4k + 1$:

$$2\sum_{i=1}^{\mathcal{N}} \frac{\eta_i^2 \cos^2\theta_i}{4} = \frac{1}{2}\sum_{i=1}^{\mathcal{N}} \eta_i^2 \cos^2\theta_i \tag{2.57}$$

   The factor 2 comes from the fact that we are counting both the upper-diagonal and the lower-diagonal contribution.

3. **All other terms** (the "boxes" in Table 2.1):

$$2\sum_{i=1}^{\mathcal{N}-1}\sum_{j=i+1}^{\mathcal{N}} \eta_i\eta_j \cos\theta_i \cos\theta_j \tag{2.58}$$

   The factor 2 derives, again, from the fact that we have upper- and lower-diagonal indices, while i cannot be equal to $\mathcal{N}$ because for $i = \mathcal{N}$ the contributions are already present in the previous eq.2.56 and 2.57. Moreover, the absence of the factor 4 at the denominator of eq.2.55 is a consequence of the following reason: removed (by the previous two points, eq.2.56 and eq.2.57) all the red and blue terms pictured in Table 2.1, we can divide all the remaining indices in 4-dimensional sets their elements are associated with equal contributions (the "boxes"). In fact,

always due to the symmetry of the system, we have that

$$\begin{aligned}\frac{1}{4}\eta_k\cos\theta_k\eta_l\cos\theta_l &= \frac{1}{4}\tilde{\eta}_{2k-1}\langle j_{z_{2k-1}}\rangle\tilde{\eta}_{2l-1}\langle j_{z_{2l-1}}\rangle = \\ &= \frac{1}{4}\tilde{\eta}_{2k-1}\langle j_{z_{2k-1}}\rangle\tilde{\eta}_{2l}\langle j_{z_{2l}}\rangle = \\ &= \frac{1}{4}\tilde{\eta}_{2k}\langle j_{z_{2k}}\rangle\tilde{\eta}_{2l-1}\langle j_{z_{2l-1}}\rangle = \\ &= \frac{1}{4}\tilde{\eta}_{2k}\langle j_{z_{2k}}\rangle\tilde{\eta}_{2l}\langle j_{z_{2l}}\rangle\end{aligned} \tag{2.59}$$

with $k, l = 1, ..., \mathcal{N}$.

So, for example, for $k = 1$ and $l = 2$ we obtain the four terms in the first box, they contribute to $\langle S_z^2\rangle$ with

$$\begin{aligned}&\frac{1}{4}\tilde{\eta}_1\langle j_{z_1}\rangle\tilde{\eta}_3\langle j_{z_3}\rangle + \frac{1}{4}\tilde{\eta}_1\langle j_{z_1}\rangle\tilde{\eta}_4\langle j_{z_4}\rangle + \frac{1}{4}\tilde{\eta}_2\langle j_{z_2}\rangle\tilde{\eta}_3\langle j_{z_3}\rangle + \frac{1}{4}\tilde{\eta}_2\langle j_{z_2}\rangle\tilde{\eta}_4\langle j_{z_4}\rangle = \\ &= \eta_1\cos\theta_1\eta_2\cos\theta_2.\end{aligned} \tag{2.60}$$

Thus we can group all this equal contributions in order to obtain the compact form of eq.(2.58).

We can now collect all the previous results for finally write down $\langle S_z^2\rangle$:

$$\langle S_z^2\rangle = \frac{1}{2}\sum_{i=1}^{\mathcal{N}}\eta_i^2 + \frac{1}{2}\sum_{i=1}^{\mathcal{N}}\eta_i^2\cos^2\theta_i + 2\sum_{i=1}^{\mathcal{N}-1}\sum_{j=i+1}^{\mathcal{N}}\eta_i\eta_j\cos\theta_i\cos\theta_j \tag{2.61}$$

Now it is just a matter of rewrite it in a more convenient form. First, let us group the sums in order to get:

$$\begin{aligned}\langle S_z^2\rangle &= \frac{1}{2}\sum_{i=1}^{\mathcal{N}}\eta_i^2\left(1+\cos^2\theta_i\right) + 2\sum_{i=1}^{\mathcal{N}-1}\sum_{j=i+1}^{\mathcal{N}}\eta_i\eta_j\cos\theta_i\cos\theta_j = \\ &= \frac{1}{2}\sum_{i=1}^{\mathcal{N}}\eta_i^2\sin^2\theta_i + \left(\sum_{i=1}^{\mathcal{N}}\eta_i^2\cos^2\theta_i + 2\sum_{i=1}^{\mathcal{N}-1}\sum_{j=i+1}^{\mathcal{N}}\eta_i\eta_j\cos\theta_i\cos\theta_j\right)\end{aligned} \tag{2.62}$$

At this point it is easy to note that the term in parentheses in the last line of the previous equation is actually

$$\sum_{i=1}^{\mathcal{N}}\eta_i^2\cos^2\theta_i + 2\sum_{i=1}^{\mathcal{N}-1}\sum_{j=i+1}^{\mathcal{N}}\eta_i\eta_j\cos\theta_i\cos\theta_j = \left(\sum_{i=1}^{\mathcal{N}}\eta_i\cos\theta_i\right)^2, \tag{2.63}$$

so that, in conclusion:

$$\langle S_z^2\rangle = \left(\sum_{i=1}^{\mathcal{N}}\eta_i\cos\theta_i\right)^2 + \frac{1}{2}\sum_{i=1}^{\mathcal{N}}\eta_i^2\sin^2\theta_i \tag{2.64}$$

We arrived to the point in which we possess all the elements for determining the particular form of ξ_U^2 in the considered model. We have that:

$$\xi_U^2 = \xi_N^2 \left(\underbrace{1 + \frac{(\Delta S_z)^2}{\langle S_z \rangle^2}}_{= \frac{\langle S_z^2 \rangle}{\langle S_z \rangle^2}} \right) = \xi_N^2 \left(1 + \frac{1}{2} \frac{\sum_{i=1}^{\mathcal{N}} \eta_i^2 \sin^2 \theta_i}{\left(\sum_{i=1}^{\mathcal{N}} \eta_i \cos \theta_i \right)^2} \right), \tag{2.65}$$

or, in a more explicit form:

$$\xi_U^2 \left(\vec{\eta}; \vec{\theta} \right) = \left\{ \frac{\left(\sum_{i=1}^{\mathcal{N}} \eta_i \right)^2}{\sum_{i=1}^{\mathcal{N}} \eta_i^2} \frac{\sum_{i=1}^{\mathcal{N}} \eta_i^2 \cos^2 \theta_i}{\left(\sum_{i=1}^{\mathcal{N}} \eta_i \cos \theta_i \right)^2} \right\} \left\{ 1 + \frac{1}{2} \frac{\sum_{i=1}^{\mathcal{N}} \eta_i^2 \sin^2 \theta_i}{\left(\sum_{i=1}^{\mathcal{N}} \eta_i \cos \theta_i \right)^2} \right\}, \tag{2.66}$$

where, as before, $\vec{x}$ indicates the $\mathcal{N}$-dimensional vector of real numbers.

In the following we will obtain a (very) similar result for a generic separable state, and then we will prove that the new parameter can take, for some particular states, values smaller than one.

2.2.2 Separable states

Suppose we have to deal with a generic separable state described by the density matrix

$$\rho = \sum_k p_k \rho_k = \sum_k p_k \rho_{k_1} \otimes ... \otimes \rho_{k_N}. \tag{2.67}$$

Here ρ_{k_i}, for $i = 1, ..., N$ refers to the i-th particle, while p_k's are positive real numbers satisfying $\sum_k p_k = 1$.
Now we need to follow the well known procedure: find, for this state, equations for $(\Delta S_x)^2$, $\langle S_x \rangle$, $\langle S_z \rangle$ and $\langle S_x^2 \rangle$ and use these results for writing down $\xi_U^2(\rho)$.

2.2.2.1 ξ_U^2 for separable states

The "ingredients" we need are the common ones:

- The variance of the collective spin measurement operator along the x direction $(\Delta S_x)^2$:

$$(\Delta S_x)^2 = \mathrm{Tr}\left(\rho S_x^2\right) - \mathrm{Tr}^2\left(\rho S_x\right) = \sum_k p_k \mathrm{Tr}\left(\rho_k S_x^2\right) - \left[\sum_k p_k \mathrm{Tr}\left(\rho_k S_x\right)\right]^2 \overset{\dagger}{\geq}$$
$$\overset{\dagger}{\geq} \sum_k p_k \left\{\mathrm{Tr}\left(\rho_k S_x^2\right) - \left[\mathrm{Tr}\left(\rho_k S_x\right)\right]^2\right\}, \tag{2.68}$$

where for the inequality marked with † we used again lemma 1.
Let us introduce the new notation $\langle A\rangle_k \equiv \mathrm{Tr}\left(\rho_k A\right)$, for a generic hermitian operator A; we can thus rewrite the last term in the curly parentheses as:

$$\left\{\mathrm{Tr}\left(\rho_k S_x^2\right) - \left[\mathrm{Tr}\left(\rho_k S_x\right)\right]^2\right\} = \langle\left(\sum_{i=1}^N \eta_i j_{x_i}\right)^2\rangle_k - \langle\sum_{i=1}^N \eta_i j_{x_i}\rangle_k^2 \overset{\dagger\dagger}{=}$$
$$\overset{\dagger\dagger}{=} \sum_{i=1}^N \eta_i^2 \langle j_{x_i}^2\rangle_k + \sum_{i\neq j} \eta_i\eta_j \langle j_{x_i}\rangle_k \langle j_{x_j}\rangle_k - \left(\sum_{i=1}^N \eta_i^2 \langle j_{x_i}\rangle_k^2 + \sum_{i\neq j} \eta_i\eta_j \langle j_{x_i}\rangle_k \langle j_{x_j}\rangle_k\right) =$$
$$= \sum_{i=1}^N \eta_i^2 \left(\Delta j_{x_i}\right)_k^2 \tag{2.69}$$

Here for equality †† we used the property $\langle j_{x_i} j_{x_j}\rangle_k = \mathrm{Tr}(\rho_k j_{x_i} \otimes j_{x_j}) = \mathrm{Tr}(\rho_k j_{x_i}) \times \mathrm{Tr}(\rho_k j_{x_j}) = \langle j_{x_i}\rangle_k \langle j_{x_j}\rangle_k$, whenever $i \neq j$. Moreover we defined $(\Delta j_{x_i})_k^2 = \langle j_{x_i}^2\rangle_k - \langle j_{x_i}\rangle_k^2$.
We can now collect the two previous results in order to obtain

$$(\Delta S_x)^2 \geq \sum_k p_k \sum_{i=1}^N \eta_i^2 \left(\Delta j_{x_i}\right)_k^2 \tag{2.70}$$

- The average value of the collective spin measurement operator $\langle S_z\rangle$:

$$\langle S_z\rangle = \mathrm{Tr}\left(\sum_k p_k \rho_k S_z\right) = \sum_k p_k \mathrm{Tr}\left(\rho_k \sum_{i=1}^N \eta_i j_{z_i}\right) = \sum_k p_k \sum_{i=1}^N \eta_i \langle j_{z_i}\rangle_k \tag{2.71}$$

- The average value $\langle S_z^2 \rangle$:

$$\begin{aligned}\langle S_z^2 \rangle &= \mathrm{Tr}\left(\sum_k p_k \rho_k S_z^2\right) = \sum_k p_k \mathrm{Tr}\left(\rho_k \sum_{i,j=1}^N \eta_i \eta_j j_{z_i} j_{z_j}\right) = \\ &= \sum_k p_k \sum_{i,j=1}^N \eta_i \eta_j \langle j_{z_i} j_{z_j} \rangle_k \overset{\dagger}{=} \sum_k p_k \left[\sum_{i=1}^N \eta_i^2 \left(\Delta j_{z_i}\right)_k^2 + \left(\sum_{i=1}^N \eta_i^2 \langle j_z \rangle_k\right)^2\right] \overset{\dagger\dagger}{\geq} \\ &\overset{\dagger\dagger}{\geq} \sum_k p_k \sum_{i=1}^N \eta_i^2 \left(\Delta j_{z_i}\right)_k^2 + \left(\sum_k p_k \sum_{i=1}^N \eta_i^2 \langle j_z \rangle_k\right)^2,\end{aligned} \tag{2.72}$$

where relation †† follows from Jensen's inequality and equality † is a direct consequence of

$$\begin{aligned}\sum_{i,j=1}^N \eta_i \eta_j \langle j_{z_i} j_{z_j} \rangle_k &= \sum_{i=1}^N \eta_i^2 \langle j_{z_i}^2 \rangle_k - \sum_{i=1}^N \eta_i^2 \langle J_z \rangle_k^2 + \sum_{i=1}^N \eta_i^2 \langle J_z \rangle_k^2 + \sum_{i \neq j} \eta_i \eta_j \overbrace{\langle j_{z_i} j_{z_j} \rangle_k}^{= \langle j_{z_i} \rangle_k \langle j_{z_j} \rangle_k} = \\ &= \sum_{i=1}^N \eta_i^2 \left(\Delta j_{z_i}\right)_k^2 + \left(\sum_{i=1}^N \eta_i^2 \langle J_z \rangle_k\right)^2\end{aligned} \tag{2.73}$$

We are finally able to write down ξ_U^2; or, better, a first lower bound for it (due to the inequality in eq.2.70):

$$\begin{aligned}&\xi_U^2(\rho) \geq \\ &\geq \frac{\left(\sum_{i=1}^N \eta_i\right)^2}{\sum_{i=1}^N \eta_i^2} \frac{\left\{\sum_k p_k \sum_{i=1}^N \eta_i^2 \left(\Delta j_{x_i}\right)_k^2\right\} \left\{\left(\sum_k p_k \sum_{i=1}^N \eta_i \langle j_{z_i} \rangle_k\right)^2 + \sum_k p_k \sum_{i=1}^N \eta_i^2 \left(\Delta j_{z_i}\right)_k^2\right\}}{\left(\sum_k p_k \sum_{i=1}^N \eta_i \langle j_{z_i} \rangle_k\right)^4} = \\ &= \frac{\left(\sum_{i=1}^N \eta_i\right)^2}{\sum_{i=1}^N \eta_i^2} \frac{\left\{\sum_k p_k \sum_{i=1}^N \eta_i^2 \left(\Delta j_{x_i}\right)_k^2\right\}}{\left(\sum_k p_k \sum_{i=1}^N \eta_i \langle j_{z_i} \rangle_k\right)^2} \left\{1 + \frac{\sum_k p_k \sum_{i=1}^N \eta_i^2 \left(\Delta j_{z_i}\right)_k^2}{\left(\sum_k p_k \sum_{i=1}^N \eta_i \langle j_{z_i} \rangle_k\right)^2}\right\}\end{aligned} \tag{2.74}$$

Let us briefly look at some properties of the function in the right hand side of the previous equation. Obviously all the terms are positive, both at numerator and denominator, so that we can deduce $\xi_U^2 \geq 0$. Moreover, there is a family of points where the function is not well defined, since the denominator takes null value. Clearly these points are given by $\sum_k p_k \sum_{i=1}^N \eta_i \langle j_{x_i} \rangle_k = 0$, and the squeezing parameter is, for such values, going to infinity. We can already say that $0 \leq \xi_U^2 \leq \infty$.

Now it is just a matter of proving that there exists some critical state for which our new squeezing parameter approaches zero. This is the main goal of the next subsection, where we first try to give some clue about the behaviour of ξ^2_U, in order to find such state, and later we will prove it can take values smaller than one.

2.2.2.2 Finding (some) critical states for which $\xi^2_U < 1$

Here we will proceed gradually; at first we will prove that the state $|\psi\rangle = |\uparrow\rangle^{\otimes^N}$ is a local minimum for which $\xi^2_U\left(|\uparrow\rangle^{\otimes^N}\right) = 1$. This will be useful later, when we will study the derivative of our squeezing parameter. In fact, we will try to identify different stationary points, one of these being given by $|\uparrow\rangle^{\otimes^N}$. Some of the others will be used for determining states for which $\xi^2_U(\rho) \ll 1$.

- $\xi^2_U\left(|\uparrow\rangle^{\otimes^N}\right) = 1$, and in this state the function takes a local minimum.

  The equality has already proven in section 2.2, eq.2.48; we only need to show it is a local minimum.
  Let us suppose $\langle j_{z_i}\rangle_k = \frac{1}{2} - \epsilon_{i,k}$, where $\epsilon_{i,k}$ is a positive real number for all k positive integers and $i = 1, ..., N$. Notice that we do not allow any of the $\epsilon_{i,k}$ to be negative due to physical consideration. We thus have:

$$\langle j_{z_i}\rangle_k = \frac{1}{2} - \epsilon_{i,k} \tag{2.75a}$$

$$(\Delta j_{z_i})^2_k = \langle j^2_{z_i}\rangle_k - \langle j_{z_i}\rangle^2_k = \frac{1}{4} - \left(\frac{1}{2} - \epsilon_{i,k}\right)^2 = \epsilon_{i,k} - \epsilon^2_{i,k} \simeq \epsilon_{i,k} \tag{2.75b}$$

$$(\Delta j_{x_i})^2_k = \langle j^2_{x_i}\rangle_k - \langle j_{x_i}\rangle^2_k = \frac{1}{4} - \langle j_{x_i}\rangle^2_k \overset{\dagger}{\geq} \frac{1}{4} - \epsilon_{i,k} + \epsilon^2_{i,k} \simeq \frac{1}{4} - \epsilon_{i,k} \tag{2.75c}$$

  In the last of the three equations, the inequality marked with † is a consequence of the quantum mechanical property

$$\langle j_{x_i}\rangle^2_k + \langle j_{z_i}\rangle^2_k \leq \frac{1}{4} \tag{2.76}$$

  that automatically implies $\langle j_{x_i}\rangle^2_k \leq \frac{1}{4} - \langle j_{z_i}\rangle^2_k = \epsilon_{i,k} - \epsilon^2_{i,k}$.
  At this point, putting equations 2.75a, 2.75b and 2.75c in eq.2.74 we can express

ξ_U^2 as a function of $\epsilon_{i,k}$ and try to find a lower bound for it:

$$\begin{aligned}
&\xi_U^2\left(\{\epsilon_{i,k}\}\right) \geq \\
&\geq \frac{\left(\sum\limits_{i=1}^{N}\eta_i\right)^2}{\sum\limits_{i=1}^{N}\eta_i^2}\left\{\frac{\sum\limits_k p_k \sum\limits_{i=1}^{N}\eta_i^2\left(\frac{1}{4}-\epsilon_{i,k}\right)}{\left(\sum\limits_k p_k \sum\limits_{i=1}^{N}\eta_i\left(\frac{1}{2}-\epsilon_{i,k}\right)\right)^2}\right\}\left\{1+\frac{\sum\limits_k p_k \sum\limits_{i=1}^{N}\eta_i^2\epsilon_{i,k}}{\left(\sum\limits_k p_k \sum\limits_{i=1}^{N}\eta_i\left(\frac{1}{2}-\epsilon_{i,k}\right)\right)^2}\right\} \simeq \\
&\simeq \frac{\left(\sum\limits_{i=1}^{N}\eta_i\right)^2}{\sum\limits_{i=1}^{N}\eta_i^2}\left\{\frac{\sum\limits_{i=1}^{N}\eta_i^2}{\left(\sum\limits_{i=1}^{N}\eta_i\right)^2}\right\}\left\{1+\frac{4\sum\limits_k p_k \sum\limits_{i=1}^{N}\eta_i^2\epsilon_{i,k}}{\left(\sum\limits_{i=1}^{N}\eta_i\right)^2}\right\} = \\
&= 1+\frac{4\sum\limits_k p_k \sum\limits_{i=1}^{N}\eta_i^2\epsilon_{i,k}}{\left(\sum\limits_{i=1}^{N}\eta_i\right)^2} \geq 1
\end{aligned} \tag{2.77}$$

Notice that, even if we showed that $|\uparrow\rangle^{\otimes N}$ is a local minimum for $\xi_U^2(\rho)$, it is *not*, in one "non-physical" situation, a stationary point! In fact, *outside the domain* allowed by quantum mechanics and in a neighbourhood of $|\uparrow\rangle^{\otimes N}$, $\xi_U^2\left(\epsilon_{i,k}\right)$ as in eq.2.77 can take values smaller than one. The difference from before is that here the $\epsilon_{i,k}$ are allowed to take negative values, that means that particles can be described by a non physical spin vector longer than one half: $\|\langle\vec{j}_i\rangle\| > \frac{1}{2}$ for some i. For example, take $p_1 = 1$, $\epsilon_{1,1} < 0$ and $\epsilon_{i,k} = 0$ for all k bigger than 2 and $i = 2, ..., N$. Then, supposing the equality in eq.2.76 (that means $\langle J_y\rangle = 0$), we have that the first inequality in eq.2.77 is saturated and thus:

$$\xi_U^2\left(\epsilon_{i,k}\right) = 1+\frac{4\sum\limits_k p_k \sum\limits_{i=1}^{N}\eta_i^2\epsilon_{i,k}}{\left(\sum\limits_{i=1}^{N}\eta_i\right)^2} = 1-\frac{4\sum\limits_k p_k \sum\limits_{i=1}^{N}\eta_i^2|\epsilon_{i,k}|}{\left(\sum\limits_{i=1}^{N}\eta_i\right)^2} < 1 \tag{2.78}$$

This behaviour of our squeezing parameter suggests us how to proceed for finding the derivative of the new squeezing parameter. We want to express $\xi_U^2(\rho)$ in function of only one (class of) variable, namely $\langle j_{z_i}\rangle_k$. We have just seen that when such variables are allowed to vary outside their domain imposed by quantum mechanics, we loose stationary points; this advise us for next substitution:

- Let us rewrite ξ_U^2 substituting $\langle j_{z_i}\rangle_k$ with $\frac{1}{2}\cos\theta_{i,k}$. From eq.2.74 we get:

$$\begin{aligned}
&\xi_U^2(\rho) \overset{\dagger}{\geq} \\
&= \frac{\left(\sum_{i=1}^{N}\eta_i\right)^2}{\sum_{i=1}^{N}\eta_i^2}\frac{\sum_k p_k\sum_{i=1}^{N}\eta_i^2\cos^2\theta_{i,k}}{\left(\sum_k p_k\sum_{i=1}^{N}\eta_i\cos\theta_{i,k}\right)^2}\left\{1+\frac{\sum_k p_k\sum_{i=1}^{N}\eta_i^2\sin^2\theta_{i,k}}{\left(\sum_k p_k\sum_{i=1}^{N}\eta_i\cos\theta_{i,k}\right)^2}\right\} \equiv \quad (2.79)\\
&\equiv \tilde{\xi}_U^2(\{\eta_i\},\{\theta_{i,k}\})
\end{aligned}$$

For obtaining this expression, in the inequality marked with †, we used eq.2.76, that in this context gives:

$$(\Delta j_{x_i})_k^2 = \langle j_{x_i}^2\rangle_k - \langle j_{x_i}\rangle_k^2 = \frac{1}{4} - \langle j_{x_i}\rangle_k^2 \geq \langle j_{z_i}\rangle_k^2 = \frac{1}{4}\cos^2\theta_{i,k} \qquad (2.80)$$

The intervals in which our variables are allowed to vary are clearly $(0,1]$ for the η_i and $[0,\pi]$ for the $\theta_{i,k}$, for all k and $i=1,...,N$. The reason for which the domains of the η_i have to be like these is the same as explained in section 2.1.1, while for the $\theta_{i,k}$, being connected with the spin of particles along the z direction, the boundaries are deriving from quantum mechanics. Here we recall that the function $\tilde{\xi}_U^2(\{\eta_i\},\{\theta_{i,k}\})$ is positive and continuous almost everywhere, being singular in all the points such that $\left(\sum_k p_k\sum_i \eta_i\cos\theta_{i,k}\right)^2 = 0$. There it goes to infinity, so that we already have $0 \leq \tilde{\xi}_U^2(\{\eta_i\},\{\theta_{i,k}\}) \leq \infty$.

Let us now compare the two equations 2.79 and 2.66. The first one is more general, describing a generic separable state, and reduces to the second one in the specific model considered in section 2.2.1. We can now proceed with taking the derivative with respect to one of the $\{\theta_{i,k}\}$, supposing the $\{\eta_i\}$ to be fixed.

- First, let us restrict the domain of the $\theta_{i,k}$ to $[0,\frac{\pi}{2}]$, for all k, $i=1,...,N$. We are allowed to do this, because whenever the variables $\langle j_{z_i}\rangle_k = \frac{1}{2}\cos\theta_{i,k}$ take different signs, we necessarily get an increase of $\tilde{\xi}_U^2(\{\theta_{i,k}\})$. This is a straightforward conclusion we can take from eq. 2.74; the numerator is not affected by these changes of signs, while the denominator necessarily decreases. Moreover, since $\tilde{\xi}_U^2(\{\theta_{i,k}\}) = \tilde{\xi}_U^2(\{-\theta_{i,k}\})$, we can consider for the $\{\theta_{i,k}\}$ only the interval for which $\cos\theta_{i,k} \geq 0$, that exactly is the one we wrote before.

- Now, let us suppose η_i fixed for all $i = 1, ..., N$ and rewrite $\tilde{\xi}^2_U(\{\eta_i\}, \{\theta_{i,k}\})$ using the following substitutions:

$$x(\{\theta_{i,k}\}) \equiv \sum_k p_k \sum_{i=1}^N \eta_i^2 \cos^2\theta_{i,k} > 0 \tag{2.81a}$$

$$y(\{\theta_{i,k}\}) \equiv \left(\sum_k p_k \sum_{i=1}^N \eta_i \cos\theta_{i,k}\right)^2 > 0 \tag{2.81b}$$

$$a \equiv \sum_{i=1}^N \eta_i^2 > 0 \tag{2.81c}$$

$$b \equiv \left(\sum_{i=1}^N \eta_i\right)^2 > 0 \tag{2.81d}$$

where we decided to ignore the cases $x = 0$ and $y = 0$, since the squeezing parameter is singular in such point. All other terms are strictly positive due to their definitions.
Equation 2.79 takes now the form:

$$\tilde{\xi}^2_U(x, y) = \frac{b}{a} x \left(\frac{a - x + y}{y^2}\right), \tag{2.82}$$

where we have to remember that the dependence over the $\{\theta_{i,k}\}$ is kept inside $x(\{\theta_{i,k}\})$ and $y(\{\theta_{i,k}\})$. What we can now easily do is to obtain the derivative of the squeezing parameter with respect to $\theta_{j,l}$:

$$\begin{aligned}\frac{\partial \tilde{\xi}^2_U(\{\theta_{i,k}\})}{\partial\theta_{j,l}} &= \frac{\partial \tilde{\xi}^2_U(x,y)}{\partial x}\frac{\partial x(\{\theta_{i,k}\})}{\partial\theta_{j,l}} + \frac{\partial \tilde{\xi}^2_U(x,y)}{\partial y}\frac{\partial y(\{\theta_{i,k}\})}{\partial\theta_{j,l}} = \\ &= \frac{b}{a}\left\{\underbrace{\frac{a - 2x + y}{y^2}\frac{\partial x}{\partial\theta_{j,l}}}_{\mathcal{A}} + \underbrace{\frac{x(2x - y - 2a)}{y^3}\frac{\partial y}{\partial\theta_{j,l}}}_{\mathcal{B}}\right\}\end{aligned} \tag{2.83}$$

Remember we are looking for the stationary points, that means all the $\{\theta_{i,k}\}$ for which eq.2.83 is null. Now, since $\frac{b}{a}$ is always strictly bigger than zero, this can only be verified if $\mathcal{A} = \mathcal{B} = 0$ *or* $\mathcal{A} = -\mathcal{B}$ for all $\theta_{j,l}$. Let us check, case by case, all the possibilities:

- Starting with the easiest one, $\mathcal{A} = \mathcal{B} = 0$, we get that the two conditions:

$$(a - 2x + y)\frac{\partial x}{\partial\theta_{j,l}} = 0 \tag{2.84a}$$

$$(2x - y - 2a)\frac{\partial y}{\partial\theta_{j,l}} = 0 \tag{2.84b}$$

have to be verified simultaneously for all $\theta_{j,l}$. Here we used the facts that x and y are bigger than zero.

Notice that both equations 2.84a and 2.84b, as products of two terms, can be satisfied in two different ways. With an argument that will be given shortly, it is possible to show that we can rewrite these conditions as:

$$\frac{\partial x}{\partial \theta_{j,l}} = -2p_l\eta_j^2 \cos\theta_{j,l} \sin\theta_{j,l} = 0 \tag{2.85a}$$

$$\frac{\partial y}{\partial \theta_{j,l}} = -2p_l\eta_j \sin\theta_{j,l} \underbrace{\sum_k p_k \sum_{i=1}^{N} \eta_i \cos\theta_{i,k}}_{>0} = -2p_l\eta_j\sqrt{y}\sin\theta_{j,l} = 0 \tag{2.85b}$$

for all $\theta_{j,l}$. It is now easy to conclude that, imposing $\mathcal{A} = \mathcal{B} = 0$, we necessarily must have $\sin\theta_{j,l} = 0$ for all $l, j = 1, ..., N$. In other words, the only separable state satisfying this is the pure state $|\uparrow\rangle^{\otimes^N}$. This is not a surprise, because we already showed that such wave vector identifies a stationary point (and in particular a local minimum) for our new squeezing parameter.

Consider now the two other conditions

$$(a - 2x + y) = 0 \tag{2.86a}$$

$$(2x - y - 2a) = 0, \tag{2.86b}$$

taken from equations 2.84a and 2.84a. We will now prove that, whenever one of them is verified, $\tilde{\xi}_U^2(\{\theta_{i,k}\})$ cannot take values less than one. Let us start by the first one (eq. 2.86a); in this case we would obtain

$$\tilde{\xi}_U^2(x,y) = \frac{b}{a}\frac{x^2}{(2x-a)^2} = \frac{\left(\sum_{i=1}^{N}\eta_i\right)^2}{\sum_{i=1}^{N}\eta_i^2}\left(\frac{\sum_k p_k \sum_{i=1}^{N}\eta_i^2\cos^2\theta_{i,k}}{\sum_k p_k \sum_{i=1}^{N}\eta_i^2\left(\cos^2\theta_{i,k} - \sin^2\theta_{i,k}\right)}\right)^2 \tag{2.87}$$

Now we can notice that, since

$$0 \leq \sum_k p_k \left(\sum_{i=1}^{N}\eta_i\cos\theta_{i,k}\right)^2 = y = 2x - a = \sum_k p_k \sum_{i=1}^{N}\eta_i^2\left(\cos^2\theta_{i,k} - \sin^2\theta_{i,k}\right), \tag{2.88}$$

we necessarily have that $0 \leq \sum_k p_k \sum_{i=1}^{N} \eta_i^2 \left(\cos^2\theta_{i,k} - \sin^2\theta_{i,k}\right) \leq \sum_k p_k \sum_{i=1}^{N} \eta_i^2 \cos^2\theta_{i,k}$, so that, in conclusion:

$$\tilde{\xi}_U^2(x,y) = \frac{\left(\sum_{i=1}^{N}\eta_i\right)^2}{\sum_{i=1}^{N}\eta_i^2}\left(\frac{\sum_k p_k \sum_{i=1}^{N}\eta_i^2\cos^2\theta_{i,k}}{\sum_k p_k \sum_{i=1}^{N}\eta_i^2\left(\cos^2\theta_{i,k}-\sin^2\theta_{i,k}\right)}\right)^2 \geq \frac{\left(\sum_{i=1}^{N}\eta_i\right)^2}{\sum_{i=1}^{N}\eta_i^2} \geq 1 \tag{2.89}$$

If we now look at eq.2.86b,we easily obtain that there exists no possible choice of the angles $\{\theta_{i,k}\}$ for satisfying $2x - y - 2a = 0$ (i.e.: $2(x-a) = y$). In fact, this equation can be read as

$$0 > -2\sum_k p_k \sum_{i=1}^{N}\eta_i^2\cos^2\theta_{i,k} = 2(x-a) = y = \left(\sum_k p_k \sum_{i=1}^{N}\eta_i\cos\theta_{i,k}\right)^2 > 0, \tag{2.90}$$

that is clearly impossible.

- Let us now consider the hardest case, in which we have $\mathcal{A} + \mathcal{B} = 0$ in eq.2.83. Writing explicitly derivatives $\frac{\partial x}{\partial\theta_{j,l}}$ and $\frac{\partial y}{\partial\theta_{j,l}}$ we can get that

$$\frac{\partial\tilde{\xi}_U^2}{\partial\theta_{j,l}} = -\frac{2p_l\eta_j\sin\theta_{j,l}}{y^2}\frac{b}{a}\left((a-2x+y)\,\eta_j\cos\theta_{j,l} + \frac{x(2x-y-2a)}{\sqrt{y}}\right) = 0. \tag{2.91}$$

Since we excluded the cases in which $a - 2x + y = 0$ and $2x - y - 2a = 0$ (for the reasons explained above), the only possible way for obtaining the equality is to have satisfied one of the two conditions

$$\sin\theta_{j,l} = 0 \tag{2.92a}$$

$$\eta_j\cos\theta_{j,l} = \frac{x}{\sqrt{y}}\frac{2x-y-2a}{2x-y-a} \tag{2.92b}$$

for all l, $j = 1, ..., N$.

Now, if eq.2.92a is always verified, we reduce to the case above. Thus, we can restrict ourselves to study the other two cases allowed by previous equations. The first one is given by eq.2.92b satisfied for all l, $j = 1, ..., N$; while the second one by eq.2.92a satisfied for some indices and eq.2.92b for all the others.

In particular, it is possible to prove that the previous one gives no solution, while the last one can provide the global minimum of the function (depending on the coefficients $\vec{\eta}$). However, since such minimum is very hard to be found, we will restrict ourselves to eq.2.92b only, in a way that will be clear in the following.

- Suppose that eq.2.92b is valid for all l, $j = 1, ..., N$. It is possible to see that, as consequence, we need the condition $\eta_j\cos\theta_{j,l} = \lambda$ (being $0 < \lambda \leq 1$ a real

number) to be verified for all l, $j = 1, ..., N$. In fact eq.2.92b, once we substitute the corresponding expressions for $x(\{\theta_{i,k}\})$, $y(\{\theta_{i,k}\})$, a and b, reads:

$$\eta_j \cos\theta_{j,l} = \frac{\sum_k p_k \sum_{i=1}^{N} \eta_i^2 \cos^2\theta_{i,k}}{\sum_k p_k \sum_{i=1}^{N} \eta_i \cos\theta_{i,k}} \times \\ \times \left\{ \frac{2\sum_k p_k \sum_{i=1}^{N} \eta_i^2 \cos^2\theta_{i,k} - \left(\sum_k p_k \sum_{i=1}^{N} \eta_i \cos\theta_{i,k}\right)^2 - 2\sum_{i=1}^{N} \eta_i^2}{2\sum_k p_k \sum_{i=1}^{N} \eta_i^2 \cos^2\theta_{i,k} - \left(\sum_k p_k \sum_{i=1}^{N} \eta_i \cos\theta_{i,k}\right)^2 - \sum_{i=1}^{N} \eta_i^2} \right\} \tag{2.93}$$

Now, since we get exactly the same equation for all l, $j = 1, ..., N$, we can conclude that the only possible way for eq.2.93 to be verified is that $\eta_j \cos\theta_{j,l} = \lambda$, for some real λ between zero and one, as said before.

However, this is *not* a stationary point; in fact, if we impose this constraint to eq.2.93, we would get (Remember $\sum_k p_k = 1$):

$$\lambda = \frac{N\lambda^2}{N\lambda} \left\{ \frac{2N\lambda - (N\lambda)^2 - 2\sum_{i=1}^{N} \eta_i^2}{2N\lambda - (N\lambda)^2 - \sum_{i=1}^{N} \eta_i^2} \right\}, \tag{2.94}$$

that after simple algebraical passages becomes equivalent to the equation

$$\sum_{i=1}^{N} \eta_i^2 = 0, \tag{2.95}$$

that clearly is impossible, due to the restrictions we have over $\vec{\eta}$. Notice we decided to neglect the case $\lambda = 0$, since in such case the function $\tilde{\xi}_U^2(x, y)$ is not well defined and approaches infinite.

- Therefore the only possibility for having some stationary point in which $\tilde{\xi}_U^2$ takes values smaller than one is in the mixed situation in which both equations 2.92a and 2.92b are satisfied, one over some indices and the other over all others. However, since this case is particularly hard to be treated, we will restrict ourself to the previous one, where all contributes $\eta_j \cos\theta_{j,l}$ are the same and given by λ. In fact, even if this is not a stationary point, and thus a (global) minimum, we can prove that for the appropriate choice of the coefficients $\vec{\eta}$, it takes the new squeezing parameter to values they are smaller than one.

  For the sake of completeness, we add that a minimum can be found putting, for example, $\eta_1 = 1$, $\eta_i = x$ for $i = 2, ..., N$, $\theta_{1,k} = y$ for all k and $\theta_{i,k} = 0$ for all k, $i = 2, ..., N$. Here both x and y are allowed to vary between zero and one, but will

turn out that the minimum is reached for a very small (but not null) value of x and a y that approaches (but never equals) $\frac{\pi}{2}$.

Before proceeding, let us summarize what we just obtained. At first, we get an expression for the new squeezing parameter $\xi_U^2(\rho)$ when we are dealing with separable states described by a density matrix ρ. Subsequently, we were able to find a lower bound for it that we called $\tilde{\xi}_U^2(\rho)$, and expressed this new function using the substitution $\langle j_{z_i}\rangle_k \to \frac{1}{2}\cos\theta_{i,k}$. This way, we restricted ourselves to remain in the boundaries imposed by quantum mechanics, and at the same time we obtained a periodic function $\tilde{\xi}_U^2(\{\theta_{i,k}\})$ in the variables $\{\theta_{i,k}\}$. Due to its periodicity, positivity and continuity considerations, we can deduce that the minimum of this function lies in one of its stationary points. One of these is the state $|\uparrow\rangle^{\otimes^N}$, for which $\tilde{\xi}_U^2\left(|\uparrow\rangle^{\otimes^N}\right) = 1$, while the others are hard to find exactly. However we suspect that one is *not* the lower bound of $\tilde{\xi}_U^2$! This will be shown in the following section, where we will prove, using our champion state for which all $\eta_i\cos\theta_{i,k}$ equals λ, that $\tilde{\xi}_U^2 \ll 1$ for a proper choice of $\vec{\eta}$.

2.2.2.3 A formal proof that $\xi_U^2 \ll 1$

As said right before, let us consider the state characterized by

$$\eta_i\cos\theta_{i,k} = \lambda \quad \text{for all } k,\ i = 1, ..., N, \tag{2.96}$$

where $0 < \lambda \leq 1$. This state does not identify a minimum, but will approach to for an intelligent choice of the coefficients $\{\eta_i\}$.
As a consequence of eq.2.96, we can rewrite $\tilde{\xi}_U^2(\{\theta_{i,k}\},\{\eta_i\})$ as (see eq.2.79):

$$\tilde{\xi}_U^2(\vec{\eta},\lambda) = \frac{\left(\sum_{i=1}^N \eta_i\right)^2}{\sum_{i=1}^N \eta_i^2}\frac{1}{N}\left\{1 + \frac{\sum_{i=1}^N \eta_i^2}{N^2\lambda^2} - \frac{1}{N}\right\} \tag{2.97}$$

Before determining explicitly the value of this function, we need to perform a little step further. Namely, find λ for which $\tilde{\xi}_U^2$ takes the smallest possible value. This goal is obviously reached with the biggest λ, that we supposed to be 1. But notice that λ is *not* independent from the $\{\eta_i\}$; in fact it has to take some value that can be reached by *all* the product terms $\eta_i\cos\theta_{i,k}$! Now, since the cosine is limited upward by unity, it is easy to see that the actual boundary in which λ is allowed to vary is $\left(0, \min_{i=1,...,N}\{\eta_i\}\right]$. Thus, supposing the minimum of the coefficients η_i is $\eta_l \equiv \min_{i=1,...,N}\{\eta_i\}$, we finally get

that eq.2.97 becomes

$$\tilde{\xi}_U^2(\vec{\eta},\lambda) = \frac{\left(\sum_{i=1}^{N}\eta_i\right)^2}{\sum_{i=1}^{N}\eta_i^2}\frac{1}{N}\left\{1+\frac{\sum_{i=1}^{N}\eta_i^2}{N^2\eta_l^2}-\frac{1}{N}\right\} \tag{2.98}$$

In the following we will introduce a model, inspired by the experimental physics but efficient and intelligent for what is our purpose as well, for the description of the η_i's. This way we can prove not only that $\tilde{\xi}_U^2$ can take values smaller than one, but also that this happens in the ordinary laboratory life.

Suppose we have N atoms, each one associated with a coefficient η_i, in a two dimensional box of width L. Now, in practice, the particles inside it are trapped with some appropriate (electrical) potential, but for simplicity we will assume that they are uniformly distributed inside the box. Moreover we imagine the laser runs in the middle of the box, hitting it in $\frac{L}{2}$, as it is possible to see in the following picture:

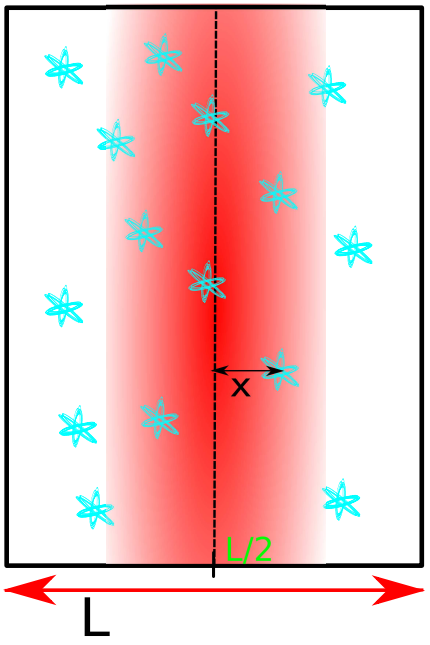

FIGURE 2.3: Experimental setup made by a box of width L, hit by a Gaussian laser in its middle. The particles' distribution is uniform in the box; the quantity of interest is the atomic distance from the symmetry axis of the beam

Since we are interested in how much such laser hits the particles, we want to know at which distance from the axis of the beam the atoms lie. Of course, as follows from our hypothesis, the probability distribution $\tilde{p}(x)$ describing the position x of any atom

with respect to such axis is constant, and in particular equals $\frac{1}{L}$:

$$\tilde{p}(x) = \begin{cases} 0 & \text{if } |x| > L \\ \frac{1}{L} & \text{if } |x| \leq L \end{cases} \tag{2.99}$$

At this point we have to assign to these particles the coefficients η_i, that have to be strictly bigger than zero and less or equal to one. We can try to describe the laser intensity with a Gaussian function, peaked in the middle of the box and decreasing towards it. According to this model, given an atom in x, its coefficient η would be

$$\eta(x) = e^{-\frac{x^2}{\alpha^2}}, \tag{2.100}$$

where α is a positive real parameter describing the Gaussian. Which is the probability distribution function $p(\eta)$ for the coefficient η? As it is possible to see from the following figure,

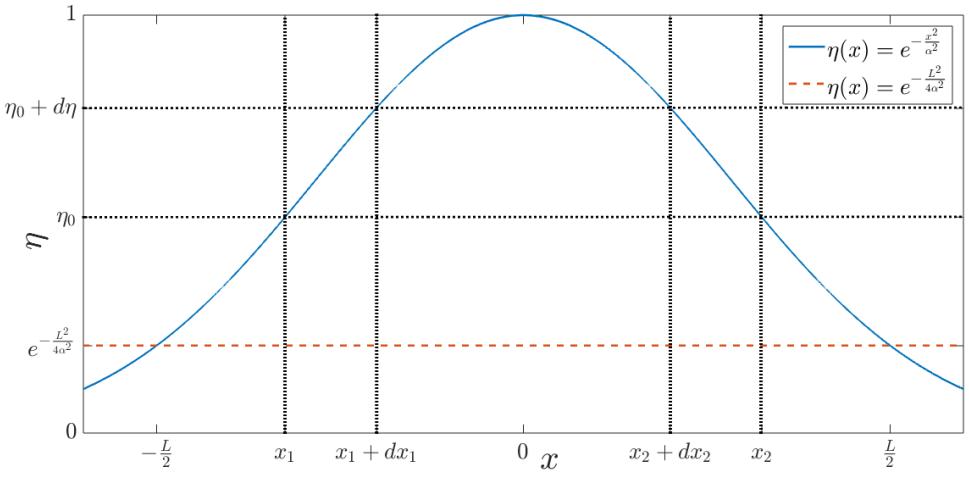

FIGURE 2.4: Gaussian function $\eta(x) = e^{-\frac{x^2}{\alpha^2}}$, for $\alpha = 0.4$. Here we also supposed $L = 1$, that changes the limits between x is allowed to vary ($x \in \left[-\frac{L}{2}, \frac{L}{2}\right]$), but does not affect the shape of the function $\eta(x)$

we have that η is included between η_0 and $\eta_0 + d\eta$ whenever the atom finds itself between x_1 and $x_1 + dx_1$ *or* x_2 and $x_2 + dx_2$. Here dx_1 is positive and dx_2 negative. In other words:

$$p(\eta)d\eta = \tilde{p}(x_1)dx_1 - \tilde{p}(x_2)dx_2 = 2\tilde{p}(x_1)dx_1 = \frac{2}{L}dx_1, \tag{2.101}$$

where we used symmetry of both the Gaussian function and $\tilde{p}(x)$ about the centre; we arbitrarily decided to keep x_1 instead of x_2. Notice that, as it is clear from Fig.2.4, $dx_1 = -dx_2$.

It is important to point out that, due to the restrictions over x, η is allowed to vary in the range $\left[e^{-\frac{1}{4\nu^2}}, 1\right]$, being ν the positive parameter defined by $\nu = \frac{\alpha}{L}$.
Now we are capable to obtain the probability distribution function $p(\eta)$; in fact, from eq.2.101, we obtain that:

$$p(\eta) = \frac{2}{L}\frac{dx_1}{d\eta} = -\frac{2}{L}\frac{dx_2}{d\eta}. \tag{2.102}$$

The inverse function that gives x depending on η is

$$x(\eta) = \begin{cases} \sqrt{-\alpha^2 \log(\eta)} = x_2(\eta) & \text{if } x \text{ is positive, } e^{-\frac{1}{4\nu^2}} \leq \eta \leq 1 \\ -\sqrt{-\alpha^2 \log(\eta)} = x_1(\eta) & \text{if } x \text{ is negative, } e^{-\frac{1}{4\nu^2}} \leq \eta \leq 1 \end{cases} \tag{2.103}$$

We can now take the derivatives of x_1 and x_2 with respect to η and obtain

$$\frac{dx_1}{d\eta} = \frac{\alpha}{2\eta\sqrt{-\log(\eta)}} = -\frac{dx_2}{d\eta}, \tag{2.104}$$

so that, in conclusion:

$$p(\eta) = \begin{cases} \frac{\nu}{\eta\sqrt{-\log(\eta)}} & \text{if } e^{-\frac{1}{4\nu^2}} \leq \eta \leq 1 \\ 0 & \text{if } \eta < e^{-\frac{1}{4\nu^2}} \text{ or } 1 < \eta. \end{cases} \tag{2.105}$$

We remember here that L represents the width of the box in which the particles lie, α is the parameter describing the Gaussian function (and henceforth the laser), and $\nu = \frac{\alpha}{L}$.
We want to remark that $p(\eta)$ is, indeed, a good definition for a probability distribution function; we can easily check the normalization by

$$\int_{-\infty}^{\infty} p(\eta)d\eta = \int_{e^{-\frac{1}{4\nu^2}}}^{1} \frac{\nu}{\eta\sqrt{-\log(\eta)}}d\eta = 1. \tag{2.106}$$

At this point, since it will become useful later, let us derive the probability distribution function $p(\eta^2)$ for η^2. It is just a matter of following the same steps as before; the only difference is that here the Gaussian function we used in eq.2.100 is elevated to the square:

$$\eta^2(x) = \left(e^{-\frac{x^2}{\alpha^2}}\right)^2 = e^{-\frac{2x^2}{\alpha^2}}. \tag{2.107}$$

This allows η^2 to vary in the bigger interval $\left[e^{-\frac{1}{2\nu^2}}, 1\right]$ and thus takes us to

$$p(\eta^2) = \begin{cases} \frac{\nu}{\eta^2\sqrt{-2\log(\eta^2)}} & \text{if } e^{-\frac{1}{2\nu^2}} \leq \eta \leq 1 \\ 0 & \text{if } \eta < e^{-\frac{1}{2\nu^2}} \text{ or } 1 < \eta. \end{cases} \tag{2.108}$$

Having the probability distribution functions for both η and η^2 it is now easy to determine the expected values $\bar{\eta}$ and $\bar{\eta^2}$:

$$\bar{\eta} = \int_{-\infty}^{\infty} \eta p(\eta) d\eta = \nu \int_{e^{-\frac{1}{4\nu^2}}}^{1} \frac{d\eta}{\sqrt{-\log \eta}} = \sqrt{\pi}\nu \operatorname{erf}\left(\frac{1}{2\nu}\right) \tag{2.109a}$$

$$\bar{\eta^2} = \int_{-\infty}^{\infty} \eta^2 p(\eta^2) d\eta^2 = \nu \int_{e^{-\frac{1}{2\nu^2}}}^{1} \frac{d\eta^2}{\sqrt{-2\log \eta^2}} = \sqrt{\frac{\pi}{2}}\nu \operatorname{erf}\left(\frac{1}{\sqrt{2}\nu}\right), \tag{2.109b}$$

where $\operatorname{erf}(x)$ is the error function

$$\operatorname{erf}(x) = \frac{2}{\sqrt{\pi}} \int_0^x e^{-t^2} dt \tag{2.110}$$

So we have now all the ingredients to test our new squeezing parameter and show how it fails. This can be done directly by generating random coefficients $\{\eta_i\}$ according to eq.2.105, or more analytically using the central limit theorem:

Theorem 1. *Let* $\{X_1, X_2, ...\}$ *be a sequence of independent and identically distributed random variables, and define the sample average*

$$S_N(X_i) = \frac{\sum_{i=1}^{N} X_i}{N}. \tag{2.111}$$

Moreover, suppose these random variables have expected value and variance respectively given by $E[X_i] = \bar{X}_i$ *and* $Var[X_i] = \sigma^2$*. Then as* N *approaches infinity, the random variables* $(S_N(X_i) - \mu)$ *converge in distribution to the normal that has null average and variance given by* $N \cdot \sigma^2$*.*

In fact, looking at eq.2.98, we are now able to estimate all terms in the right hand side. First, let us take $\eta_l = e^{-\frac{1}{4\nu^2}}$, that is a good approximation for the lowest possible coefficient $\eta_l = \min_{i=1,..,N} \eta_i$. In particular, $e^{-\frac{1}{4\nu^2}}$ approaches η_l from below, that is an essential characteristic for λ, as we have seen before ($0 \leq \lambda \leq \eta_l$).
Let us look more properly into the sums $\sum_{i=1}^{N} \eta_i$ and $\sum_{i=1}^{N} \eta_i^2$. *If* we suppose all the coefficients η_i to be independent one from the other, then we can consider them as independent and identically distributed random variables. Then we are satisfying hypotheses

of theorem 1 and can conclude that, as N approaches infinity,

$$S_N(\eta) - \bar{\eta} = \frac{\sum_{i=1}^{N} \eta_i}{N} - \bar{\eta} \to 0 \tag{2.112a}$$

$$S_N(\eta^2) - \bar{\eta^2} = \frac{\sum_{i=1}^{N} \eta_i^2}{N} - \bar{\eta^2} \to 0 \tag{2.112b}$$

In other words, slightly modifying these last two equations and supposing the equality to zero:

$$\sum_{i=1}^{N} \eta_i = N\bar{\eta} \tag{2.113a}$$

$$\sum_{i=1}^{N} \eta_i^2 = N\bar{\eta^2} \tag{2.113b}$$

We can now put these last results in equation 2.98, and obtain a function depending only on the number of particles N and on the fraction $\nu = \frac{\alpha}{L}$:

$$\begin{aligned} \tilde{\xi}_U^2(\nu, N) &= \frac{(N\bar{\eta})^2}{N\bar{\eta^2}} \frac{1}{N} \left\{ 1 + \frac{N\bar{\eta^2}}{N^2 e^{-\frac{1}{2\nu^2}}} - \frac{1}{N} \right\} = \\ &= \frac{\sqrt{2\pi}\nu \operatorname{erf}^2\left(\frac{1}{2\nu}\right)}{\operatorname{erf}\left(\frac{1}{\sqrt{2}\nu}\right)} \left\{ 1 + \frac{\sqrt{\pi}\nu \operatorname{erf}\left(\frac{1}{\sqrt{2}\nu}\right)}{\sqrt{2} N e^{-\frac{1}{2\nu^2}}} - \frac{1}{N} \right\} \end{aligned} \tag{2.114}$$

We can now plot this function, in order to see how it behaves:

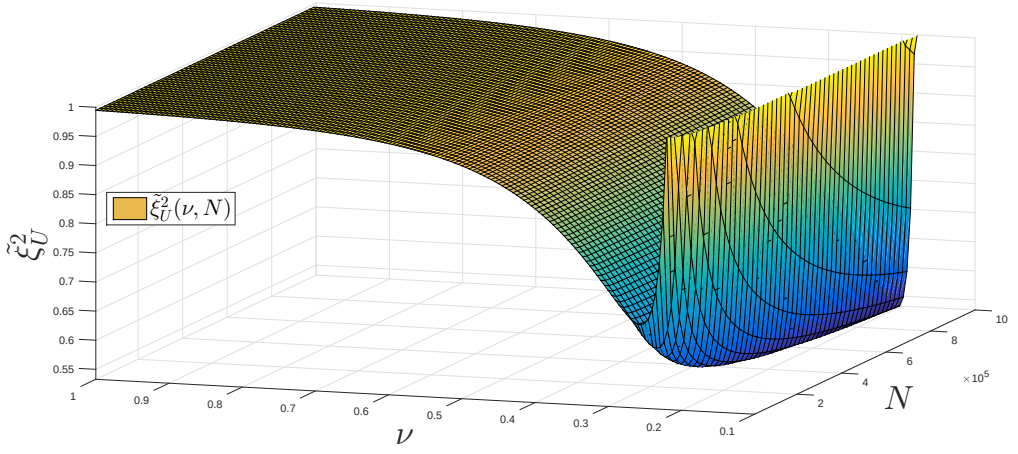

FIGURE 2.5: Plot of the function $\tilde{\xi}_U^2(\nu, N)$, obtained using eq.2.114

As it is possible to see, $\tilde{\xi}_U^2(\nu, N)$ becomes smaller than one in almost all the chosen domain. In fact, except for very small values of ν, whenever N is big enough $\tilde{\xi}_U^2(\nu, N) < 1$

always.

Let us look a little more in detail to the properties of $\tilde{\xi}^2_U(\nu, N)$:

- In the limit $\nu \to 0$ we obviously have (from the definition of the error function) that

$$\operatorname{erf}\left(\frac{1}{2\nu}\right) \to 1 \tag{2.115a}$$

$$\operatorname{erf}\left(\frac{1}{\sqrt{2}\nu}\right) \to 1, \tag{2.115b}$$

  so that

$$\tilde{\xi}^2_U(\nu \to 0, N) \simeq \sqrt{2\pi}\nu \left\{1 + \frac{\sqrt{\pi}\nu e^{\frac{1}{2\nu^2}}}{\sqrt{2}N} - \frac{1}{N}\right\} \to \infty \tag{2.116}$$

  for N fixed. This is not really surprising, since we modified the squeezing parameter ξ^2 with the factor $\frac{\langle S_z^2\rangle}{\langle S_z\rangle^2}$ for avoiding the bad behaviour of ξ^2 whenever we had few η_i much bigger than all the others (like here). What we did not expect, is that it is still possible, for ξ^2_U, to take values smaller than one, as showed by Fig.2.5.

- In the limit $\nu \to \infty$ we can rewrite the error function $\operatorname{erf}(x)$ using its series expansion:

$$\operatorname{erf}(x) = \frac{2}{\sqrt{\pi}} \sum_{n=0}^{\infty} \frac{(-1)^n x^{2n+1}}{n!(2n+1)} \underset{x\to 0}{\simeq} \frac{2}{\sqrt{\pi}} x \tag{2.117}$$

  Putting eq.2.117 in eq.2.114 we can now obtain that

$$\tilde{\xi}^2_U(\nu \to \infty, N) \simeq 1 - \frac{1}{N} + \frac{1}{N} = 1, \tag{2.118}$$

  in concordance with Fig.2.5. This tells us that, taking the coefficients $\{\eta_i\}$ distributed according to $p(\eta)$ and assuming $\eta_i \cos\theta_{i,k} = \lambda$ for all k, $i = 1, ..., N$, it is actually easy to obtain a value for $\tilde{\xi}^2_U$ that is smaller than one.
  How much smaller? This is the next and final step we will do in this section, where we will derive $\tilde{\xi}^2_U(\nu, N)$ with respect to ν and N, in order to discover where is the global minimum of the function.

Let us go back to eq.2.114. In order to discover its minimum, let us derive it, first with respect to N and subsequently to ν.

$$\frac{\partial \tilde{\xi}^2_U(\nu, N)}{\partial N} = -\frac{1}{N^2}\left[\underbrace{\frac{\sqrt{2\pi}\nu \operatorname{erf}^2\left(\frac{1}{2\nu}\right)}{\operatorname{erf}\left(\frac{1}{\sqrt{2}\nu}\right)}}_{\mathcal{A}} \underbrace{\left(\frac{\sqrt{\pi}\nu \operatorname{erf}\left(\frac{1}{\sqrt{2}\nu}\right)}{\sqrt{2}e^{-\frac{1}{2\nu^2}}} - 1\right)}_{\mathcal{B}}\right] \tag{2.119}$$

Let us now point out that both terms $\mathcal{A}$ and $\mathcal{B}$ are bigger than zero, the first one as a consequence of the positivity of the error function in the considered domain ($\nu \geq 0$), while for the second it follows from a little more accurate analysis we don't report here. As a consequence of the positivity of $\mathcal{A}$, $\mathcal{B}$ and N^2 we can conclude that the derivative $\frac{\partial \tilde{\xi}^2_U(\nu,N)}{\partial N}$ is negative everywhere, and thus that $\tilde{\xi}^2_U(\nu, N)$ decreases whenever N increases. Conversely, once we focus our attention on ν, we are able to find a stationary point that is a minimum as well. This can be qualitatively deduced analysing the plot in Fig.2.5, where is clear that, once we fixed $N \gg 1$, there exists a value of ν that minimizes the function. Let us write the derivative with respect to ν:

$$\begin{aligned}\frac{\partial \tilde{\xi}^2_U(\nu,N)}{\partial \nu} &= \frac{e^{-\frac{1}{2\nu^2}}\operatorname{erf}\left(\frac{1}{2\nu}\right)}{N\nu\operatorname{erf}^2\left(\frac{1}{\sqrt{2}\nu}\right)}\times \\ &\times\left\{-2e^{-\frac{1}{4\nu^2}}\operatorname{erf}\left(\frac{1}{\sqrt{2}\nu}\right)\left[\sqrt{2}(N-1)+e^{\frac{1}{2\nu^2}}\sqrt{\pi}\nu\operatorname{erf}\left(\frac{1}{\sqrt{2}\nu}\right)\right]+\operatorname{erf}\left(\frac{1}{2\nu}\right)\times\right. \\ &\left.\times\left[2(N-1)+e^{\frac{1}{2\nu^2}}(N-1)\sqrt{2\pi}\nu\operatorname{erf}\left(\frac{1}{\sqrt{2}\nu}\right)+e^{\frac{1}{\nu^2}}\pi(2\nu^2-1)\operatorname{erf}^2\left(\frac{1}{\sqrt{2}\nu}\right)\right]\right\}\end{aligned} \tag{2.120}$$

Whatever it means, we can ask a calculator to solve it numerically in a positive neighbourhood of zero (where we think the minimum lies), and obtain the approximate value ν_{Min} that minimizes the function $\tilde{\xi}^2_U(\nu, N)$ whenever N is fixed. In the following Fig.2.6, we plotted the function $\tilde{\xi}^2_U(\nu = \nu_{Min}, N)$, that represents the minimum value that our squeezing parameter can reach in the used hypotheses and with N fixed.

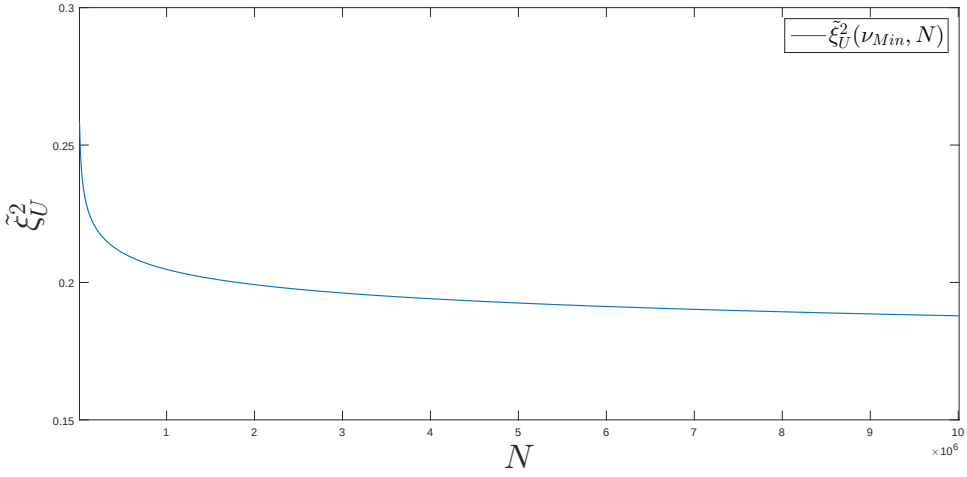

FIGURE 2.6: Plot of the function $\tilde{\xi}^2_U(\nu_{Min}, N)$

We would like to make a last comment before passing to the next argument. More

in detail, we want to show that $\tilde{\xi}_U^2(\nu, N) \to 0$ asymptotically. Let us rewrite the function

$$\tilde{\xi}_U^2(\nu, N) = \underbrace{\frac{\sqrt{2\pi}\nu \operatorname{erf}^2\left(\frac{1}{2\nu}\right)}{\operatorname{erf}\left(\frac{1}{\sqrt{2}\nu}\right)}}_{\mathcal{C}} \underbrace{\left\{1 + \frac{\sqrt{\pi}\nu \operatorname{erf}\left(\frac{1}{\sqrt{2}\nu}\right)}{\sqrt{2}Ne^{-\frac{1}{2\nu^2}}} - \frac{1}{N}\right\}}_{\mathcal{D}}, \tag{2.121}$$

putting in evidence the two factors $\mathcal{C}$ and $\mathcal{D}$. If we now study these two terms in some limits of interest, we get that

$$\mathcal{D} = 1 + \frac{\sqrt{\pi}\nu \operatorname{erf}\left(\frac{1}{\sqrt{2}\nu}\right)}{\sqrt{2}Ne^{-\frac{1}{2\nu^2}}} - \frac{1}{N} \underset{N\to\infty}{\to} 1, \tag{2.122}$$

while for $\mathcal{C}$ we obtain

$$\mathcal{C} = \frac{\sqrt{2\pi}\nu \operatorname{erf}^2\left(\frac{1}{2\nu}\right)}{\operatorname{erf}\left(\frac{1}{\sqrt{2}\nu}\right)} \underset{\nu\to 0}{\simeq} \sqrt{2\pi}\nu \to 0. \tag{2.123}$$

The limit $\nu \to 0$ has been studied before, in eq.2.116, where we proved that $\tilde{\xi}_U^2(\nu \to 0, N) \to \infty$ for a fixed N. But if we look at eq.2.121 more carefully, we notice that letting $\nu \to 0$ *and* $N \gg e^{\frac{1}{2\nu^2}}$, we restrict ourselves in the case in which eq.2.122 and 2.123 are both satisfied, so that in conclusion

$$\tilde{\xi}_U^2(\nu, N) \underset{\substack{\nu\to 0 \\ N\gg e^{\frac{1}{2\nu^2}}}}{\longrightarrow} 0 \tag{2.124}$$

Chapter 3

How we detect entanglement?

Let us briefly summarize what we obtained in chapter 2. We started with the commonly used definition of the squeezing parameter ξ_R^2, as introduced by Wineland et al. in [18] and we showed that, generalizing the measurement operator to the "weighted" one $\vec{S}$ (see eq.2.1), it is possible to obtain values for ξ_N^2 smaller than one for separable states. In particular, we introduced a model for which $\xi_N^2 \to \frac{2}{N}$, pointing out the difficulty, during the experiments, to find out if a particular state is entangled or not. Subsequently, we tried to generalize the squeezing parameter, introducing the factor $\frac{\langle S_z^2 \rangle}{\langle S_z \rangle^2}$, that was supposed to correct the bad behaviour and to recover the useful inequality $\xi_U^2 \geq 1$ for separable states. But, after having accurately studied ξ_U^2, we proved that this parameter can approach the null value under some (more strict) hypotheses as well. Therefore we decide to take a step back and study the relations between $\langle S_z \rangle$ and $(\Delta S_x)^2$, using a slightly modified version of the Lagrange multiplier method, as done before by Anders Sørensen in [37].

More in the details, at first we will use the model introduced in section 2.2.2.3, for obtaining a first plot of $(\Delta S_x)^2$ with respect to $\langle S_z \rangle$. Later on, we will give the general results derived supposing the coefficients $\{\eta_i\}$ are following a generic probability distribution. As final step, we will consider the cases in which the number of particles is not fixed, but can vary during time, and the one where the coefficients $\{\eta_i\}$ are allowed to change during the experiment.

3.1 A practical approach

3.1.1 The Lagrange multiplier method

The Lagrange multiplier method (in its easiest version) is usually used for determining the minima of a function $f(x)$ under some given boundary $g(x) = 0$. The procedure consists of defining

$$\Gamma(x, \mu) = f(x) + \mu g(x) \tag{3.1}$$

and to impose the constraint

$$\frac{\partial \Gamma(x, \mu)}{\partial \mu} = 0, \tag{3.2}$$

that is equivalent to the boundary $g(x) = 0$. Finding the minima for $\Gamma(x, \mu)$ is now equivalent to finding the ones for $f(x)$ along $g(x) = 0$. The parameter μ is referred in the literature as "Lagrange multiplier".
As said above, we will use a slightly modified version; instead of $f(x)$ and $g(x)$ we will use $(\Delta S_x)^2$ and $\langle S_z \rangle$, so that

$$\Gamma = (\Delta S_x)^2 - \mu \langle S_z \rangle, \tag{3.3}$$

where we decided to change the arbitrary sign of μ for convenience.
Here the biggest difference from the ordinary method is that $\langle S_z \rangle$ is not considered a boundary, and is allowed to take values different than zero. As consequence, we do not impose the constraint $\frac{\partial \Gamma}{\partial \mu} = 0$ any more, but still we want to minimize Γ with respect to $(\Delta S_x)^2$ and $\langle S_z \rangle$. In fact, once we find the minimum possible value Γ_{Min} of Γ, we have that:

$$(\Delta S_x)^2 = \Gamma + \mu \langle S_z \rangle \geq \Gamma_{Min} + \mu \langle S_z \rangle, \tag{3.4}$$

that identifies the lowest bound for $(\Delta S_x)^2$ we were aiming for. Now, if both $(\Delta S_x)^2$ and $\langle S_z \rangle$ are determined using a generic separable state, we must conclude that the limit pointed out in eq.3.4 has to be the uncrossable lowest bound characterizing all such states. But this is exactly what we want: a sufficient condition for discriminating if the wave vector describing the system is entangled or not! In fact, whenever we obtain experimental values of $(\Delta S_x)^2$ and $\langle S_z \rangle$ that lie below the curve plotted using eq.3.4, we can deduce immediately that the system is entangled.

In the following, we will give an example which is experimentally feasible, to explain the procedure laid out in the above paragraph. Later we will deduce the general procedure for getting the curve defining the lowest limit reachable by the considered state.

3.1.2 A useful example

Let us consider the experimental situation we introduced in section 2.2.2.3, where we derived a simple model describing the coefficients $\{\eta_i\}$. This has to be the starting point for our analysis, since, as we have seen, both $(\Delta S_x)^2$ and $\langle S_z \rangle$ are depending on these coefficients, and any estimate of such quantities needs to have some clue about the $\{\eta_i\}$. The main results we will use here are given by eq.2.105 and 2.108, together with eq.2.109a and 2.109b; essentially the probability distributions $p(\eta)$ and $p(\eta^2)$ with associated averages. Moreover, let us recall that, for a generic separable state described by a density matrix ρ as in eq.2.67, we have:

$$(\Delta S_x)^2 = \frac{1}{4} \sum_k p_k \sum_{i=1}^{N} \eta_i^2 \cos^2 \theta_{i,k} \tag{3.5a}$$

$$\langle S_z \rangle = \frac{1}{2} \sum_k p_k \sum_{i=1}^{N} \eta_i \cos \theta_{i,k}, \tag{3.5b}$$

as derived in equations 2.70 and 2.71. We performed the substitution $\langle j_{z_i} \rangle_k \to \frac{1}{2} \cos \theta_{i,k}$, with the $\theta_{i,k}$'s being inside the interval $[0, \pi]$. To be precise, eq.3.5a is *not* an equality, but an inequality, being the term in the left hand side bigger or equal to the one in the right. However, since we are interested in minimizing it, we will ignore this fact and suppose the inequality is saturated. As we have seen before, this is equivalent to the supposition $\langle j_{y_i} \rangle_k = 0$ for all k, $i = 1, ..., N$.

For simplifying the following calculations, we will restrict the domain of the $\theta_{i,k}$'s to the interval $\left[0, \frac{\pi}{2}\right]$. This does not affect the research of the minimum possible value of $(\Delta S_x)^2$ for a given $\langle S_z \rangle$, since allowing $\cos \theta_{i,k}$ to change sign does not alter $(\Delta S_x)^2$, but only $\langle S_z \rangle$, that could reach smaller values. It follows that to the same variance would be associated a smaller spin along z; consequently we can deduce that every lowest value of $(\Delta S_x)^2$ associated to some $\langle S_z \rangle$ is obtained with the cosines having the same sign. For the above choice of domains for the $\theta_{i,k}$'s, we can restrict the interval in which μ is allowed to vary as well. A priori, since we do not have any hypothesis about this variable, we have that $\mu \in (-\infty, \infty)$; but once we look at eq.3.3 we can guess that the minimum of Γ is reached for positive μ. In fact, since $\langle S_z \rangle$ can only take positive values (due to the restriction of the interval in which the $\theta_{i,k}$'s are allowed to vary), a negative μ can only increase the value of Γ.

At this point, it is just a matter of following the Lagrange (modified) method, as explained before; so let us introduce the function to be minimized:

$$\Gamma(\{\eta_i\},\{\theta_{i,k}\},\mu) = (\Delta S_x)^2 - \mu\langle S_z\rangle = \frac{1}{4}\sum_k p_k \sum_{i=1}^{N} \eta_i^2 \cos^2\theta_{i,k} - \frac{\mu}{2}\sum_k p_k \sum_{i=1}^{N} \eta_i \cos\theta_{i,k}. \tag{3.6}$$

Let us, for instance, fix the $\{\eta_i\}$ and μ. Thus we have that $\Gamma(\{\theta_{i,k}\})$ is a continuous and periodic function in all the variables $\{\theta_{i,k}\}$, so that a minimum needs to lie in one of its stationary points. Consequently, let us derive Γ with respect to a generic $\theta_{j,l}$:

$$\frac{\partial\Gamma(\{\theta_{i,k}\})}{\partial\theta_{j,l}} = \frac{p_l\eta_j \sin\theta_{j,l}}{2}\left(\mu - \eta_j\cos\theta_{j,l}\right) \tag{3.7}$$

As it is possible to see, there are two ways for having null derivative (remember that the η_i's vary in the interval $\left[e^{-\frac{1}{4\nu^2}},1\right]$ and μ in $[0,\infty]$):

$$\sin\theta_{j,l} = 0 \tag{3.8a}$$

$$\eta_j\cos\theta_{j,l} = \mu, \text{ for } \frac{\mu}{\eta_j} \leq 1, \text{ i.e. } \mu \leq \eta_j \tag{3.8b}$$

For completeness, let us write down the second derivative of Γ with respect to $\theta_{j,l}$:

$$\frac{\partial^2\Gamma(\{\theta_{i,k}\})}{\partial^2\theta_{j,l}} = \frac{p_l\eta_j}{2}\left[\mu\left(\cos\theta_{j,l} + \sin\theta_{j,l}\right) - \eta_j\cos(2\theta_{j,l})\right]. \tag{3.9}$$

We can now ask ourselves which one between conditions 3.8a and 3.8b (when allowed) corresponds to a minimum. We have that:

- Whenever $\mu > \eta_j$, eq.3.8b is never satisfied, so that the only possibility to have the derivative $\frac{\partial\Gamma}{\partial\theta_{j,l}}$ equal to zero is to have $\sin\theta_{j,l} = 0$. This allows $\theta_{j,l}$ to be equal to 0 or π; it is easy to check that the second derivative is positive only for the first one (remember $\mu > \eta_j$), so that we can conclude that this is the only minimum. The smallest possible contribution of $\theta_{j,l}$ to Γ would be, in this case,

$$\frac{1}{4}p_l\eta_j^2\cos^2\theta_{j,l} - \frac{\mu}{2}p_l\eta_j\cos\theta_{j,l} \underset{\mu>\eta_j}{\rightarrow} \frac{1}{4}p_l\eta_j^2 - \frac{\mu}{2}p_l\eta_j \tag{3.10}$$

- Suppose now $\mu \leq \eta_j$. Here both eq. 3.8a and 3.8b can be satisfied; we only need to check which one represents the minimum. Looking at the second derivative (eq.3.9), we get that it is positive for $\eta_j\cos\theta_{j,l} = \mu$ and negative for $\sin\theta_{j,k} = 0$. Therefore we conclude that $\cos\theta_{j,l} = \frac{\mu}{\eta_j}$ is, indeed, the minimum, and the smallest

contribution is given by

$$\frac{1}{4}p_l\eta_j^2\cos^2\theta_{j,l} - \frac{\mu}{2}p_l\eta_j\cos\theta_{j,l} \underset{\mu\leq\eta_j}{\rightarrow} -\frac{1}{4}\mu^2 \tag{3.11}$$

Depending on μ, we have now all the ingredients for determining the minimum possible values of Γ. In fact, since we supposed the particles - and thus the coefficients η_i - to be independent, what we derived before can be applied for all l, $j = 1, ..., N$, in order to reach the global minimum Γ_{Min} of Γ. Here we must divide the domain of μ in three parts: the first one given by $\mu \leq \min_{i=1,...,N}\{\eta_i\}$, the second by $\min_{i=1,...,N}\{\eta_i\} < \mu \leq \max_{i=1,...,N}\{\eta_i\}$ and the third one by $\mu > \max_{i=1,...,N}\{\eta_i\}$; so that

$$\mu \leq \min\{\eta_i\} \rightarrow \Gamma_{Min} = \frac{\mu^2 N}{4} - \mu\frac{\mu N}{2} \tag{3.12a}$$

$$\min\{\eta_i\} < \mu \leq \max\{\eta_i\} \rightarrow \Gamma_{Min} = \frac{1}{4}\left(\sum_{\mu^2\leq\eta_i^2}\mu^2 + \sum_{\mu^2>\eta_i^2}\eta_i^2\right) - \frac{\mu}{2}\left(\sum_{\mu\leq\eta_i}\mu + \sum_{\mu>\eta_i}\eta_i\right) \tag{3.12b}$$

$$\mu > \max\{\eta_i\} \rightarrow \Gamma_{Min} = \frac{1}{4}\sum_{i=1}^{N}\eta_i^2 - \frac{\mu}{2}\sum_{i=1}^{N}\eta_i \tag{3.12c}$$

In eq.3.12b, the sums are to be taken over all the coefficients η_i that are bigger or smaller than μ, as specified.

At this point it is straightforward to determine, case by case, the average spin $\langle S_z\rangle$ and the variance $(\Delta S_x)^2$. In fact, remembering that $\Gamma = (\Delta S_x)^2 - \mu\langle S_z\rangle$ (or just imposing the constraints 3.8a and 3.8b to eq. 3.5a and 3.5b), we are able to obtain:

Range	$\mu \leq \min\{\eta_i\}$	$\min\{\eta_i\} < \mu \leq \max\{\eta_i\}$	$\mu > \max\{\eta_i\}$
$\langle S_z\rangle$	$\frac{\mu N}{2}$	$\frac{1}{2}\left(\sum_{\mu\leq\eta_i}\mu + \sum_{\mu>\eta_i}\eta_i\right)$	$\frac{1}{2}\sum_{i=1}^{N}\eta_i$
$(\Delta S_x)^2$	$\frac{\mu^2 N}{4}$	$\frac{1}{4}\left(\sum_{\mu^2\leq\eta_i^2}\mu^2 + \sum_{\mu^2>\eta_i^2}\eta_i^2\right)$	$\frac{1}{4}\sum_{i=1}^{N}\eta_i^2$

TABLE 3.1: In this Table we collected the results for $\langle S_z\rangle$ and $(\Delta S_x)^2$ in the different ranges in which μ is allowed to vary

Notice that, since all the quantities involved are *not* dependent on k any more, and that $\sum_k p_k = 1$, we are allowed to neglect these summations.

The results reported in Table 3.1 is valid for every probability distributions $p(\eta)$ and $p(\eta^2)$ describing the coefficients involved! We next employ what we found in section 2.2.2.3, in order to be practically able to use what we just obtained here.

In the following we will determine, term by term, all the quantities in Table 3.1:

- We already met $\sum_{i=1}^{N} \eta_i$ and $\sum_{i=1}^{N} \eta_i^2$ in section 2.2.2.3. There we showed that, according to the central limit theorem (theorem 1), we can write these sums as:

$$\sum_{i=1}^{N} \eta_i = N\bar{\eta} = N \int_{-\infty}^{\infty} \eta p(\eta) d\eta = N\sqrt{\pi}\nu \operatorname{erf}\left(\frac{1}{2\nu}\right) \tag{3.13a}$$

$$\sum_{i=1}^{N} \eta_i^2 = N\bar{\eta^2} = N \int_{-\infty}^{\infty} \eta^2 p(\eta^2) d\eta^2 = N\sqrt{\frac{\pi}{2}}\nu \operatorname{erf}\left(\frac{1}{\sqrt{2}\nu}\right) \tag{3.13b}$$

The remaining terms are harder to understand. For this reason, we will explain in details where they are coming from and then we will derive an appropriate expression in terms of the probability distributions we have at our disposal.

- Let us start with $\frac{1}{2}\left(\sum_{\mu\leq\eta_i} \mu + \sum_{\mu>\eta_i} \eta_i\right)$. First, recall that it represents $\langle S_z \rangle$ in the considered range; in fact it is coming from $\langle S_z \rangle = \frac{1}{2}\sum_k p_k \sum_{i=1}^{N} \eta_i \cos\theta_{i,k}$. More precisely we found that, depending on the value of μ, the cosines have to take one of the two different values allowed by eq. 3.8a or 3.8b. This was the only way for letting Γ to reach its minimum Γ_{Min}. Now, if $\mu \leq \min\{\eta_i\}$ or $\mu \geq \max\{\eta_i\}$, only one of these equations has to be verified (respectively the second and the first), so that we do not have to split the sum in two and obtain the results reported in Table 3.1. But in the particular considered case, where $\min\{\eta_i\} \leq \mu \leq \max\{\eta_i\}$, we necessarily have that some of the coefficients are bigger than μ and some smaller. From this fact, we need to split the sum in two; respectively one part consisting of all coefficients bigger than μ, for which $\eta_i \cos\theta_{i,k} = \mu$; and the other of all the ones smaller, for which $\cos\theta_{i,k} = 1$. In conclusion what we get is exactly $\frac{1}{2}\left(\sum_{\mu\leq\eta_i} \mu + \sum_{\mu>\eta_i} \eta_i\right)$; remember that we loose the dependence over k and thus can neglect $\sum_k p_k = 1$. At this point, it is just a matter to estimate the two sums.

  Let us start rewriting

$$\sum_{\mu\leq\eta_i} \mu = \mu \sum_{\mu\leq\eta_i} 1 = \mu N(\mu \leq \eta_i) = \mu N P(\mu \leq \eta), \tag{3.14}$$

  where $N(\mu \leq \eta_i)$ is the number of coefficients η_i such that $\mu \leq \eta_i$, and $P(\mu \leq \eta)$ represents the probability of having μ smaller or equal to η (according to the probability distribution $p(\eta)$). Determining $P(\mu \leq \eta)$ is quite easy; from probability

theory we have

$$P(\mu \leq \eta) = \int_{\mu}^{\infty} p(\eta) d\eta = \nu \int_{\mu}^{1} \frac{d\eta}{\eta\sqrt{-\log \eta}} = 2\nu\sqrt{-\log \mu}, \tag{3.15}$$

so that, for the first sum:

$$\sum_{\mu \leq \eta_i} \mu = 2N\nu\mu\sqrt{-\log \mu}. \tag{3.16}$$

In a similar way we can obtain an expression for the second sum, for which we get:

$$\sum_{\mu > \eta_i} \eta_i \overset{\dagger}{=} NP(\mu > \eta)\bar{\eta}(\mu > \eta), \tag{3.17}$$

where $P(\mu > \eta)$ is the probability of having μ bigger than η, and $\bar{\eta}(\mu > \eta)$ is the average value of η we obtain considering $p_{tr}(\eta)$, that is the probability distribution $p(\eta)$ truncated to the value of μ (see the following Fig.3.1).

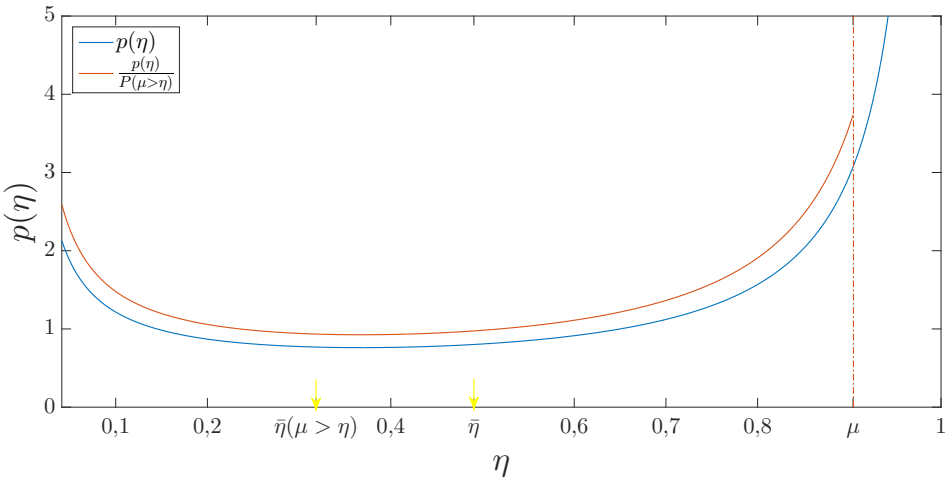

FIGURE 3.1: Plot of the functions $p(\eta)$ and $p_{tr}(\eta)$ ($p(\eta)$ truncated), with parameter $\nu = 0.28$. Notice that $p_{tr}(\eta)$ has been renormalized, as consequence of the restriction of its domain. In the coordinate axis are marked the values of $\mu = 0.9$, $\bar{\eta} = 0.49$ and $\bar{\eta}(\mu > \eta) = 0.32$.

In eq.3.17, the equality marked with † is a consequence of the central limit theorem (theorem 1). Here we have to be careful, since the hypotheses of such theorem are *not* necessarily satisfied; it depends on μ. In fact, since we allow μ to vary, at some point it will approach the minimum between the η_i's, $\min\{\eta_i\}$, where there could be a very small number of particles described by coefficients η_i *smaller* than μ. In this case we are not allowed to use theorem 1, that only works for a big statistical sample. We will discuss about this problem later; for now we just neglect it and

suppose theorem 1 valid everywhere.
Going to eq.3.17 back, since

$$P(\mu > \eta) = \int_{-\infty}^{\mu} p(\eta)d\eta = 1 - P(\mu \leq \eta) = 1 - 2\nu\sqrt{-\log\mu}, \tag{3.18}$$

the only remaining computation we have to perform is $\bar{\eta}(\mu > \eta)$. As said above, it represents the average of η obtained with the probability density function truncated up to μ (see Fig.3.1). In other words, giving $p_{tr}(\eta)$ first:

$$p_{tr}(\eta) = \begin{cases} \frac{p(\eta)}{P(\mu>\eta)} & \text{if } e^{-\frac{1}{4\nu^2}} \leq \eta \leq \mu \\ 0 & \text{if } \eta < e^{-\frac{1}{4\nu^2}} \text{ or } \mu < \eta, \end{cases} \tag{3.19}$$

we get that $\bar{\eta}(\mu > \eta)$ is given by

$$\bar{\eta}(\mu > \eta) = \int_{-\infty}^{\infty} \eta p_{tr}(\eta)d\eta = \frac{\int_{e^{-\frac{1}{4\nu^2}}}^{\mu} \eta p(\eta)d\eta}{P(\mu > \eta)} = \frac{\sqrt{\pi}\nu\left[\text{erf}\left(\frac{1}{2\nu}\right) - \text{erf}\left(\sqrt{-\log\mu}\right)\right]}{P(\mu > \eta)}. \tag{3.20}$$

In conclusion, we are finally able to write down the second sum

$$\sum_{\mu>\eta_i} \eta_i = NP(\mu > \eta)\bar{\eta}(\mu > \eta) = \sqrt{\pi}N\nu\left[\text{erf}\left(\frac{1}{2\nu}\right) - \text{erf}\left(\sqrt{-\log\mu}\right)\right], \tag{3.21}$$

and consequently $\langle S_z \rangle$ for $\min\{\eta_i\} \leq \mu \leq \max\{\eta_i\}$:

$$\begin{aligned} \langle S_z \rangle &= \frac{1}{2}\sum_k p_k \sum_{i=1}^{N} \eta_i \cos\theta_{i,k} = \frac{1}{2}\left(\sum_{\mu\leq\eta_i} \mu + \sum_{\mu>\eta_i} \eta_i\right) = \\ &= \frac{N\nu}{2}\left\{2\mu\sqrt{-\log\mu} + \sqrt{\pi}\left[\text{erf}\left(\frac{1}{2\nu}\right) - \text{erf}\left(\sqrt{-\log\mu}\right)\right]\right\}. \end{aligned} \tag{3.22}$$

- The other term we need to analyse is $\frac{1}{4}\left(\sum_{\mu^2\leq\eta_i^2} \mu^2 + \sum_{\mu^2>\eta_i^2} \eta_i^2\right)$. The discussion about it proceeds analogously to the previous one; in fact, except the fact that it comes from $(\Delta S_x)^2 = \frac{1}{4}\sum_k p_k \sum_{i=1}^{N} \eta_i^2 \cos^2\theta_{i,k}$ instead of $\langle S_z \rangle$, there are no big differences from before. Therefore, let us just collect the results we would obtain following the same procedure:

$$\sum_{\mu^2\leq\eta_i^2} \mu^2 = \mu^2 \sum_{\mu^2\leq\eta_i^2} = \mu^2 N(\mu^2 \leq \eta^2) = N\mu^2 P(\mu^2 \leq \eta^2), \tag{3.23}$$

where we necessarily have that $P(\mu^2 \leq \eta^2)$, i.e.: the probability to have μ^2 smaller than μ^2, is given by

$$P(\mu^2 \leq \eta^2) = \int_{\mu^2}^{1} p(\eta^2) d\eta^2 = P(\mu \leq \eta) = 2\nu\sqrt{-\log \mu}. \tag{3.24}$$

As consequence, we can write the first sum as:

$$\sum_{\mu^2 \leq \eta_i^2} \mu^2 = 2N\nu\mu^2\sqrt{-\log \mu}, \tag{3.25}$$

while for the second we have:

$$\sum_{\mu^2 > \eta_i^2} \eta_i^2 = NP(\mu^2 > \eta^2)\bar{\eta^2}(\mu^2 > \eta^2). \tag{3.26}$$

Here $P(\mu^2 > \eta^2)$ represents the probability to have μ^2 bigger than η^2, that can be obtained by $P(\mu^2 > \eta^2) = 1 - P(\mu^2 \leq \eta^2)$. Similarly as before, $\bar{\eta^2}(\mu^2 > \eta^2)$ is the average value of η^2 obtained considering $p_{tr}(\eta^2)$ (the probability distribution $p(\eta^2)$ truncated to the value of μ^2). This is given by:

$$p_{tr}(\eta^2) = \begin{cases} \frac{p(\eta^2)}{P(\mu^2 > \eta^2)} & \text{if } e^{-\frac{1}{2\nu^2}} \leq \eta^2 \leq \mu^2 \\ 0 & \text{if } \eta^2 < e^{-\frac{1}{2\nu^2}} \text{ or } \mu^2 < \eta^2, \end{cases} \tag{3.27}$$

so that we finally have:

$$\begin{aligned} \bar{\eta^2}(\mu^2 > \eta^2) = \int_{-\infty}^{\infty} \eta^2 p_{tr}(\eta^2) d\eta^2 = \frac{\int_{\exp\left(-\frac{1}{2\nu^2}\right)}^{\mu^2} \eta^2 p(\eta^2) d\eta^2}{P(\mu^2 > \eta^2)} = \\ = \frac{\sqrt{\frac{\pi}{2}}\nu \left[\operatorname{erf}\left(\frac{1}{\sqrt{2}\nu}\right) - \operatorname{erf}\left(\sqrt{-2\log \mu}\right)\right]}{P(\mu^2 > \eta^2)}. \end{aligned} \tag{3.28}$$

In conclusion, the second sum can be rewritten as

$$\sum_{\mu^2 > \eta_i^2} \eta_i^2 = NP(\mu^2 > \eta^2)\bar{\eta^2}(\mu^2 > \eta^2) = \sqrt{\frac{\pi}{2}} N\nu \left[\operatorname{erf}\left(\frac{1}{\sqrt{2}\nu}\right) - \operatorname{erf}\left(\sqrt{-2\log \mu}\right)\right], \tag{3.29}$$

so that $(\Delta S_x)^2$, for $\min\{\eta_i\} \leq \mu \leq \max\{\eta_i\}$ becomes

$$(\Delta S_x)^2 = \frac{1}{4}\sum_k p_k \sum_{i=1}^{N} \eta_i^2 \cos^2\theta_{i,k} = \frac{1}{4}\left(\sum_{\mu^2\leq\eta_i^2} \mu^2 + \sum_{\mu^2>\eta_i^2} \eta_i^2\right) = \\ = \frac{N\nu}{4}\left\{2\mu^2\sqrt{-\log\mu} + \sqrt{\frac{\pi}{2}}\left[\operatorname{erf}\left(\frac{1}{\sqrt{2}\nu}\right) - \operatorname{erf}\left(\sqrt{-2\log\mu}\right)\right]\right\}. \tag{3.30}$$

As a last comment, we make clear that eq.3.26 is obtained using the central limit theorem, and therefore present the same problem we pointed out for eq.3.17, whenever μ approaches the minimum possible value of the squared η_i's.

At this point we are finally able to rewrite Table 3.1 for the particular model used for the description of the coefficients $\{\eta_i\}$. Using equations 3.13a, 3.13b, 3.22 and 3.30 we get

Range	$\mu \leq \min\{\eta_i\}$	$\min\{\eta_i\} < \mu \leq \max\{\eta_i\}$	$\mu > \max\{\eta_i\}$
$\langle S_z\rangle$	$\frac{\mu N}{2}$	$\frac{N\nu}{2}\{2\mu\sqrt{-\log\mu}+$ $+\sqrt{\pi}\left[\operatorname{erf}\left(\frac{1}{2\nu}\right) - \operatorname{erf}\left(\sqrt{-\log\mu}\right)\right]\}$	$\frac{N\sqrt{\pi}\nu}{2}\operatorname{erf}\left(\frac{1}{2\nu}\right)$
$(\Delta S_x)^2$	$\frac{\mu^2 N}{4}$	$\frac{N\nu}{4}\{2\mu^2\sqrt{-\log\mu}+$ $+\sqrt{\frac{\pi}{2}}\left[\operatorname{erf}\left(\frac{1}{\sqrt{2}\nu}\right) - \operatorname{erf}\left(\sqrt{-2\log\mu}\right)\right]\}$	$\frac{N\sqrt{\frac{\pi}{2}}\nu}{4}\operatorname{erf}\left(\frac{1}{\sqrt{2}\nu}\right)$

TABLE 3.2: Here we reported the same results as in Table 3.1, having imposed the conditions deriving from the particular model for the $\{\eta_i\}$ we are using.

For each value of μ between zero and one (whenever $\mu > 1$, $\langle S_z\rangle$ and $(\Delta S_x)^2$ are fixed), we obtain correspondent $\langle S_z\rangle$ and $(\Delta S_x)^2$. Therefore we are able to plot the second one with respect to the first one, both renormalised. This is done by dividing them for the biggest possible values they can assume, respectively (as it follows from eq.3.5a and 3.5b)

$$\langle S_z\rangle_{CSS} = \frac{1}{2}\sum_{i=1}^{N}\eta_i = \frac{N\sqrt{\pi}\nu}{2}\operatorname{erf}\left(\frac{1}{2\nu}\right) \tag{3.31a}$$

$$(\Delta S_x)^2_{CSS} = \frac{1}{4}\sum_{i=1}^{N}\eta_i^2 = \frac{N\sqrt{\frac{\pi}{2}}\nu}{4}\operatorname{erf}\left(\frac{1}{\sqrt{2}\nu}\right). \tag{3.31b}$$

We decided to use the appendix "$_{CSS}$" because the maximal values refer to the coherent spin state (see eq.1.12). The following Fig.3.2 represents the behaviour of $\frac{(\Delta S_x)^2}{(\Delta S_x)^2_{CSS}}$ with respect to $\frac{\langle S_z\rangle}{\langle S_z\rangle_{CSS}}$:

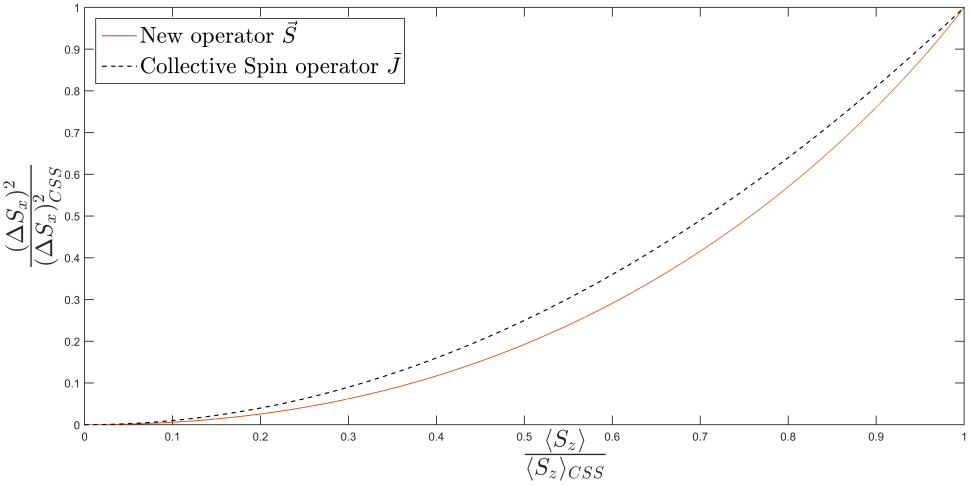

FIGURE 3.2: $\frac{(\Delta S_x)^2}{(\Delta S_x)^2_{CSS}}$ as function of $\frac{\langle S_z\rangle}{\langle S_z\rangle_{CSS}}$. For drawing this plot, we supposed $\min\{\eta_i\} = e^{-\frac{1}{4\nu^2}}$ and $\max\{\eta_i\} = 1$, they are good approximations whenever the number of particles $N \gg 1$ and $\nu \gg \frac{1}{N}$.

Before commenting this plot, let us explain why we were allowed to apply the central limit theorem in the critical cases mentioned before. There are two of them, respectively one for $\langle S_z\rangle$ and one for $(\Delta S_x)^2$, both in the range $\min\{\eta_i\} < \mu \leq \max\{\eta_i\}$ (see Table 3.1). Case by case we have:

- For $\langle S_z\rangle = \frac{1}{2}\left(\sum_{\mu\leq\eta_i}\mu + \sum_{\mu>\eta_i}\eta_i\right)$, we have seen that (eq.3.16 and 3.21):

$$\begin{cases} \sum_{\mu\leq\eta_i}\mu & = \mu N P(\mu\leq\eta) = 2N\nu\mu\sqrt{-\log\mu} \\ \sum_{\mu>\eta_i}\eta_i & \overset{Thm\ 1}{=} N P(\mu>\eta)\bar{\eta}(\mu>\eta), \end{cases} \tag{3.32}$$

  where the equality holds whenever hypotheses of theorem 1 hold. This means, practically, whenever the sum $\sum_{\mu>\eta_i}\eta_i$ runs over big numbers of particles. But, as pointed out before, μ is allowed to vary from $\min\{\eta_i\}$ to $\max\{\eta_i\}$, so that the possibility to have particles described by coefficients $\eta_i < \mu$ is few, whenever $\mu \to \min\{\eta_i\}$. But what happens when this is actually the case?
  Suppose $\mu = e^{-\frac{1}{4\nu^2}} + x$, for a positive, small x. The upper sum in eq.3.32 can be rewritten as:

$$\sum_{\mu\leq\eta_i}\mu = 2N\nu\mu\sqrt{-\log\mu} \underset{\mu\simeq e^{-\frac{1}{4\nu^2}}+x}{\to} N\left[e^{-\frac{1}{4\nu^2}} + x\left(2\nu^2+1\right)\right] \tag{3.33}$$

The problem is that we cannot do the same for the lower sum; in fact the equation characterizing it is not valid for $\mu \to \min\{\eta_i\}$ any more! What we can do is to obtain the biggest possible value it can reach, namely substituting all the coefficients η_i involved with one (the maximum value allowed by their domain), i.e. switch $\bar{\eta}(\mu > \eta)$ with 1:

$$\sum_{\mu>\eta_i} \eta_i \leq \sum_{\mu>\eta_i} 1 = NP(\mu > \eta) = N(1 - 2\nu\sqrt{-\log\mu}). \tag{3.34}$$

Now, the right hand side of this equation can be evaluated for $\mu = e^{-\frac{1}{4\nu^2}} + x$. Using Taylor expansion:

$$N(1 - 2\nu\sqrt{-\log\mu}) \underset{\mu\simeq e^{-\frac{1}{4\nu^2}}+x}{\to} 2e^{\frac{1}{4\nu^2}} N\nu^2 x, \tag{3.35}$$

so that, in conclusion

$$\sum_{\mu>\eta_i} \eta_i \leq \sum_{\mu>\eta_i} 1 \underset{\mu\simeq e^{-\frac{1}{4\nu^2}}+x}{\to} 2e^{\frac{1}{4\nu^2}} N\nu^2 x. \tag{3.36}$$

In particular, for $x \to 0$, we get

$$\begin{cases} \sum\limits_{\mu\leq\eta_i} \mu & \underset{\mu\simeq e^{-\frac{1}{4\nu^2}}+x}{\to} N\left[e^{-\frac{1}{4\nu^2}} + x\left(2\nu^2+1\right)\right] \underset{x\simeq 0}{\to} Ne^{-\frac{1}{4\nu^2}} \\ \sum\limits_{\mu>\eta_i} \eta_i & \leq \sum\limits_{\mu>\eta_i} 1 \underset{\mu\simeq e^{-\frac{1}{4\nu^2}}+x}{\to} 2e^{\frac{1}{4\nu^2}} N\nu^2 x \underset{x\simeq 0}{\to} 0, \end{cases} \tag{3.37}$$

and therefore we can deduce that, at least for an appropriate choice of the parameters ν and N,

$$\sum_{\mu>\eta_i} \eta_i \ll \sum_{\mu\leq\eta_i} \mu \tag{3.38}$$

in the limit $\mu \to e^{-\frac{1}{4\nu^2}}$. In other words, it does not matter if the central limit theorem is not satisfied; when it happens, the contribution of the corresponding sum is negligible with respect to the other, as shown in the following Fig.3.3.

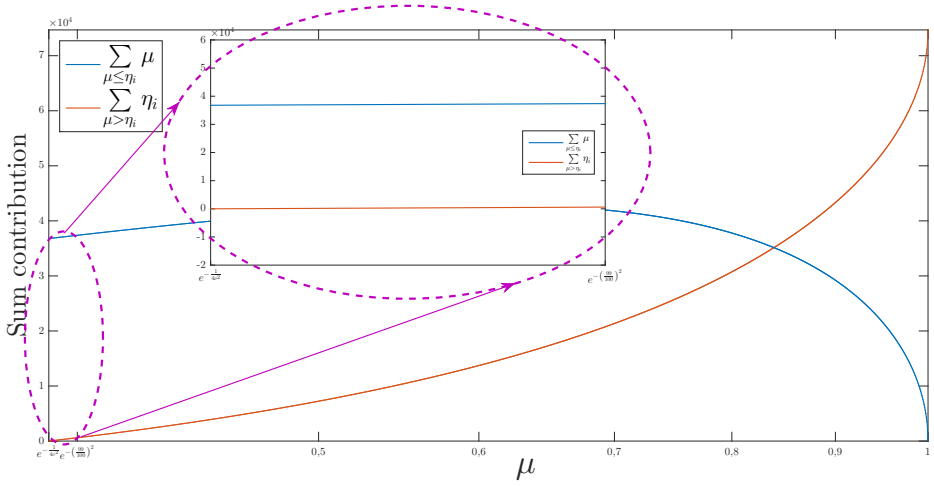

FIGURE 3.3: Values taken by the two sums $\sum_{\mu\leq\eta_i}\mu$ and $\sum_{\mu>\eta_i}\eta_i$ varying μ. As it is possible to see, for $\mu\to e^{-\frac{1}{4\nu^2}}$ the first one is predominant, as explained in the text. Here $N=10^5$ and $\nu=0.5$. The ellipsis encloses the interval in which we suppose the central limit theorem is not verified (see text below): $\mu\in\left[0,e^{-\left[\frac{1}{2\nu}\left(1-\frac{1000}{N}\right)\right]^2}\right]=\left[0,e^{-\left(\frac{99}{100}\right)^2}\right]$

What does "appropriate choice of the parameter" actually mean? Of course, for any pair (ν,N), at $\mu=e^{-\frac{1}{4\nu^2}}$ we get that $\sum_{\mu>\eta_i}\eta_i\leq\sum_{\mu>\eta_i}1=0$, so that we always obtain $\sum_{\mu>\eta_i}\eta_i\ll\sum_{\mu\leq\eta_i}\mu$. But we request that this constraint is valid in a neighbourhood of $\mu=e^{-\frac{1}{4\nu^2}}$ as well! Here, with the model in use for the description of the coefficients, it is pretty well satisfied, at least for N and ν not very small. However, it is for the experimentalist to decide if, for a given setup, the central limit theorem can be applied in the whole domain of μ.

For example, let us consider that the hypotheses of the central limit theorem are satisfied whenever $N(\mu>\eta)\geq 10^3$, and to discard all the experimental setups for which $\frac{\sum_{\mu>\eta_i}\eta_i}{\sum_{\mu\leq\eta_i}\mu}\leq 10^3$. Here $N(\mu>\eta)$ represents the expected number of particles whose coefficients are smaller than μ: $N(\mu>\eta)=NP(\mu>\eta)$. Now, the first condition identify the "critical" interval for μ in which we have to check if the second condition is verified. In fact, $N(\mu>\eta)\geq 10^3$ means that

$$10^3\leq N(\mu>\eta)=NP(\mu>\eta)=N\left(1-2\nu\sqrt{-log(\mu)}\right), \tag{3.39}$$

is valid whenever

$$\mu\geq e^{-\left[\frac{1}{2\nu}\left(1-\frac{10^3}{N}\right)\right]^2}. \tag{3.40}$$

In the Fig.3.3 this interval is pointed out by the violet ellipse; as it is possible to see the second condition is well satisfied inside it.

- These passage are to be repeated identically for $(\Delta S_x)^2 = \frac{1}{4}\left(\sum_{\mu^2\leq\eta_i^2}\mu^2 + \sum_{\mu^2>\eta_i^2}\eta_i^2\right)$. Here we have that (eq.3.25 and 3.29):

$$\begin{cases} \sum_{\mu^2\leq\eta_i^2}\mu^2 & = \mu^2 NP(\mu^2\leq\eta^2) = 2N\nu\mu^2\sqrt{-\log\mu} \\ \sum_{\mu^2>\eta_i^2}\eta_i^2 & \overset{Thm\ 1}{=} NP(\mu^2>\eta^2)\bar{\eta^2}(\mu^2>\eta^2), \end{cases} \tag{3.41}$$

so that, taking $\mu^2 = \left(e^{-\frac{1}{4\nu^2}} + x\right)^2$,

$$\begin{cases} \sum_{\mu^2\leq\eta_i^2}\mu^2 & \underset{\mu^2\simeq\left(e^{-\frac{1}{4\nu^2}}+x\right)^2}{\to} N\left[e^{-\frac{1}{2\nu^2}} + xe^{-\frac{1}{4\nu^2}}\left(2\nu^2+1\right)\right] \underset{x\simeq 0}{\to} Ne^{-\frac{1}{2\nu^2}} \\ \sum_{\mu^2>\eta_i^2}\eta_i^2 & \leq \sum_{\mu^2>\eta_i^2} 1 \underset{\mu^2\simeq\left(e^{-\frac{1}{4\nu^2}}+x\right)^2}{\to} 2e^{\frac{1}{4\nu^2}}N\nu^2 x \underset{x\simeq 0}{\to} 0. \end{cases} \tag{3.42}$$

For the last equation, as the central limit theorem is not applicable, we estimated the upper limit substituting the coefficients η_i^2 of the involved particles with one, i.e.: the biggest possible value they can assume.
The conclusions are the same as before: for $\mu^2 = e^{-\frac{1}{2\nu^2}}$ we have that

$$\sum_{\mu^2>\eta_i^2}\eta_i^2 \ll \sum_{\mu^2\leq\eta_i^2}\mu^2, \tag{3.43}$$

but if we request this condition to be satisfied in a neighbourhood of such point, we need first to choose such neighbourhood, and then, using the expansion in eq.3.42, evaluate how the sums behave in such interval. Notice that, as the probability distribution functions $p(\eta)$ and $p(\eta^2)$ are similar, since the second describes the squared variable of the first, it is usually not necessary to perform a double check.

Let us go back to Fig.3.2 and to Table 3.2, that has been used for the plot. As explained before, this has been drawn deriving, for each μ in the interval $[0,1]$, both $\langle S_z\rangle$ and $(\Delta S_x)^2$. What we would like to have, however, is an equation of $(\Delta S_x)^2$ expressed in terms of $\langle S_z\rangle$. As it is possible to see from the Table 3.2, this is not easily obtainable, at least for the range $\min\{\eta_i\} < \mu \leq \max\{\eta_i\}$. In fact, the presence of the variable μ inside the error function makes it difficult to get the inverse function. Nevertheless, what we can do without great effort is to obtain expressions in some limits of interest. Let us suppose that $\min\{\eta_i\} = e^{-\frac{1}{4\nu^2}}$ and that $\max\{\eta_i\} = 1$. This is an excellent compromise whenever the number of particles N is big enough. Then we have, for each one of the three ranges in which μ can vary:

- $\mu \leq \min\{\eta_i\}$
  Here $(\Delta S_x)^2$ and $\langle S_z \rangle$ are given by (see Table 3.2)

$$\langle S_z \rangle = \frac{\mu N}{2} \tag{3.44a}$$

$$(\Delta S_x)^2 = \frac{\mu^2 N}{4}, \tag{3.44b}$$

  so that it is actually very easy to obtain

$$(\Delta S_x)^2 = \frac{\langle S_z \rangle^2}{N} \quad \text{for } 0 \leq \langle S_z \rangle \leq \frac{N e^{-\frac{1}{4\nu^2}}}{2}. \tag{3.45}$$

  It is interesting here to note that eq.3.45 is the result we would obtain, for the whole domain $\mu \in [0, 1]$, if we had all the coefficients equal to one. This is equivalent to ask, in our model, a very big ν. In this case, looking at eq.2.109a, we have:

$$\bar{\eta} \underset{\nu \to \infty}{\to} 1 \tag{3.46a}$$

$$1 \geq \eta_i \geq e^{-\frac{1}{4\nu^2}} \underset{\nu \to \infty}{\to} 1, \tag{3.46b}$$

  so that $\min\{\eta_i\} \to 1$ as well. In conclusion, eq.3.45 would be extended to the whole domain, showing that in such limit our model recovers the lowest bound identified by the squeezing parameter (see eq.1.16). This is a result that we actually needed to achieve, since we are generalizing ξ^2 to a more realistic situation.

- $\mu > \max\{\eta_i\}$
  This case does not have any interest; in fact, $(\Delta S_x)^2$ and $\langle S_z \rangle$ do not depend on μ and are therefore constant. The challenging one is the following

- $\max\{\eta_i\} < \mu \leq \max\{\eta_i\}$
  Let us first rewrite the quantities of interest. From Table 3.1:

$$\langle S_z \rangle = \frac{N\nu}{2} \left\{ 2\mu \sqrt{-\log \mu} + \sqrt{\pi} \left[\operatorname{erf}\left(\frac{1}{2\nu} \right) - \operatorname{erf}\left(\sqrt{-\log \mu} \right) \right] \right\} \tag{3.47a}$$

$$(\Delta S_x)^2 = \frac{N\nu}{4} \left\{ 2\mu^2 \sqrt{-\log \mu} + \sqrt{\frac{\pi}{2}} \left[\operatorname{erf}\left(\frac{1}{\sqrt{2}\nu} \right) - \operatorname{erf}\left(\sqrt{-2\log \mu} \right) \right] \right\}. \tag{3.47b}$$

  As these two functions are invertible, it would be possible to express μ as a function of $\langle S_z \rangle$, and later substitute it in eq.3.47b to obtain the expression for the curve in Fig.3.2. But this would involve a great effort for a small reward. In fact, the equation we would obtain would be extremely complicated; at this point it is easier to directly use the plot given before.
  However, not all is lost! Indeed, in the limit $\mu \to 1$ we are able to take Fourier expansions of both eq.3.47a and 3.47b, and obtain a linear approximation to $(\Delta S_x)^2$,

expressed in function of $\langle S_z \rangle$. Notice that for $\mu = 1$ we have that both $\langle S_z \rangle$ and $(\Delta S_x)^2$ take their maxima.

Let us set $\mu = 1 - x$, being x a small, positive real number. Thus we have:

$$\begin{aligned}
&\langle S_z \rangle = \\
&= \frac{N\nu}{2}\left\{2(1-x)\sqrt{-\log(1-x)} + \sqrt{\pi}\left[\operatorname{erf}\left(\frac{1}{2\nu}\right) - \operatorname{erf}\left(\sqrt{-\log(1-x)}\right)\right]\right\} = \\
&= \frac{N\nu}{2}\left\{\sqrt{\pi}\operatorname{erf}\left(\frac{1}{2\nu}\right) - \frac{4}{3}x^{\frac{3}{2}} - \frac{1}{5}x^{\frac{5}{2}} - + o(x^{\frac{7}{2}})\right\} = \\
&= \frac{N\nu}{2}\left\{\sqrt{\pi}\operatorname{erf}\left(\frac{1}{2\nu}\right) - \frac{4}{3}x^{\frac{3}{2}}\right\} + o(x^{\frac{5}{2}})
\end{aligned} \tag{3.48}$$

and

$$\begin{aligned}
&(\Delta S_x)^2 = \\
&= \frac{N\nu}{4}\left\{2(1-x)^2\sqrt{-\log(1-x)} + \sqrt{\frac{\pi}{2}}\left[\operatorname{erf}\left(\frac{1}{\sqrt{2}\nu}\right) - \operatorname{erf}\left(\sqrt{-2\log(1-x)}\right)\right]\right\} = \\
&= \frac{N\nu}{4}\left\{\sqrt{\frac{\pi}{2}}\operatorname{erf}\left(\frac{1}{\sqrt{2}\nu}\right) - \frac{8}{3}x^{\frac{3}{2}} + \frac{6}{5}x^{\frac{5}{2}} + o(x^{\frac{7}{2}})\right\} = \\
&= \frac{N\nu}{4}\left\{\sqrt{\frac{\pi}{2}}\operatorname{erf}\left(\frac{1}{\sqrt{2}\nu}\right) - \frac{8}{3}x^{\frac{3}{2}}\right\} + o(x^{\frac{5}{2}}).
\end{aligned} \tag{3.49}$$

The linear approximation is now obtainable neglecting all but the first expansion terms of eq. 3.48 and 3.49,

$$\langle S_z \rangle \simeq \frac{N\nu}{2}\left\{\sqrt{\pi}\operatorname{erf}\left(\frac{1}{2\nu}\right) - \frac{4}{3}x^{\frac{3}{2}}\right\} \tag{3.50a}$$

$$(\Delta S_x)^2 \simeq \frac{N\nu}{4}\left\{\sqrt{\frac{\pi}{2}}\operatorname{erf}\left(\frac{1}{\sqrt{2}\nu}\right) - \frac{8}{3}x^{\frac{3}{2}}\right\}, \tag{3.50b}$$

so that

$$\frac{4}{3}x^{\frac{3}{2}} \simeq \sqrt{\pi}\operatorname{erf}\left(\frac{1}{2\nu}\right) - \frac{2\langle S_z \rangle}{N\nu} \tag{3.51}$$

and consequently

$$(\Delta S_x)^2 \simeq \langle S_z \rangle + \sqrt{\frac{\pi}{2}}\frac{N\nu}{4}\left\{\operatorname{erf}\left(\frac{1}{\sqrt{2}\nu}\right) - 2\sqrt{2}\operatorname{erf}\left(\frac{1}{2\nu}\right)\right\}. \tag{3.52}$$

Let us make some comments about these last results.

First, this curve intersect the real one at the point $x = 0$, i.e.: $\mu = 1$ and $\langle S_z \rangle = \langle S_z \rangle_{CSS}$. Moreover, as a consequence of the fact that we cut the series expansions in eq.3.48 and 3.49 at the first term, we cannot require that $(\Delta S_x)^2$, as expressed in eq.3.52,

approximates well the real curve. In fact, it drift away very near to the tangent point (see Fig.3.4 later). However, there are two reasons for which eq.3.52 is very useful:

1. In experiments, the average spin of the system $\langle S_z \rangle$ usually approaches the maximum allowed value $\langle S_z \rangle_{CSS}$. We remember that, according to this model, it is represented by eq.3.31a:

$$\langle S_z \rangle_{CSS} = \frac{1}{2} \sum_{i=1}^{N} \eta_i = \frac{N\sqrt{\pi}\nu}{2} \operatorname{erf}\left(\frac{1}{2\nu}\right). \tag{3.53}$$

   Therefore, the knowledge about how $(\Delta S_x)^2$ behaves for $\langle S_z \rangle \to \langle S_z \rangle_{CSS}$ is generally sufficient.

2. The linear approximation lies *below* the real curve whenever $\langle S_z \rangle \to \langle S_z \rangle_{CSS}$.
   Let us denote the approximations to $\langle S_z \rangle$ and $(\Delta S_x)^2$ as (see eq.3.50a and 3.50b):

$$\langle S_z \rangle_{app}(x) = \frac{N\nu}{2} \left\{ \sqrt{\pi} \operatorname{erf}\left(\frac{1}{2\nu}\right) - \frac{4}{3} x^{\frac{3}{2}} \right\} \tag{3.54a}$$

$$(\Delta S_x)^2_{app}(x) = \frac{N\nu}{4} \left\{ \sqrt{\frac{\pi}{2}} \operatorname{erf}\left(\frac{1}{\sqrt{2}\nu}\right) - \frac{8}{3} x^{\frac{3}{2}} \right\}. \tag{3.54b}$$

   As we have seen, from these equation it is possible to obtain an expression of $(\Delta S_x)^2_{app}$ depending on $\langle S_z \rangle_{app}$:

$$(\Delta S_x)^2_{app}(\langle S_z \rangle_{app}) = \langle S_z \rangle_{app} + \sqrt{\frac{\pi}{2}} \frac{N\nu}{4} \left\{ \operatorname{erf}\left(\frac{1}{\sqrt{2}\nu}\right) - 2\sqrt{2} \operatorname{erf}\left(\frac{1}{2\nu}\right) \right\}; \tag{3.55}$$

   now we want to prove that this curve $(\Delta S_x)^2_{app}(\langle S_z \rangle_{app})$ lies below the real one, obtained using Table 3.2. From eq.3.48 and 3.49 we have that, for $\langle S_z \rangle \to \langle S_z \rangle_{CSS}$:

$$\begin{aligned} \langle S_z \rangle &= \frac{N\nu}{2} \left\{ \sqrt{\pi} \operatorname{erf}\left(\frac{1}{2\nu}\right) - \frac{4}{3} x^{\frac{3}{2}} - \frac{1}{5} x^{\frac{5}{2}} + o(x^{\frac{7}{2}}) \right\} \leq \\ &\leq \frac{N\nu}{2} \left\{ \sqrt{\pi} \operatorname{erf}\left(\frac{1}{2\nu}\right) - \frac{4}{3} x^{\frac{3}{2}} \right\} = \langle S_z \rangle_{app} \end{aligned} \tag{3.56}$$

   and

$$\begin{aligned} (\Delta S_x)^2 &= \frac{N\nu}{4} \left\{ \sqrt{\frac{\pi}{2}} \operatorname{erf}\left(\frac{1}{\sqrt{2}\nu}\right) - \frac{8}{3} x^{\frac{3}{2}} + \frac{6}{5} x^{\frac{5}{2}} + o(x^{\frac{7}{2}}) \right\} \geq \\ &\geq \frac{N\nu}{4} \left\{ \sqrt{\frac{\pi}{2}} \operatorname{erf}\left(\frac{1}{\sqrt{2}\nu}\right) - \frac{8}{3} x^{\frac{3}{2}} \right\} = (\Delta S_x)^2_{app} \end{aligned} \tag{3.57}$$

At this point it is just a matter of simple algebra to obtain

$$\frac{(\Delta S_x)^2}{\langle S_z \rangle} \geq \frac{(\Delta S_x)^2_{app}}{\langle S_z \rangle_{app}}. \tag{3.58}$$

In words, this exactly means that for $\langle S_z \rangle \to \langle S_z \rangle_{CSS}$, the linear approximation is smaller than the real curve.

This fact is of particular interest, because whenever we prove that some experimental point $\left(\langle S_z \rangle_{exp}, (\Delta S_x)^2_{exp}\right)$ lies below $(\Delta S_x)^2_{app}\,(\langle S_z \rangle_{app})$, we can automatically deduce that the theoretical curve expressing the lowest possible value of $(\Delta S_x)^2$ for the model in use passes over it. And, since we derived such curve for a generic separable state, we can infer the system we are dealing with is entangled.

At this point we are able to plot $(\Delta S_x)^2$ "numerically" with respect to $\langle S_z \rangle$ (see Fig.3.2), to explicitly obtain an expression of the variance with respect to the average spin for $0 \leq \langle S_z \rangle \leq \frac{N e^{-\frac{1}{4\nu^2}}}{2}$ (eq.3.45) and to write down a linear approximation to $(\Delta S_x)^2$ in the point $\langle S_z \rangle = \langle S_z \rangle_{CSS}$ (eq.3.55). In the following we will give a final comment regarding this example. In particular, the goal is to see how much can $(\Delta S_x)^2$ vary with respect to $\langle S_z \rangle$, letting parameters N and ν changing. It is already clear from Table 3.2 that N is just a scale factor, that vanishes once we renormalise: something we usually do to have enough statistics. On the contrary, ν changes the curve of Fig.3.2, as it is possible to see in the next Fig.3.4.

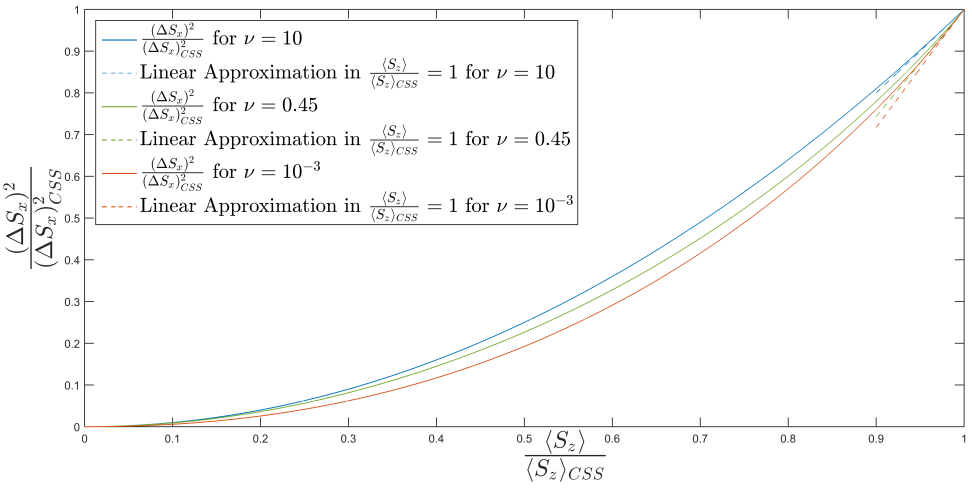

FIGURE 3.4: Renormalized curves $\frac{(\Delta S_x)^2}{(\Delta S_x)^2_{CSS}}$ vs $\frac{\langle S_z \rangle}{\langle S_z \rangle_{CSS}}$ for ν equal to 10 (*blue*), 0.45 (*green*) and 10^-3 (*red*). In the plot are drawn the linear approximations as well, in the range $\frac{\langle S_z \rangle}{\langle S_z \rangle_{CSS}} \in [0.9, 1]$

First, let us remember that here we renormalized $\langle S_z \rangle$ and $(\Delta S_x)^2$, i.e.: we plotted $\frac{(\Delta S_x)^2}{(\Delta S_x)^2_{CSS}}$ with respect to $\frac{\langle S_z \rangle}{\langle S_z \rangle_{CSS}}$. This means that the equation of the linear approximation becomes, from eq.3.55 and using eq.3.31a:

$$\frac{(\Delta S_x)^2_{app}}{(\Delta S_x)^2_{CSS}} \left(\frac{\langle S_z \rangle_{app}}{\langle S_z \rangle_{CSS}} \right) = \frac{\langle S_z \rangle_{CSS}}{(\Delta S_x)^2_{CSS}} \left\{ \frac{\langle S_z \rangle_{app}}{\langle S_z \rangle_{CSS}} + \left[\frac{\text{erf}\left(\frac{1}{\sqrt{2}\nu}\right)}{2\sqrt{2}\,\text{erf}\left(\frac{1}{2\nu}\right)} - 1 \right] \right\}. \tag{3.59}$$

Now, since the function $\frac{(\Delta S_x)^2_{app}}{(\Delta S_x)^2_{CSS}} \left(\frac{\langle S_z \rangle_{app}}{\langle S_z \rangle_{CSS}} \right)$ is always forced to pass through the point $(1, 1)$, what we can do is to study its slope m there. Using eq.3.31a and 3.31b we get that

$$m(\nu) = \frac{\langle S_z \rangle_{CSS}}{(\Delta S_x)^2_{CSS}} = \frac{2\sqrt{2}\,\text{erf}\left(\frac{1}{2\nu}\right)}{\text{erf}\left(\frac{1}{\sqrt{2}\nu}\right)}, \tag{3.60}$$

and with such expression we can draw the next plot, where we study how the slope m changes varying the parameter ν.

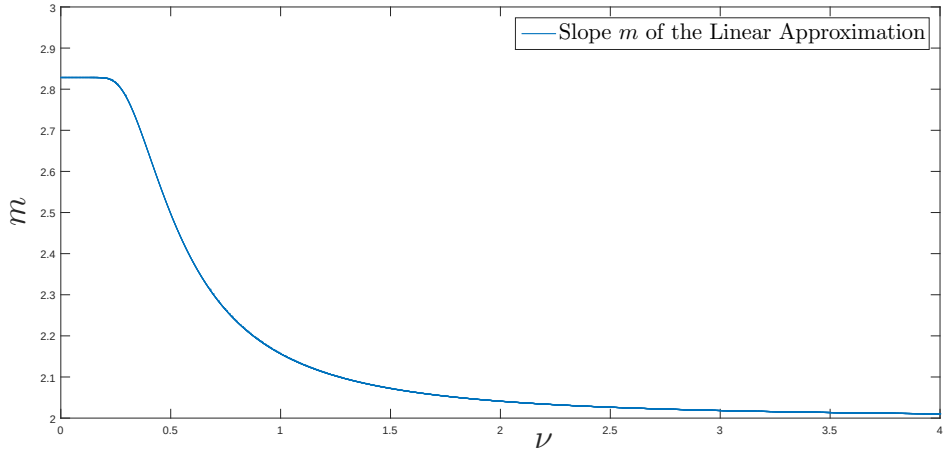

FIGURE 3.5: Slope of the linear approximation $\frac{(\Delta S_x)^2_{app}}{(\Delta S_x)^2_{CSS}} \left(\frac{\langle S_z \rangle_{app}}{\langle S_z \rangle_{CSS}} \right)$ varying ν

It seems that $m(\nu)$ is allowed to vary in the interval $\left[2, 2\sqrt{2}\right]$, and that it takes its smallest value for $\nu \to \infty$, while its biggest for $\nu = 0$. In fact, from the definition of the error function and its series expansion in eq.2.117, it follows that

$$m(\nu = 0) = \frac{2\sqrt{2}\,\text{erf}\,(\infty)}{\text{erf}\,(\infty)} = 2\sqrt{2} \tag{3.61a}$$

$$m(\nu \to \infty) = \frac{2\sqrt{2}\,\text{erf}\left(\frac{1}{2\nu}\right)}{\text{erf}\left(\frac{1}{\sqrt{2}\nu}\right)} \simeq \frac{2\sqrt{2}\left(\frac{2}{\sqrt{\pi}}\frac{1}{2\nu}\right)}{\left(\frac{2}{\sqrt{\pi}}\frac{1}{\sqrt{2}\nu}\right)} = 2, \tag{3.61b}$$

as wanted. We just need to check that $m(\nu)$ is monotonically decreasing; and this will be done through the derivative:

$$\frac{\partial m}{\partial \nu}(\nu) = \frac{e^{-\frac{1}{2\nu^2}} \overbrace{\left[4\,\mathrm{erf}\left(\frac{1}{2\nu}\right) - 2\sqrt{2}e^{\frac{1}{4\nu^2}}\,\mathrm{erf}\left(\frac{1}{\sqrt{2}\nu}\right)\right]}^{\mathcal{A}}}{\sqrt{\pi}\nu^2\,\mathrm{erf}^2\left(\frac{1}{\sqrt{2}\nu}\right)}. \tag{3.62}$$

Since ν is only allowed to be positive, the denominator of the last equation has to be bigger or equal than zero in all the domain of the function. Therefore, the sign of the derivative is determined by the numerator, and in particular by the term marked with $\mathcal{A}$.

We would like to prove $\mathcal{A} \leq 0$ for every possible ν. Now, as it is difficult to work with the error function, and since $m(\nu)$ appears to behave nicely (see fig.3.5), we will only check the sign of the derivative (i.e.: factor $\mathcal{A}$) for $\nu \to \infty$ and $\nu \to 0$.

- For $\nu \to \infty$ we can use the series expansions of the exponential and of the error function (eq.2.117):

$$\begin{aligned}
&\mathcal{A} = \\
&= 4\,\mathrm{erf}\left(\frac{1}{2\nu}\right) - 2\sqrt{2}e^{\frac{1}{4\nu^2}}\,\mathrm{erf}\left(\frac{1}{\sqrt{2}\nu}\right) \underset{\nu\to\infty}{\longrightarrow} \\
&\underset{\nu\to\infty}{\longrightarrow} 4\left(\frac{2}{\sqrt{\pi}}\frac{1}{2\nu}\right) - 2\sqrt{2}\left(1+\frac{1}{4\nu^2}\right)\left(\frac{2}{\sqrt{\pi}}\frac{1}{\sqrt{2}\nu}\right) = \\
&= -\frac{1}{\sqrt{\pi}\nu^3} \leq 0;
\end{aligned} \tag{3.63}$$

  so that we can conclude that m stretches to value 2 from above.

- For $\nu \to 0$ the error functions approaches to one, so that

$$\begin{aligned}
&\mathcal{A} = \\
&= 4\,\mathrm{erf}\left(\frac{1}{2\nu}\right) - 2\sqrt{2}e^{\frac{1}{4\nu^2}}\,\mathrm{erf}\left(\frac{1}{\sqrt{2}\nu}\right) \underset{\nu\to 0}{\longrightarrow} \\
&\underset{\nu\to 0}{\longrightarrow} 4 - 2\sqrt{2}e^{\frac{1}{4\nu^2}} \to -\infty.
\end{aligned} \tag{3.64}$$

In conclusion, we can say that $m(\nu)$ is a decreasing function in the two considered limits, and that it seems to take all values between $2\sqrt{2} \leq m < 2$.

Before starting the theoretical approach (just a matter of repeat what we have done here), let us summarize what we obtained. We supposed to have an experiment with a fixed number of particles N, described by coefficients $\{\eta_i\}$ following the probability

distribution $p(\eta)$. Given the system in a separable state, we determined which is the minimum of the variance $(\Delta S_x)^2$ for any possible value of the average spin $\langle S_z \rangle$. In our particular case, we found some difficulties to obtain a function of $(\Delta S_x)^2$ explicitly dependent on $\langle S_z \rangle$, but we solved this problem in a linear approximation. Thus, whit a set of experimental data, we have a powerful method to discern if the system is entangled (squeezed) or not.

3.2 Theory

Here there are many levels of generality we can achieve. The easiest one is the one we used in our previous example, where we have a fixed number of particles and the coefficients $\{\eta_i\}$ are not varying in time. But clearly these are not reasonable requests if we are dealing with repeated runs of the same experimental setup, where particles are "free" to move, not only within the box, but even in and outside it. In the next sections we will give a formal procedure to follow, in order to obtain results similar to the one showed in Table 3.2 for a generic probability distribution $p(\eta)$ and for a varying number of particles N.

3.2.1 Fixed N, fixed $\{\eta_i\}$

The first case we will study is the one in which we deal with an ideal experiment where the number N and the probability distribution function $p(\eta)$ describing the particles are not varying in time. In other words, we will obtain the same results we gave in section 3.1.2, for generic $p(\eta)$ and $p(\eta^2)$. We recall here that, even if we are calling $p(\eta)$ and $p(\eta^2)$ with the same letter "p", they refer to two different functions; we use this notation just for simplicity.

Therefore, let $p(\eta)$ and $p(\eta^2)$ be our probability distribution functions. In the hypothesis in which the particles are *not* interacting, i.e.: they are independent, the central limit theorem allows us to take the conclusion

$$\sum_{i=1}^{N} \eta_i \overset{Thm\ 1}{=} N\bar{\eta} = \int_{-\infty}^{\infty} \eta p(\eta) d\eta \tag{3.65a}$$

$$\sum_{i=1}^{N} \eta_i^2 \overset{Thm\ 1}{=} N\bar{\eta^2} = \int_{-\infty}^{\infty} \eta^2 p(\eta^2) d\eta^2. \tag{3.65b}$$

Moreover, let us remember that for a generic separable state we found that

$$(\Delta S_x)^2 = \frac{1}{4}\sum_k p_k \sum_{i=1}^{N} \eta_i^2 \cos^2\theta_{i,k} \tag{3.66a}$$

$$\langle S_z\rangle = \frac{1}{2}\sum_k p_k \sum_{i=1}^{N} \eta_i \cos\theta_{i,k}, \tag{3.66b}$$

as derived in eq.2.70 and 2.71. Again, all the $\theta_{i,k}$, in principle, are allowed to vary between $[0,\pi]$, but we restrict this domain to $\left[0,\frac{\pi}{2}\right]$ for the same reasons explained in section 2.2.2.3. In fact, our goal is to determine the minimum value that the variance $(\Delta S_x)^2$ can assume given any value of the spin $\langle S_z\rangle$. This will be performed using the (modified) Lagrange method; introducing (again, as in eq.3.6) the function

$$\Gamma(\{\eta_i\},\{\theta_{i,k}\},\mu) = (\Delta S_x)^2 - \mu\langle S_z\rangle = \frac{1}{4}\sum_k p_k \sum_{i=1}^{N} \eta_i^2 \cos^2\theta_{i,k} - \frac{\mu}{2}\sum_k p_k \sum_{i=1}^{N} \eta_i \cos\theta_{i,k}, \tag{3.67}$$

we want now to find its lowest value $\Gamma_{Min}(\{\eta_i\},\mu)$, in order to achieve our goal. Being, by definition, $\Gamma_{Min}(\{\eta_i\},\mu)$ the minimum of $\Gamma(\{\eta_i\},\{\theta_{i,k}\},\mu)$ with respect to the variables $\{\theta_{i,k}\}$, we have that

$$(\Delta S_x)^2 = \Gamma(\{\eta_i\},\{\theta_{i,k}\},\mu) + \mu\langle S_z\rangle \geq \Gamma_{Min}(\{\eta_i\},\mu) + \mu\langle S_z\rangle. \tag{3.68}$$

In other words, we are able to find a curve that saturate the inequality in eq.3.68:

$$(\Delta S_x)^2 = \Gamma_{Min}(\{\eta_i\},\mu) + \mu\langle S_z\rangle. \tag{3.69}$$

For the sake of clarity, let us explain that in the last equation 3.69 the *only* variable is μ (the coefficients $\{\eta_i\}$ are to be considered fixed), not only for Γ, but for $(\Delta S_x)^2$ and for $\langle S_z\rangle$ as well. In fact, once we impose the constraint that lead Γ to Γ_{Min}, we loose the dependence over the $\{\theta_{i,k}\}$ for all the terms.
Let us now explain how to find $\Gamma_{Min}(\{\eta_i\},\mu)$. First, due to eq.3.66a and 3.66b, we can deduce that $\Gamma_{Min}(\{\eta_i\},\{\theta_{i,k}\},\mu)$ is periodic and continuous in the variables $\{\theta_{i,k}\}$, so that its minimum has to be located in one of the stationary point, found through the derivative:

$$\frac{\partial\Gamma(\{\theta_{i,k}\})}{\partial\theta_{j,l}} = \frac{p_l\eta_j\sin\theta_{j,l}}{2}\left(\mu - \eta_j\cos\theta_{j,l}\right). \tag{3.70}$$

Without repeating ourselves too much, let us say that the constraint $\frac{\partial\Gamma(\{\theta_{i,k}\})}{\partial\theta_{j,l}} = 0$ leads to the two conditions

$$\sin\theta_{j,l} = 0 \tag{3.71a}$$

$$\eta_j \cos\theta_{j,l} = \mu, \text{ for } \mu \leq \eta_j, \tag{3.71b}$$

where both of them are to be verified, depending on μ. Recall that we can consider μ to be positive, since for negative values we necessarily have that Γ increases, as it is clear from eq.3.67. More in particular, with the aid of the second derivative, in the previous section we found that (equations 3.12a, 3.12b and 3.12c):

1. For $\mu \leq \min\{\eta_i\}$ the condition expressed by eq.3.71a is always verified, so that

$$\Gamma_{Min} = -\frac{\mu^2 N}{4} \tag{3.72}$$

and

$$\langle S_z\rangle = \frac{\mu N}{2} \tag{3.73a}$$

$$(\Delta S_x)^2 = \frac{\mu^2 N}{4}. \tag{3.73b}$$

2. The case given by $\min\{\eta_i\} < \mu \leq \min\{\eta_i\}$ is, again, the most complicated. In fact, both constraints 3.71a and 3.71b are verified; the first one for all the particles described by coefficients η_i bigger or equal than μ, the second strictly smaller. As consequence we have that

$$\Gamma_{Min} = \frac{1}{4}\left(\sum_{\mu^2\leq\eta_i^2}\mu^2 + \sum_{\mu^2>\eta_i^2}\eta_i^2\right) - \frac{\mu}{2}\left(\sum_{\mu\leq\eta_i}\mu + \sum_{\mu>\eta_i}\eta_i\right) \tag{3.74}$$

and

$$\langle S_z\rangle = \frac{1}{2}\left(\sum_{\mu\leq\eta_i}\mu + \sum_{\mu>\eta_i}\eta_i\right) \tag{3.75a}$$

$$(\Delta S_x)^2 = \frac{1}{4}\left(\sum_{\mu^2\leq\eta_i^2}\mu^2 + \sum_{\mu^2>\eta_i^2}\eta_i^2\right); \tag{3.75b}$$

the significance of these terms has been explained before. In short, we had to split the sums describing $\langle S_z\rangle$ and $(\Delta S_x)^2$ in two, due to the fact that we have two constraints.

3. For $\mu > \max\{\eta_i\}$ the condition expressed by eq.3.71b is always verified, so that

$$\Gamma_{Min} = \frac{1}{4}\sum_{i=1}^{N}\eta_i^2 - \frac{\mu}{2}\sum_{i=1}^{N}\eta_i \tag{3.76}$$

and

$$\langle S_z\rangle = \frac{1}{2}\sum_{i=1}^{N}\eta_i \tag{3.77a}$$

$$(\Delta S_x)^2 = \frac{1}{4}\sum_{i=1}^{N}\eta_i^2. \tag{3.77b}$$

As it is possible to see, here μ is *not* present in the expressions for $(\Delta S_x)^2$ and $\langle S_z\rangle$; in fact all the range in which both of them are allowed to vary is exhausted, and now they remain constant to their maximum.

What we just obtained is exactly Table 3.1, that for completeness we copy here:

Range	$\mu \leq \min\{\eta_i\}$	$\min\{\eta_i\} < \mu \leq \max\{\eta_i\}$	$\mu > \max\{\eta_i\}$
$\langle S_z\rangle$	$\frac{\mu N}{2}$	$\frac{1}{2}\left(\sum_{\mu\leq\eta_i}\mu + \sum_{\mu>\eta_i}\eta_i\right)$	$\frac{1}{2}\sum_{i=1}^{N}\eta_i$
$(\Delta S_x)^2$	$\frac{\mu^2 N}{4}$	$\frac{1}{4}\left(\sum_{\mu^2\leq\eta_i^2}\mu^2 + \sum_{\mu^2>\eta_i^2}\eta_i^2\right)$	$\frac{1}{4}\sum_{i=1}^{N}\eta_i^2$

TABLE 3.3: In this Table we collected the results for $\langle S_z\rangle$ and $(\Delta S_x)^2$ in the different ranges in which μ is allowed to vary

It is now of great interest, and actually our main goal, to derive expressions for the terms in Table 3.3 using the probability distributions functions $p(\eta)$ and $p(\eta^2)$. Therefore, let us just create a second list in which, for each point of it, we derive such expressions both for $\langle S_z\rangle$ and $(\Delta S_x)^2$. We will try to be concise, since the proceeding will be no different from the one already done in section 2.2.2.3 with the particular distributions we had there.

1. $\mu \leq \min\{\eta_i\}$

   - For $\langle S_z\rangle$ we have that
   $$\langle S_z\rangle = \frac{\mu N}{2}, \tag{3.78}$$
   - while for $(\Delta S_x)^2$:
   $$(\Delta S_x)^2 = \frac{\mu^2 N}{4}. \tag{3.79}$$

Here there is no need to plug in the additional informations given by the $p(\eta)$ and $p(\eta^2)$; the curve created by the couple $\left(\langle S_z\rangle, (\Delta S_x)^2\right)$ represents an impassable limit for all separable states. In other words, for all the probability distributions describing our particles, we can identify a range, going from zero to some value smaller than one, in which the curve described by eq.3.69 is following the same equation

$$(\Delta S_x)^2 = \frac{\langle S_z\rangle^2}{N}, \tag{3.80}$$

obtainable from eq.3.78 and 3.79. For being more precise, since the interval in which this holds is given by $\mu \in [0, \min\{\eta_i\}]$, we have that the previous equation is valid whenever

$$\langle S_z\rangle \in \left[0, \frac{N}{2}\min\{\eta_i\}\right], \tag{3.81}$$

as follows from eq.3.78.

2. $\min\{\eta_i\} < \mu \leq \max\{\eta_i\}$

   - Here $\langle S_z\rangle$ is given by

$$\langle S_z\rangle = \frac{1}{2}\left(\sum_{\mu\leq\eta_i}\mu + \sum_{\mu>\eta_i}\eta_i\right), \tag{3.82}$$

   so that we have to plug in $p(\eta)$. In fact, as already seen, the first of the two sums can be seen as:

$$\sum_{\mu\leq\eta_i}\mu = \mu\sum_{\mu\leq\eta_i}1, \tag{3.83}$$

   where $\sum_{\mu\leq\eta_i}1$ represents the number of particles $N(\mu\leq\eta)$ having coefficients $\eta_i \geq \mu$. In other words:

$$\sum_{\mu\leq\eta_i}\mu = \mu\sum_{\mu\leq\eta_i}1 = \mu N(\mu\leq\eta) = \mu NP(\mu\leq\eta), \tag{3.84}$$

   being $P(\mu\leq\eta)$ the probability of having $\eta\geq\mu$:

$$P(\mu\leq\eta) = \int_{\mu}^{\infty} p(\eta)d\eta. \tag{3.85}$$

   The second sum of eq.3.82 consists of all coefficients η_i's they are strictly smaller than μ. Therefore, in terms of $p(\eta)$:

$$\sum_{\mu>\eta_i}\eta_i \overset{Thm\ 1}{=} N(\mu>\eta)\bar{\eta}(\mu>\eta) = NP(\mu>\eta)\bar{\eta}(\mu>\eta), \tag{3.86}$$

where $N(\mu > \eta)$ is the number of particles having $\eta_i < \mu$, and as consequence $P(\mu > \eta)$ is the probability of having $\eta < \mu$. $\bar{\eta}(\mu > \eta)$ represents the average of η according to the truncated probability function $p_{tr}(\eta)$, obtained from $p(\eta)$ by:

$$p_{tr}(\eta) = \begin{cases} \frac{p(\eta)}{P(\mu>\eta)} & \text{if } \eta_{Min} \leq \eta \leq \mu \\ 0 & \text{if } \eta < \eta_{Min} \text{ or } \mu < \eta, \end{cases} \tag{3.87}$$

as we have seen in eq.3.19. η_{Min} is the smallest possible value that η can take, according to $p(\eta)$. In conclusion, we have that

$$\bar{\eta}(\mu > \eta) = \int_{-\infty}^{\infty} \eta p_{tr}(\eta) d\eta, \tag{3.88}$$

so that

$$\sum_{\mu>\eta_i} \eta_i = NP(\mu > \eta)\bar{\eta}(\mu > \eta) = N \int_{\eta_{Min}}^{\mu} \eta p(\eta) d\eta, \tag{3.89}$$

and finally (eq.3.84 and 3.89)

$$\begin{aligned} \langle S_z \rangle &= \frac{1}{2} \left[\mu N P(\mu \leq \eta) + NP(\mu > \eta)\bar{\eta}(\mu > \eta) \right] = \\ &= \frac{1}{2} \left(\mu N \int_{\mu}^{\infty} p(\eta) d\eta + N \int_{\eta_{Min}}^{\mu} \eta p(\eta) d\eta \right). \end{aligned} \tag{3.90}$$

We recall that, in general, the central limit theorem (theorem 1) is *not* always satisfied when $\mu \to \eta_{Min}$ in eq.3.86. Usually this fact is not important, since very likely in such limit

$$\sum_{\mu^2>\eta_i^2} \eta_i^2 \ll \sum_{\mu^2 \leq \eta_i^2} \mu^2, \tag{3.91}$$

as consequence of the facts $P(\mu > \eta) \to 0$ and $P(\mu \leq \eta) \to 1$. But there is the possibility that this does not hold for some exotic probability distribution $p(\eta)$, so that a control is always needed, or at least suggested.

- For $(\Delta S_x)^2$ the discussion proceeds analogously:

$$(\Delta S_x)^2 = \frac{1}{4} \left(\sum_{\mu^2 \leq \eta_i^2} \mu^2 + \sum_{\mu^2>\eta_i^2} \eta_i^2 \right), \tag{3.92}$$

where the first of the two sums can be seen as:

$$\sum_{\mu^2 \leq \eta_i^2} \mu^2 = \mu^2 \sum_{\mu^2 \leq \eta_i^2} 1 = \mu^2 N(\mu^2 \leq \eta^2) = \mu^2 NP(\mu^2 \leq \eta^2), \tag{3.93}$$

with $N(\mu^2 \leq \eta^2)$ representing the number of particles described by coefficients bigger or equal than μ. Consequently, $P(\mu^2 \leq \eta^2)$ is the probability of obtaining $\eta \geq \mu$, that, according to the definitions of $p(\eta)$ and $p(\eta^2)$, necessarily is equal to $P(\mu \leq \eta)$.
The second sum in eq.3.92 is given by

$$\sum_{\mu^2 > \eta_i^2} \eta_i^2 \overset{Thm\ 1}{=} N(\mu^2 > \eta^2)\bar{\eta^2}(\mu^2 > \eta^2) = NP(\mu^2 > \eta^2)\bar{\eta^2}(\mu^2 > \eta^2), \quad (3.94)$$

where $N(\mu^2 > \eta^2)$ and $P(\mu^2 > \eta^2)$ are what everyone is expecting from them and

$$\bar{\eta^2}(\mu^2 > \eta^2) = \int_{-\infty}^{\infty} \eta^2 p_{tr}(\eta^2) d\eta^2. \quad (3.95)$$

In this case $p_{tr}(\eta^2)$ is defined as

$$p_{tr}(\eta^2) = \begin{cases} \frac{p(\eta^2)}{P(\mu^2 > \eta^2)} & \text{if } \eta_{Min}^2 \leq \eta^2 \leq \mu^2 \\ 0 & \text{if } \eta^2 < \eta_{Min}^2 \text{ or } \mu^2 < \eta^2, \end{cases}, \quad (3.96)$$

so that, in conclusion:

$$\begin{aligned} (\Delta S_x)^2 &= \frac{1}{4}\left[\mu^2 NP(\mu^2 \leq \eta^2) + NP(\mu^2 > \eta^2)\bar{\eta^2}(\mu^2 > \eta^2)\right] = \\ &= \frac{1}{4}\left(\mu^2 N \int_{\mu^2}^{\infty} p(\eta^2) d\eta^2 + N \int_{\eta_{Min}}^{\mu} \eta^2 p(\eta^2) d\eta^2\right). \end{aligned} \quad (3.97)$$

Naturally, the same considerations about the central limit theorem, used for eq.3.94, are to be taken, and the same precautions adopted.

3. $\mu > \max\{\eta_i\}$
This is probably the less interesting case, since for any value of μ satisfying this constraint, $\langle S_z \rangle$ and $(\Delta S_x)^2$ are constant. Both of them have spanned their own range, namely $[0, \langle S_z \rangle_{CSS}]$ and $\left[0, (\Delta S_x)^2_{CSS}\right]$ in the previous two points, so that they reached their maximum and keep it fixed. Written in mathematical language we have

$$\langle S_z \rangle = \langle S_z \rangle_{CSS} = \frac{1}{2}\sum_{i=1}^{N} \eta_i = \frac{N}{2}\bar{\eta} \quad (3.98a)$$

$$(\Delta S_x)^2 = (\Delta S_x)^2_{CSS} = \frac{1}{4}\sum_{i=1}^{N} \eta_i^2 = \frac{N}{4}\bar{\eta^2}, \quad (3.98b)$$

where $\bar{\eta}$ and $\bar{\eta^2}$ are given by eq.3.65a and 3.65b.

At this point we probably are able to give the most interesting result of this section, namely Table 3.3 with the boxes filled with the new results we just obtained:

Range	$\mu \leq \min\{\eta_i\}$	$\min\{\eta_i\} < \mu \leq \max\{\eta_i\}$	$\mu > \max\{\eta_i\}$
$\langle S_z \rangle$	$\frac{\mu N}{2}$	$\frac{1}{2}\left[\mu N P(\mu \leq \eta) + N P(\mu > \eta)\bar{\eta}(\mu > \eta)\right]$	$\frac{N}{2}\bar{\eta}$
$(\Delta S_x)^2$	$\frac{\mu^2 N}{4}$	$\frac{1}{4}\left[\mu^2 N P(\mu^2 \leq \eta^2) + N P(\mu^2 > \eta^2)\bar{\eta^2}(\mu^2 > \eta^2)\right]$	$\frac{N}{4}\bar{\eta^2}$

TABLE 3.4: $\langle S_z \rangle$ and $(\Delta S_x)^2$ in the different ranges in which μ is allowed to vary, for a generic probability distribution function $p(\eta)$.

And now, just like in section 3.1.2, we are able to plot the curve such that for any value of $\langle S_z \rangle$ associates the smallest possible $(\Delta S_x)^2$, for a separable state. If we are lucky, we are able to obtain this curve analytically; otherwise we can draw it numerically. This depends on the probability distribution functions $p(\eta)$ and $p(\eta^2)$, they can give rise to very nasty functions inside Table 3.4.

3.2.2 Varying N, fixed $\{\eta_i\}$

What if we do not know exactly how many particles there are inside our experimental setup? We will use a little trick: we imagine that the time needed for performing the experiment is short enough for *not* letting any particle to come in or outside the box. This way, the generalization becomes very easy: we just need to evaluate the number of particles $\bar{N}$ inside the box at the moment of the experiment, and later perform the same analysis of before. In fact, once we fix the number of particles, it is just a matter of following the same step as in previous section 3.2.1 replacing N with our estimator $\bar{N}$. This way, Table 3.4 becomes:

Range	$\mu \leq \min\{\eta_i\}$	$\min\{\eta_i\} < \mu \leq \max\{\eta_i\}$	$\mu > \max\{\eta_i\}$
$\langle S_z \rangle$	$\frac{\mu \bar{N}}{2}$	$\frac{1}{2}\left[\mu \bar{N} P(\mu \leq \eta) + \bar{N} P(\mu > \eta)\bar{\eta}(\mu > \eta)\right]$	$\frac{\bar{N}}{2}\bar{\eta}$
$(\Delta S_x)^2$	$\frac{\mu^2 \bar{N}}{4}$	$\frac{1}{4}\left[\mu^2 \bar{N} P(\mu^2 \leq \eta^2) + \bar{N} P(\mu^2 > \eta^2)\bar{\eta^2}(\mu^2 > \eta^2)\right]$	$\frac{\bar{N}}{4}\bar{\eta^2}$

TABLE 3.5: Generalization of Table 3.4 for the case in which the number of particles is not precisely known.

Let us now discuss two important point relevant to this section. The first one concerns how to estimate N in order to get $\bar{N}$, while the second repeated measurements.

The natural way for obtaining $\bar{N}$ is to suppose that there exists a probability distribution function $p(N)$ describing the number of particles. In the easiest case this distribution will be a Gaussian peaked on its average $\bar{N}$, but there could easily be some complications. An example, given by the real life, is that the incoming laser has a small probability to act up, so that it does not detect a percentage of the particles inside

the box. This malfunction can be modelled by saying that we have less particle in the setup. Now, if this percentage of "lost" particles is fixed, we can model this behaviour by saying that the probability distribution function for N presents two peaks: one for all the times in which the laser works properly, the other for the ones in which it does not.

Let us now speak about repeated measurements. It is very common, when people deal with the experiments, that a result is obtained through the average of many runs. Now, for any of these run, we must admit that we could not have the control of the number of particles, we can just estimate it! In this case we can, again, rely on the central limit theorem; in fact we are dealing here with repeated measurements of one system that, run after run, presents the same statistical properties. Then, according to theorem 1, the mean of these measurements converge to the normal distribution having the average of any single run. As a consequence, Table 3.5 is still valid if we need to check the result obtained with a big number of repeated measurements.
Moreover, if the function $f\left(\frac{\langle S_z\rangle}{\langle S_z\rangle_{CSS}}\right)$, expressing the lowest bound for $\frac{(\Delta S_x)^2}{(\Delta S_x)^2_{CSS}}$, is convex, then its average over repeated runs of the experiment can only take a bigger value than the one we would obtain with a single run with the same normalized spin $\overline{\left(\frac{\langle S_z\rangle}{\langle S_z\rangle_{CSS}}\right)}$. Here, supposing we have M trials, each of them denoted with letter "i", we have used the notation:

$$\overline{\left(\frac{\langle S_z\rangle}{\langle S_z\rangle_{CSS}}\right)} = \frac{1}{M}\sum_{i=1}^{M}\frac{\langle S_z\rangle_i}{\langle S_z\rangle_{i_{CSS}}}. \tag{3.99}$$

Notice that, as the number of particles varies, $\langle S_z\rangle_{i_{CSS}}$ is not fixed run after run; for this reason we appended to it the subscript "i". The proof comes straightforward: $\overline{\left(\frac{(\Delta S_x)^2}{(\Delta S_x)^2_{CSS}}\right)}$ being the value that the normalized variance get by averaging the results we obtained running the experiment many times,

$$\begin{aligned}\overline{\left(\frac{(\Delta S_x)^2}{(\Delta S_x)^2_{CSS}}\right)} = \frac{1}{M}\sum_{i=1}^{M}\frac{(\Delta S_x)^2_i}{(\Delta S_x)^2_{i_{CSS}}} \geq \frac{1}{M}\sum_{i=1}^{M} f\left(\frac{\langle S_z\rangle_i}{\langle S_z\rangle_{i_{CSS}}}\right) \overset{\text{convexity}}{\geq} \\ \overset{\text{convexity}}{\geq} f\left(\frac{1}{M}\sum_{i=1}^{M}\frac{\langle S_z\rangle_i}{\langle S_z\rangle_{i_{CSS}}}\right) = f\left(\overline{\frac{\langle S_z\rangle}{\langle S_z\rangle_{CSS}}}\right).\end{aligned} \tag{3.100}$$

This is always true; but let us think about the assumption we made in this last equation. We defined

$$\overline{\left(\frac{(\Delta S_x)^2}{(\Delta S_x)^2_{CSS}}\right)} = \frac{1}{M}\sum_{i=1}^{M}\frac{(\Delta S_x)^2_i}{(\Delta S_x)^2_{i_{CSS}}}, \tag{3.101}$$

that means that we need to know, for any experimental shot "i", which is the maximum value $(\Delta S_x)^2_{i_{CSS}}$ for the variance. This assumption clearly exceed our possibilities, since, if the number of particles is oscillating, we can only guess what $(\Delta S_x)^2_{i_{CSS}}$ is, being it

dependent over N. Therefore, a more general proof comes by defining

$$\overline{\left(\frac{(\Delta S_x)^2}{(\Delta S_x)^2_{CSS}}\right)} = \frac{\overline{(\Delta S_x)^2}}{\overline{(\Delta S_x)^2_{CSS}}} \tag{3.102a}$$

$$\overline{\left(\frac{\langle S_z\rangle}{\langle S_z\rangle_{CSS}}\right)} = \frac{\overline{\langle S_z\rangle}}{\overline{\langle S_z\rangle_{CSS}}}, \tag{3.102b}$$

where:

$$\overline{\langle S_z\rangle} = \langle S_z\rangle_{exp} = \sum_{N=0}^{\infty} p_N \langle S_z\rangle_{exp} \tag{3.103a}$$

$$\overline{\langle S_z\rangle_{CSS}} = \sum_{N=0}^{\infty} p_N \langle S_z(N)\rangle_{CSS} = \frac{\sum_{N=0}^{\infty} p_N \sum_{i=1}^{N} \eta_i}{2} \overset{\dagger}{=} \frac{\sum_{N=0}^{\infty} p_N N\bar{\eta}}{2} \tag{3.103b}$$

$$\overline{(\Delta S_x)^2} = (\Delta S_x)^2_{exp} = \sum_{N=0}^{\infty} p_N \, (\Delta S_x)^2_{exp} \tag{3.103c}$$

$$\overline{(\Delta S_x)^2_{CSS}} = \sum_{N=0}^{\infty} p_N \, (\Delta S_x)^2_{CSS}\,(N) = \frac{\sum_{N=0}^{\infty} p_N \sum_{i=1}^{N} \eta_i^2}{4} \overset{\dagger}{=} \frac{\sum_{N=0}^{\infty} p_N N\bar{\eta^2}}{4}. \tag{3.103d}$$

Here, appendix "$_{exp}$" refers to the averages obtained experimentally (in M runs):

$$\langle S_z\rangle_{exp} = \frac{\sum_{i=1}^{M} \langle S_z\rangle_i}{M} \tag{3.104a}$$

$$(\Delta S_x)^2_{exp} = \frac{\sum_{i=1}^{M} (\Delta S_x)^2_i}{M}, \tag{3.104b}$$

while letter "N" to the number of particles. Therefore $\langle S_z(N)\rangle_{CSS}$ and $(\Delta S_x)^2_{CSS}\,(N)$ are, respectively, the maxima spin average and variance, given a setup with N atoms (as stated in eq.3.103b and 3.103d). p_N represents the probability of having N particles; these coefficients can be determined through the distribution function $p(N)$ and clearly we must have $\sum_{N=0}^{\infty} p_N = 1$. As a conclusive comment of the last set of equations 3.103a, 3.103b, 3.103c and 3.103d, let us say that the two equalities marked with †, where we used the central limit theorem, are allowed *only if* the probability distribution functions $p(\eta)$ and $p(\eta^2)$ are not dependent over the number of particles N. In fact, if it is not the case, we would not be able to plug in the averages $\bar{\eta}$ and $\bar{\eta^2}$, being them varying with N.

At this point we have, following similar passages as in eq.3.100:

$$\begin{aligned}
\overline{\left(\frac{(\Delta S_x)^2}{(\Delta S_x)^2_{CSS}}\right)} &= \frac{\overline{(\Delta S_x)^2}}{\overline{(\Delta S_x)^2_{CSS}}} = \frac{\sum_{N=0}^{\infty} p_N (\Delta S_x)^2_{exp}}{\sum_{K=0}^{\infty} p_K (\Delta S_x)^2_{CSS}(K)} = \\
&= \frac{\sum_{N=0}^{\infty} p_N (\Delta S_x)^2_{CSS}(N) \frac{(\Delta S_x)^2_{exp}}{(\Delta S_x)^2_{CSS}(N)}}{\sum_{K=0}^{\infty} p_K (\Delta S_x)^2_{CSS}(K)} \overset{\dagger\dagger}{\geq} \\
&\overset{\dagger\dagger}{\geq} \frac{\sum_{N=0}^{\infty} p_N (\Delta S_x)^2_{CSS}(N) f\left(\frac{\langle S_z\rangle_{exp}}{\langle S_z(N)\rangle_{CSS}}\right)}{\sum_{K=0}^{\infty} p_K (\Delta S_x)^2_{CSS}(K)} \overset{convexity}{\geq} \\
&\overset{convexity}{\geq} f\left(\frac{\sum_{N=0}^{\infty} p_N (\Delta S_x)^2_{CSS}(N) \frac{\langle S_z\rangle_{exp}}{\langle S_z(N)\rangle_{CSS}}}{\sum_{K=0}^{\infty} p_K (\Delta S_x)^2_{CSS}(K)}\right) = \\
&= f\left(\frac{\sum_{N=0}^{\infty} p_N N \bar{\eta^2} \frac{2\langle S_z\rangle_{exp}}{N\bar{\eta}}}{\sum_{K=0}^{\infty} p_K K \bar{\eta^2}}\right) = \\
&= f\left(\frac{2\sum_{N=0}^{\infty} p_N \langle S_z\rangle_{exp}}{\sum_{K=0}^{\infty} p_K K \bar{\eta}}\right) = f\left(\frac{\sum_{N=0}^{\infty} p_N \langle S_z\rangle_{exp}}{\sum_{K=0}^{\infty} p_K \langle S_z(K)\rangle_{CSS}}\right) = \\
&= f\left(\frac{\overline{\langle S_z\rangle}}{\overline{\langle S_z\rangle_{CSS}}}\right) = f\left(\overline{\frac{\langle S_z\rangle}{\langle S_z\rangle_{CSS}}}\right).
\end{aligned} \tag{3.105}$$

The relation marked with †† follows from eq.3.100, with $(\Delta S_x)^2_{i_{CSS}} = (\Delta S_x)^2_{CSS}(N)$ for all $i = 1, ..., M$.

We just found, again and with more general hypothesis, that $\overline{\left(\frac{(\Delta S_x)^2}{(\Delta S_x)^2_{CSS}}\right)} \geq f\left(\overline{\frac{\langle S_z\rangle}{\langle S_z\rangle_{CSS}}}\right)$. Therefore, and this is a very important result, it is *not* possible to break down the theoretical curve f (derived thanks to Table 3.5) by averaging many times the outcomes of an experimental setup, at least when the probability distribution functions for the coefficients $\{\eta_i\}$ are not dependent over the particles number N. In the case this condition does not hold, it would be necessary to check if the same conclusion can be taken or not.

3.2.3 N not fixed and $\{\eta_i\}$ varying in time

As a conclusion of this theoretical part, let us consider the case in which some of the probability distributions we are dealing with here - namely $p(\eta)$ and $p(\eta^2)$ - are allowed to vary in time. This generalized model should be used whenever the experimental setup

changes during the measurement, but still we suppose there are no fluctuations on the number of particles during a single run.
Since now time is a variable, let us rewrite:

$$p(\eta) \to p(\eta, t) \tag{3.106a}$$

$$p(\eta^2) \to p(\eta^2, t), \tag{3.106b}$$

where for any value of t these functions represent probability distribution functions. The means of all these variables at t is thus given by:

$$\bar{\eta}(t) = \int_{-\infty}^{\infty} \eta p(\eta, t) d\eta \tag{3.107a}$$

$$\bar{\eta^2}(t) = \int_{-\infty}^{\infty} \eta^2 p(\eta^2, t) d\eta^2. \tag{3.107b}$$

Now, since the time is *not* dependent on η and η^2, if we want to determine the expected value of any of these quantities in some time interval, the only thing we have to do is to average, so that:

$$\bar{\eta}_T = \frac{\int_{t_1}^{t_2} \bar{\eta}(t) dt}{t_2 - t_1} \tag{3.108a}$$

$$\bar{\eta^2}_T = \frac{\int_{t_1}^{t_2} \bar{\eta^2}(t) dt}{t_2 - t_1}. \tag{3.108b}$$

In these last equations, we used the appendix "$_T$" to refer to the averages in some time interval $T = t_2 - t_1$. Now, supposing T represents the duration of the measurement, what we should do is to generalize Table 3.3 first and Table 3.4 later for these time dependent probability distributions.
The previous one does not present any difference, except the fact that now, instead of N, we have the mean value $\bar{N}$, just like in the previous section 3.2.2. The real difference can be found once we plug in the probability distribution functions, in order to obtain the last Table. In fact, following the same steps as before (the only difference here is that we need to integrate over time as well), we can get:

Range	$\mu \leq \min\{\eta_i\}$	$\min\{\eta_i\} < \mu \leq \max\{\eta_i\}$	$\mu > \max\{\eta_i\}$
$\langle S_z \rangle$	$\frac{\mu\bar{N}}{2}$	$\frac{1}{2}\left[\mu\bar{N}P_T(\mu \leq \eta) + \bar{N}P_T(\mu > \eta)\bar{\eta}_T(\mu > \eta)\right]$	$\frac{\bar{N}}{2}\bar{\eta}_T$
$(\Delta S_x)^2$	$\frac{\mu^2\bar{N}}{4}$	$\frac{1}{4}\left[\mu^2\bar{N}P_T(\mu^2 \leq \eta^2) + \bar{N}P_T(\mu^2 > \eta^2)\bar{\eta^2}_T(\mu^2 > \eta^2)\right]$	$\frac{\bar{N}}{4}\bar{\eta^2}_T$

TABLE 3.6: Generalization of Table 3.4 for the case in which the number of particles is not precisely known, and the probability distribution functions describing the coefficients are time dependent. T refers to the needed time for getting the measurement.

In this conclusive Table, as it is possible to guess, we used the appendix $_T$ to indicate the time average of the correspondent quantities, just as in eq.3.108a and 3.108b.

Chapter 4

How "good" is the entanglement?

So far, we have introduced the new measurement operator $\vec{S} = \sum \eta_i \vec{J}_i$, with which we proved that the inequality $\xi^2 \geq 1$ is not valid any more. Subsequently, using a more general argument, we derived the relation between $(\Delta S_x)^2$ and $\langle S_z \rangle$ for a generic separable state. This has been done for any probability distribution $p(\eta)$ regarding the coefficients $\{\eta_i\}$ and under different hypotheses in section 3.2. Here we will try to give an answer to the question: "What about entanglement?"
As we will see, it is extremely hard to get a similar result even for the simplest case of two particle entanglement. In the following, we will study the two particles case and try to generalize it step after step.

4.1 2-particle entanglement

Let us suppose we have only two particles, and that these can be entangled. Expecting, as usual, to have a two level system, a basis would be given by

$$\{|\uparrow\uparrow\rangle, |\uparrow\downarrow\rangle, |\downarrow\uparrow\rangle, |\downarrow\downarrow\rangle\}, \tag{4.1}$$

where the first arrow in every element refers to the first particle and the second to the second. Therefore a generic state $|\psi\rangle$ describing the system would be:

$$|\psi\rangle = C_{\uparrow\uparrow}|\uparrow\uparrow\rangle + C_{\downarrow\uparrow}|\uparrow\downarrow\rangle + C_{\uparrow\downarrow}|\downarrow\uparrow\rangle + C_{\downarrow\downarrow}|\downarrow\downarrow\rangle, \tag{4.2}$$

with normalization criterion given by $|C_{\uparrow\uparrow}|^2 + |C_{\downarrow\uparrow}|^2 + |C_{\uparrow\downarrow}|^2 + |C_{\downarrow\downarrow}|^2 = 1$. The four coefficients marked with C are in general complex numbers.
What we should do now is to obtain some expressions for $(\Delta S_x)^2$ and $\langle S_z \rangle$ regarding the state described in eq.4.2. Once we have them, the proceeding is analogous to what

we have done in section 3.1; we will use the modified Lagrange multiplier method in order to obtain the curve minimizing $(\Delta S_x)^2$ with respect to $\langle S_z \rangle$. At the end we will compare this curve to the one obtained for the corresponding separable state. We have that:

- $S_z = \eta_1 j_{z_1} + \eta_2 j_{z_2}$. Computing term by term we have that:

$$\begin{aligned}\langle j_{z_1} \rangle = \langle j_{z_1} \otimes \mathbb{I}_2 \rangle = \langle \psi | j_{z_1} \otimes \mathbb{I}_2 | \psi \rangle = \\ = \left[C^*_{\uparrow\uparrow} \langle \uparrow\uparrow | + C^*_{\downarrow\uparrow} \langle \uparrow\downarrow | + C^*_{\uparrow\downarrow} \langle \downarrow\uparrow | + C^*_{\downarrow\downarrow} \langle \downarrow\downarrow | \right] \times (j_{z_1} \otimes \mathbb{I}_2) \times \\ \times \left[C_{\uparrow\uparrow} | \uparrow\uparrow \rangle + C_{\downarrow\uparrow} | \uparrow\downarrow \rangle + C_{\uparrow\downarrow} | \downarrow\uparrow \rangle + C_{\downarrow\downarrow} | \downarrow\downarrow \rangle \right] \overset{\dagger}{=} \\ \overset{\dagger}{=} \frac{1}{2} \left(|C_{\uparrow\uparrow}|^2 + |C_{\uparrow\downarrow}|^2 - |C_{\downarrow\uparrow}|^2 - |C_{\downarrow\downarrow}|^2 \right).\end{aligned} \tag{4.3}$$

The equality marked with † is a consequence of the fact that

$$\begin{aligned}j_{z_1} \otimes \mathbb{I}_2 = \left(\frac{|\uparrow\rangle_1\langle\uparrow| - |\downarrow\rangle_1\langle\downarrow|}{2} \right) \otimes (|\uparrow\rangle_2\langle\uparrow| + |\downarrow\rangle_2\langle\downarrow|) = \\ = \frac{|\uparrow\uparrow\rangle\langle\uparrow\uparrow| + |\uparrow\downarrow\rangle\langle\uparrow\downarrow| - |\downarrow\uparrow\rangle\langle\downarrow\uparrow| - |\downarrow\downarrow\rangle\langle\downarrow\downarrow|}{2},\end{aligned} \tag{4.4}$$

where, for example, $|\uparrow\rangle_1\langle\uparrow|$ refers to the projection operator acting only over the first particle. Remembering the orthonormal property of the basis, it is now straightforward to obtain how the last equality in eq.4.3 is obtained.
Following the same steps we can now determine

$$\langle j_{z_2} \rangle = \langle \mathbb{I}_1 \otimes j_{z_2} \rangle = \frac{1}{2} \left(|C_{\uparrow\uparrow}|^2 - |C_{\uparrow\downarrow}|^2 + |C_{\downarrow\uparrow}|^2 - |C_{\downarrow\downarrow}|^2 \right), \tag{4.5}$$

where the sign difference follows directly writing down

$$\mathbb{I}_1 \otimes j_{z_2} = \frac{|\uparrow\uparrow\rangle\langle\uparrow\uparrow| - |\uparrow\downarrow\rangle\langle\uparrow\downarrow| + |\downarrow\uparrow\rangle\langle\downarrow\uparrow| - |\downarrow\downarrow\rangle\langle\downarrow\downarrow|}{2}. \tag{4.6}$$

In conclusion, from eq.4.3 and 4.5, we have that

$$\begin{aligned}\langle S_z \rangle = \langle \eta_1 j_{z_1} + \eta_2 j_{z_2} \rangle = \eta_1 \langle j_{z_1} \rangle + \eta_2 \langle j_{z_2} \rangle = \\ = \frac{\eta_1}{2} \left(|C_{\uparrow\uparrow}|^2 + |C_{\uparrow\downarrow}|^2 - |C_{\downarrow\uparrow}|^2 - |C_{\downarrow\downarrow}|^2 \right) + \frac{\eta_2}{2} \left(|C_{\uparrow\uparrow}|^2 - |C_{\uparrow\downarrow}|^2 + |C_{\downarrow\uparrow}|^2 - |C_{\downarrow\downarrow}|^2 \right).\end{aligned} \tag{4.7}$$

- $S_x = \eta_1 j_{x_1} + \eta_2 j_{x_2}$. Skipping some mathematical steps identical as before, we can obtain that, in this case,

$$\begin{aligned} j_{x_1} \otimes \mathbb{I}_2 &= \left(\frac{|\uparrow\rangle_1\langle\downarrow| + |\downarrow\rangle_1\langle\uparrow|}{2} \right) \otimes (|\uparrow\rangle_2\langle\uparrow| + |\downarrow\rangle_2\langle\downarrow|) = \\ &= \frac{|\uparrow\uparrow\rangle\langle\downarrow\uparrow| + |\uparrow\downarrow\rangle\langle\downarrow\downarrow| + |\downarrow\uparrow\rangle\langle\uparrow\uparrow| + |\downarrow\downarrow\rangle\langle\uparrow\downarrow|}{2}; \end{aligned} \tag{4.8}$$

as consequence:

$$\begin{aligned} \langle j_{x_1} \rangle &= \langle j_{x_1} \otimes \mathbb{I}_2 \rangle = \langle \psi | j_{x_1} \otimes \mathbb{I}_2 | \psi \rangle = \\ &= \frac{1}{2} \left(C^*_{\uparrow\uparrow} C_{\downarrow\uparrow} + C^*_{\uparrow\downarrow} C_{\downarrow\downarrow} + C^*_{\downarrow\uparrow} C_{\uparrow\uparrow} + C^*_{\downarrow\downarrow} C_{\uparrow\downarrow} \right) = \\ &= \frac{1}{2} \left[C^*_{\uparrow\uparrow} C_{\downarrow\uparrow} + \left(C^*_{\uparrow\uparrow} C_{\downarrow\uparrow} \right)^* + C^*_{\uparrow\downarrow} C_{\downarrow\downarrow} + \left(C^*_{\uparrow\downarrow} C_{\downarrow\downarrow} \right)^* \right] = \\ &= \Re(C^*_{\uparrow\uparrow} C_{\downarrow\uparrow}) + \Re(C^*_{\uparrow\downarrow} C_{\downarrow\downarrow}) = \\ &= [\Re(C_{\uparrow\uparrow})\Re(C_{\downarrow\uparrow}) + \Im(C_{\uparrow\uparrow})\Im(C_{\downarrow\uparrow})] + [\Re(C_{\uparrow\downarrow})\Re(C_{\downarrow\downarrow}) + \Im(C_{\uparrow\downarrow})\Im(C_{\downarrow\downarrow})] . \end{aligned} \tag{4.9}$$

In the previous equation we used $\Re$ and $\Im$ for denoting, respectively, the real and imaginary part of a complex number.
Similarly,

$$\mathbb{I}_1 \otimes j_{x_2} = \frac{|\uparrow\uparrow\rangle\langle\uparrow\downarrow| + |\uparrow\downarrow\rangle\langle\uparrow\uparrow| + |\downarrow\uparrow\rangle\langle\downarrow\downarrow| + |\downarrow\downarrow\rangle\langle\downarrow\uparrow|}{2} \tag{4.10}$$

and

$$\begin{aligned} \langle j_{x_2} \rangle &= \langle \mathbb{I}_1 \otimes j_{x_2} \rangle = \langle \psi | \mathbb{I}_1 \otimes j_{x_2} | \psi \rangle = \\ &= \Re(C^*_{\uparrow\uparrow} C_{\uparrow\downarrow}) + \Re(C^*_{\downarrow\uparrow} C_{\downarrow\downarrow}) = \\ &= [\Re(C_{\uparrow\uparrow})\Re(C_{\uparrow\downarrow}) + \Im(C_{\uparrow\uparrow})\Im(C_{\uparrow\downarrow})] + [\Re(C_{\downarrow\uparrow})\Re(C_{\downarrow\downarrow}) + \Im(C_{\downarrow\uparrow})\Im(C_{\downarrow\downarrow})] . \end{aligned} \tag{4.11}$$

We are now able to collect the results shown in equations 4.9 and 4.11 in order to write down $\langle S_x \rangle$:

$$\begin{aligned} \langle S_x \rangle &= \langle \eta_1 j_{x_1} + \eta_2 j_{x_2} \rangle = \eta_1 \langle j_{x_1} \rangle + \eta_2 \langle j_{x_2} \rangle = \\ &= \eta_1 \left(\Re(C^*_{\uparrow\uparrow} C_{\downarrow\uparrow}) + \Re(C^*_{\uparrow\downarrow} C_{\downarrow\downarrow}) \right) + \eta_2 \left(\Re(C^*_{\uparrow\uparrow} C_{\uparrow\downarrow}) + \Re(C^*_{\downarrow\uparrow} C_{\downarrow\downarrow}) \right) . \end{aligned} \tag{4.12}$$

- $S_x^2 = (\eta_1 j_{x_1} + \eta_2 j_{x_2})^2 = \eta_1^2 j_{x_1}^2 + \eta_2^2 j_{x_2}^2 + 2\eta_1\eta_2 j_{x_1} j_{x_2}$. Here we used the fact that the commutator $[j_{x_1}, j_{x_2}]$ is null, so that $j_{x_1} j_{x_2} = j_{x_2} j_{x_1}$. As follows from the general properties of Pauli matrices, we have that

$$j_{x_1}^2 = j_{x_2}^2 = \frac{\mathbb{I}}{4}, \tag{4.13}$$

so that:

$$\langle S_x^2\rangle = \eta_1^2\langle j_{x_1}^2\rangle + \eta_2^2\langle j_{x_2}^2\rangle + 2\eta_1\eta_2\langle j_{x_1}j_{x_2}\rangle = \frac{\eta_1^2+\eta_2^2}{4} + 2\eta_1\eta_2\langle j_{x_1}j_{x_2}\rangle. \tag{4.14}$$

Therefore, the only term we have to compute is $\langle j_{x_1}j_{x_2}\rangle$. Following a similar procedure to the previous one, we can rewrite

$$\begin{aligned} j_{x_1}j_{x_2} = j_{x_1}\otimes j_{x_2} &= \left(\frac{|\uparrow\rangle_1\langle\downarrow| + |\downarrow\rangle_1\langle\uparrow|}{2}\right)\otimes\left(\frac{|\uparrow\rangle_2\langle\downarrow| + |\downarrow\rangle_2\langle\uparrow|}{2}\right) = \\ &= \frac{|\uparrow\uparrow\rangle\langle\downarrow\downarrow| + |\uparrow\downarrow\rangle\langle\downarrow\uparrow| + |\downarrow\uparrow\rangle\langle\uparrow\downarrow| + |\downarrow\downarrow\rangle\langle\uparrow\uparrow|}{4}, \end{aligned} \tag{4.15}$$

so that, using the orthonormal property again:

$$\begin{aligned} \langle j_{x_1}j_{x_2}\rangle &= \langle j_{x_1}\otimes j_{x_2}\rangle = \langle\psi|j_{x_1}\otimes j_{x_2}|\psi\rangle = \\ &= \frac{1}{4}\left(C_{\uparrow\uparrow}^*C_{\downarrow\downarrow} + C_{\uparrow\downarrow}^*C_{\downarrow\uparrow} + C_{\downarrow\uparrow}^*C_{\uparrow\downarrow} + C_{\downarrow\downarrow}^*C_{\uparrow\uparrow}\right) = \\ &= \frac{1}{4}\left[C_{\uparrow\uparrow}^*C_{\downarrow\downarrow} + \left(C_{\uparrow\uparrow}^*C_{\downarrow\downarrow}\right)^* + C_{\uparrow\downarrow}^*C_{\downarrow\uparrow} + \left(C_{\uparrow\downarrow}^*C_{\downarrow\uparrow}\right)^*\right] = \\ &= \frac{1}{2}\left[\Re(C_{\uparrow\uparrow}^*C_{\downarrow\downarrow}) + \Re(C_{\uparrow\downarrow}^*C_{\downarrow\uparrow})\right] = \\ &= \frac{1}{2}\left\{[\Re(C_{\uparrow\uparrow})\Re(C_{\downarrow\downarrow}) + \Im(C_{\uparrow\uparrow})\Im(C_{\downarrow\downarrow})] + [\Re(C_{\uparrow\downarrow})\Re(C_{\downarrow\uparrow}) + \Im(C_{\uparrow\downarrow})\Im(C_{\downarrow\uparrow})]\right\}. \end{aligned} \tag{4.16}$$

We are now finally able to write down $\langle S_x^2\rangle$, the last ingredient we needed for the Lagrange function Γ:

$$\begin{aligned} \langle S_x^2\rangle &= \eta_1^2\langle j_{x_1}^2\rangle + \eta_2^2\langle j_{x_2}^2\rangle + 2\eta_1\eta_2\langle j_{x_1}j_{x_2}\rangle = \\ &= \frac{\eta_1^2+\eta_2^2}{4} + \eta_1\eta_2\left[\Re(C_{\uparrow\uparrow}^*C_{\downarrow\downarrow}) + \Re(C_{\uparrow\downarrow}^*C_{\downarrow\uparrow})\right]. \end{aligned} \tag{4.17}$$

Let us summarize what we just obtained. For $\langle S_z\rangle$ we have, as expressed in eq.4.7:

$$\langle S_z\rangle = \frac{\eta_1+\eta_2}{2}\left(|C_{\uparrow\uparrow}|^2 - |C_{\downarrow\downarrow}|^2\right) + \frac{\eta_1-\eta_2}{2}\left(|C_{\uparrow\downarrow}|^2 - |C_{\downarrow\uparrow}|^2\right), \tag{4.18}$$

while it follows from eq.4.12 and 4.17 that $(\Delta S_x)^2$ becomes:

$$\begin{aligned} (\Delta S_x)^2 &= \langle S_x^2\rangle - \langle S_x\rangle^2 = \\ &= \frac{\eta_1^2+\eta_2^2}{4} + \eta_1\eta_2\left[\Re(C_{\uparrow\uparrow}^*C_{\downarrow\downarrow}) + \Re(C_{\uparrow\downarrow}^*C_{\downarrow\uparrow})\right] \\ &- \left\{\eta_1\left[\Re(C_{\uparrow\uparrow}^*C_{\downarrow\uparrow}) + \Re(C_{\uparrow\downarrow}^*C_{\downarrow\downarrow})\right] + \eta_2\left[\Re(C_{\uparrow\uparrow}^*C_{\uparrow\downarrow}) + \Re(C_{\downarrow\uparrow}^*C_{\downarrow\downarrow})\right]\right\}^2. \end{aligned} \tag{4.19}$$

It is now clear that, once we put these expressions in the Lagrange function $\Gamma = (\Delta S_x)^2 - \mu\langle S_z\rangle$, its minimization becomes a hard task. Let us first take a simplified approach by

considering all the coefficients $\{C_{\uparrow\uparrow}, C_{\uparrow\downarrow}, C_{\downarrow\uparrow}, C_{\downarrow\downarrow}\}$ to be real numbers, and moreover two of them to be null: $C_{\uparrow\downarrow} = C_{\downarrow\uparrow} = 0$. It follows that we can express the state vector $|\psi\rangle$ as

$$|\psi\rangle = C_{\uparrow\uparrow}|\uparrow\uparrow\rangle + C_{\downarrow\downarrow}|\downarrow\downarrow\rangle, \tag{4.20}$$

with normalization condition $C_{\uparrow\uparrow}^2 + C_{\downarrow\downarrow}^2 = 1$. This reminds us the fundamental trigonometric relation, so that we choose to make the substitutions

$$C_{\uparrow\uparrow} = \cos x \tag{4.21a}$$

$$C_{\downarrow\downarrow} = \sin x, \tag{4.21b}$$

with x being a real number inside the interval $[-\pi, \pi]$, in order to span all the possibilities for the coefficients. The state describing the system (eq.4.20) becomes now

$$|\psi\rangle = |\uparrow\uparrow\rangle \cos x + |\downarrow\downarrow\rangle \sin x, \tag{4.22}$$

that simplify the terms in the Lagrange Γ function a lot. In fact, collecting the main results we have (eq.4.7 and 4.19):

$$\langle S_z \rangle = \frac{\eta_1 + \eta_2}{2} \left(\cos^2 x - \sin^2 x\right) = \frac{\eta_1 + \eta_2}{2} \cos(2x) \tag{4.23a}$$

$$(\Delta S_x)^2 = \frac{\eta_1^2 + \eta_2^2}{4} + \eta_1 \eta_2 \cos x \sin x = \frac{\eta_1^2 + \eta_2^2}{4} + \frac{\eta_1 \eta_2}{2} \sin(2x), \tag{4.23b}$$

and consequently

$$\Gamma(x, \mu) = (\Delta S_x)^2 - \mu \langle S_z \rangle = \frac{\eta_1^2 + \eta_2^2}{4} + \frac{\eta_1 \eta_2}{2} \sin(2x) - \mu \frac{\eta_1 + \eta_2}{2} \cos(2x). \tag{4.24}$$

As a first comment, notice that this function is, due to the factor 2 inside the arguments of sine and cosine, π-periodic. Therefore, without loss of generality, we can restrict the interval in which x is allowed to vary to $\left[-\frac{\pi}{2}, \frac{\pi}{2}\right]$. At this point we want to follow the standard procedure; minimize Γ deriving in the x variable, and subsequently determine how $\langle S_z \rangle$ and $(\Delta S_x)^2$ vary with respect to μ. As before, the minimum has to be found in a stationary point, being Γ periodic and continuous in x; μ can be any real numbers. The derivative is given by

$$\frac{\partial \Gamma}{\partial x}(x, \mu) = \eta_1 \eta_2 \cos(2x) + \mu (\eta_1 + \eta_2) \sin(2x), \tag{4.25}$$

so that the stationary points, identified by $\frac{\partial \Gamma}{\partial x}(x, \mu) = 0$, are:

$$x_{1,2} = \arctan\left(\frac{\eta_1 \eta_2}{\mu (\eta_1 + \eta_2)}\right) - k \frac{\pi}{2} \operatorname{sgn}(\mu). \tag{4.26}$$

Here, due to the x's domain, k can assume only the values 0 or 1; let us call x_1 the point identified by $k = 0$ and x_2 the one by $k = 1$. k cannot take other values since, for any possible μ, we have only two stationary points; if μ is negative, the argument of arctan identifies a number between $-\frac{\pi}{2}$ and 0, so that we can find another solution adding $\frac{\pi}{2}$. Otherwise, having μ positive, we can obtain the second stationary point by subtracting $\frac{\pi}{2}$, as stated in eq.4.26. Necessarily, one of these represents a minimum and the other a maximum; this is a consequence of the fact that we have a continuous periodic function with only two stationary points.
Which of the two is the one minimizing Γ? Let us call this point x_{min}, that in the practice will be determined checking which, between $\Gamma(x_1)$ and $\Gamma(x_2)$ takes the smallest values. We can now collect what we obtained, that is: what we will need for drawing the usual curve. As before, Γ_{min} represents the function Γ once we plugged in the constraint $x = x_{min}$:

$$\Gamma_{min}(\mu) = \frac{\eta_1^2 + \eta_2^2}{4} + \frac{\eta_1\eta_2}{2}\sin(2x_{min}) - \mu\frac{\eta_1 + \eta_2}{2}\cos(2x_{min}) \tag{4.27a}$$

$$\langle S_z\rangle(\mu) = \frac{\eta_1 + \eta_2}{2}\cos(2x_{min}) \tag{4.27b}$$

$$(\Delta S_x)^2(\mu) = \frac{\eta_1^2 + \eta_2^2}{4} + \frac{\eta_1\eta_2}{2}\sin(2x_{min}). \tag{4.27c}$$

As a final comment, let us prove that the function $\Gamma_{min}(\mu)$ is even. This will be done analysing the two cases in which μ is, respectively, positive and negative.

- $\mu \geq 0$

  Let us remember that, in this case,

$$x_1 = \arctan\left(\frac{\eta_1\eta_2}{\mu(\eta_1 + \eta_2)}\right) \in \left[0, \frac{\pi}{2}\right] \tag{4.28a}$$

$$x_2 = \arctan\left(\frac{\eta_1\eta_2}{\mu(\eta_1 + \eta_2)}\right) - \frac{\pi}{2} \in \left[-\frac{\pi}{2}, 0\right), \tag{4.28b}$$

  and minimizing Γ means to find for which k the function

$$\begin{aligned}\Gamma(\mu) = \frac{\eta_1^2 + \eta_2^2}{4} + \frac{\eta_1\eta_2}{2}\sin\left[2\arctan\left(\frac{\eta_1\eta_2}{\mu(\eta_1 + \eta_2)}\right) - k\pi\right] + \\ - \mu\frac{\eta_1 + \eta_2}{2}\cos\left[2\arctan\left(\frac{\eta_1\eta_2}{\mu(\eta_1 + \eta_2)}\right) - k\pi\right]\end{aligned} \tag{4.29}$$

takes the smallest value. Now, since $\sin(a-\pi) = -\sin a$ and $\cos(a-\pi) = -\cos a$, we have that

$$\begin{cases} k & = 0 \text{ (i.e.: } x_1) \\ \Gamma & = \frac{\eta_1^2+\eta_2^2}{4} + \frac{\eta_1\eta_2}{2}\sin\left[2\arctan\left(\frac{\eta_1\eta_2}{\mu(\eta_1+\eta_2)}\right)\right] - \mu\frac{\eta_1+\eta_2}{2}\cos\left[2\arctan\left(\frac{\eta_1\eta_2}{\mu(\eta_1+\eta_2)}\right)\right] \end{cases} \tag{4.30}$$

and

$$\begin{cases} k & = 1 \text{ (i.e.: } x_2) \\ \Gamma & = \frac{\eta_1^2+\eta_2^2}{4} - \frac{\eta_1\eta_2}{2}\sin\left[2\arctan\left(\frac{\eta_1\eta_2}{\mu(\eta_1+\eta_2)}\right)\right] + \mu\frac{\eta_1+\eta_2}{2}\cos\left[2\arctan\left(\frac{\eta_1\eta_2}{\mu(\eta_1+\eta_2)}\right)\right]. \end{cases} \tag{4.31}$$

- $\mu < 0$

  Here we have that

$$x_1 = -\arctan\left(\frac{\eta_1\eta_2}{|\mu|\,(\eta_1+\eta_2)}\right) \in \left[-\frac{\pi}{2}, 0\right) \tag{4.32a}$$

$$x_2 = -\arctan\left(\frac{\eta_1\eta_2}{\mu\,(\eta_1+\eta_2)}\right) + \frac{\pi}{2} \in \left[0, \frac{\pi}{2}\right], \tag{4.32b}$$

  and, as before, minimizing Γ means to find for which k the function

$$\begin{aligned} \Gamma(\mu) = \frac{\eta_1^2+\eta_2^2}{4} - \frac{\eta_1\eta_2}{2}\sin\left[2\arctan\left(\frac{\eta_1\eta_2}{|\mu|\,(\eta_1+\eta_2)}\right) - k\pi\right] + \\ - \mu\frac{\eta_1+\eta_2}{2}\cos\left[2\arctan\left(\frac{\eta_1\eta_2}{|\mu|\,(\eta_1+\eta_2)}\right) - k\pi\right] \end{aligned} \tag{4.33}$$

  takes the smallest value. In the last equation we used the properties of the trigonometric functions. Therefore, differently as before, we have that

$$\begin{cases} k & = 0 \text{ (i.e.: } x_1) \\ \Gamma & = \frac{\eta_1^2+\eta_2^2}{4} - \frac{\eta_1\eta_2}{2}\sin\left[2\arctan\left(\frac{\eta_1\eta_2}{|\mu|(\eta_1+\eta_2)}\right)\right] + \mu\frac{\eta_1+\eta_2}{2}\cos\left[2\arctan\left(\frac{\eta_1\eta_2}{|\mu|(\eta_1+\eta_2)}\right)\right] \end{cases} \tag{4.34}$$

  and

$$\begin{cases} k & = 1 \text{ (i.e.: } x_2) \\ \Gamma & = \frac{\eta_1^2+\eta_2^2}{4} + \frac{\eta_1\eta_2}{2}\sin\left[2\arctan\left(\frac{\eta_1\eta_2}{|\mu|(\eta_1+\eta_2)}\right)\right] - \mu\frac{\eta_1+\eta_2}{2}\cos\left[2\arctan\left(\frac{\eta_1\eta_2}{|\mu|(\eta_1+\eta_2)}\right)\right]. \end{cases} \tag{4.35}$$

At this point we can look carefully to the four systems of two equations 4.30 and 4.31, regarding the first case $\mu \geq 0$, and 4.34 and 4.35 for $\mu < 0$. What we immediately notice is that the Γ functions takes the same value for a pair of μ and k. In particular we have

that

$$\begin{cases} (\mu \geq 0 \wedge k = 0) \vee (\mu < 0 \wedge k = 1) \\ \Gamma = \frac{\eta_1^2+\eta_2^2}{4} + \frac{\eta_1\eta_2}{2} \sin\left[2 \arctan\left(\frac{\eta_1\eta_2}{|\mu|(\eta_1+\eta_2)}\right)\right] - \mu\frac{\eta_1+\eta_2}{2} \cos\left[2 \arctan\left(\frac{\eta_1\eta_2}{|\mu|(\eta_1+\eta_2)}\right)\right] \end{cases} \tag{4.36a}$$

$$\begin{cases} (\mu \geq 0 \wedge k = 1) \vee (\mu < 0 \wedge k = 0) \\ \Gamma = \frac{\eta_1^2+\eta_2^2}{4} - \frac{\eta_1\eta_2}{2} \sin\left[2 \arctan\left(\frac{\eta_1\eta_2}{|\mu|(\eta_1+\eta_2)}\right)\right] + \mu\frac{\eta_1+\eta_2}{2} \cos\left[2 \arctan\left(\frac{\eta_1\eta_2}{|\mu|(\eta_1+\eta_2)}\right)\right] \end{cases} \tag{4.36b}$$

The conclusion we can take is that, whatever the sign of μ is, the two stationary points x_1 and x_2 identify the same two values for Γ: the same maximum and the same minimum. Consequently, changing the sign of μ does *not* change the value that Γ_{min} is taking when we impose the constraint $x = x_{min}$ (at most, switches x_{min} from x_1 to x_2, or vice versa). In other words, we can say that we are in presence of a symmetry. In fact, the Γ function is even:

$$\Gamma(-\mu) = \Gamma(\mu), \tag{4.37}$$

that is a fundamental requirement for our system since, once we take negative values for $\langle S_z \rangle$, we want the curve that associates to this observable the minimum possible $(\Delta S_x)^2$ to be exactly the same as the one for positive $\langle S_z \rangle$. Therefore, we can restrict the interval in which μ is allowed to vary to $[0, \infty]$, that corresponds to say that we are dealing with positive $\langle S_z \rangle$.

We have now all the elements to plot the usual curve, that identifies the smallest value of $(\Delta S_x)^2$ for any possible $\langle S_z \rangle$. We will put, together with such function, the one associated to the generic separable state of two particles. In this case, since we will decide which values the coefficients η_1 and η_2 will take, we only need the results shown in Table 3.3. In other words, supposing $\eta_1 \leq \eta_2$, we have:

Range	$\mu \leq \eta_1$	$\eta_1 < \mu \leq \eta_2$	$\mu > \eta_2$
$\langle S_z \rangle_{sep}$	μ	$\frac{1}{2}(\mu + \eta_1)$	$\frac{\eta_1+\eta_2}{2}$
$(\Delta S_x)^2_{sep}$	$\frac{\mu^2}{2}$	$\frac{1}{4}(\mu^2 + \eta_2^2)$	$\frac{\eta_1^2+\eta_2^2}{4}$

TABLE 4.1: $\langle S_z \rangle$ and $(\Delta S_x)^2$ in the different ranges in which μ is allowed to vary, for a generic separable state made by two particles

As introduced in Table 4.1, we will use the suffixes "$_{sep}$" and "$_{ent}$" for referring ourselves to the separable and the entangled cases respectively.

We can now give the following Figure 4.1, where we actually plotted the normalized

variables $\frac{(\Delta S_x)^2}{(\Delta S_x)^2_{CSS}}$ and $\frac{\langle S_z\rangle}{\langle S_z\rangle_{CSS}}$.

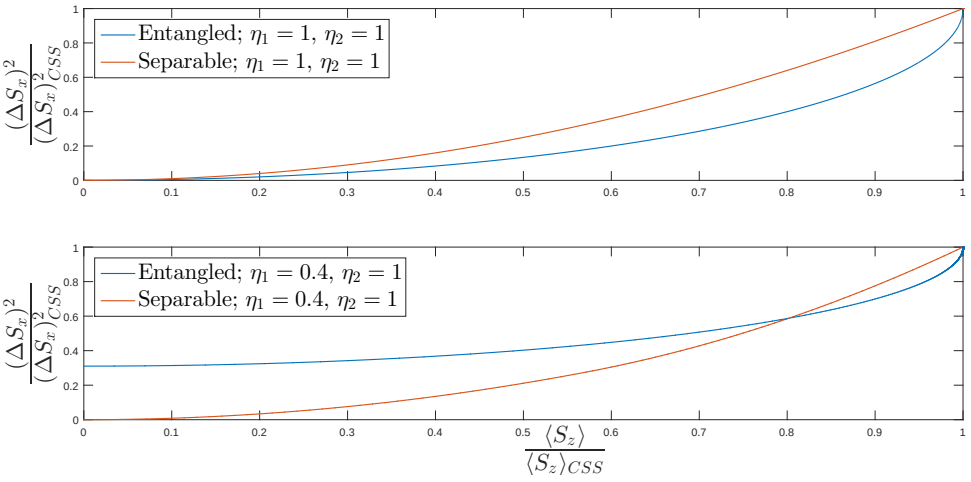

FIGURE 4.1: $\frac{(\Delta S_x)^2}{(\Delta S_x)^2_{CSS}}$ with respect to $\frac{\langle S_z\rangle}{\langle S_z\rangle_{CSS}}$; the *red* curve refers to the separable state and the *blue* to the entangled. In the upper plot we took η_1 and η_2 both equal to one; In the lower one $\eta_1 = 0.4$ and $\eta_2 = 1$.

For $\langle S_z\rangle_{CSS}$ we considered (look at eq.4.23a)

$$\langle S_z\rangle_{CSS} = \frac{\eta_1 + \eta_2}{2}, \tag{4.38}$$

while for $(\Delta S_x)^2_{CSS}$ we impose:

$$(\Delta S_x)^2_{CSS} = \frac{\eta_1^2 + \eta_2^2}{4}. \tag{4.39}$$

Notice that $(\Delta S_x)^2_{ent}$ can, in principle, take bigger values (as it follows from eq.4.23b); however, due to the constraints we impose in the minimization procedure, $(\Delta S_x)^2_{ent}$ never exceed $(\Delta S_x)^2_{CSS}$ as we defined it. Therefore our definition is, indeed, appropriate.

As it is possible to see from the Figure 4.1, there are big portions of the plots in which the curve representing the entangled system lies below the other, so that there is the actual possibility to identify entanglement using these functions. Notice that as much the coefficients η_1 and η_2 differ, as much the entanglement becomes harder to detect. However, as the two particles are correlated, we can think them to interact between themselves, so that we can imagine them to be very near in the space and thus described by very similar coefficients.

4.1.1 The general case

So far we have seen that it is possible, having entanglement between two particles, to obtain a variance that lies below the lowest limit allowed by separable states. This result has been obtained analytically, simplifying the wave function describing the two particles' state to $|\psi\rangle = C_{\uparrow\uparrow}|\uparrow\uparrow\rangle + C_{\downarrow\downarrow}|\downarrow\downarrow\rangle$. But what happens when we consider the general case, with the wave function expressed by eq.4.2? For instance, we require that the theoretical curve describing the lowest limit for the entangled case always lies *below* the one for the separable. This is a straightforward consequence of the fact that the most general two particles' entangled state contains all the possible separable wave vectors already into itself. Therefore, a plot like the second one in Fig.4.1 cannot be true any more for the general case. So let us derive the usual curves in order to find out their properties and to obtain a powerful instrument for the description of a system made of N particles, which can be entangled in pairs of two (see the following section 4.1.2).

At first let us say that, after having trivially attempted to solve analytically the usual Lagrange multiplier problem (with $\langle S_z\rangle$ and $(\Delta S_x)^2$ given by eq.4.18 and 4.19), we encountered an insurmountable difficulty. The stationary points of the Γ function are here identified by high rank polynomials, for which there does not exist a known solution. Therefore the only possible approach results to be the numerical one. However, this is not discouraging; in fact, even if for sake of completeness we would like to obtain all results without approximations, the important curve is the one regarding separable state, for which an analytical expression is known from previous section 3.2.
All the next results have been derived using the Lagrange method explained above.

At this point, let us present what we obtained. In the following Fig.4.2 we plotted the minimum of $\left(\frac{(\Delta S_x)^2}{(\Delta S_x)^2_{CSS}}\right)$ for the state $|\psi\rangle$, with respect to the variables $\frac{\langle S_z\rangle}{\langle S_z\rangle_{CSS}}$ and $\frac{\eta_1}{\eta_2}$. Notice that, as all these quantities are normalized, once we fix the ratio $\frac{\eta_1}{\eta_2}$, we do not have dependence over the coefficients η_1 and η_2 any more.

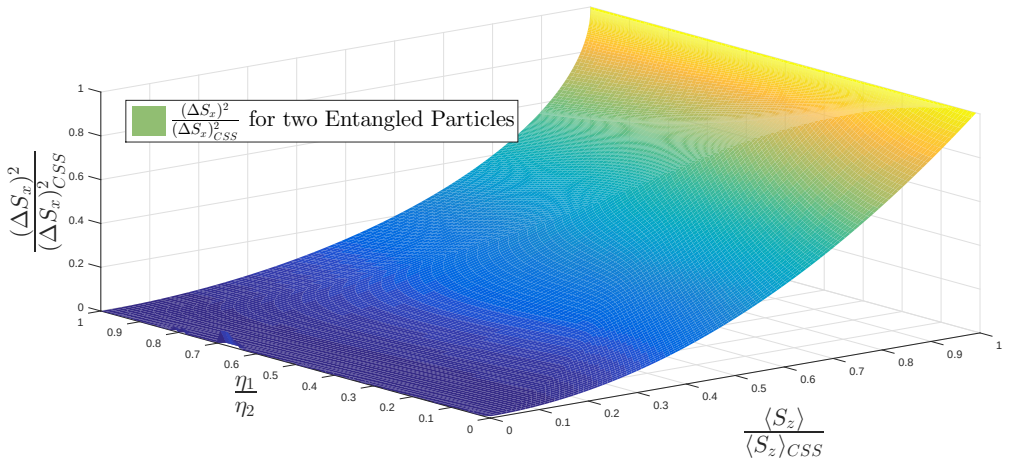

FIGURE 4.2: Normalized variance for two entangled particles for different values of $\frac{\eta_1}{\eta_2}$ and normalized spin

As it follows from this graph, there are two very important properties that need to be mentioned:

- $\left(\frac{(\Delta S_x)^2}{(\Delta S_x)^2_{CSS}}\right)$ is a *convex* and *increasing* function with respect to its variable $\frac{\langle S_z \rangle}{\langle S_z \rangle_{CSS}}$.
- Supposed η_1 to be less or equal to η_2, $\left(\frac{(\Delta S_x)^2}{(\Delta S_x)^2_{CSS}}\right)$ is *decreasing* with respect to $\frac{\eta_1}{\eta^2}$. This property, that does not appear clearly from Fig.4.2, can be deduced from the following plot, where we draw three curves $\left(\frac{(\Delta S_x)^2}{(\Delta S_x)^2_{CSS}}\right)$, for three meaningful values of $\frac{\eta_1}{\eta_2}$.

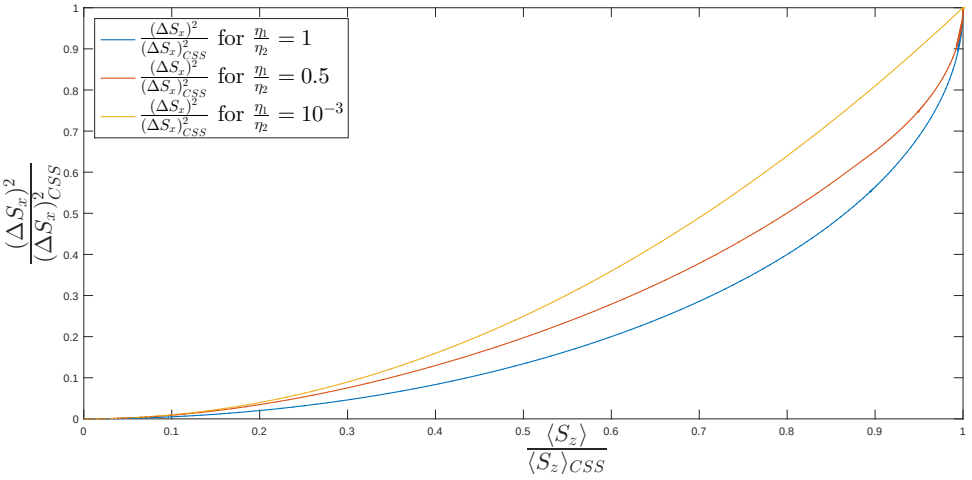

FIGURE 4.3: Three plots of $\left(\frac{(\Delta S_x)^2}{(\Delta S_x)^2_{CSS}}\right)$ for $\frac{\eta_1}{\eta_2}$ being equal to 1 (*blue*), 0.5 (*red*) and 10^{-3} (*yellow*)

As it is possible to see, the curve associated to the smallest $\frac{\eta_1}{\eta_2}$ is the one lying above all the others. As this ratio increases, $\left(\frac{(\Delta S_x)^2}{(\Delta S_x)^2_{CSS}}\right)$ takes smaller and smaller values, until it hits the curve described by $\frac{\eta_1}{\eta_2} = 1$. In other words, $\left(\frac{(\Delta S_x)^2}{(\Delta S_x)^2_{CSS}}\right)$ is *decreasing* with respect to $\frac{\eta_1}{\eta 2}$, as announced.

So far we exhausted the case of two entangled particles. We considered the most general wave vector (eq.4.2) and we obtained an absolute, not crossable limit for the normalized variance for such state, given any possible pair of coefficients η_1 and η_2 (see Fig.4.2). We mentioned two fundamental properties for such limit, they will be very useful in the following. In fact, what we will do next, is to generalize the main result obtained in section 3.1 for separable states, well summarized (in the example of section 3.1.2) by Fig.3.4, to any state made by an even number N of particles they can be entangled in pairs. In other words, given a probability distribution function $p(\eta)$ for the coefficients $\{\eta_i\}$, we will derive the minimum possible value of $\left(\frac{(\Delta S_x)^2}{(\Delta S_x)^2_{CSS}}\right)$ allowing to 2-particle entanglement, consequently giving a sufficient criteria for saying if in our system three (or more) particles are correlated.

Notice that, for the curve corresponding to $\eta_1 = \eta_2$, there already exists an analytical expression. In fact $\eta_1 = \eta_2$ is equivalent to say that we are using the collective spin operator $\vec{J}$ instead of $\vec{S}$. Anders S. Sørensen derived, in his paper [37], that the relation the two entangled particles have to satisfy is:

$$\frac{(\Delta J_x)^2}{(\Delta J_x)^2_{CSS}} \geq 1 - \sqrt{1 - \left(\frac{\langle J_z\rangle}{\langle J_z\rangle_{CSS}}\right)^2} \equiv f\left(1, \frac{\langle J_z\rangle}{\langle J_z\rangle_{CSS}}\right). \tag{4.40}$$

The reason for which we introduced the notation f will be clear later, when we will use such function. The first argument of f is the ratio $\frac{\eta_1}{\eta_2}$, so that, for being precise, $f(k, x)$ is the function represented in Fig.4.2, that in the particular case $k = 1$ takes the specific form of eq.4.40.

4.1.2 N particles with allowed entanglement in pairs

As said before, the goal of this section is to study the minima for the variance of a system made by an even number of particles N, that can be entangled in pairs. This will be done in three fundamental steps: at first, we will consider a specific case regarding 4 atoms; subsequently we will generalize it and in conclusion we will increase the number of particles to an even N first, odd later.

4.1.2.1 4 particles

The most generic density matrix describing a system formed by 4 particles that can be entangled in pairs is given by

$$\rho = p_1(\rho_{1,2} \otimes \rho_{3,4}) + p_2(\rho_{1,3} \otimes \rho_{2,4}) + p_3(\rho_{1,4} \otimes \rho_{2,3}), \tag{4.41}$$

where p_1, p_2 and p_3 are three positive real numbers such that $p_1 + p_2 + p_3 = 1$ and $\rho_{i,j}$ is the most general density matrix of the two entangled particles i and j ($i \neq j$). In other words, $\rho_{i,j}$ is the projector operator obtained using the state of eq.4.2, referred to atoms i-th and j-th.

At first, consider the simplified case in which $p_1 = 1$, and henceforth $p_2 = p_3 = 0$. We have that

$$\rho = \rho_{1,2} \otimes \rho_{3,4}, \tag{4.42}$$

so that it results in a particularly easy problem to determine the usual, necessary quantities $\langle S_z \rangle$ and $(\Delta S_x)^2$. In fact:

- $\langle S_z \rangle = \langle S_z \rangle_{1,2} + \langle S_z \rangle_{3,4}$, where we defined $\langle A \rangle_{i,j} = \mathrm{Tr}\,(A\rho_{i,j})$, for $i \neq j$. The proof of this equality proceeds straightforward, remembering that, whenever we have two operators A and B acting respectively over the two subsystems indicated with the same letters and described by $\rho = \rho_A \otimes \rho_B$, we have that

$$\langle A \otimes B \rangle = \mathrm{Tr}\,[(A \otimes B)\rho] = \mathrm{Tr}\,(A\rho_A \otimes B\rho_B) = \mathrm{Tr}\,(A\rho_A)\,\mathrm{Tr}\,(B\rho_B)\,. \tag{4.43}$$

  In fact, since $S_z = \eta_1 j_{z_1} + \eta_2 j_{z_2} + \eta_3 j_{z_3} + \eta_4 j_{z_4}$ and

$$\begin{aligned} \langle j_{z_1} \rangle &= \mathrm{Tr}\,(j_{z_1}\rho) = \mathrm{Tr}\,[(j_{z_1} \otimes \mathbb{I}_2 \otimes \mathbb{I}_3 \otimes \mathbb{I}_4)\,(\rho_{1,2} \otimes \rho_{3,4})] = \\ &= \mathrm{Tr}\,[(j_{z_1} \otimes \mathbb{I}_2)\,\rho_{1,2}\,(\mathbb{I}_3 \otimes \mathbb{I}_4)\,\rho_{3,4}] \overset{\text{eq.4.43}}{=} \mathrm{Tr}\,(j_{z_1}\rho_{1,2}) \cdot 1 = \langle j_{z_1} \rangle_{1,2}, \end{aligned} \tag{4.44}$$

  we have that $\langle j_{z_1} \rangle = \langle j_{z_1} \rangle_{1,2}$, $\langle j_{z_2} \rangle = \langle j_{z_2} \rangle_{1,2}$, $\langle j_{z_3} \rangle = \langle j_{z_3} \rangle_{3,4}$ and $\langle j_{z_4} \rangle = \langle j_{z_4} \rangle_{3,4}$ and therefore

$$\begin{aligned} \langle S_z \rangle &= \eta_1 \langle j_{z_1} \rangle + \eta_2 \langle j_{z_2} \rangle + \eta_3 \langle j_{z_3} \rangle + \eta_4 \langle j_{z_4} \rangle = \\ &= \langle \eta_1 j_{z_1} + \eta_2 j_{z_2} \rangle_{1,2} + \langle \eta_3 j_{z_3} + \eta_4 j_{z_4} \rangle_{3,4} = \langle S_z \rangle_{1,2} + \langle S_z \rangle_{3,4}, \end{aligned} \tag{4.45}$$

  as we wanted.

- With the same arguments that we used for deriving eq.4.45, we can obtain, for S_x, that

$$\langle S_x \rangle = \langle S_x \rangle_{1,2} + \langle S_x \rangle_{3,4} \tag{4.46}$$

- As usual, slightly more complex calculations are needed for determining $\langle S_x^2 \rangle$. In fact, here we have to deal with all crossed terms, obtained writing down explicitly S_x^2 in all its components. Remembering that $j_{x_i}^2 = \frac{\mathbb{I}}{4}$ for any i-th particle, we have that:

$$\begin{aligned} S_x^2 = \frac{\eta_1^2 + \eta_2^2}{4} + 2\eta_1\eta_2 j_{x_1} j_{x_2} + \frac{\eta_3^2 + \eta_4^2}{4} + 2\eta_3\eta_4 j_{x_3} j_{x_4} + \\ + 2\eta_1\eta_3 j_{x_1} j_{x_3} + 2\eta_1\eta_4 j_{x_1} j_{x_4} + 2\eta_2\eta_3 j_{x_2} j_{x_3} + 2\eta_2\eta_4 j_{x_2} j_{x_4}. \end{aligned} \tag{4.47}$$

  Now, using eq.4.43 and noticing that $\langle j_{x_i} j_{x_j} \rangle = \langle j_{x_i} \rangle \langle j_{x_j} \rangle$, whenever particles i and j are *not* entangled, we can conclude

$$\begin{aligned} \langle S_x^2 \rangle = \frac{\eta_1^2 + \eta_2^2}{4} + 2\eta_1\eta_2 \langle j_{x_1} j_{x_2} \rangle_{1,2} + \frac{\eta_3^2 + \eta_4^2}{4} + 2\eta_3\eta_4 \langle j_{x_3} j_{x_4} \rangle_{3,4} + \\ + 2\eta_1\eta_3 \langle j_{x_1} \rangle_{1,2} \langle j_{x_3} \rangle_{3,4} + 2\eta_1\eta_4 \langle j_{x_1} \rangle_{1,2} \langle j_{x_4} \rangle_{3,4} + \\ + 2\eta_2\eta_3 \langle j_{x_2} \rangle_{1,2} \langle j_{x_3} \rangle_{3,4} + 2\eta_2\eta_4 \langle j_{x_2} \rangle_{1,2} \langle j_{x_4} \rangle_{3,4} = \\ = \langle S_x^2 \rangle_{1,2} + \langle S_x^2 \rangle_{3,4} + (\text{Crossed Terms}). \end{aligned} \tag{4.48}$$

  Here, in "(Crossed Terms)" we collected all the contributions given by second and third rows of eq.4.48.

Before writing down explicitly $(\Delta S_x)^2$, let us determine $\langle S_x \rangle^2$:

$$\begin{aligned} \langle S_x \rangle^2 = (\langle S_x \rangle_{1,2} + \langle S_x \rangle_{3,4})^2 = \langle S_x \rangle_{1,2}^2 + \langle S_x \rangle_{3,4}^2 + 2\langle S_x \rangle_{1,2} \langle S_x \rangle_{3,4} = \\ = \langle S_x \rangle_{1,2}^2 + \langle S_x \rangle_{3,4}^2 + (\text{Crossed Terms}). \end{aligned} \tag{4.49}$$

Notice that the crossed terms are the same as before. This can be seen from the fact $\langle S_x \rangle_{1,2} = \eta_1 \langle j_{x_1} \rangle_{1,2} + \eta_2 \langle j_{x_2} \rangle_{1,2}$ and $\langle S_x \rangle_{3,4} = \eta_3 \langle j_{x_3} \rangle_{3,4} + \eta_4 \langle j_{x_4} \rangle_{3,4}$. Then simple algebra shows that they are actually equal, so that we can conclude (eq.4.48 and 4.49):

$$(\Delta S_x)^2 = \langle S_x^2 \rangle - \langle S_x \rangle^2 = \langle S_x^2 \rangle_{1,2} + \langle S_x^2 \rangle_{3,4} - \langle S_x \rangle_{1,2}^2 - \langle S_x \rangle_{3,4}^2 = (\Delta S_x)_{1,2}^2 + (\Delta S_x)_{3,4}^2 . \tag{4.50}$$

In this last equation we introduced the notation $(\Delta S_x)_{i,j}^2 = \langle S_x^2 \rangle_{i,j} - \langle S_x \rangle_{i,j}^2$, for $i \neq j$. We can now collect the results we obtained:

$$\langle S_z \rangle = \langle S_z \rangle_{1,2} + \langle S_z \rangle_{3,4} \tag{4.51a}$$

$$(\Delta S_x)^2 = (\Delta S_x)_{1,2}^2 + (\Delta S_x)_{3,4}^2 , \tag{4.51b}$$

so that, once we plug in the normalization, we get:

$$\frac{\langle S_z\rangle}{\langle S_z\rangle_{CSS}} = \frac{\langle S_z\rangle_{1,2_{CSS}}}{\langle S_z\rangle_{CSS}}\frac{\langle S_z\rangle_{1,2}}{\langle S_z\rangle_{1,2_{CSS}}} + \frac{\langle S_z\rangle_{3,4_{CSS}}}{\langle S_z\rangle_{CSS}}\frac{\langle S_z\rangle_{3,4}}{\langle S_z\rangle_{3,4_{CSS}}} \tag{4.52a}$$

$$\frac{(\Delta S_x)^2}{(\Delta S_x)^2_{CSS}} = \frac{(\Delta S_x)^2_{1,2_{CSS}}}{(\Delta S_x)^2_{CSS}}\frac{(\Delta S_x)^2_{1,2}}{(\Delta S_x)^2_{1,2_{CSS}}} + \frac{(\Delta S_x)^2_{3,4_{CSS}}}{(\Delta S_x)^2_{CSS}}\frac{(\Delta S_x)^2_{3,4}}{(\Delta S_x)^2_{3,4_{CSS}}}, \tag{4.52b}$$

where $\langle S_z\rangle_{i,j_{CSS}}$ and $(\Delta S_x)^2_{i,j_{CSS}}$ represent the maximum value the average spin and the variance can take, respectively, in the minimization procedure (as stated in eq.4.38 and 4.39 for $i = 1$ and $j = 2$). As usual, the appendices indicate the particles we are referring to. Moreover, as it follows directly from eq.4.51a and 4.51b, $\langle S_z\rangle_{CSS}$ and $(\Delta S_x)^2_{CSS}$ are given by the sums of the maximum values the average spin and variance can assume over the two subsystems. Collecting all these results together, we have that:

$$\langle S_z\rangle_{1,2_{CSS}} \overset{\text{eq.4.38}}{=} \frac{\eta_1+\eta_2}{2} \tag{4.53a}$$

$$\langle S_z\rangle_{3,4_{CSS}} \overset{\text{eq.4.38}}{=} \frac{\eta_3+\eta_4}{2} \tag{4.53b}$$

$$\langle S_z\rangle_{CSS} = \langle S_z\rangle_{1,2_{CSS}} + \langle S_z\rangle_{3,4_{CSS}} = \frac{\eta_1+\eta_2+\eta_3+\eta_4}{2} \tag{4.53c}$$

$$(\Delta S_x)^2_{1,2_{CSS}} \overset{\text{eq.4.39}}{=} \frac{\eta_1^2+\eta_2^2}{4} \tag{4.53d}$$

$$(\Delta S_x)^2_{3,4_{CSS}} \overset{\text{eq.4.39}}{=} \frac{\eta_3^2+\eta_4^2}{4} \tag{4.53e}$$

$$(\Delta S_x)^2_{CSS} = (\Delta S_x)^2_{1,2_{CSS}} + (\Delta S_x)^2_{3,4_{CSS}} = \frac{\eta_1^2+\eta_2^2+\eta_3^2+\eta_4^2}{4}. \tag{4.53f}$$

Now, looking at the two equations 4.52a and 4.52b, we can get the minimum that $\frac{(\Delta S_x)^2}{(\Delta S_x)^2_{CSS}}$ can assume, for four particles and a density matrix as in eq.4.42. In fact, for any couple of two entangled particles i, j,

$$\frac{(\Delta S_x)^2_{i,j}}{(\Delta S_x)^2_{i,j_{CSS}}} \geq f\left(\frac{\eta_i}{\eta_j}, \frac{\langle S_z\rangle_{i,j}}{\langle S_z\rangle_{i,j_{CSS}}}\right), \tag{4.54}$$

where $f(k, x)$ is the function obtained numerically in the section 4.1.1, and drawn in Fig.4.2. In fact, $(\Delta S_x)^2_{i,j}$ and $\langle S_z\rangle_{i,j}$ refer to the average spin and variance calculated through $\rho_{i,j}$, the density matrix given by the state (the appendices refer to the particle we are considering)

$$|\psi\rangle = C_{\uparrow\uparrow}|\uparrow_i\uparrow_j\rangle + C_{\downarrow\uparrow}|\uparrow_i\downarrow_j\rangle + C_{\uparrow\downarrow}|\downarrow_i\uparrow_j\rangle + C_{\downarrow\downarrow}|\downarrow_i\downarrow_j\rangle, \tag{4.55}$$

i.e.: the same state of eq.4.2. And therefore the same state for which we numerically determined the minimum possible variance $f\left(\frac{\eta_i}{\eta_j}, \frac{\langle S_z\rangle_{i,j}}{\langle S_z\rangle_{i,j_{CSS}}}\right)$ (for simplicity let us assume $\eta_i \leq \eta_j$). As we stated above, this function is *convex*, *increasing* with respect to $\frac{\langle S_z\rangle_{i,j}}{\langle S_z\rangle_{i,j_{CSS}}}$

and *decreasing* with respect to $\frac{\eta_i}{\eta_j}$ (here $\frac{\eta_i}{\eta_j}$ is allowed to vary in the interval $(0,1]$). In conclusion, we can rewrite eq.4.52b in the following way:

$$\begin{aligned}\frac{(\Delta S_x)^2}{(\Delta S_x)^2_{CSS}} &= \frac{(\Delta S_x)^2_{1,2_{CSS}}}{(\Delta S_x)^2_{CSS}}\frac{(\Delta S_x)^2_{1,2}}{(\Delta S_x)^2_{1,2_{CSS}}} + \frac{(\Delta S_x)^2_{3,4_{CSS}}}{(\Delta S_x)^2_{CSS}}\frac{(\Delta S_x)^2_{3,4}}{(\Delta S_x)^2_{3,4_{CSS}}} \overset{eq.4.54}{\geq} \\ &\overset{eq.4.54}{\geq} \frac{(\Delta S_x)^2_{1,2_{CSS}}}{(\Delta S_x)^2_{CSS}} f\left(\frac{\eta_1}{\eta_2}, \frac{\langle S_z\rangle_{1,2}}{\langle S_z\rangle_{1,2_{CSS}}}\right) + \frac{(\Delta S_x)^2_{3,4_{CSS}}}{(\Delta S_x)^2_{CSS}} f\left(\frac{\eta_3}{\eta_4}, \frac{\langle S_z\rangle_{3,4}}{\langle S_z\rangle_{3,4_{CSS}}}\right) \overset{\dagger}{\geq} \\ &\overset{\dagger}{\geq} \frac{(\Delta S_x)^2_{1,2_{CSS}}}{(\Delta S_x)^2_{CSS}} f\left(1, \frac{\langle S_z\rangle_{1,2}}{\langle S_z\rangle_{1,2_{CSS}}}\right) + \frac{(\Delta S_x)^2_{3,4_{CSS}}}{(\Delta S_x)^2_{CSS}} f\left(1, \frac{\langle S_z\rangle_{3,4}}{\langle S_z\rangle_{3,4_{CSS}}}\right) \overset{\dagger\dagger}{\geq} \\ &\overset{\dagger\dagger}{\geq} f\left(1, \frac{(\Delta S_x)^2_{1,2_{CSS}}}{(\Delta S_x)^2_{CSS}}\frac{\langle S_z\rangle_{1,2}}{\langle S_z\rangle_{1,2_{CSS}}} + \frac{(\Delta S_x)^2_{3,4_{CSS}}}{(\Delta S_x)^2_{CSS}}\frac{\langle S_z\rangle_{3,4}}{\langle S_z\rangle_{3,4_{CSS}}}\right),\end{aligned} \tag{4.56}$$

where for the relations marked with † and †† we used the facts that $f(k,x)$ is decreasing with respect to k and convex with respect to x, respectively. Notice that, in order to use the convexity property:

$$\frac{(\Delta S_x)^2_{1,2_{CSS}}}{(\Delta S_x)^2_{CSS}} + \frac{(\Delta S_x)^2_{3,4_{CSS}}}{(\Delta S_x)^2_{CSS}} = 1, \tag{4.57}$$

as it follows directly from the definitions in eq.4.53f.

Let us now look at eq.4.56, and let us try to understand what it means. For any value of the normalized average spin of the whole system, $\frac{\langle S_z\rangle}{\langle S_z\rangle_{CSS}}$ as in eq.4.52a, we can find the minimum of the normalized variance $\frac{(\Delta S_x)^2}{(\Delta S_x)^2_{CSS}}$, determining the smallest value that the last term in eq.4.56 can assume. In other words, if we denote with $\frac{(\Delta S_x)^2_{Min}}{(\Delta S_x)^2_{CSS}}\left(\frac{\langle S_z\rangle}{\langle S_z\rangle_{CSS}}\right)$ the lowest value that the variance $\frac{(\Delta S_x)^2}{(\Delta S_x)^2_{CSS}}$ can take for the given average spin $\frac{\langle S_z\rangle}{\langle S_z\rangle_{CSS}}$, and remembering that the function $f(k,x)$ is *increasing* with respect to x, we can deduce that

$$\begin{aligned}&\frac{(\Delta S_x)^2_{Min}}{(\Delta S_x)^2_{CSS}}\left(\frac{\langle S_z\rangle}{\langle S_z\rangle_{CSS}}\right) = \\ &= f\left(1, \min_{\langle S_z\rangle_{1,2}+\langle S_z\rangle_{3,4}=\langle S_z\rangle}\left\{\frac{(\Delta S_x)^2_{1,2_{CSS}}}{(\Delta S_x)^2_{CSS}}\frac{\langle S_z\rangle_{1,2}}{\langle S_z\rangle_{1,2_{CSS}}} + \frac{(\Delta S_x)^2_{3,4_{CSS}}}{(\Delta S_x)^2_{CSS}}\frac{\langle S_z\rangle_{3,4}}{\langle S_z\rangle_{3,4_{CSS}}}\right\}\right).\end{aligned} \tag{4.58}$$

What does $\min_{\langle S_z\rangle_{1,2}+\langle S_z\rangle_{3,4}=\langle S_z\rangle}\left\{\frac{(\Delta S_x)^2_{1,2_{CSS}}}{(\Delta S_x)^2_{CSS}}\frac{\langle S_z\rangle_{1,2}}{\langle S_z\rangle_{1,2_{CSS}}} + \frac{(\Delta S_x)^2_{3,4_{CSS}}}{(\Delta S_x)^2_{CSS}}\frac{\langle S_z\rangle_{3,4}}{\langle S_z\rangle_{3,4_{CSS}}}\right\}$ exactly mean? And why did we put it here? As stated above, we want to find the minimum of $\frac{(\Delta S_x)^2}{(\Delta S_x)^2_{CSS}}$ for a given average spin $\frac{\langle S_z\rangle}{\langle S_z\rangle_{CSS}}$. Now, in general, there are many ways one can obtain $\langle S_z\rangle$ varying $\langle S_z\rangle_{1,2}$ and $\langle S_z\rangle_{3,4}$; which is the correct one, i.e.: the one that minimizes eq.4.56? Here we remembered that $f(k,x)$ is increasing in x, so that we have to find the

couple of $\langle S_z\rangle_{1,2}$ and $\langle S_z\rangle_{3,4}$ that minimize, for the given $\langle S_z\rangle$, the second argument of the function $f(k,x)$. This is what we expressed in eq.4.58.

Before proceeding to the next passage, that will generalize what we just obtained by the use of the density matrix in eq.4.41, let us just collect the most important results:

- For four particles described by the operator in eq.4.42 it is possible to find a lower bound for the variance, that in general is smaller than the one obtainable using the collective spin operator $\vec{J} = \vec{j_1} + \vec{j_2}$. We will come back later to this point, giving a specific example. Intuitively it is a consequence of the fact that, in the absence of the coefficients η_1, η_2, η_3 and η_4, the argument of the last term in eq.4.56 is fixed to:

$$\begin{aligned} &\frac{(\Delta S_x)^2_{1,2_{CSS}}}{(\Delta S_x)^2_{CSS}} \frac{\langle S_z\rangle_{1,2}}{\langle S_z\rangle_{1,2_{CSS}}} + \frac{(\Delta S_x)^2_{3,4_{CSS}}}{(\Delta S_x)^2_{CSS}} \frac{\langle S_z\rangle_{3,4}}{\langle S_z\rangle_{3,4_{CSS}}} \xrightarrow[\vec{S}\to\vec{J}]{} \\ &\frac{(\Delta J_x)^2_{1,2_{CSS}}}{(\Delta J_x)^2_{CSS}} \frac{\langle J_z\rangle_{1,2}}{\langle J_z\rangle_{1,2_{CSS}}} + \frac{(\Delta J_x)^2_{3,4_{CSS}}}{(\Delta J_x)^2_{CSS}} \frac{\langle J_z\rangle_{3,4}}{\langle J_z\rangle_{3,4_{CSS}}} = \\ &= \frac{\langle J_z\rangle_{1,2} + \langle J_z\rangle_{3,4}}{\langle J_z\rangle_{CSS}} = \frac{\langle J_z\rangle}{\langle J_z\rangle_{CSS}}, \end{aligned} \tag{4.59}$$

  so that we do not have the possibility to move ourselves along the x axis of $f(k,x)$. The "$_{CSS}$" quantities, referred to the collective spin operator $\vec{J}$, are obtainable from the more general ones with $\vec{S}$ by substituting all the coefficients $\{\eta_i\}$ with 1.

- As it follows from eq. 4.56, for reaching the lowest possible value of the variance we need to impose some constraints over the $\{\eta_i\}$. In particular, we need to have that the entangled particles are described by the same coefficients. For example, if $\eta_1 = \eta_2 \neq \eta 3 = \eta_4$, we necessarily have that in the smallest limit the entangled atoms are the couples $(1,2)$ and $(3,4)$. Otherwise it is impossible (except in the limiting cases $\frac{\langle S_z\rangle}{\langle S_z\rangle_{CSS}} = 0$ or $\frac{\langle S_z\rangle}{\langle S_z\rangle_{CSS}} = 1$), to saturate the inequality of eq.4.56.

Let us now discuss the most general case for four particles, allowing the density matrix describing the system to take the form of eq.4.41. Following the same steps as before, we will first determine $\langle S_z\rangle$ and $(\Delta S_x)^2$. These comes directly from eq.4.51a and 4.51b, using the linearity property of the trace:

$$\langle S_z\rangle = p_1\left(\langle S_z\rangle_{1,2} + \langle S_z\rangle_{3,4}\right) + p_2\left(\langle S_z\rangle_{1,3} + \langle S_z\rangle_{2,4}\right) + p_3\left(\langle S_z\rangle_{1,4} + \langle S_z\rangle_{2,3}\right) \tag{4.60a}$$

$$\langle S_x\rangle = p_1\left(\langle S_x\rangle_{1,2} + \langle S_x\rangle_{3,4}\right) + p_2\left(\langle S_x\rangle_{1,3} + \langle S_x\rangle_{2,4}\right) + p_3\left(\langle S_x\rangle_{1,4} + \langle S_x\rangle_{2,3}\right). \tag{4.60b}$$

For obtaining $(\Delta S_x)^2$, let us first write down $\langle S_x\rangle^2$ in an intelligent way:

$$\begin{aligned}\langle S_x\rangle^2 = \left[p_1\left(\langle S_x\rangle_{1,2}+\langle S_x\rangle_{3,4}\right)+p_2\left(\langle S_x\rangle_{1,3}+\langle S_x\rangle_{2,4}\right)+p_3\left(\langle S_x\rangle_{1,4}+\langle S_x\rangle_{2,3}\right)\right]^2 \overset{\dagger}{\leq} \\ \overset{\dagger}{\leq} p_1\left(\langle S_x\rangle_{1,2}+\langle S_x\rangle_{3,4}\right)^2+p_2\left(\langle S_x\rangle_{1,3}+\langle S_x\rangle_{2,4}\right)^2+p_3\left(\langle S_x\rangle_{1,4}+\langle S_x\rangle_{2,3}\right)^2 .\end{aligned} \tag{4.61}$$

Here, the inequality marked with † is a direct consequence of the Jensen's inequality (see lemma 1). Notice that all the squared terms $(\langle S_x\rangle_{i,j}+\langle S_x\rangle_{k,l})^2$, (i,j,k,l) being permutations of the numbers $(1,2,3,4)$, give rise to crossed terms. These crossed terms, as happened for equations 4.49, are the same we obtain writing down $\langle S_x^2\rangle$ (due to the linearity; see eq.4.48):

$$\begin{aligned}\langle S_x^2\rangle = p_1\left(\langle S_x^2\rangle_{1,2}+\langle S_x^2\rangle_{3,4}\right)+p_2\left(\langle S_x^2\rangle_{1,3}+\langle S_x^2\rangle_{2,4}\right)+ \\ +p_3\left(\langle S_x^2\rangle_{1,4}+\langle S_x^2\rangle_{2,3}\right)+(\text{Crossed Terms}).\end{aligned} \tag{4.62}$$

Therefore we can deduce that the variance for the whole system satisfy the relation

$$\begin{aligned}(\Delta S_x)^2 \geq p_1\left[(\Delta S_x)^2_{1,2}+(\Delta S_x)^2_{3,4}\right]+ \\ +p_2\left[(\Delta S_x)^2_{1,3}+(\Delta S_x)^2_{2,4}\right]+p_3\left[(\Delta S_x)^2_{1,4}+(\Delta S_x)^2_{2,3}\right].\end{aligned} \tag{4.63}$$

Now, looking at this last equation and remembering what we obtained previously in this section, we can set the lowest bound:

$$\begin{aligned}&(\Delta S_x)^2 \geq p_1\left[(\Delta S_x)^2_{1,2}+(\Delta S_x)^2_{3,4}\right]+p_2\left[(\Delta S_x)^2_{1,3}+(\Delta S_x)^2_{2,4}\right]+ \\ &+p_3\left[(\Delta S_x)^2_{1,4}+(\Delta S_x)^2_{2,3}\right]\overset{\dagger\dagger}{\geq}(\Delta S_x)^2_{1,2}+(\Delta S_x)^2_{3,4}\overset{eq.4.58}{\geq} \\ &\overset{eq.4.58}{\geq} f\left(1,\min_{\langle S_z\rangle_{1,2}+\langle S_z\rangle_{3,4}=\langle S_z\rangle}\left\{\frac{(\Delta S_x)^2_{1,2_{CSS}}}{(\Delta S_x)^2_{CSS}}\frac{\langle S_z\rangle_{1,2}}{\langle S_z\rangle_{1,2_{CSS}}}+\frac{(\Delta S_x)^2_{3,4_{CSS}}}{(\Delta S_x)^2_{CSS}}\frac{\langle S_z\rangle_{3,4}}{\langle S_z\rangle_{3,4_{CSS}}}\right\}\right),\end{aligned} \tag{4.64}$$

where the second inequality †† is a consequence of the second property stated above (deduced from eq.4.56). We decided to pick $\eta_1=\eta_2$ and $\eta_3=\eta_4$, in order to satisfy the constraint $\frac{\eta_i}{\eta_j}=1$ for the first and second couple of particles.
We finally concluded the most general case for four particles, with entanglement allowed between couples of them. In the following section we will generalize this result to any even number N of atom.

4.1.2.2 N particles

The generalization of the main result obtained in section 4.1.2.1, namely eq.4.64, turns out to be particularly easy. In fact, there is no substantial difference between four and N particles: using linearity and Jensen inequality we can determine analogous results for $\langle S_z \rangle$ and $(\Delta S_x)^2$, and therefore the lowest values the variance can take for different spins along the z axis. But let us proceed with order, starting by giving the density matrix and proceeding to our common objective.

Being, as before, $\rho_{i,j}$ (for $i \neq j$) the most general operator describing a couple of entangled atoms, we have that the most general density matrix for the system is:

$$\rho = \sum_k p_k \rho_{k_1,k_2} \otimes ... \otimes \rho_{k_{N-1},k_N}. \tag{4.65}$$

Here, $\sum_k p_k = 1$ and the appendices k_i, $i = 1, ..., N$, refer to the not commutative permutations of the indices, as we had in eq.4.41 for $N = 4$. However, since the limit of the variance is reached when all the entangled atoms have the same coefficients, we can set all the p_k's equal to zero except the first one and consider the following density matrix

$$\rho = \rho_{1,2} \otimes \rho_{3,4} \otimes ... \otimes \rho_{N-1,N}. \tag{4.66}$$

As said above, here we have $\eta_1 = \eta_2$, $\eta_3 = \eta_4$,..., $\eta_{N-1} = \eta_N$.
At this point, using linearity, it is particularly easy to obtain the equivalent of eq.4.45 and 4.46:

$$\langle S_z \rangle = \langle S_z \rangle_{1,2} + ... + \langle S_z \rangle_{N-1,N} \tag{4.67a}$$

$$\langle S_x \rangle = \langle S_x \rangle_{1,2} + ... + \langle S_x \rangle_{N-1,N}. \tag{4.67b}$$

For S_x^2, we can, again, divide it in two parts: the first one given by $S^2_{x_{1,2}} + ... + S^2_{x_{N-1,N}}$ and the second by the well known crossed terms, as in eq.4.48. Here $S^2_{x_{i,j}} = \left(\eta_i j_{x_i} + \eta_j j_{x_j}\right)^2$, for all $i \neq j$. Therefore we have:

$$\langle S_x^2 \rangle = \langle S_x^2 \rangle_{1,2} + ... + \langle S_x^2 \rangle_{N-1,N} + (\text{Crossed Terms}). \tag{4.68}$$

And, without surprise, these crossed terms are the same ones we would find computing

$$\langle S_x \rangle^2 = \langle S_x \rangle^2_{1,2} + ... + \langle S_x \rangle^2_{N-1,N} + (\text{Crossed Terms}), \tag{4.69}$$

so that, in conclusion:

$$\langle S_z \rangle = \langle S_z \rangle_{1,2} + ... + \langle S_z \rangle_{N-1,N} \tag{4.70a}$$

$$(\Delta S_x)^2 = (\Delta S_x)^2_{1,2} + ... + (\Delta S_x)^2_{N-1,N}\,. \tag{4.70b}$$

For what concerns the normalization (that we need for finding the minimum normalized variance), knowing that $(i \neq j)$

$$\langle S_z \rangle_{i,j_{CSS}} = \frac{\eta_i + \eta_j}{2} \overset{\dagger}{=} \eta_i = \eta_j \tag{4.71a}$$

$$(\Delta S_x)^2_{i,j_{CSS}} = \frac{\eta_i^2 + \eta_j^2}{4} \overset{\dagger}{=} \frac{\eta_i^2}{2} = \frac{\eta_j^2}{2}, \tag{4.71b}$$

the maxima values that $\langle S_z \rangle$ and $(\Delta S_x)^2$ can assume are

$$\langle S_z \rangle_{CSS} = \langle S_z \rangle_{1,2_{CSS}} + ... + \langle S_z \rangle_{N-1,N_{CSS}} \overset{\dagger}{=} \sum_{k=1}^{\frac{N}{2}} \eta_{2k} \tag{4.72a}$$

$$(\Delta S_x)^2_{CSS} = (\Delta S_x)^2_{1,2_{CSS}} + ... + (\Delta S_x)^2_{N-1,N_{CSS}} \overset{\dagger}{=} \sum_{k=1}^{\frac{N}{2}} \frac{\eta_{2k}^2}{2}. \tag{4.72b}$$

In these last four equations, equalities marked with † represent a consequence of the fact that, for the considered couples of entangled particles (i, j), the coefficients η_i and η_j are equal.

At this point we have got everything we need for proceeding in the conclusive step: obtain a result equivalent to eq.4.64 for an even number N of particles. We have, being f the same function we have encountered in the previous section 4.1.2.1:

$$\begin{aligned}
&\frac{(\Delta S_x)^2}{(\Delta S_x)^2_{CSS}} = \frac{(\Delta S_x)^2_{1,2_{CSS}}}{(\Delta S_x)^2_{CSS}} \frac{(\Delta S_x)^2_{1,2}}{(\Delta S_x)^2_{1,2_{CSS}}} + ... + \frac{(\Delta S_x)^2_{N-1,N_{CSS}}}{(\Delta S_x)^2_{CSS}} \frac{(\Delta S_x)^2_{N-1,N}}{(\Delta S_x)^2_{N-1,N_{CSS}}} \geq \\
&\geq \frac{(\Delta S_x)^2_{1,2_{CSS}}}{(\Delta S_x)^2_{CSS}} f\left(\frac{\eta_1}{\eta_2}, \frac{\langle S_z \rangle_{1,2}}{\langle S_z \rangle_{1,2_{CSS}}}\right) + ... + \frac{(\Delta S_x)^2_{N-1,N_{CSS}}}{(\Delta S_x)^2_{CSS}} f\left(\frac{\eta_{N-1}}{\eta_N}, \frac{\langle S_z \rangle_{N-1,N}}{\langle S_z \rangle_{N-1,N_{CSS}}}\right) \overset{\dagger}{=} \\
&\overset{\dagger}{=} \frac{(\Delta S_x)^2_{1,2_{CSS}}}{(\Delta S_x)^2_{CSS}} f\left(1, \frac{\langle S_z \rangle_{1,2}}{\langle S_z \rangle_{1,2_{CSS}}}\right) + ... + \frac{(\Delta S_x)^2_{N-1,N_{CSS}}}{(\Delta S_x)^2_{CSS}} f\left(1, \frac{\langle S_z \rangle_{N-1,N}}{\langle S_z \rangle_{N-1,N_{CSS}}}\right) \overset{\dagger\dagger}{\geq} \\
&\overset{\dagger\dagger}{\geq} f\left(1, \frac{(\Delta S_x)^2_{1,2_{CSS}}}{(\Delta S_x)^2_{CSS}} \frac{\langle S_z \rangle_{1,2}}{\langle S_z \rangle_{1,2_{CSS}}} + ... + \frac{(\Delta S_x)^2_{N-1,N_{CSS}}}{(\Delta S_x)^2_{CSS}} \frac{\langle S_z \rangle_{N-1,N}}{\langle S_z \rangle_{N-1,N_{CSS}}}\right) = \\
&= f\left(1, \frac{\sum_{k=1}^{\frac{N}{2}} \eta_{2k} \langle S_z \rangle_{2k-1,2k}}{\sum_{k=1}^{\frac{N}{2}} \eta_{2k}^2}\right) \underset{Thm.1}{\longrightarrow} f\left(1, \frac{2}{N\bar{\eta^2}} \sum_{k=1}^{\frac{N}{2}} \eta_{2k} \langle S_z \rangle_{2k-1,2k}\right),
\end{aligned} \tag{4.73}$$

where equality marked with † is a consequence of the fact that, for all entangled couple (i,j), $\eta_i = \eta_j$; inequality †† follows from convexity of the $f(k,x)$ function in its second argument. The last passage, where we used the central limit theorem for plugging in what we know about the coefficients $\{\eta_i\}$, needs N to be big.
As before, since $f(k,x)$ is also *increasing* with respect to x (the average spin in our case), we need to find the smallest possible value that the second argument of f can take, given any total average spin $\langle S_z \rangle$. This can be done numerically, knowing the probability distribution functions $p(\eta)$ and $p(\eta^2)$. In fact, generating the $\frac{N}{2}$ coefficients η_{2k} according to their distribution, we can always find, for any $\langle S_z \rangle$,

$$\min_{\langle S_z \rangle = \langle S_z \rangle_{1,2} + \ldots + \langle S_z \rangle_{N-1,N}} \left\{ \sum_{k=1}^{\frac{N}{2}} \eta_{2k} \langle S_z \rangle_{2k-1,2k} \right\}, \tag{4.74}$$

and therefore obtain the theoretical minimum for the normalized variance:

$$\frac{(\Delta S_x)^2_{Min}}{(\Delta S_x)^2_{CSS}} \left(\frac{\langle S_z \rangle}{\langle S_z \rangle_{CSS}} \right) = f \left(1, \frac{2 \min_{\langle S_z \rangle = \langle S_z \rangle_{1,2} + \ldots + \langle S_z \rangle_{N-1,N}} \left\{ \sum_{k=1}^{\frac{N}{2}} \eta_{2k} \langle S_z \rangle_{2k-1,2k} \right\}}{N \bar{\eta^2}} \right). \tag{4.75}$$

This represents a statistical minimum, that is always possible to find knowing $p(\eta)$ and $p(\eta^2)$.
To give an idea, let us derive it for our previous model, introduced in section 2.2.2.3 and analysed more in details later in section 3.1.2. There we supposed to have $p(\eta)$ and $p(\eta^2)$ given by eq.2.105 and 2.108, so that we can determine $\bar{\eta^2}$ (see eq.2.109b) and generate $\frac{N}{2}$ coefficients η_{2k} according to $p(\eta)$. In the following Figure 4.4 we plotted several curves, of which the lowest one (*plain red*) exactly represents the obtained statistical minimum $\frac{(\Delta S_x)^2_{Min}}{(\Delta S_x)^2_{CSS}}$, in the considered model, with parameters ν equal to 0.3 and $N = 10^3$. For a comparison, we also draw the curves representing the minima variances for:

- (*blue dashed*) a generic *separable* state, using, instead of $\vec{S}$, the collective spin operator $\vec{J}$;
- (*blue plain*) the same *separable* state, but considering $\vec{S}$ and probability distribution functions $p(\eta)$ and $p(\eta^2)$ described by the parameters $\nu = 0.3$ and $N = 10^3$;
- (*red dashed*) a generic state where we allow to 2-particles *entanglement*, using the collective spin operator $\vec{J}$.

The red and blue dashed curves, that are obtained, we remember, using $\vec{J}$ instead of $\vec{S}$, are derived by substituting all the coefficients $\{\eta_i\}$ with one. Of course, these are the

same theoretical curves derived by others (see, for example, Anders Sørensen's article [37]) and used as entanglement criteria.

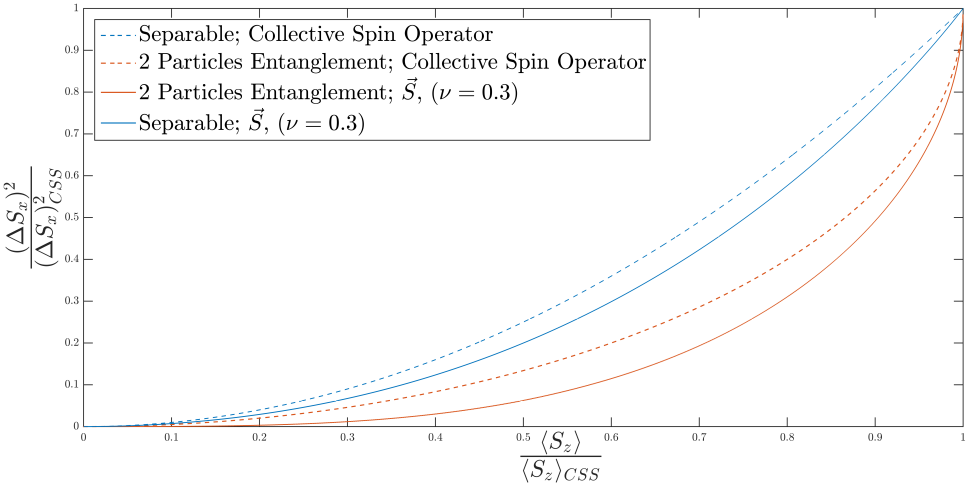

FIGURE 4.4: Minima variances for separable (blue) and 2-particles entangled (red) states. For each couple, the one lying above is obtained using the collective spin operator $\vec{J}$; the one below using $\vec{S}$. Here and $\nu = 0.3$

As it is possible to see from the Fig.4.4, the curves obtained through $\vec{S}$ lie *below* the ones obtained through $\vec{J}$.

For finally concluding about the entanglement of pairs, we will generalize what we found here by considering *odd* numbers N of particles (see Section 4.1.2.3).

4.1.2.3 Generalization to odd numbers of particles

Let us go back to the system in which we allow two particle entanglement. As a conclusive comment we want to understand what happens when the number of considered particles is odd. At first, let us collect the curves describing the minima normalized variances for a single and two possibly entangled particles. This is done in the following picture:

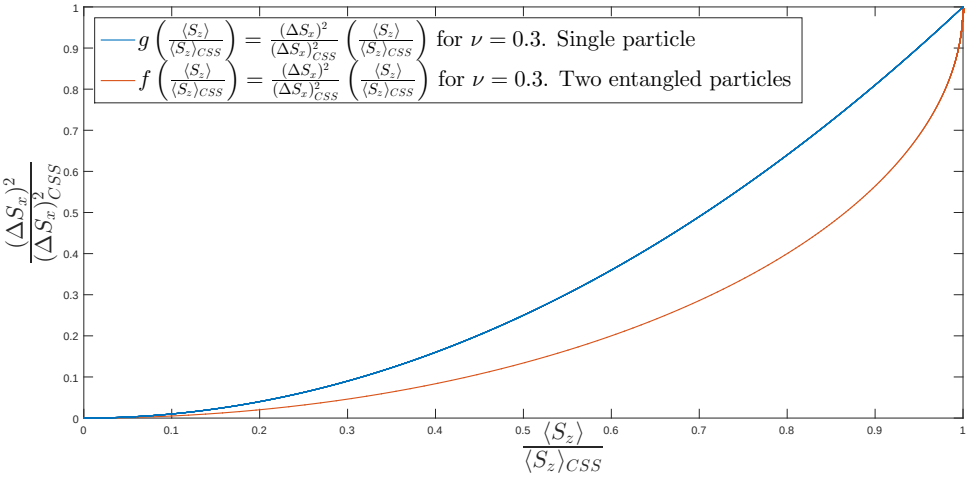

FIGURE 4.5: Reported here we have the curves describing the minima normalized variances for one single particle (*blue*) and an entangled couple (*red*). These functions have been taken from the figures 4.6 and 4.2 respectively. More in particular, for the entangled couple we picked up $\eta_1 = \eta_2$ that, as we have seen, identify the lowest curve

So far nothing new, these are curves we have already seen in the previous sections; the point is that we will use them now for proving the intuitive fact that the contribution of the not entangled particle in a state of N (odd) atoms cannot be smaller of the one of an entangle couple. Notice that we are referring to the situation in which both the variance and the average spin are normalized.

Let us start by giving the density matrix of our state. In general, since we are allowing here for entanglement between two atoms, it is a vector product between not entangled single particle density matrices ρ_i and entangled pairs $\rho_{i,j}$, $i \neq j$. However, since the minimum contribution of a correlated pair is always smaller than the one of a single atom, we will consider only states in which $N-1$ particles are entangled in $\frac{N-1}{2}$ couples, and the N-th atom is a free, lonely one. Written in a mathematical language:

$$\rho = \sum_k p_k \left(\underbrace{\rho_{k_1,k_2} \otimes ... \otimes \rho_{k_{N-2},k_{N-1}}}_{pairs} \otimes \underbrace{\rho_{k_N}}_{single} \right) = \sum_k p_k \rho_k, \tag{4.76}$$

where as usual the p_k's are positive numbers they sum up to one and $\{k_1, ..., k_N\}$ represent permutations of the numbers $1, ..., N$.

If a more rigorous proof of this fact is needed, we can start by considering the most general density matrix we can have:

$$\rho = \sum_k p_k \rho_k = \sum_k p_k \left(\rho_{k_1} \otimes \rho_{k_2} \otimes ... \right), \tag{4.77}$$

where now every ρ_{k_i} can describe a single particle *or* an entangled couple. For instance, let us say

$$\rho_{k_1} = \rho_1 \tag{4.78a}$$

$$\rho_{k_2} = \rho_2 \tag{4.78b}$$

$$\rho_{k_3} = \rho_{1,2}, \tag{4.78c}$$

where a single numerical index states that the density matrix refers to a single particle, while a double one to an entangled couple. We agree that this operator ρ, as in eq.4.77, includes in itself all possible states of our system, so it actually represents the most complete one. Now, using linearity of the trace operator and Jensen inequality (lemma 1), we can write

$$\langle S_z \rangle = \sum_k p_k \left(\langle S_z \rangle_{k_1} + \langle S_z \rangle_{k_2} + ... \right) \tag{4.79a}$$

$$(\Delta S_x)^2 \overset{lemma1}{\geq} \sum_k p_k \left[(\Delta S_x)^2_{k_1} + (\Delta S_x)^2_{k_2} + ... \right], \tag{4.79b}$$

where we introduced the notations $(\Delta S_x)^2_{k_i} = \langle S_{x^2} \rangle_{k_i} - \langle S_x \rangle^2_{k_i}$ and $\langle A \rangle_{k_i} = \mathrm{Tr}\left(A \rho_{k_i}\right)$ for any operator A acting on subsystem ρ_{k_i}. Equations 4.79a and 4.79b, besides the mentioned properties, are consequence of the fact that all ρ_{k_i}'s are independent. The procedure for deriving these results does not include anything new compared to what we have already seen, for instance, in eq.4.93a and eq.4.95.

At this point it is straightforward to understand why the lowest limit for the variance of this system has to be reached for a density matrix of the form of eq.4.76. Let us take the first three terms in the series described by eq.4.79a and 4.79b, namely the ones determined by the matrices ρ_{k_1}, ρ_{k_2} and ρ_{k_3}. Moreover, suppose these three operators are exactly the ones we introduced above, in equations 4.78a, 4.78b and 4.78c. These refer to the first two particles, but while ρ_{k_1} and ρ_{k_2} are distinguishable and do not account for entanglement, ρ_{k_3} does. Therefore ρ_{k_3} is more general than the first two, including in itself the possibility of having two separable particles. The conclusion we take is that the minimum that $\frac{(\Delta S_x)^2_{k_3}}{(\Delta S_x)^2_{CSS_{1,2}}}$ can assume, is always smaller or equal than the one of $\frac{(\Delta S_x)^2_{k_1} + (\Delta S_x)^2_{k_2}}{(\Delta S_x)^2_{CSS_{1,2}}}$. Therefore we can neglect the not necessary single-particles density matrices in eq.4.77, and suppose our system to be the most entangled possible, i.e.: to be composed by $\frac{N-1}{2}$ entangled couples and a single atom. In other words, we obtain back the density matrix 4.76.

As usual, we are considering normalized quantities; here we used the same normalization as before:

$$(\Delta S_x)_{CSS_{1,2}} = \frac{\eta_1^2 + \eta_2^2}{4}, \tag{4.80}$$

that is the value that the variance take for the coherent spin state of the first two particles.

Let us go back to the main problem; from eq.4.76 it is easy to determine out from this density matrix the usual quantities $\langle S_z\rangle$, $\langle S_x\rangle$ and $\langle S_x^2\rangle$. The procedure is, in fact, the same we followed in the equations 4.67a, 4.67b and 4.68 before and in 4.93a, 4.93b and 4.93c later. We have that

$$\langle S_z\rangle = \sum_k p_k \left(\langle S_z\rangle_{k_1,k_2} + ... + \langle S_z\rangle_{k_{N-2},k_{N-1}} + \langle S_z\rangle_{k_N}\right) \tag{4.81a}$$

$$\langle S_x\rangle = \sum_k p_k \left(\langle S_x\rangle_{k_1,k_2} + ... + \langle S_x\rangle_{k_{N-2},k_{N-1}} + \langle S_x\rangle_{k_N}\right) \tag{4.81b}$$

$$\langle S_x^2\rangle = \sum_k p_k \left[\langle S_x^2\rangle_{k_1,k_2} + ... + \langle S_x^2\rangle_{k_{N-2},k_{N-1}} + \langle S_x^2\rangle_{k_N} + (\text{C.T.})\right], \tag{4.81c}$$

where we used the notation

$$\langle S_{z,x}\rangle_{k_i,k_j} = \text{Tr}\left[\rho_k \left(\eta_{k_i} j_{z,x_{k_i}} + \eta_{k_j} j_{z,x_{k_j}}\right)\right] \equiv \text{Tr}\left(\rho_{k_i,k_j} S_{z,x}\right) \tag{4.82a}$$

$$\langle S_x^2\rangle_{k_i,k_j} = \text{Tr}\left[\rho_k \left(\eta_{k_i} j_{x_{k_i}} + \eta_{k_j} j_{x_{k_j}}\right)^2\right] \equiv \text{Tr}\left(\rho_{k_i,k_j} S_x^2\right) \tag{4.82b}$$

$$\langle S_{z,x}\rangle_{k_N} = \text{Tr}\left[\rho_k \eta_{k_N} j_{x_{k_N}}\right] \equiv \text{Tr}\left(\rho_{k_N} S_{z,x}\right) \tag{4.82c}$$

$$\langle S_x^2\rangle_{k_N} = \text{Tr}\left[\rho_k \eta_{k_N} j_{x_{k_N}}^2\right] \equiv \text{Tr}\left(\rho_{k_N} S_x^2\right). \tag{4.82d}$$

It is important to make clear that in "(C.T.)" (eq.4.81c), where we collected *some* of the crossed terms derived from squaring the operator S_x, there are all the contributions of the kind $\langle \eta_{k_i} j_{x_{k_i}}\rangle\langle \eta_{k_j} j_{x_{k_j}}\rangle$. All of them refer to non entangled particles k_i and k_j, that is the reason for which we are allowed to write them in this form instead of $\langle \eta_{k_i} j_{x_{k_i}} \eta_{k_j} j_{x_{k_j}}\rangle$. The crossed terms regarding the entangled pairs are already collected in eq.4.82b. Therefore, once we subtract $\langle S_x\rangle^2$ to $\langle S_x^2\rangle$ in order to get $(\Delta S_x)^2$, what we called "(C.T.)" sums up to zero with its counterpart deriving from squaring $\langle S_x\rangle$. In conclusion:

$$(\Delta S_x)^2 \geq \sum_k p_k \left[(\Delta S_x)^2_{k_1,k_2} + ... + (\Delta S_x)^2_{k_{N-2},k_{N-1}} + (\Delta S_x)^2_{k_N}\right], \tag{4.83}$$

where the inequality follows from Jensen's lemma 1 and

$$(\Delta S_x)^2_{k_i,k_j} = \langle S_x^2\rangle_{k_i,k_j} - \langle S_x\rangle^2_{k_i,k_j} \tag{4.84a}$$

$$(\Delta S_x)^2_{k_N} = \langle S_x^2\rangle_{k_N} - \langle S_x\rangle^2_{k_N}. \tag{4.84b}$$

From now on, let us call $f\left(\frac{\langle S_z\rangle}{\langle S_z\rangle_{CSS}}\right)$ and $g\left(\frac{\langle S_z\rangle}{\langle S_z\rangle_{CSS}}\right)$ the functions representing, given a value of the average spin, the minimum possible variance for one single particle and

an entangled pair respectively, as stated in the legend of Fig.4.5. Therefore we have:

$$\begin{aligned}
\frac{(\Delta S_x)^2}{(\Delta S_x)^2_{CSS}}\left(\frac{\langle S_z\rangle}{\langle S_z\rangle_{CSS}}\right) &\geq \sum_k p_k\left[\frac{(\Delta S_x)^2_{CSS_{k_1,k_2}}}{(\Delta S_x)^2_{CSS}}\frac{(\Delta S_x)^2_{k_1,k_2}}{(\Delta S_x)^2_{CSS_{k_1,k_2}}}+...\right.\\
&\left.\ldots+\frac{(\Delta S_x)^2_{CSS_{k_{N-2},k_{N-1}}}}{(\Delta S_x)^2_{CSS}}\frac{(\Delta S_x)^2_{k_{N-2},k_{N-1}}}{(\Delta S_x)^2_{CSS_{k_{N-2},k_{N-1}}}}+\frac{(\Delta S_x)^2_{CSS_{k_N}}}{(\Delta S_x)^2_{CSS}}\frac{(\Delta S_x)^2_{k_N}}{(\Delta S_x)^2_{CSS_{k_N}}}\right]\overset{\dagger^1}{\geq}\\
&\overset{\dagger^1}{\geq}\sum_k p_k\left[\frac{(\Delta S_x)^2_{CSS_{k_1,k_2}}}{(\Delta S_x)^2_{CSS}}f\left(\frac{\langle S_z\rangle_{k_1,k_2}}{\langle S_z\rangle_{CSS_{k_1,k_2}}}\right)+...\right.\\
&\left.\ldots+\frac{(\Delta S_x)^2_{CSS_{k_{N-2},k_{N-1}}}}{(\Delta S_x)^2_{CSS}}f\left(\frac{\langle S_z\rangle_{k_{N-2},k_{N-1}}}{\langle S_z\rangle_{CSS_{k_{N-2},k_{N-1}}}}\right)+\frac{(\Delta S_x)^2_{CSS_{k_N}}}{(\Delta S_x)^2_{CSS}}g\left(\frac{\langle S_z\rangle_{k_N}}{\langle S_z\rangle_{CSS_{k_N}}}\right)\right]\overset{\dagger^2}{\geq}\\
&\overset{\dagger^2}{\geq}\sum_k p_k\left[\frac{(\Delta S_x)^2_{CSS_{k_1,k_2}}}{(\Delta S_x)^2_{CSS}}f\left(\frac{\langle S_z\rangle_{k_1,k_2}}{\langle S_z\rangle_{CSS_{k_1,k_2}}}\right)+...\right.\\
&\left.\ldots+\frac{(\Delta S_x)^2_{CSS_{k_{N-2},k_{N-1}}}}{(\Delta S_x)^2_{CSS}}f\left(\frac{\langle S_z\rangle_{k_{N-2},k_{N-1}}}{\langle S_z\rangle_{CSS_{k_{N-2},k_{N-1}}}}\right)+\frac{(\Delta S_x)^2_{CSS_{k_N}}}{(\Delta S_x)^2_{CSS}}f\left(\frac{\langle S_z\rangle_{k_N}}{\langle S_z\rangle_{CSS_{k_N}}}\right)\right]\overset{\dagger^3}{\geq}\\
&\overset{\dagger^3}{\geq}f\left(\sum_k p_k\left[\frac{(\Delta S_x)^2_{CSS_{k_1,k_2}}}{(\Delta S_x)^2_{CSS}}\frac{\langle S_z\rangle_{k_1,k_2}}{\langle S_z\rangle_{CSS_{k_1,k_2}}}+...\right.\right.\\
&\left.\left.\ldots+\frac{(\Delta S_x)^2_{CSS_{k_{N-2},k_{N-1}}}}{(\Delta S_x)^2_{CSS}}\frac{\langle S_z\rangle_{k_{N-2},k_{N-1}}}{\langle S_z\rangle_{CSS_{k_{N-2},k_{N-1}}}}+\frac{(\Delta S_x)^2_{CSS_{k_N}}}{(\Delta S_x)^2_{CSS}}\frac{\langle S_z\rangle_{k_N}}{\langle S_z\rangle_{CSS_{k_N}}}\right]\right)\overset{\dagger^4}{\geq}\\
&\overset{\dagger^4}{\geq}f\left(\min_{\langle S_z\rangle=\sum_k p_k\left(\langle S_z\rangle_{k_1,k_2}+...+\langle S_z\rangle_{k_N}\right)}\left\{\sum_k p_k\left[\frac{(\Delta S_x)^2_{CSS_{k_1,k_2}}}{(\Delta S_x)^2_{CSS}}\frac{\langle S_z\rangle_{k_1,k_2}}{\langle S_z\rangle_{CSS_{k_1,k_2}}}+...\right.\right.\right.\\
&\left.\left.\left.\ldots+\frac{(\Delta S_x)^2_{CSS_{k_{N-2},k_{N-1}}}}{(\Delta S_x)^2_{CSS}}\frac{\langle S_z\rangle_{k_{N-2},k_{N-1}}}{\langle S_z\rangle_{CSS_{k_{N-2},k_{N-1}}}}+\frac{(\Delta S_x)^2_{CSS_{k_N}}}{(\Delta S_x)^2_{CSS}}\frac{\langle S_z\rangle_{k_N}}{\langle S_z\rangle_{CSS_{k_N}}}\right]\right\}\right),
\end{aligned}\tag{4.85}$$

where we defined, with a slightly different notation than before,

$$\langle S_z\rangle_{CSS_{k_i,k_j}} = \frac{\eta_{k_i}+\eta_{k_j}}{2} \tag{4.86a}$$

$$(\Delta S_x)^2_{CSS_{k_i,k_j}} = \frac{\eta^2_{k_i}+\eta^2_{k_j}}{4} \tag{4.86b}$$

$$\langle S_z\rangle_{CSS_{k_N}} = \frac{\eta_{k_N}}{2} \tag{4.86c}$$

$$(\Delta S_x)^2_{CSS_{k_N}} = \frac{\eta^2_{k_N}}{4}. \tag{4.86d}$$

Let us now explain all the inequalities marked with † in eq.4.85:

- In the relation $\dagger^1$ we just plugged in the minimizing functions f and g we derived previously and recalled, with the figure 4.5, at the beginning of this section.
- $\dagger^2$ is a straightforward consequence of the fact that, for any allowed $x \in [0,1]$, $g(x) \leq f(x)$. It is important to note here that with this approximation (substitute g with f) we do not obtain an optimal lower limit; being precise we should keep the function g through all the calculations! However, this way the algebra results

to be much simpler; moreover in the limit $N \gg 1$, g's contribution is negligible with respect to the sum of f's ones.

- In $\dagger^3$ we simply used the convexity of the function f. Recalling the previous point, here is where the algebra is much simplified by the substitution $g \to f$. In fact, the convexity argument needs that the coefficients sum up to one! This is always the case for the p_k, but we need the last term $\frac{(\Delta S_x)^2_{CSS_{k_N}}}{(\Delta S_x)^2_{CSS}}$ in order to have

$$\frac{(\Delta S_x)^2_{CSS_{k_1,k_2}}}{(\Delta S_x)^2_{CSS}} + ... + \frac{(\Delta S_x)^2_{CSS_{k_{N-2},k_{N-1}}}}{(\Delta S_x)^2_{CSS}} + \frac{(\Delta S_x)^2_{CSS_{k_N}}}{(\Delta S_x)^2_{CSS}} = 1. \tag{4.87}$$

- In the last inequality $\dagger^4$ we used the property of monotonically increasing of the function f, just as we did in previous sections, in equations 4.64 and 4.75.

As a final passage, in order to conclude the case regarding entanglement for two particles, let us rewrite eq.4.85 plugging in the probability distribution function for the coefficients $p(\eta)$:

$$\begin{aligned} &\frac{(\Delta S_x)^2}{(\Delta S_x)^2_{CSS}} \left(\frac{\langle S_z \rangle}{\langle S_z \rangle_{CSS}} \right) \geq \\ &\geq f \left(\min_{\langle S_z \rangle = \langle S_z \rangle_{1,2} + ... + \langle S_z \rangle_{N-2,N-1} + \langle S_z \rangle_N} \left\{ \frac{2 \sum_{i=1}^{\frac{N-1}{2}} \eta_{2i} \langle S_z \rangle_{2i-1,2i} + \eta_N \langle S_z \rangle_N}{N \bar{\eta}^2} \right\} \right). \end{aligned} \tag{4.88}$$

Here we need to give some explanations. First, we imposed the condition that the coefficients of all entangled couples are the same. As we have seen in section 4.1.2, this is a condition that has to be verified in order to achieve the inferior limit. Second, we neglected the sum over the p_k, because its result is one, and in order to attain the minimum of f's argument in eq.4.85, we can consider all the terms to be independent from k.

In the following, we will try to obtain a better criterion for 2-particle entanglement. However, before doing it, we will take a little detour and get a new minimization curve for $(\Delta S_x)^2$ in the separable case. In fact, for obtaining eq.4.75, we used a different approach than the one we introduced in Section 3.1. Even if in both of them we used the Lagrange method, in the second one we derived the result *straight* through it, while in the first we obtained the lowest bound for the simplest situation (two entangled particles), and then we used it in the general one. There are no reason for which this method should fail in the separable case, and therefore we will see what we can obtain.

4.2 Detour: The separable case again

In order to check what we obtained in Section 3.1, we will here try to achieve a similar result - a lowest bound for $(\Delta S_x)^2$ for a separable state - with a different method. More in particular, we will exploit the single particle normalized curve (Fig.4.6) for obtaining the general one for N particles, using convexity as we did in eq.4.73.

Therefore, let us first derive the mentioned curve for one atom. Now, since it has to be *normalized*, it is sufficient to note that

$$\frac{\langle S_z \rangle}{\langle S_z \rangle_{CSS}} = \frac{\langle \eta J_z \rangle}{\langle \eta J_z \rangle_{CSS}} = \frac{\langle J_z \rangle}{\langle J_z \rangle_{CSS}} \tag{4.89a}$$

$$\frac{(\Delta S_x)^2}{(\Delta S_x)^2_{CSS}} = \frac{\eta^2 (\Delta J_x)^2}{\eta^2 (\Delta J_x)^2_{CSS}} = \frac{(\Delta J_x)^2}{(\Delta J_x)^2_{CSS}}, \tag{4.89b}$$

being η the coefficient describing the only atom we have. It is *not* surprising that, in this case, there is no "η" dependence in $\frac{(\Delta S_x)^2}{(\Delta S_x)^2_{CSS}}$. In fact, through the normalization we are reducing the degrees of freedom for the particles' coefficients by one, and since we only have one η, we end up with no dependence over it. This also is the reason for which we had a single axis for $\frac{\eta_1}{\eta_2}$ in Fig.4.2, instead that two axes, one for η_1 and the other for η_2.
As consequence of equations 4.89a and 4.89b, we automatically recover the "entanglement criterion" reported in the literature (see, for example, the article [37])

$$\frac{(\Delta J_x)^2}{(\Delta J_x)^2_{CSS}} \geq \left(\frac{\langle J_z \rangle}{\langle J_z \rangle_{CSS}} \right)^2, \tag{4.90}$$

that is the squeezing parameter

$$\xi_R^2 = \frac{(\Delta J_x)^2}{\langle J_z \rangle^2} \geq 1. \tag{4.91}$$

Of course, having here only one atom, we cannot speak about entanglement.
In the last equation 4.91 we used that, for one particle, the maximum values that the variance and the average spin are allowed to assume are, respectively, $\frac{1}{4}$ and $\frac{1}{2}$.
In conclusion, the curve minimizing the normalized variance of a single atom is a simple quadratic function (see eq.4.90), drawn in the following figure

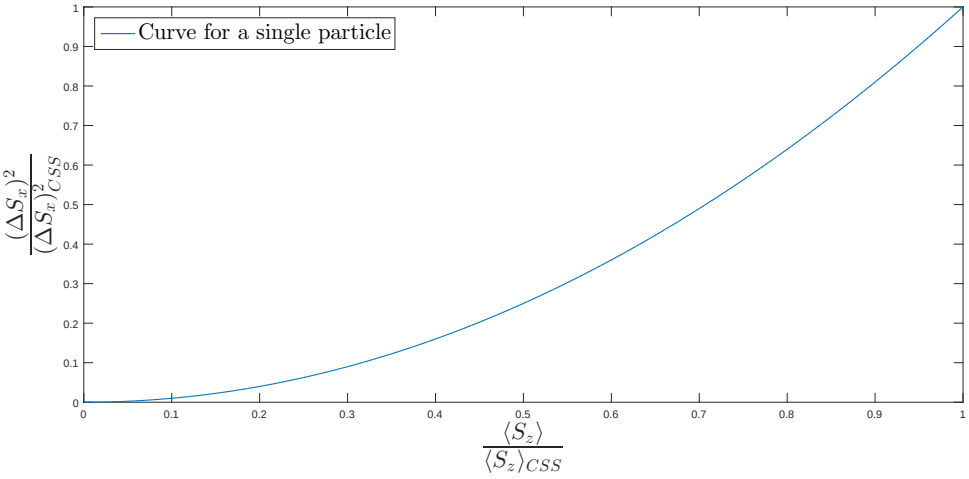

FIGURE 4.6: Minimum normalized variance for a single particle. As reported in the literature, the curve is simply a quadratic - see eq.4.90.

At this point, let us consider back the same separable density matrix as in eq.2.67:

$$\rho = \sum_k p_k \rho_k = \sum_k p_k \rho_{k_1} \otimes ... \otimes \rho_{k_N}. \tag{4.92}$$

Then we have, without surprise, that $\langle S_z \rangle$, $\langle S_x \rangle$ and $\langle S_x^2 \rangle$ are given by:

$$\langle S_z \rangle = \mathrm{Tr}\left(\rho S_z\right) = \sum_k p_k \sum_{i=1}^N \eta_i \mathrm{Tr}\left(\rho_k j_{z_i}\right) = \sum_k p_k \sum_{i=1}^N \eta_i \langle j_{z_i} \rangle_k = \sum_k p_k \sum_{i=1}^N \langle S_{z_i} \rangle_k \tag{4.93a}$$

$$\langle S_x \rangle = \mathrm{Tr}\left(\rho S_x\right) = \sum_k p_k \sum_{i=1}^N \eta_i \langle j_{x_i} \rangle_k = \sum_k p_k \sum_{i=1}^N \langle S_{x_i} \rangle_k \tag{4.93b}$$

$$\langle S_x^2 \rangle = \mathrm{Tr}\left[\rho \left(\underbrace{\sum_{i=1}^N \eta_i j_{x_i}}_{S_x}\right)^2\right] \overset{\dagger}{=} \sum_k p_k \sum_{i=1}^N \eta_i^2 \underbrace{\langle j_{x_i}^2 \rangle_k}_{\frac{1}{4}} + (\text{C.T.}) = \sum_k p_k \sum_{i=1}^N \langle S_{x_i}^2 \rangle_k + (\text{C.T.}) \tag{4.93c}$$

Here we used the same notation we introduced before, $\langle A \rangle_k \equiv \mathrm{Tr}\left(\rho_k A\right)$. In the equality marked with †, we collected all the terms of the kind $p_k \langle j_{x_i} j_{x_j} \rangle_k$, for all $i \neq j$, in the so-called "Crossed Term" (C.T.).

As a last step before being able to write down $(\Delta S_x)^2$, let us compute $\langle S_x \rangle^2$. We have,

with little algebra

$$\langle S_x\rangle^2 = \left(\sum_k p_k \sum_{i=1}^N \eta_i \langle j_{x_i}\rangle_k\right)^2 \overset{\dagger\dagger}{\leq} \sum_k p_k \left(\sum_{i=1}^N \eta_i \langle j_{x_i}\rangle_k\right)^2 = \sum_k p_k \langle S_{x_i}\rangle_k^2 + (\text{C.T.}), \tag{4.94}$$

Where inequality †† is a straightforward consequence of Jensen's theorem we outlined in lemma 1.

At this point, similarly as before in the previous section, once we subtract $\langle S_x\rangle^2$ to $\langle S_x^2\rangle$ in order to get $(\Delta S_x)^2$, the crossed terms (C.T.) cancel themselves. This is, again, a consequence of the fact that, in absence of entanglement, $\langle j_{x_i} j_{x_j}\rangle_k = \langle j_{x_i}\rangle\langle j_{x_j}\rangle_k$ for all $i \neq j$. Finally (from eq.4.93c and 4.94):

$$(\Delta S_x)^2 = \langle S_x^2\rangle - \langle S_x\rangle^2 \geq \sum_k p_k \sum_{i=1}^N \left[\langle S_{x_i}^2\rangle_k - \langle S_{x_i}\rangle_k^2\right] = \sum_k p_k \sum_{i=1}^N (\Delta S_{x_i})_k^2, \tag{4.95}$$

where we defined $(\Delta S_{x_i})_k^2 \equiv \langle S_{x_i}^2\rangle_k - \langle S_{x_i}\rangle_k^2$.

At this point we can determine, using the convexity of the quadratic function, a new lowest bound for the normalized variance in the separable case. In fact, recalling that the normalization is done by dividing for the maximum values reached by the coherent spin state

$$\langle S_z\rangle_{CSS} = \frac{1}{2}\sum_{i=1}^N \eta_i \tag{4.96a}$$

$$(\Delta S_x)_{CSS}^2 = \frac{1}{4}\sum_{i=1}^N \eta_i^2, \tag{4.96b}$$

we have that:

$$\begin{aligned}
\frac{(\Delta S_x)^2}{(\Delta S_x)_{CSS}^2}\left(\frac{\langle S_z\rangle}{\langle S_z\rangle_{CSS}}\right) &\geq \sum_k p_k \sum_{i=1}^N \frac{(\Delta S_{x_i})_k^2}{(\Delta S_x)_{CSS}^2} = \\
&= \sum_k p_k \sum_{i=1}^N \frac{(\Delta S_{x_i})_{k_{CSS}}^2}{(\Delta S_x)_{CSS}^2}\frac{(\Delta S_{x_i})_k^2}{(\Delta S_{x_i})_{k_{CSS}}^2} \overset{\text{eq. 4.90}}{\geq} \\
&\overset{\text{eq. 4.90}}{\geq} \sum_k p_k \sum_{i=1}^N \frac{(\Delta S_{x_i})_{k_{CSS}}^2}{(\Delta S_x)_{CSS}^2}\left(\frac{\langle S_{z_i}\rangle_k}{\langle S_{z_i}\rangle_{k_{CSS}}}\right)^2 \overset{\text{lemma 1}}{\geq} \\
&\overset{\text{lemma 1}}{\geq} \left(\sum_k p_k \sum_{i=1}^N \frac{(\Delta S_{x_i})_{k_{CSS}}^2}{(\Delta S_x)_{CSS}^2}\frac{\langle S_{z_i}\rangle_k}{\langle S_{z_i}\rangle_{k_{CSS}}}\right)^2.
\end{aligned} \tag{4.97}$$

In the last equation we denoted with $\langle S_{z_i}\rangle_{k_{CSS}}$ and $(\Delta S_{x_i})^2_{k_{CSS}}$ the maxima values for the average spin and variance that the i-th particle can obtain respectively; namely

$$\langle S_{z_i}\rangle_{k_{CSS}} = \frac{\eta_i}{2} \tag{4.98a}$$

$$(\Delta S_{x_i})^2_{k_{CSS}} = \frac{\eta_i^2}{4}. \tag{4.98b}$$

Moreover, for using Jensen's inequality (lemma 1), we needed $\sum_k p_k \sum_{i=1}^{N} \frac{(\Delta S_{x_i})^2_{k_{CSS}}}{(\Delta S_x)^2_{CSS}} = 1$. This is ensured from the facts $\sum_k p_k = 1$ and $\sum_{i=1}^{N} \frac{(\Delta S_{x_i})^2_{k_{CSS}}}{(\Delta S_x)^2_{CSS}} = 1$. Notice that there is no explicit dependence over k in the terms $(\Delta S_{x_i})^2_{k_{CSS}}$.
Let us now look back at eq.4.97. Similarly to the previous section, where we derived an analogous result for a system in which two particles' entanglement is allowed (eq.4.75), this equation express the minimum value that the normalized variance of the system can achieve, once we fix the normalized average spin. However, one more step is needed! In fact, given $\frac{\langle S_z\rangle}{\langle S_z\rangle_{CSS}}$, the argument of the last term in eq.4.75 is not uniquely determined. Since $\langle S_z\rangle = \sum_k p_k \sum_{i=1}^{N} \langle S_{z_i}\rangle_k$, there is, in general, quite a lot of freedom in the choices of the $\langle S_{z_i}\rangle_k$'s and the p_k's. Remember here that we are trying to figure out which is the minimum value that the variance can assume; therefore, since the quadratic function is monotonically increasing and, de facto, we can adjust its argument, we need to find the lowest value it can assume:

$$\min_{\langle S_z\rangle = \sum_k p_k \langle S_{z_1}\rangle_k + \ldots + \langle S_{z_N}\rangle_k} \left\{ \sum_k p_k \sum_{i=1}^{N} \frac{(\Delta S_{x_i})^2_{k_{CSS}}}{(\Delta S_x)^2_{CSS}} \frac{\langle S_{z_i}\rangle_k}{\langle S_{z_i}\rangle_{k_{CSS}}} \right\}. \tag{4.99}$$

Substituting now what we wrote in equations 4.98a and 4.98b, we finally have that

$$\frac{(\Delta S_x)^2}{(\Delta S_x)^2_{CSS}} \left(\frac{\langle S_z\rangle}{\langle S_z\rangle_{CSS}} \right) \geq \left(\min_{\langle S_z\rangle = \langle S_{z_1}\rangle + \ldots + \langle S_{z_N}\rangle} \left\{ \frac{2\sum_{i=1}^{N} \eta_i \langle S_{z_i}\rangle}{N\bar{\eta^2}} \right\} \right)^2, \tag{4.100}$$

where we plugged in the average of the squared coefficients $\bar{\eta^2}$ (big N is required) and neglected the sum over k. This can be done since, considering particles having equivalent coefficients, there is a unique way for getting the minimum expressed in eq.4.99, that does not depend over the coefficients p_k that can be summed to one. Knowing the probability distribution $p(\eta)$ of the coefficients, it is possible to draw this function. For example, generating N coefficients according to $p(\eta)$, we can identify the argument of the quadratic function and draw a plot. In the next figure we report it (*blue* curve), considering the model introduced above in sections 2.2.2.3 and 3.1.2. For comparison,

we decided to include the curve we derived with the Lagrange method (section 3.1.2, *red*) and the one obtained considering the collective spin operator (*black dashed*) as well.

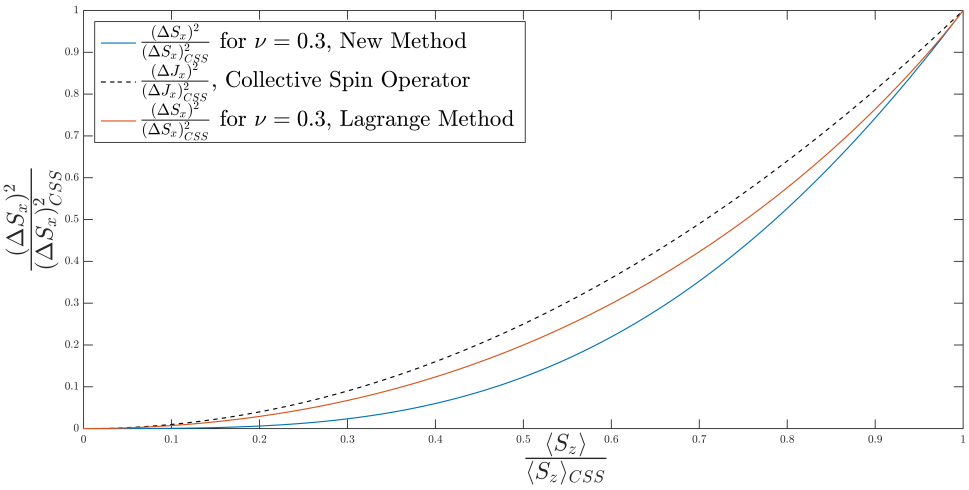

FIGURE 4.7: In this graph we report three curves, obtained with the parameter $\nu = 0.3$ (for the *red* and *blue* ones). All of them represent the minimum possible normalized variance; the *black* one is obtained using the collective spin operator, while the *red* and *blue* with the more general $\vec{S} = \sum_{i=1}^{N} \eta_i \vec{j}_i$. The difference of the latter two is given by the method used in their derivation: for the first one we used Lagrange, while the second follows from eq.4.100

As it is possible to see, the curves obtained with the Lagrange method (*red*) and the convexity of the single particle function (*blue*) are *not* the same. Should we take the conclusion that - at least for one of them - we did something wrong? Fortunately not (at least not so soon); in fact Jensen's inequality is saturated to an equality *only* under some particular conditions (for example the coefficients being all equal), so that this method is not particularly efficient. On the other hand, every point along the *red* curve corresponds to a specific, real state, so that we can deduce that the Lagrange method give rise to a better constraint. Of course both the methods are valid, but not equivalent.

4.3 A better boundary for N particles entangled in pairs

Similarly to what happened in the separable case (see the conclusion of previous section 4.2), the curves obtained for N particles entangled in pairs (Fig.4.4) are not efficient. In fact, unless all the coefficients $\{\eta_i\}$ are the same, the convexity inequality used in their derivation is never saturated along the whole curve, giving therefore a bad criterion.

The natural question arising in this context is therefore: "Can we obtain something

better?" Take, for instance, the separable case. The big advantage we had there is that we were able to minimize the Lagrange function Γ directly for the general case of N atoms, without the need of going through evaluating the incriminated inequality. But this is not true any more when we allow to have correlations between particles; in fact now $\langle j_{x_i} j_{x_j} \rangle = \langle j_{x_i} \rangle \langle j_{x_j} \rangle$, for all $i \neq j$ is not true any more. From one side, this is the reason for which the limit for entangled atoms is actually lower; but from the other side it prevents us from obtaining the optimal criterion.

What we will do next is to use the information we obtained in section 4.1.1 - and more in particular eq.4.40 - to obtain the optimal criterion, plugging the informations directly in the Lagrange function Γ and therefore avoiding the deleterious convexity argument.

4.3.1 The "Optimal criterion"

As said above, the way for obtaining the optimal criterion passes through the Lagrange multiplier method. The additional informations we will plug in are:

- For any entangled couple of particles (i, j), in order to achieve the minimum, the coefficients have to be equal:
$$\eta_i = \eta_j. \tag{4.101}$$
This is a straightforward consequence of the second property deduced from Fig.4.2.

- The most general density matrix describing the system is the one given in eq.4.65. However, for our purpose it is easier to consider the one written in eq.4.66, that we recall to be
$$\rho = \rho_{1,2} \otimes \rho_{3,4} \otimes ... \otimes \rho_{N-1,N} = \bigotimes_{k=1}^{\frac{N}{2}} \rho_{2k-1,2k}. \tag{4.102}$$
As discussed above (see section 4.1.2.2), these two are completely equivalent for our purposes. Moreover, we have supposed N to be an even number. Generalization to odd N can be done in the same fashion as we did in section 4.1.2.3.

At this point we are able to write down the average spin and variance for our system. In the following we are referring to section 4.1.2.2. Skipping some algebra - that can be found in the equations 4.70a and 4.70b - and using the same notation as before, we

have:

$$\langle S_z\rangle = \langle S_z\rangle_{1,2} + ... + \langle S_z\rangle_{N-1,N} = \sum_{k=1}^{\frac{N}{2}} \langle S_z\rangle_{2k-1,2k} \tag{4.103a}$$

$$(\Delta S_x)^2 = (\Delta S_x)^2_{1,2} + ... + (\Delta S_x)^2_{N-1,N} = \sum_{k=1}^{\frac{N}{2}} (\Delta S_x)^2_{2k-1,2k}\,. \tag{4.103b}$$

We also remember that the values that we will use for the normalization are:

$$\langle S_z\rangle_{CSS} = \langle S_z\rangle_{1,2_{CSS}} + ... + \langle S_z\rangle_{N-1,N_{CSS}} \overset{\dagger}{=} \sum_{k=1}^{\frac{N}{2}} \eta_{2k} \tag{4.104a}$$

$$(\Delta S_x)^2_{CSS} = (\Delta S_x)^2_{1,2_{CSS}} + ... + (\Delta S_x)^2_{N-1,N_{CSS}} \overset{\dagger}{=} \sum_{k=1}^{\frac{N}{2}} \frac{\eta^2_{2k}}{2}, \tag{4.104b}$$

where we used in † that

$$\langle S_z\rangle_{2k-1,2k_{CSS}} = \eta_k \tag{4.105a}$$

$$(\Delta S_x)^2_{2k-1,2k_{CSS}} = \frac{\eta^2_k}{2}. \tag{4.105b}$$

At this stage we finally have all the ingredients to write down our Lagrange function $\Gamma(\mu, \langle S_z\rangle, (\Delta S_x)^2)$:

$$\Gamma = (\Delta S_x)^2 - \mu\langle S_z\rangle = \sum_{k=1}^{\frac{N}{2}} \left\{(\Delta S_x)^2_{2k-1,2k} - \mu\langle S_z\rangle_{2k-1,2k}\right\}. \tag{4.106}$$

Now, with the intention of plugging in the information contained in eq.4.40, we rewrite such relation as

$$\frac{(\Delta S_x)^2_{2k-1,2k}}{(\Delta S_x)^2_{2k-1,2k_{CSS}}} \geq 1 - \sqrt{1 - \left(\frac{\langle S_z\rangle_{2k-1,2k}}{\langle S_z\rangle_{2k-1,2k_{CSS}}}\right)^2} \text{ for } k = 1, ..., \frac{N}{2}; \tag{4.107}$$

this way we made clear that this inequality can be used for all entangled pairs we are dealing with in the Lagrange function. Notice that we were able to substitute $\vec{S}$ by the collective spin operator $\vec{J}$ for the two following reasons:

- The density matrix $\rho = \bigotimes_{k=1}^{\frac{N}{2}} \rho_{2k-1,2k}$ consists of the vector product of the independent sub-matrices $\rho_{2k-1,2k}$, $k = 1, ..., \frac{N}{2}$

- In the case in which the entangled pair $(2k-1, 2k)$ is described by the same coefficient η_k, we get that

$$\frac{\langle S_z\rangle_{2k-1,2k}}{\langle S_z\rangle_{2k-1,2k_{CSS}}} = \frac{\langle J_z\rangle_{2k-1,2k}}{\langle J_z\rangle_{2k-1,2k_{CSS}}} \tag{4.108a}$$

$$\frac{(\Delta S_x)^2_{2k-1,2k}}{(\Delta S_x)^2_{2k-1,2k_{CSS}}} = \frac{(\Delta J_x)^2_{2k-1,2k}}{(\Delta J_x)^2_{2k-1,2k_{CSS}}} \tag{4.108b}$$

But let us come back to the main problem; it is useful now to slightly modify the form of the Γ function. Starting from eq.4.106, it is easy to obtain:

$$\begin{aligned}
\Gamma &= \sum_{k=1}^{\frac{N}{2}} \left\{ (\Delta S_x)^2_{2k-1,2k} - \mu \langle S_z\rangle_{2k-1,2k} \right\} = \\
&= \sum_{k=1}^{\frac{N}{2}} \left\{ (\Delta S_x)^2_{2k-1,2k_{CSS}} \frac{(\Delta S_x)^2_{2k-1,2k}}{(\Delta S_x)^2_{2k-1,2k_{CSS}}} - \mu \langle S_z\rangle_{2k-1,2k_{CSS}} \frac{\langle S_z\rangle_{2k-1,2k}}{\langle S_z\rangle_{2k-1,2k_{CSS}}} \right\} = \\
&= \sum_{k=1}^{\frac{N}{2}} \left\{ \frac{\eta_k^2}{2} \frac{(\Delta S_x)^2_{2k-1,2k}}{(\Delta S_x)^2_{2k-1,2k_{CSS}}} - \mu\eta_k \frac{\langle S_z\rangle_{2k-1,2k}}{\langle S_z\rangle_{2k-1,2k_{CSS}}} \right\}.
\end{aligned} \tag{4.109}$$

It is therefore clear how we can use the inequality 4.107; in fact, plugging it in this last equation, we are able to minimize the Γ function and make it dependent over the variables μ and $\langle J_z\rangle_{2k-1,2k}$ only. Notice that, since we are trying to find a lower bound, this minimization is not deleterious. We get:

$$\begin{aligned}
\Gamma &\geq \sum_{k=1}^{\frac{N}{2}} \left\{ \frac{\eta_k^2}{2} \left[1 - \sqrt{1 - \left(\frac{\langle S_z\rangle_{2k-1,2k}}{\langle S_z\rangle_{2k-1,2k_{CSS}}} \right)^2} \right] - \mu\eta_k \frac{\langle S_z\rangle_{2k-1,2k}}{\langle S_z\rangle_{2k-1,2k_{CSS}}} \right\} \equiv \\
&\equiv \tilde{\Gamma}\left(\mu, \left\{ \frac{\langle S_z\rangle_{2k-1,2k}}{\langle S_z\rangle_{2k-1,2k_{CSS}}} \right\} \right)
\end{aligned} \tag{4.110}$$

It is important to make clear that, as consequence of the fact that eq.4.107 is an inequality that can always be saturated, we are still in the optimality condition. In other words, for all possible values $\left\{ \frac{\langle S_z\rangle_{2k-1,2k}}{\langle S_z\rangle_{2k-1,2k_{CSS}}} \right\}$ and μ, Γ represents a physically real state. We remember that, in general, $\left\{ \frac{\langle S_z\rangle_{2k-1,2k}}{\langle S_z\rangle_{2k-1,2k_{CSS}}} \right\}$ and μ are allowed to vary inside the intervals $[-1, 1]$ and $(-\infty, \infty)$ respectively. In the following we will reduce them through symmetry considerations.

From now on, it is just a matter of following the same steps of section 3.2: find the minimum possible value of the Γ function for any μ, and then determine the associated normalized averaged spin $\frac{\langle S_z\rangle}{\langle S_z\rangle_{CSS}}$ and variance $\frac{(\Delta S_x)^2}{(\Delta S_x)^2_{CSS}}$. This result will be achieved by

studying the first and second derivatives of $\tilde{\Gamma}\left(\mu, \left\{\frac{\langle S_z\rangle_{2k-1,2k}}{\langle S_z\rangle_{2k-1,2k_{CSS}}}\right\}\right)$. For clearness, let us denote $\frac{\langle S_z\rangle_{2k-1,2k}}{\langle S_z\rangle_{2k-1,2k_{CSS}}}$ with x_k. We have

$$\frac{\partial\tilde{\Gamma}(\mu,\{x_k\})}{\partial x_k} = \eta_k\left(\frac{\eta_k}{2}\frac{x_k}{\sqrt{1-x_k^2}} - \mu\right), \tag{4.111}$$

from which it is easy to find the only stationary point

$$x_{k_{min}} = \frac{2|\mu|\,\mathrm{sgn}(\mu)}{\sqrt{\eta_k^2+4\mu^2}}. \tag{4.112}$$

Notice that the Γ function is symmetric with respect to the transformation

$$\left(\mu, \left\{\frac{\langle S_z\rangle_{2k-1,2k}}{\langle S_z\rangle_{2k-1,2k_{CSS}}}\right\}\right) \rightarrow \left(-\mu, -\left\{\frac{\langle S_z\rangle_{2k-1,2k}}{\langle S_z\rangle_{2k-1,2k_{CSS}}}\right\}\right), \tag{4.113}$$

so that, without loss of generality, we can restrict the intervals in which x_k and μ can vary to $[0,1]$ and $[0,\infty)$ respectively. In addition to the same argument used in section 3.1.2, here we also imposed that all the $\left\{\frac{\langle S_z\rangle_{2k-1,2k}}{\langle S_z\rangle_{2k-1,2k_{CSS}}}\right\}$ have the same sign.
Is this point a minimum? The second derivative is always bigger than zero,

$$\frac{\partial^2\tilde{\Gamma}(\mu,\{x_k\})}{\partial x_k^2} = \frac{\eta_k^2}{2\left(1-x_k^2\right)^{\frac{3}{2}}} > 0 \;\forall\; x_k \in [0,1], \tag{4.114}$$

that ensures us the stationary point is a minimum.
At this point, since this is valid for any $k = 1, ..., \frac{N}{2}$, we can plug in this constraint in the Γ function for obtaining its lowest possible value Γ_{min}:

$$\begin{aligned}\Gamma_{min}(\mu) &= \sum_{k=1}^{\frac{N}{2}}\frac{\eta_k^2}{2}\left[1-\sqrt{1-x_{k_{min}}^2}\right] - \mu\sum_{k=1}^{\frac{N}{2}}\eta_k x_{k_{min}} = \\ &= \sum_{k=1}^{\frac{N}{2}}\frac{\eta_k^2}{2}\left[1-\frac{\eta_k}{\sqrt{\eta_k^2+4\mu^2}}\right] - \mu\sum_{k=1}^{\frac{N}{2}}\eta_k\frac{\mu}{\sqrt{\eta_k^2+4\mu^2}}.\end{aligned} \tag{4.115}$$

Finally, using these results we can determine the minimum average spin $\langle S_z\rangle$ and variance $(\Delta S_x)^2$ for the system of $\frac{N}{2}$ pairs of entangled particle. In fact, using the equation 4.103a we have

$$\langle S_z\rangle = \sum_{k=1}^{\frac{N}{2}}\langle S_z\rangle_{2k-1,2k} = \sum_{k=1}^{\frac{N}{2}}\eta_k x_{k_{min}} = 2\mu\sum_{k=1}^{\frac{N}{2}}\frac{\eta_k}{\sqrt{\eta_k^2+4\mu^2}}, \tag{4.116}$$

while from 4.103b and 4.107, supposing this latter inequality saturated, we get

$$\begin{aligned}(\Delta S_x)^2 &= \sum_{k=1}^{\frac{N}{2}} (\Delta S_x)^2_{2k-1,2k} = \sum_{k=1}^{\frac{N}{2}} \frac{\eta_k^2}{2} \frac{(\Delta S_x)^2_{2k-1,2k}}{(\Delta S_x)^2_{2k-1,2k_{CSS}}} = \\ &= \sum_{k=1}^{\frac{N}{2}} \frac{\eta_k^2}{2} \left[1 - \sqrt{1 - x^2_{k_{min}}}\right] = \sum_{k=1}^{\frac{N}{2}} \frac{\eta_k^2}{2} \left[1 - \frac{\eta_k}{\sqrt{\eta_k^2 + 4\mu^2}}\right].\end{aligned} \tag{4.117}$$

Therefore, including the normalization, we achieve the important results:

$$\frac{\langle S_z \rangle}{\langle S_z \rangle_{CSS}} = \left(\sum_{j=1}^{\frac{N}{2}} \eta_j\right)^{-1} \sum_{k=1}^{\frac{N}{2}} \mu \frac{2\eta_k}{\sqrt{\eta_k^2 + 4\mu^2}} \tag{4.118a}$$

$$\frac{(\Delta S_x)^2}{(\Delta S_x)^2_{CSS}} = \left(\sum_{j=1}^{\frac{N}{2}} \eta_j^2\right)^{-1} \sum_{k=1}^{\frac{N}{2}} \eta_k^2 \left[1 - \frac{\eta_k}{\sqrt{\eta_k^2 + 4\mu^2}}\right]. \tag{4.118b}$$

Why these two equations are so important? Because they allow to determine the now optimal curve that identifies the minimum possible normalized variance $\frac{(\Delta S_x)^2}{(\Delta S_x)^2_{CSS}}$ with respect to the average spin $\frac{\langle S_z \rangle}{\langle S_z \rangle_{CSS}}$, when we allow to 2-particle entanglement.
Why is such curve optimal? Because, differently from before, here for any value of the average spin and any set of coefficients $\{\eta_k\}$, the variance corresponds to a precise state of the system.
How are we going to determine, in practice, this curve? There are two possible ways we already used in the previous sections. The first and easiest one, is to generate the $\frac{N}{2}$ coefficients $\{\eta_k\}$ according to their probability distribution $p(\eta)$ and use directly equations 4.118a and 4.118b. The second, "analytic", way is in general harder, because it requires to determine non trivial probability distribution functions. In fact, besides $p(\eta)$ and $p(\eta^2)$, necessary for deriving $\bar{\eta}$ and $\bar{\eta^2}$, we need to know $p\left(\frac{\eta}{\sqrt{\eta^2+4\mu^2}}\right)$ and $p\left(\frac{\eta^3}{\sqrt{\eta^2+4\mu^2}}\right)$ for the relative averages $\overline{\left(\frac{\eta}{\sqrt{\eta^2+4\mu^2}}\right)}$ and $\overline{\left(\frac{\eta^3}{\sqrt{\eta^2+4\mu^2}}\right)}$. However, once we know them, we have:

$$\frac{\langle S_z \rangle}{\langle S_z \rangle_{CSS}} = \frac{2\mu}{\bar{\eta}} \overline{\left(\frac{\eta}{\sqrt{\eta^2 + 4\mu^2}}\right)} \tag{4.119a}$$

$$\frac{(\Delta S_x)^2}{(\Delta S_x)^2_{CSS}} = 1 - \frac{1}{\bar{\eta^2}} \overline{\left(\frac{\eta^3}{\sqrt{\eta^2 + 4\mu^2}}\right)}, \tag{4.119b}$$

they unequivocally identify the curve of interest that describes the behaviour of the system once the number of atoms N is big enough for having an appropriate statistic.

The two couples of equations 4.118a, 4.118b and 4.119a, 4.119b represent everything we can say about our system without knowing the coefficients $\{\eta_k\}$ - i.e.: their probability distribution $p(\eta)$. In the following we will use once again the simplified model of sections 2.2.2.3 and 3.1.2, in order to confront this new curve with the one derived using convexity.

4.3.2 A practical example

As said above, let us suppose to have the distribution $p(\eta)$ of eq.2.105 describing our $\frac{N}{2}$ coefficients for N particles. There are now two ways of proceeding, as we discussed at the end of the previous section. However, even for such simplified model the derivations of $p\left(\frac{\eta}{\sqrt{\eta^2+4\mu^2}}\right)$ and $p\left(\frac{\eta^3}{\sqrt{\eta^2+4\mu^2}}\right)$ are already not trivial. Henceforth we decide to simply generate the coefficients according to $p(\eta)$ and to use the first mentioned method only.

In the first of the next two figures (4.8) it is possible to see the histogram with the coefficients $\{\eta_k\}$ we used for the derivation of the curves plotted in the second figure (4.9). Along with the histogram we draw the theoretical distribution $p(\eta)$, while in the plot the three curves represent the minimum possible variance $\frac{(\Delta S_x)^2}{(\Delta S_x)^2_{CSS}}$ with respect to the average spin $\frac{\langle S_z\rangle}{\langle S_z\rangle_{CSS}}$. All refer to the situation of pairs of entangled particles; the differences are:

- The *black dashed* curve is the theoretical one obtained first by Anders Sørensen in [37], using the collective spin operator $\vec{J}$ instead of $\vec{S}$ (see eq.4.40)
- The *blue* curve is the one described by eq.4.75 and already plotted in Fig.4.4 (*plain red* there). The convexity inequality has been used in its derivation
- Finally, the *red* curve represents the fresh, optimal criterion derived using equations 4.118a, 4.118b and the coefficients $\{\eta_k\}$ collected in the histogram of the next Fig.4.8.

The histogram with the coefficients is

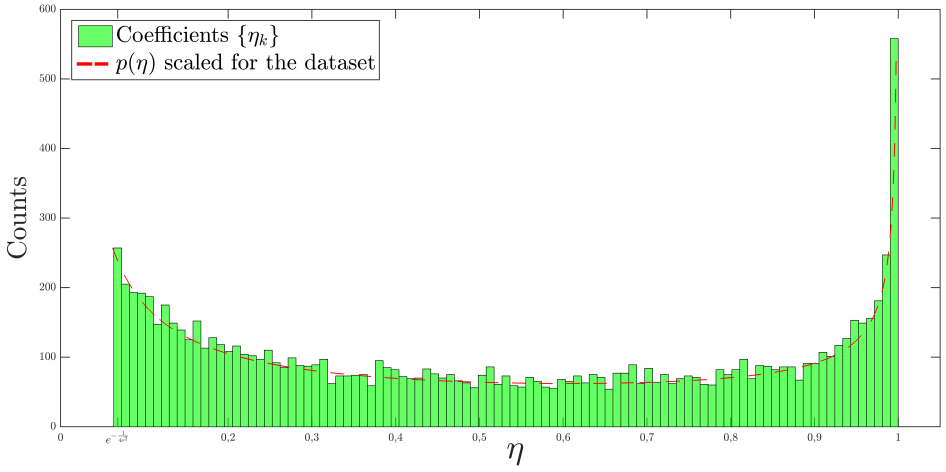

FIGURE 4.8: Histogram with the coefficients $\{\eta_k\}$ generated according with the probability distribution $p(\eta)$, as in eq.2.105, plotted in red and scaled for the considered dataset. The total number of generated coefficients is $\frac{N}{2} = 10^4$

while the plot with the three mentioned curves is:

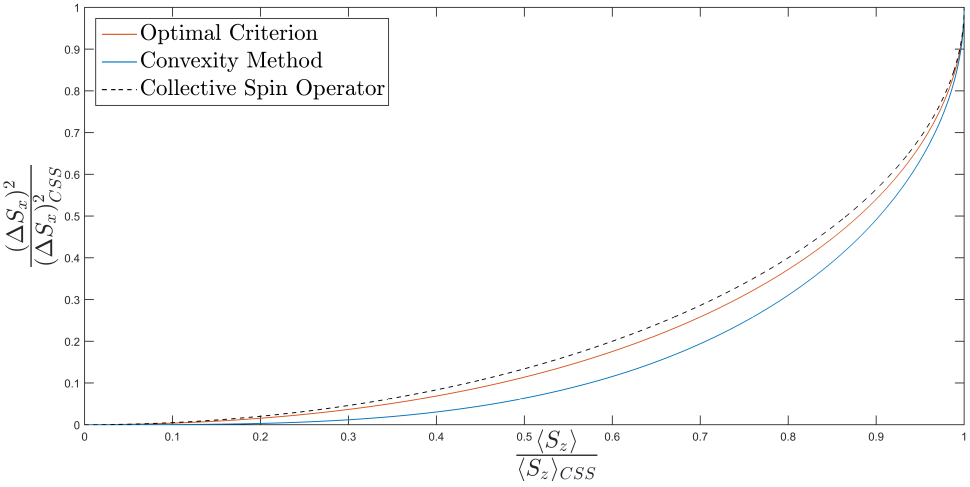

FIGURE 4.9: The *dashed black* curve here is drawn using eq.4.40 directly. The *blue* line represents the criterion derived using the convexity inequality, while the *red* one is the optimal. For these latter two the coefficients $\{\eta_k\}$ collected in the histogram 4.8 have been used

As it is possible to see, the two curves representing the two-particle entanglement criteria for operator $\vec{S}$ are significantly different. The one obtained using the convexity argument lies far below the optimal one, thus confirming our prediction according to which the new criterion is much better than the old one.

4.4 k-particle entanglement

Let us briefly summarize what we have done so far in this chapter:

1. We started by taking two particles, described by any coefficients η_1 and η_2, and numerically derived their minimum possible variance with respect to the average spin and the fraction $\frac{\eta_1}{\eta_2}$ (see fig.4.2)

2. We deduced, from our numerical calculations, that the two-particle curve $\frac{(\Delta S_x)^2}{(\Delta S_x)^2_{CSS}}$ $\left(\frac{\eta_1}{\eta_2}, \frac{\langle S_z \rangle}{\langle S_z \rangle_{CSS}}\right)$ satisfy two important properties: it is *convex* with respect to its second argument, and *reaches the minimum* whenever $\eta_1 = \eta_2$. The latter one allows us to use eq.4.40, the curve determined in [37], as reference curve; this will be important in the following

3. At this point we took a collection of N particles, and we allowed them to be correlated in pairs. Which is the criterion for having *more* than two-particle entanglement? We derived a first one (eq.4.75), using the two previously cited properties (convexity method)

4. We extended this result to an *odd* number of atoms

5. We took a small detour to the separable case again and, using the same convexity-based procedure we described in the previous points, we derived a new entanglement criterion (Fig.4.7). We concluded that this method is *not* efficient, since it is based on an inequality that, in general, is not saturated for the majority of the states

6. We designed a new procedure, that uses the Lagrange method for determining the minimum variance directly for N particles entangled in pairs. This new method - that we called "Optimal" - is based on the fact that for reaching the minimum, the coefficients of the entangled pairs have to be equal. This way, we can plug in eq.4.40 in the Lagrange function and minimize it

7. The conclusion we draw is that this Optimal method is significantly better than the convexity-based one.

In the following, our goal is to generalize the Optimality method - that, ironically, will not be optimal any more - to the case of k-particles entanglement.

At first, similarly to what we have done before (section 4.1.1), we will think at the case of k atoms described by the most general state vector and any coefficients $(\eta_1, ..., \eta_k)$.

The result we are aiming to, is to prove that the minimum possible variance is achieved when all the $\{\eta_j\}_{j=1}^k$ are the same. In such case we are able to use, within the Lagrange method, the well known results obtained with the collective spin operator (see [37]), and obtain a natural generalization of the optimal method to k-particles entanglement. However, we remember that this result was determined numerically before, minimizing a function of seven complex variables and one real. In principle, the same procedure can be repeated here, now with k^2-1 complex variables (of the wave function) and $k-1$ real (the coefficients); but we believe too much computational resources would be required, already with reasonable small values for k. We tried to find an alternative way to reach the desired conclusion, but it seems to be at least very challenging without directly computing the function. Therefore, for now, we must limit ourselves to a reasonable assumption

Conjecture 1. *Let us suppose to have a k-tuple of particles, each one described by a coefficient η_j allowed to vary in the range $(0,1]$, for all $j=1,...,k$. Then the minimum normalized variance $\frac{(\Delta S_x)^2}{(\Delta S_x)^2_{CSS}}$, as a function of the normalized spin $\frac{\langle S_z\rangle}{\langle S_z\rangle_{CSS}}$ is achieved whenever all the $\{\eta_j\}_{j=1}^k$ are equal.*

Using this conjecture we are able to take a step further in the Optimal procedure for k-tuples of entangled particles. What we still need to know is the equivalent of the relation 4.40 for $k>2$. In fact, the analytical equation for the desired criterion is known only for two atoms; all the others have been derived numerically (see [37]). What we will do in the next section, is to find a lower bound for the normalized variance of the collective spin operator $\frac{(\Delta J_x)^2}{(\Delta J_x)^2_{CSS}}$ with respect to the average spin $\frac{\langle J_z\rangle}{\langle J_z\rangle_{CSS}}$. The reason for which we are using $\vec{J}$ instead of $\vec{S}$ is that, whenever all the coefficients are the same, they are completely equivalent. Moreover, for the collective spin operator we know the commutation relations that are not valid for $\vec{S}$ any more.

4.4.1 Lower bound for the k-particle state

Let us suppose to have k particles, described by the same coefficients $\eta_1 = ... = \eta_k$. For this reason, up to a normalization constant, the collective spin operator $\vec{J}$ is completely equivalent to $\vec{S}$:

$$\vec{S} = \eta\vec{J}. \tag{4.120}$$

As consequence, we can work with $\vec{J}$ instead of $\vec{S}$.
There are two main inequalities we will use for determining the lower bound of the normalized variance $\frac{(\Delta J_x)^2}{(\Delta J_x)^2_{CSS}}$ with respect to the average spin $\frac{\langle J_z\rangle}{\langle J_z\rangle_{CSS}}$:

- The first one is the *Heisenberg Uncertainty Relation*. It states that, for *any* operators A and B acting on the system, the product of their variances is related with their commutator according to

$$(\Delta A)^2(\Delta B)^2 \geq \left|\frac{\langle[A,B]\rangle}{2}\right|^2, \tag{4.121}$$

being $[A,B] = AB - BA$. In our case, with $A = J_x$ and $B = J_y$, we have $[J_x, J_y] = iJ_z$, and therefore we recover the well known

$$(\Delta J_x)^2(\Delta J_y)^2 \geq \frac{\langle J_z\rangle^2}{4} \tag{4.122}$$

- The second one is a consequence of the quantization of spin. In general, for a state made by a collection of k particles of spin $\frac{1}{2}$, the inequality

$$\langle J_x^2\rangle + \langle J_y^2\rangle + \langle J_z^2\rangle \leq \frac{k}{2}\left(\frac{k}{2}+1\right) \tag{4.123}$$

holds. This is equivalent to say that the biggest eigenvalue of the operator $\vec{J}^2$ is $\max_J\{J(J-1)\}$, J being what we called "spin of the system", $J = \frac{k}{2}, \frac{k}{2}-1, \frac{k}{2}-2, ...$ down to 0 or $\frac{1}{2}$, depending if k is even or odd. Relation 4.123, together with the fact $\langle J_z^2\rangle \geq \langle J_z\rangle^2$ - consequence of the positivity of the variance - finally yields the second main inequality

$$\langle J_x^2\rangle + \langle J_y^2\rangle + \langle J_z\rangle^2 \leq \frac{k}{2}\left(\frac{k}{2}+1\right) \tag{4.124}$$

Now we can use the latter eq.4.124 to minimize the product $(\Delta J_x)^2(\Delta J_y)^2$

$$\begin{aligned}
&(\Delta J_x)^2(\Delta J_y)^2 = (\Delta J_x)^2(\langle J_y^2\rangle - \langle J_y\rangle^2) \overset{eq.4.124}{\leq} \\
&\overset{eq.4.124}{\leq} (\Delta J_x)^2\left(\frac{k}{2}\left(\frac{k}{2}+1\right) - \langle J_x^2\rangle - \langle J_y\rangle^2 - \langle J_z\rangle^2\right) = \\
&= (\Delta J_x)^2\left[\frac{k}{2}\left(\frac{k}{2}+1\right) - \langle J_z\rangle^2\right] + (\Delta J_x)^2\left[\underbrace{-\langle J_x^2\rangle + \langle J_x\rangle^2}_{-(\Delta J_x)^2}\underbrace{-\langle J_x\rangle^2 - \langle J_y\rangle^2}_{\leq 0}\right] \leq \\
&\leq (\Delta J_x)^2\left[\frac{k}{2}\left(\frac{k}{2}+1\right) - \langle J_z\rangle^2\right] - \left[(\Delta J_x)^2\right]^2,
\end{aligned} \tag{4.125}$$

that can be related directly to the average spin $\langle J_z\rangle$ using eq.4.122:

$$(\Delta J_x)^2\left[\frac{k}{2}\left(\frac{k}{2}+1\right) - \langle J_z\rangle^2\right] - \left[(\Delta J_x)^2\right]^2 \geq \frac{\langle J_z\rangle^2}{4}. \tag{4.126}$$

At this point we can rewrite this last inequality as

$$\left[(\Delta J_x)^2\right]^2 - (\Delta J_x)^2 \left[\frac{k}{2}\left(\frac{k}{2}+1\right) - \langle J_z\rangle^2\right] + \frac{\langle J_z\rangle^2}{4} \leq 0, \tag{4.127}$$

in which we recognize the equation of a parabola in the variable $(\Delta J_x)^2$. Remembering that we are dealing with a system of k particles - that means that

$$\langle J_z\rangle \in \left[-\frac{k}{2}, \frac{k}{2}\right] \tag{4.128a}$$

$$(\Delta J_x)^2 \in \left[-\frac{k}{4}, \frac{k}{4}\right], \tag{4.128b}$$

the only way inequality 4.127 can be satisfied is

$$(\Delta J_x)^2 \geq \frac{1}{2}\left\{\frac{k}{2}\left(\frac{k}{2}+1\right) - \langle J_z\rangle^2 - \sqrt{\left[\frac{k}{2}\left(\frac{k}{2}+1\right) - \langle J_z\rangle^2\right]^2 - \langle J_z\rangle^2}\right\}. \tag{4.129}$$

Notice that we still need to normalize the variance $(\Delta J_x)^2$ and the average spin $\langle J_z\rangle$, in order to have a lower bound we can use for our operator $\vec{S}$. Knowing that

$$\langle J_z\rangle_{CSS} = \frac{k}{2} \tag{4.130a}$$

$$(\Delta J_x)^2_{CSS} = \frac{k}{4}, \tag{4.130b}$$

we can easily get:

$$\frac{(\Delta J_x)^2}{(\Delta J_x)^2_{CSS}} \geq 1 + \frac{k}{2}\left[1 - \frac{\langle J_z\rangle^2}{\langle J_z\rangle^2_{CSS}}\right] - \sqrt{\left[1 + \frac{k}{2}\left(1 - \frac{\langle J_z\rangle^2}{\langle J_z\rangle^2_{CSS}}\right)\right]^2 - \frac{\langle J_z\rangle^2}{\langle J_z\rangle^2_{CSS}}}. \tag{4.131}$$

This is a very important relation for us; in fact, it will allow us to perform what we called "Optimal method", the procedure with which we can determine the lower bound for the variance of N particles entangled in k-tuples. The details will be given later in the following sections. At the moment, let us make clear that the criteria we would obtain using this method are not really optimal. In fact, differently from inequality 4.40 - valid for $k = 2$ - that can always be saturated, eq.4.131 does *not* provide a strict lower limit, meaning that it exceeds the real minimum. In order to better understand what it means, in the next figure 4.10 we draw the real optimal limit, for $k = 2$, given by eq.4.40 (*red* curve), and the lower bound determined through eq.4.131 (*blue* curve). For the reason explained before, these do not coincide; the blue line lies below the red one.

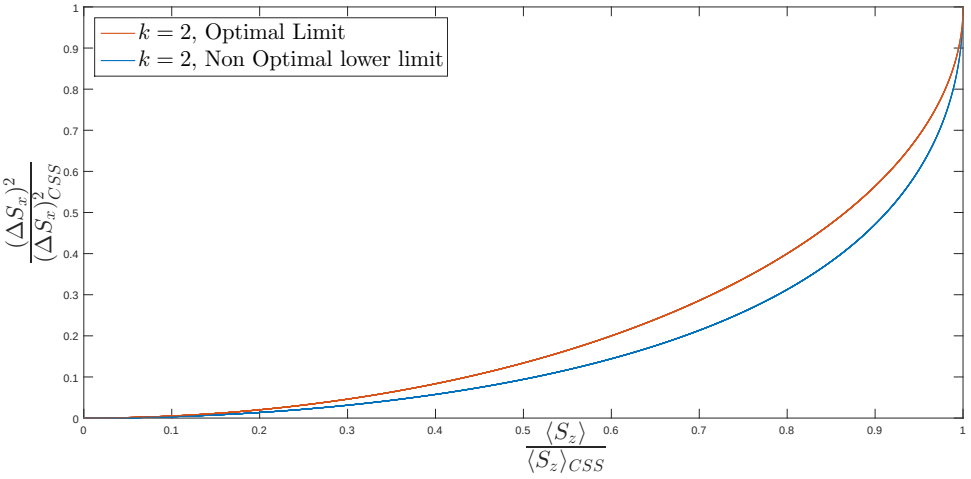

FIGURE 4.10: Two different lower bounds for the normalized variance $\frac{(\Delta J_x)^2}{(\Delta J_x)^2_{CSS}}$ with respect to $\frac{\langle J_z \rangle}{\langle J_z \rangle_{CSS}}$. In *red*, the optimal curve obtained through eq.4.40; in *blue* the one derived with eq.4.131

In conclusion, let us point out the two positive aspects of the lower bound given by inequality 4.131:

- First - and this is actually the most important one - it works for any number of atoms k. This is a fundamental requirement, because we will need such relation for determining the different k-particle entanglement criteria
- On the other side, even if it is not the optimal limit, it asymptotically reduces to it in the limit of big and even k. This has been proven by Ander Sørensen in [37].

4.4.2 N particles with allowed entanglement in k-tuplets

So far, we have determined a lower bound for the variance of k particles. In the following, similarly to what we did in the previous section 4.3.1, we will use it for N atoms, now possibly entangled in k-tuplets. We will call the criteria derived this way "Optimal", even if they do not really are. The reason for this ambiguity is that the procedure we will follow here is the natural generalization of the optimal method used before for $k = 2$. Moreover, as explained above, such generalization is not optimal only because eq.4.131 does *not* represent a strict lower bound for the normalized variance of k particle. If, in the future, such bound will be known, the real optimal criteria can be easily determined, simply substituting it to the weaker bound represented by eq.4.131.

Let us start with order, by describing the system we are going to analyse. Remember that we want to minimize the normalized variance $\frac{(\Delta J_x)^2}{(\Delta J_x)^2_{CSS}}$ with respect to the

average spin $\frac{\langle J_z\rangle^2}{\langle J_z\rangle^2_{CSS}}$. Keeping this in mind, the reasonable assumptions we are taking are:

1. All atoms in any k-tuplet have the same coefficient η. This follows directly from the conjecture 1, according to which the contribution of a k-tuplet is the lowest when such condition is verified

2. The number N of particles is a very big multiple of k:

$$N = nk, \text{ with } n \in \mathbb{N},\ n \gg 1 \tag{4.132}$$

   Let us comment this requirement. At first, we need $n \gg 1$ because we demand to have enough statistics. All the k-tuplets will have one characteristic coefficient η_j, with $j = 1, ..., n$, so that, at the end, we will have n different coefficients. In order to have a non fluctuating lower bound, this number needs to be big, exactly as N needed to be big in the separable case, and $\frac{N}{2} = n$ for $k = 2$ in the 2-particle entanglement situation.
   Why $N = nk$? Analogously to what we have done in section 4.1.2.3, the most general density matrix describing the system is

$$\rho = \sum_l p_l \rho_l = \sum_l p_l \left(\rho_{l_1} \otimes \rho_{l_2} \otimes ...\right), , \tag{4.133}$$

   where, here, each of the ρ_{l_i} describes a single particle *or* a number of atoms less or equal to k. Now, it is clear that the smallest normalized variance is obtained when all of the ρ_{l_i} refer to entangled k-tuplets. If N is *not* a multiple of k, we end up with having some free or less entangled particles in our system. However, generalizing what we said before, when $N \gg k$ and $N \neq nk$, we can obtain a non optimal lower bound by adding "virtual" particles up to $N = nk$. This bound will asymptotically tend to the optimal when $\frac{N}{k} \to \infty$

3. Proceeding with the previous point 2, we can give the density matrix for our system:

$$\rho = \sum_l p_l \rho_l = \sum_l p_l \bigotimes_{j=1}^{n} \rho_{l_j}, \tag{4.134}$$

   where now all of the ρ_{l_j} consist of k particles. Using linearity and lemma 1, we can further simplify this operator, by saying that the minimum variance can only be obtained without the "l" superposition. We finally end up with

$$\rho = \bigotimes_{j=1}^{n} \rho_j, \tag{4.135}$$

the natural generalization to k particles of equation 4.102.

Now that we have described our environment, we can proceed with determining the quantities we will use in the Lagrange Γ function: $\frac{(\Delta S_x)^2}{(\Delta S_x)^2_{CSS}}$ and $\frac{\langle S_z\rangle}{\langle S_z\rangle_{CSS}}$. Introducing the notation we will use in this section,

$$\langle A\rangle_j \equiv \mathrm{Tr}\left(A\rho_j\right), \tag{4.136}$$

where A is a generic operator acting on the system, we have:

$$\langle S_z\rangle = \sum_{j=1}^{n}\eta_j\langle J_z\rangle_j = \sum_{j=1}^{n}\langle S_z\rangle_j \tag{4.137a}$$

$$(\Delta S_x)^2 = \sum_{j=1}^{n}\eta_j^2(\Delta J_x)_j^2 = \sum_{j=1}^{n}(\Delta S_x)_j^2. \tag{4.137b}$$

These last relations are obtained the same way we got equations 4.70a and 4.70b, we also defined $(\Delta J_x)_j^2 \equiv \langle J_z^2\rangle_j - \langle J_z\rangle_j^2$ and $(\Delta S_x)_j^2 \equiv \langle S_z^2\rangle_j - \langle S_z\rangle_j^2$. As last ingredient, we need the normalization, both for the collective quantities $(\Delta S_x)^2$ and $\langle S_z\rangle$, and for the smaller terms $(\Delta S_x)_j^2$ and $\langle S_z\rangle_j$, with $j = 1, ..., n$. For these latter ones, indicated with $(\Delta S_x)^2_{j_{CSS}}$ and $\langle S_z\rangle_{j_{CSS}}$, we can use equations 4.130a and 4.130b, that, together with 4.120 yield:

$$\langle S_z\rangle_{j_{CSS}} = k\frac{\eta_j}{2} \tag{4.138a}$$

$$(\Delta S_x)^2_{j_{CSS}} = k\frac{\eta_j^2}{4}. \tag{4.138b}$$

Using these it is now trivial to determine the normalization for the collective quantities as well:

$$\langle S_z\rangle_{CSS} = \sum_{j=1}^{n}\langle S_z\rangle_{j_{CSS}} = \sum_{j=1}^{n}k\frac{\eta_j}{2} \tag{4.139a}$$

$$(\Delta S_x)^2_{j_{CSS}} = \sum_{j=1}^{n}(\Delta S_x)^2_{j_{CSS}} = \sum_{j=1}^{n}k\frac{\eta_j^2}{4}, \tag{4.139b}$$

the final step before proceeding with the actual minimization of the Lagrange Γ function $\Gamma((\Delta S_x)^2, \langle S_z\rangle, \mu) = (\Delta S_x)^2 - \mu\langle S_z\rangle$. Collecting together the terms referring to the same density matrix ρ_j, the Γ function takes the form:

$$\begin{aligned}\Gamma((\Delta S_x)^2, \langle S_z\rangle, \mu) &= \sum_{j=1}^{n}\left[(\Delta S_x)_j^2 - \mu\langle S_z\rangle_j\right] = \\ &= \sum_{j=1}^{n}\left[(\Delta S_x)^2_{j_{CSS}}\frac{(\Delta S_x)_j^2}{(\Delta S_x)^2_{j_{CSS}}} - \mu\langle S_z\rangle_{j_{CSS}}\frac{\langle S_z\rangle_j}{\langle S_z\rangle_{j_{CSS}}}\right],\end{aligned} \tag{4.140}$$

where in the last passage we made explicit the dependence over the normalized quantities of the k-tuples. From this equation and using the two relations 4.138a and 4.138b, we can rewrite the Lagrange function as:

$$\Gamma(\{(\Delta S_x)_j^2\},\{\langle S_z\rangle_j\},\mu)=\sum_{j=1}^{n}\left[\frac{k\eta_j^2}{4}\frac{(\Delta S_x)_j^2}{(\Delta S_x)_{j_{CSS}}^2}-\mu\frac{k\eta_j}{2}\frac{\langle S_z\rangle_j}{\langle S_z\rangle_{j_{CSS}}}\right], \tag{4.141}$$

that, plugging in the lower bound of eq.4.131, finally becomes

$$\begin{aligned}&\Gamma\left(\left\{\frac{\langle S_z\rangle_j}{\langle S_z\rangle_{j_{CSS}}}\right\},\mu\right)=\\&=\sum_{j=1}^{n}\left\{\frac{k\eta_j^2}{4}\left[1+\frac{k}{2}\left(1-\frac{\langle S_z\rangle_j^2}{\langle S_z\rangle_{j_{CSS}}^2}\right)-\sqrt{\left[1+\frac{k}{2}\left(1-\frac{\langle S_z\rangle_j^2}{\langle S_z\rangle_{j_{CSS}}^2}\right)\right]^2-\frac{\langle S_z\rangle_j^2}{\langle S_z\rangle_{j_{CSS}}^2}}\right]+\right.\\&\left.-\mu\frac{k\eta_j}{2}\frac{\langle S_z\rangle_j}{\langle S_z\rangle_{j_{CSS}}}\right\}.\end{aligned} \tag{4.142}$$

Notice that we supposed the inequality 4.131 to be saturated; a natural requirement since we are interested in the minimum of the Γ function. Looking now more carefully to the right hand side of eq.4.142, we notice that it is made of n independent contributions, each of them can be minimized autonomously. In order to do that, we can compute the first and second derivative with respect to $\frac{\langle S_z\rangle_j}{\langle S_z\rangle_{j_{CSS}}}$. Before actually doing that, let us briefly comment about the ranges in which the variables inside the Γ function are allowed to vary. In principle, μ and every $\frac{\langle S_z\rangle_j}{\langle S_z\rangle_{j_{CSS}}}$ reside in the ranges $(-\infty,\infty)$ and $[-1,1]$ respectively. However, we can restrict these intervals to $\mu\in[0,\infty)$ and $\frac{\langle S_z\rangle_j}{\langle S_z\rangle_{j_{CSS}}}\in[0,1]$, for all $j=1,...,n$, due to the following reasons:

- The Lagrange Γ function is symmetric with respect to the transformation

$$\left(\mu,\frac{\langle S_z\rangle_j}{\langle S_z\rangle_{j_{CSS}}}\right)\rightarrow\left(-\mu,-\frac{\langle S_z\rangle_j}{\langle S_z\rangle_{j_{CSS}}}\right) \tag{4.143}$$

- Looking at the definition of the Γ function, it is clear that the signs of the variables μ and $\langle S_z\rangle$ have to be the same, in order to achieve the lowest possible result

- Similarly, the signs of all the $\langle S_z\rangle_j$ have to be the same as well, in order to maximize $|\langle S_z\rangle|$ and therefore minimize Γ

Let us now proceed with the determination of the derivatives. For not overcharging the next formulae, let us denote $\frac{\langle S_z\rangle_j}{\langle S_z\rangle_{j_{CSS}}}$ with x_j. We have:

$$\frac{\partial\Gamma}{\partial x_l} = \frac{k\eta_l^2}{4}x_l\left[\frac{1+k\left[1+\frac{k}{2}\left(1-x_l^2\right)\right]}{\sqrt{\left(1-x_l^2\right)\left[\left(1+\frac{k}{2}\right)^2-\frac{k^2}{4}x_l^2\right]}}-k\right]-\mu\frac{\eta_l}{2} \tag{4.144}$$

and

$$\frac{\partial^2\Gamma}{\partial x_l^2} = \frac{k\eta_l^2}{4}\left\{-k+\frac{1-k^2x_l^2+k\left[1+\frac{k}{2}\left(1-x_l^2\right)\right]}{\sqrt{\left(1-x_l^2\right)\left[\left(1+\frac{k}{2}\right)^2-\frac{k^2}{4}x_l^2\right]}}+\frac{x_l^2\left[1+\frac{k}{2}\left(1+\frac{k}{2}\left[1-x_l^2\right]\right)\right]^2}{\left(\left(1-x_l^2\right)\left[\left(1+\frac{k}{2}\right)^2-\frac{k^2}{4}x_l^2\right]\right)^{\frac{3}{2}}}\right\}. \tag{4.145}$$

For the minima we have to identify the points $x_{j_{min}}$, inside the range $[0,1]$, for which $\frac{\partial\Gamma}{\partial x_l}(x_l = x_{l_{min}}) = 0$ and $\frac{\partial^2\Gamma}{\partial x_l^2}(x_l = x_{l_{min}}) > 0$. However, equations 4.144 and 4.145 are not analytically solvable. We need to find the minimum numerically, through the help of a calculator. In general, it is not even assured that a suitable set $\{x_{j_{min}}\}_{j=1}^n$ exists for the whole μ and x_j domains; or that this set is unique! For this purpose, we checked for the whole ranges $(0,1]$, in which the η_j's are allowed to vary, and $[0,\infty)$, within which resides μ. For the latter one and for big values of μ we just noticed that the term in the squared brackets in the right hand side of eq.4.144 tends to infinity whenever $x_l \to 1$. This way we can conclude that, asymptotically, $x_{l_{min}} \underset{\mu\to\infty}{\longrightarrow} 1$. It never happened, during the checking, to see an anomaly. We always found one and only one value $x_{j_{min}}$, for which the second derivative was always positive.

Having found the minimum for any $j = 1, ..., n$, we are now able to determine the expressions for the normalized minimum variance $\frac{(\Delta S_x)^2}{(\Delta S_x)^2_{CSS}}$ with respect to the average spin $\frac{\langle S_z\rangle}{\langle S_z\rangle_{CSS}}$. Without having an analytical expression for the $\{x_{j_{min}}\}_{j=1}^n$, we only need to substitute them to $\left\{\frac{\langle S_z\rangle_j}{\langle S_z\rangle_{j_{CSS}}}\right\}_{j=1}^n$ in the following equations for the normalized spin and variance. Remember that we have to plug in the constraint given by the lower bound of eq.4.131 in the latter one. Starting from equations 4.137a and 4.137b, we have:

$$\frac{\langle S_z\rangle}{\langle S_z\rangle_{CSS}} = \frac{1}{\langle S_z\rangle_{CSS}}\sum_{j=1}^n\langle S_z\rangle_{j_{CSS}}\frac{\langle S_z\rangle_j}{\langle S_z\rangle_{j_{CSS}}} = \left(\sum_{l=1}^n\eta_l\right)^{-1}\sum_{j=1}^n\eta_j x_{j_{min}} \tag{4.146}$$

and

$$\frac{(\Delta S_x)^2}{(\Delta S_x)^2_{CSS}} = \frac{1}{(\Delta S_x)^2_{CSS}} \sum_{j=1}^{n} (\Delta S_x)^2_{j_{CSS}} \frac{(\Delta S_x)^2_j}{(\Delta S_x)^2_{j_{CSS}}} \overset{eq.4.131}{=} \frac{1}{(\Delta S_x)^2_{CSS}} \times$$
$$\times \sum_{j=1}^{n} \frac{k\eta_j^2}{4} \left[1 + \frac{k}{2} \left(1 - \frac{\langle S_z \rangle_j^2}{\langle S_z \rangle^2_{j_{CSS}}} \right) - \sqrt{\left[1 + \frac{k}{2} \left(1 - \frac{\langle S_z \rangle_j^2}{\langle S_z \rangle^2_{j_{CSS}}} \right) \right]^2 - \frac{\langle S_z \rangle_j^2}{\langle S_z \rangle^2_{j_{CSS}}}} \right] =$$
$$= \left(\sum_{l=1}^{n} \eta_l^2 \right)^{-1} \sum_{j=1}^{n} \eta_j^2 \left[1 + \frac{k}{2} \left(1 - x^2_{j_{min}} \right) - \sqrt{\left[1 + \frac{k}{2} \left(1 - x^2_{j_{min}} \right) \right]^2 - x^2_{j_{min}}} \right]. \tag{4.147}$$

This is the key equation representing the final goal of this thesis. It gives us, for any value of μ and for any $k \in \mathbb{N}$, the minimum normalized variance with respect to the average spin. Differently from the case $k = 2$, where it was given an analytical expression for the minimum $x_{l_{min}}$ (eq.4.112), here we are not able to express $\frac{(\Delta S_x)^2}{(\Delta S_x)^2_{CSS}}$ and $\frac{\langle S_z \rangle}{\langle S_z \rangle_{CSS}}$ with respect to the probability distribution function $p(\eta)$, as we did in the equations 4.119a and 4.119b. Therefore, the only possible way to practically draw the desired curve for a particular distribution $p(\eta)$, is to use what in section 4.3.1 we called "simplified method". It consists of generating a statistically large number n of coefficients $\{\eta_j\}$, numerically determine $x_{j_{min}}$ for each of these and then plot the function using equations 4.146 and 4.147. This is what we are going to do in the next section, where we will use again our simplified model for determining the $\{\eta_j\}$.

Before we actually do it, however, let us comment more in details what these curves represent. As said, these are entanglement criteria; but what does it exactly means that we have k-particle entanglement? In general we think that our system is separable or correlated, and hence we would naively think that there has to be only one curve that determines if our atomic sample is entangled or not. And this is true; this curve does exist, and is the one derived using Table 3.4 and represented (for various parameters, with the simplified model of sections 2.2.2.3 and 3.1.2) in Fig3.4. The curves we will obtain with equations 4.146 and 4.147 regard the *quality* of entanglement we have. In fact, for every state described by an experimental point that lies *below* a curve with a certain k, we are sure that there are *at least* $k + 1$ entangled particles. For this reason, from now on, we will refer to these curves as "k-particle" entanglement criteria'.

4.4.3 Another practical example

With the procedure we explained in the previous section 4.4.2, we can plot the criteria for having more than k-particle entanglement, for every natural number k. More in particular, let us consider the same coefficients $\{\eta_i\}_{i=1}^n$ we collected in the histogram

4.9, generated using the distribution $p(\eta)$ of eq.2.105. With these, we are able to give the following figure, where:

- The *dashed* curves are obtained through the collective spin operator $\vec{J}$. Their equations are given, for any value of k, by eq.4.131
- The *plain* curves represent the new criteria, derived using equations 4.146 and 4.147 for the same values of k of before

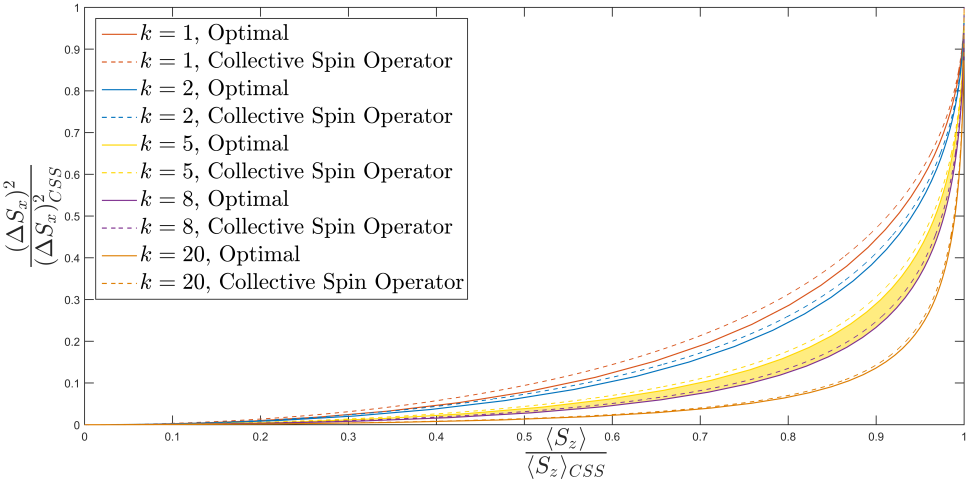

FIGURE 4.11: Various curves, referring to $k = 1, 2, 5, 8, 20$. The *dashed* ones are derived through eq.4.131, the plain using 4.146 and 4.147

Let us give an interpretation to the previous plot. Each couple of curves *plain+dashed* refers to a particular value of k. If we perform an experiment - in which the particles are described by our particular distribution $p(\eta)$ - these lines represent a powerful way for determining the measure of entanglement we have. For instance, if our experimental point hits the *yellow* region in the plane below the curve with $k = 5$, we can conclude that there are at least 6 particles entangled in our sample. Notice that, if we had access to normalized variance and average spin of the collective spin operator, we would only need the *dashed* line. The *plains* were born after we realized that such requirement is likely to be excessive, and we supposed to be able to measure the quantities relative to $\vec{S}$ only. Notice that, even though (with this particular model) the dashed and plain curves lie very near to each other, if we do not have access to $\frac{(\Delta J_x)^2}{(\Delta J_x)^2_{CSS}}$ and $\frac{\langle J_z \rangle}{\langle J_z \rangle_{CSS}}$, we can only use the plains as k-particles entanglement criteria.

Chapter 5

Experimental Application

5.1 The experiment

In this section we introduce the experiment we will analyse later. It is important to underline that all this work, that we will take and use for proving experimental k-particle entanglement, has been done by J.Appel, P.J.Windpassinger, D.Oblak, U.B.Hoff, N.Kjærgaard and E.S.Polzik. My particular contribution to the experiment has to be considered null, and I am particularly grateful to all these authors for such great opportunity: use their results for giving to this thesis a prestige that would not have reached otherwise. Most of this section 5.1 is taken as presented in the article of reference [19], including Figures and Legends. We will comment on the results obtained by these author in the following section 5.2; our analysis and conclusions will be done afterwards, in 5.3 and 5.4.

The goal of the experiment is to demonstrate squeezing - and therefore entanglement - for $\gtrsim 10^5$ cold Caesium atoms via a Quantum Non Demolition (QND) measurement [38–49]. In particular, there are two key features they need to be performed:

- The *Projection noise squeezing*, by the mentioned QND measure
- The determination of the *loss of atomic coherence* $|\langle J \rangle|$, a natural consequence of the QND probing.

Together, these demonstrate the existence of multipartite quantum correlation in ensemble.

5.1.1 Experimental setup

Using a Magneto Optical Resonator (MOT), Cs atoms are cooled and loaded into a Far Off Resonant Optical Dipole Trap (FORT) [50–52], aligned to overlap with the probe arm of a Mach-Zender Interferometer (MZI; see [40, 53], Fig.5.1)

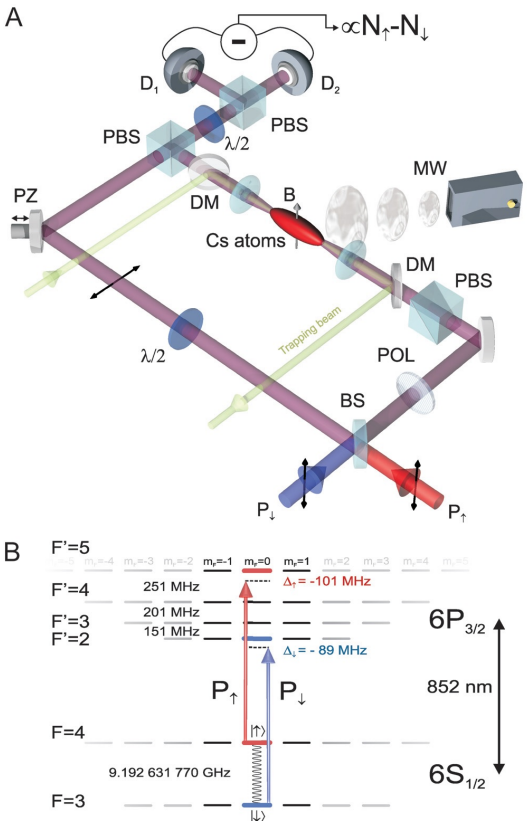

FIGURE 5.1: Experimental Setup. *(A)* An ensemble of $\sim 10^5$ Cs atoms cooled to ≈ 50 μK are confined in one arm of a MZI by a trapping beam. The atoms are prepared in a coherent superposition of the clock states $|\uparrow\rangle$ and $|\downarrow\rangle$ by applying a microwave (MW) $\frac{\pi}{2}$-pulse. Two linearly polarized probe beams $P_\uparrow$ and $P_\downarrow$ enter the interferometer via separate ports of the input Beam Splitter (BS). An arrangement of polarizers (POL) and polarizing Beam Splitters (PBS) and Half Wave Plates ($\frac{\lambda}{2}$) is used to adjust the powers and polarizations of the probe and reference beams. The combined Phase Shift of the two probes is measured in a balanced homodyne configuration. (B) Simplified level scheme of Cs showing the D2 line and the detunings of the clock state-sensitive probes, $P_\uparrow$ and $P_\downarrow$. Figure and legend taken from [19]

Atoms are loaded into the FORT from a standard Magneto-Optical Trap (MOT) superimposed onto the FORT, which collects and cools atoms to ≈ 50 μK. After the FORT is loaded, the MOT light is extinguished and a magnetic field B of ~ 2 Gauss is applied, defining a quantization axis orthogonal to the trapping beam. At this stage, the atoms occupy the $(F = 4)$ ground level, but are distributed amongst the magnetic sublevels.To polarize the atoms in one of the clock states, a combination of π-polarized laser light

resonant to the $6S_{\frac{1}{2}}(F=4) \rightarrow 6P_{\frac{3}{2}}(F'=4)$ and $6S_{\frac{1}{2}}(F=3) \rightarrow 6P_{\frac{3}{2}}(F'=4)$ transition is applied, optically pumping the atoms towards the $(F=4, m_F=0)$ state with 80% efficiency. Purification of clock state atoms proceeds by transferring the $(F=4, m_F=0)$ state atoms to the $(F=3, m_F=0)$ state using a resonant π-pulse on the clock transition and blowing away remaining atoms residing in the $(F=4)$ level. The coherent spin state (CSS) preparation is completed by putting the ensemble in an equal superposition of the clock states $\bigotimes_{i=1}^{N_A}\left(\frac{|\uparrow\rangle+|\downarrow\rangle}{\sqrt{2}}\right)_i$ by applying a resonant $\frac{\pi}{2}$ microwave pulse at the clock frequency. Next, successive QND measurements on the sample are performed, after which all atoms are pumped into the $(F=4)$ level to determine the total atom number N_A. The sequence is repeated several thousands times for various N_A. A schematic representation of the experimental sequence is shown in Fig.5.2 (top).

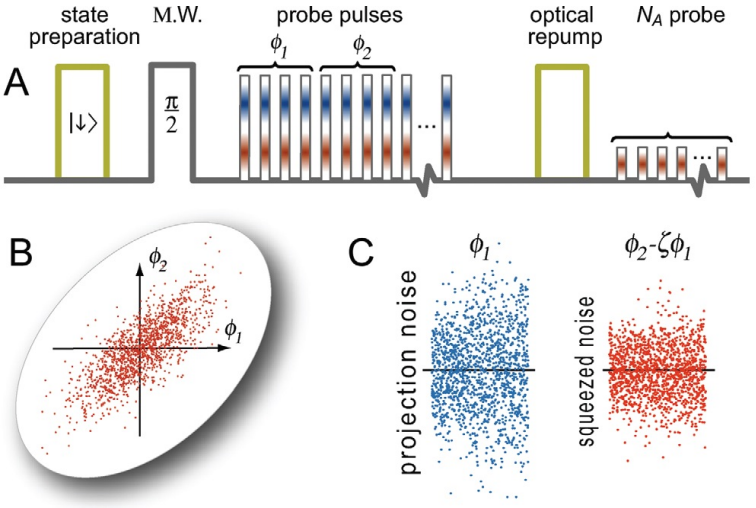

FIGURE 5.2: Pulse sequence and noise data. (A) Atoms are prepared in state $|\downarrow\rangle$ by an optical pumping sequence and then rotated to the superposition state $\frac{1}{\sqrt{2}}(|\uparrow\rangle + |\downarrow\rangle)$ by a microwave $\frac{\pi}{2}$-pulse before the train of 10 probe pulses is applied. Combining the results of several pulses, we can change the effective QND measurement strength. The first effective probe pulse measurement result ϕ_1 yields the statistics of the J_z for the CSS. The second effective pulse measurement result ϕ_2 verifies the squeezing, provided it is sufficiently correlated with ϕ_1. N_A is measured at the end of each sequence. (B) Correlations between the first and the second pulse measurements. (C) The projection noise manifested in the random scattering of about 2000 measurements of ϕ_1; and the spin squeezed state (SSS) displayed as the reduced noise in ϕ_2 when the QND result is used as $(\phi_2 - \zeta\phi_1)$. Figure and legend taken from [19]

5.1.2 Measurement of the projection noise

The dispersive measurement of the clock state average spin $\langle J_z \rangle$ (see [46] and [39]) is realized by detecting the state-dependent phase shift of the off-resonant probe laser light, $P_\downarrow$ and $P_\uparrow$. $P_\downarrow$ is coupled to the state $|\downarrow\rangle = 6S_{\frac{1}{2}}(F = 3, m_F = 0)$, while $P_\uparrow$ to $|\uparrow\rangle = 6S_{\frac{1}{2}}(F = 4, m_F = 0)$ (see Fig.5.1, bottom).
Denoting the photosignal as n, we define

$$\phi = \frac{\Delta n}{n} = \frac{\delta n}{n} + k_\uparrow N_\uparrow + k_\downarrow N_\downarrow \stackrel{\dagger}{=} \frac{\delta n}{n} + k\Delta N \stackrel{\dagger\dagger}{=} \frac{\delta n}{n} + 2kJ_z. \tag{5.1}$$

Here, we defined $N_\uparrow$ and $N_\downarrow$ to be, respectively, the number of particle in $|\uparrow\rangle$ and $|\downarrow\rangle$; $\Delta N \equiv N_\uparrow - N_\downarrow$ and $\delta n = \delta n_\uparrow + \delta n_\downarrow$ is the total shot noise contribution. In the equality marked with † we used $k_\uparrow = k_\downarrow = k$ and †† is a trivial consequence of the fact

$$J_z = \frac{\Delta N}{2}. \tag{5.2}$$

We can compute the variance $\mathrm{var}(\phi)$ of ϕ as a function of the variance $\mathrm{var}(\Delta N)$ of ΔN:

$$\mathrm{var}(\phi) = \frac{1}{n} + k^2 \mathrm{var}(\Delta N). \tag{5.3}$$

Now, for atoms in a coherent spin state, ve have $\mathrm{var}(\Delta N) = N_A$, so that eq.5.3 predicts a linear increase of the projection noise with the number of atoms. This has been observed, as it is possible to see from Fig.5.3, *blue* points.

5.1.3 Conditional noise reduction by QND measurement

The ability to measure the atomic spin projection with a sensitivity limited by the shot noise of light allows to produce a conditionally spin squeezed atomic state. After preparation of the Coherent spin state, n_1 photons have been used to measure J_z and obtain a measurement result ϕ_1, which is randomly distributed around zero with a variance $\frac{1}{n_1} + k^2 N_A$ (Fig.5.2 and eq.5.3). By using the information obtained in the first measurement it is possible, to a certain degree, to predict the outcome ϕ_2 of a successive J_z measurement performed on the same ensemble of atoms. The best estimate for ϕ_2 is $\zeta\phi_1$, which results in a conditionally reduced variance

$$\mathrm{var}(\phi_2 - \zeta\phi_1) = \frac{1}{n_2} + \frac{1}{1+\kappa^2} k^2 N_A, \tag{5.4}$$

that displays a reduction of the projection noise by $\frac{1}{1+\kappa^2}$ (*red* diamonds in Fig.5.3). The *measurement strength* $\kappa^2 = n_1 k^2 N_A$ describes the ratio of the atomic noise to the shot noise of light, and $\zeta = \frac{\mathrm{cov}(\phi_1,\phi_2)}{\mathrm{var}(\phi_1)} = \frac{\kappa^2}{1+\kappa^2}$. A Quantum Non Demolition measurement

with finite strength κ^2 leads to finite correlation between the two measures, as shown in Fig.5.2, bottom left.

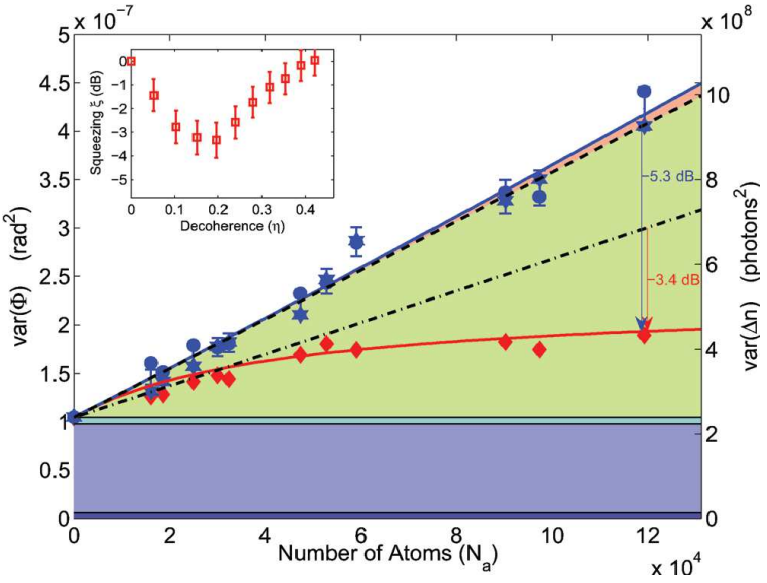

FIGURE 5.3: Projection noise and spin squeezing. In *blue*, the variances of ϕ_1 (*points*) and ϕ_2 (*stars*), referring to atoms in a CSS. The *solid blue* line is a quadratic fit, that resembles eq.5.3; the *black dashed* line is the CSS projection noise and the *black dash-dotted* one the equivalent CSS projection noise reduced by the loss of atomic coherence. The *red diamonds* correspond to the conditionally reduced variance of $\phi_2 - \zeta\phi_1$, fitted with the *solid red* line, that is the reduced noise of squeezed spin state. According to the scaling behaviour, it is possible to classify different noise contributions. Classical fluctuations are represented by the *cyan* (empty interferometer) and *red* (atom-light interaction related) area. The *blue* area represents the optical shot noise (*light* blue) and detector noise (*dark* blue). Finally, the *green* area is the projection noise. In the Inset, metrologically relevant spin squeezing ξ as a function of the decoherence parameter ε. Figure and legend taken from [19]

5.1.4 Decoherence

Spontaneous emission caused by the Quantum Non Demolition probes is a fundamental, irreversible decoherence mechanism which affects the squeezed spin state in two ways. First, it changes the value of J_z by redistributing atomic population via inelastic Raman scattering. This effect is practically absent because of the two colours QND scheme used here. The second and main effect is due to the reduction of the coherence between the clock levels. This results in a shortening of the mean collective spin vector $|\langle J\rangle| \rightarrow (1-\varepsilon)|\langle J\rangle|$, and hence to the reduction in Ramsey fringe amplitude. The degree of spin squeezing depends on the fraction ε of atoms which decohere as a result of spontaneous photon scattering during dispersive QND probing. The Quantum

Non Demolition measurement strength can be cast as $\kappa^2 \propto d\varepsilon$, where d is the resonant optical depth of the sample (see [54]). This highlights the trade-off between information gained through strong coupling and coherence lost due to spontaneous emission. ε is determined through the reduction in the Ramsey fringe amplitude in a separate echo spectroscopy experiment (as in [53] and [40]). The reduction in echo fringe amplitude as a result of the probe light thus provides an upper bound for the decoherence inflicted.

5.1.5 Squeezing and entanglement

The noise measurement data presented in Fig.5.3 correspond to $\varepsilon = 20\%$, as measured in Echo spectroscopy. According to the spin squeezing inequality, that states that for any separable state

$$\xi^2 \equiv N_A \frac{\mathrm{var}(J_z)}{|\langle J \rangle|^2} \geq 1, \tag{5.5}$$

spin squeezing and entanglement can be claimed if $\xi^2 < 1$. In this context, this means that, for a given N_A, the conditionally reduced variance of the verification measurement (*red* diamonds in Fig.5.2) is less than the projection noise scaled down by the factor $(1-\varepsilon)^2$ (*dash-dotted black* line in the same graph). In the inset of Fig.5.2 the maximum N_A-bin of the data has been considered, and ξ is plotted versus ε. Maximum squeezing $\xi = -(3.4 \pm 0.7)$ dB is observed with $\varepsilon = 20\%$, corresponding to probing the atoms with $1.3 \cdot 10^7$ photons. The squeezing reduces as ε increases further, confirming the notion that though a stronger measurement enables more precise estimation of J_z, this reduction in spin noise eventually ceases to be spectroscopically relevant as a result of decoherence.

5.1.6 Conclusion of the experiment

A reduction of projection noise to $-(5.3 \pm 0.6)$ dB and metrologically relevant spin squeezing and entanglement of $-(3.4 \pm 0.7)$ dB have been demonstrated. Furthermore, it has been shown that there exists an optimal balance between decoherence and the measurement strength for generation of spin squeezing. Notice that, since the measurement precision improves with the number of atoms, it is important that entanglement with over than 10^5 particles has been proven.

5.2 Comment to the experiment

Let us start by pointing out some minor facts, mostly due to the different notation and reference frame taken into account by us and the authors of [19]:

- For simplicity, in the experiment the variance is defined as $\frac{\text{var}(\Delta N)}{2} = \text{var}(J_z) = (\Delta J_z)^2$, while in the rest of this work we referred to the variance computed along the x-axis, $(\Delta J_x)^2$. This clearly does not represent a problem; the orientation of the reference frame is arbitrary, as far as we remain consistent with the definition of the related quantities - the squeezing parameter, for instance.

- Regarding the *squeezing parameter* ξ^2, in section 5.1.5, eq.5.5, the direction for the mean value of the total spin has not been defined. For us, in eq.1.14, it was J_z. Here it cannot, since the variance is defined as $(\Delta J_z)^2$, so it has to be one of the remaining, J_x or J_y. Notice that, because of symmetry, it does not make any difference between these two.

Let us now go to the main argument: the entanglement inequality used in the experiment [19], eq.5.5. Previously, in all chapters of this thesis until this last one, we tried to convince the reader that the spin squeezing does not represent an adequate criterion in many of the real life situation. This does not mean that it is false, but just that the Observables it is made of - J_z^2, J_z and J_x in this case - cannot precisely be determined using the experimental setup considered here. The atoms, trapped in the FORT, are distributed around in the chamber and shined by the probes $P_\downarrow$ and $P_\uparrow$ in different ways. As consequence we are not, strictly speaking, measuring the components of the collective spin operator $\vec{J} = \sum_{i=1}^{N_A} \vec{j}_i$, but of our old friend $\vec{S} = \sum_{i=1}^{N_A} \eta_i \vec{j}_i$. $\vec{j}_i$, as usual, represents the spin of the single particle, for $i = 1, ..., N_A$; the $\{\eta_i\}_{i=1}^{N_A}$ are the coefficients to be assigned to every atom, related with the intensity of the probes in the position it occupies.
In fact, the authors of experiment [19] calculate $\langle J_z \rangle$, using the relation

$$\langle J_z \rangle = \frac{N_\uparrow - N_\downarrow}{2} = \frac{1}{2} \int_0^{2\pi} \int_0^{\infty} \mathrm{d}\theta r \mathrm{d}r I_P(r) \pi w^2 \left[n_{A_\uparrow}(r,\theta) - n_{A_\downarrow}(r,\theta) \right], \tag{5.6}$$

where w is a constant factor, $I_P(r)$ is the (equal) intensity of the probing beams at a distance r of their main axis and $n_{A_\downarrow}$, $n_{A_\uparrow}$ are the atomic densities of atoms in $|\downarrow\rangle$ and $|\uparrow\rangle$ respectively. What eq.5.6 means, is that every atom contributes proportionally to the intensity I_P that it feels. In other words, what has been called here with $\langle J_z \rangle$, is exactly $\langle S_z \rangle$, up to a negligible multiplicative constant that depends on the definition of the $\{\eta_i\}_{i=1}^{N_A}$.
Similarly, we believe that the variance $\text{var}(\phi)$, derived experimentally and used for the plots of Fig.5.3, is not directly related with $(\Delta J_z)^2 = \frac{\text{var}(\Delta N)}{2}$, but with $(\Delta S_z)^2$. The argument is exactly the same: each particle contributes differently to the differential phase shift ϕ - according to its distance to the probing beams - and therefore it is not $\vec{J}$ to be measured, but $\vec{S}$.

We conclude that what is measured in the experiment are, indeed, $(\Delta S_z)^2$ and the decoherence ε that refers to the shortening of the mean vector $|\langle S\rangle| \to (1-\varepsilon)|\langle S\rangle|$. From the Inset of Fig.5.3, where is represented the squeezing parameter ξ^2 with respect to the decoherence ε, we can thus determine the experimental points $\left(|\langle S\rangle|, (\Delta S_z)^2\right)$, where $|\langle S\rangle|$ is the mean spin, along y or x. In the next figure we represent such points.

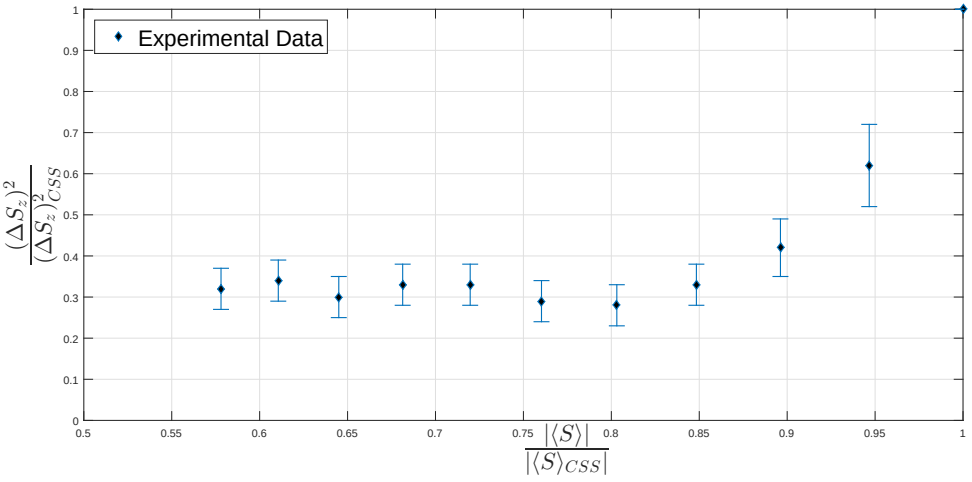

FIGURE 5.4: Experimental points relative to the normalized spin squeezed state (*blue*). These data are derived directly from the Inset of Fig.5.3, using equations 5.7a and 5.7b

Being precise, the data plotted in the last Fig.5.4 are to be interpreted as normalized with the coherent spin state: $\left(\frac{|\langle S\rangle|}{|\langle S\rangle|_{CSS}}, \frac{(\Delta S_z)^2}{(\Delta S_z)^2_{CSS}}\right)$. The relations we used for drawing the data are (the squeezing parameter ξ^2 is expressed in Decibel):

$$\frac{|\langle S\rangle|}{|\langle S\rangle_{CSS}|} = 1-\varepsilon \tag{5.7a}$$

$$\frac{(\Delta S_z)^2}{(\Delta S_z)^2_{CSS}} = \left(\frac{|\langle S\rangle|}{|\langle S\rangle_{CSS}|}\right)^2 \cdot 10^{\frac{\xi^2}{10}}. \tag{5.7b}$$

Here, for using a slightly more familiar notation, we introduced the appendix $_{CSS}$ that, exactly as in the previous chapters, refer to the maximal value of the related observable in the separable case. So, for instance, in eq.5.7a ε represents the shortening of the spin vector from $|\langle S\rangle_{CSS}|$ to $|\langle S\rangle|$. Regarding eq.5.7b, we need to be more careful. In fact, we are not dealing with the collective spin operator any more, but with $\vec{S}$, and we need to consider this in the definition of the squeezing parameter ξ^2 by changing it. As

discussed in section 1.4, ξ^2 becomes, under these circumstances:

$$\xi^2 = N_A \frac{(\Delta J_z)^2}{|\langle J \rangle|^2} \underset{\vec{J}\to\vec{S}}{\longrightarrow} \frac{\left(\sum_{i=1}^{N_a} \eta_i\right)^2}{\sum_{i=1}^{N_a} \eta_i^2} \frac{(\Delta S_z)^2}{|\langle S \rangle|^2}, \tag{5.8}$$

where

$$\frac{\left(\sum_{i=1}^{N_a} \eta_i\right)^2}{\sum_{i=1}^{N_a} \eta_i^2} = \frac{|\langle S \rangle_{CSS}|^2}{(\Delta J_z)^2_{CSS}}. \tag{5.9}$$

The reason for which we are allowed to freely take the experimental values of ξ^2 reported in Fig.5.3 and use them directly in the derivations of $\frac{|\langle S \rangle|}{|\langle S \rangle_{CSS}|}$ and $\frac{(\Delta S_z)^2}{(\Delta S_z)^2_{CSS}}$ (as we did in equations 5.7a and 5.7b), is the following. Because they are experimental, and not theoretical, we believe they already refer to the generalized version of the squeezing parameter, as expressed in the right hand side of eq.5.8. All the numbers we need to plug in for ξ^2 are, up to a multiplicative constant that disappears at the moment of the renormalization, taken directly from the readouts of the detectors. N_A itself is not calculated theoretically, but included via the maximum value of $|\langle J \rangle|$; the one corresponding to the coherent spin state, that naturally becomes $|\langle S \rangle|$ in our interpretation.

Here we explained why, we believe, it is necessary to use $\vec{S}$ instead than the collective spin operator $\vec{J}$. Consequently, the spin squeezing inequality, that states that $\xi^2 < 1$ for any entangled state, is not valid any more, as discussed previously in chapter 2. We need to find a new criterion for determining if the System is correlated or not. But this is what this whole work is about, and what we have done in chapters 3 and 4 theoretically! Therefore, in the next section 5.3, we will use the concepts and analytics developed so far for deriving this criterion, as well with the k-particle entanglement ones we are now able to obtain.

From now on, in order to be in accordance with the notation used in the previous chapters, we will change reference frame, so that the variance we will refer to is the one along the x axis, and the main component of the spin the z one.

5.3 Our analysis

In the previous section 5.1 we described how the experiment is designed, and we explained why we need to use our new entanglement criteria for determining if the state of the system is entangled. We now analytically evaluate the minimum normalized variance

$\frac{(\Delta S_x)^2}{(\Delta S_x)^2_{CSS}}$ with respect to the average spin $\frac{\langle S_z \rangle}{\langle S_z \rangle_{CSS}}$, for any k-particle entanglement we desire. In other words, find the distribution function $p(\eta)$.

We will start by determining $\rho(r, z)$, associated with the probability of having a particle at distances r and z, respectively from the main axis of the FORT as shown in Fig.5.5. Afterwards, we will generate a statistical relevant number n of "virtual" particles and get the set of coefficients $\{\eta_i\}_{i=1}^n$ by plugging them inside the equation $\eta(r, z)$. $\eta(r, z)$ is the function that relates the value of η with the coordinates r and z of the atom.

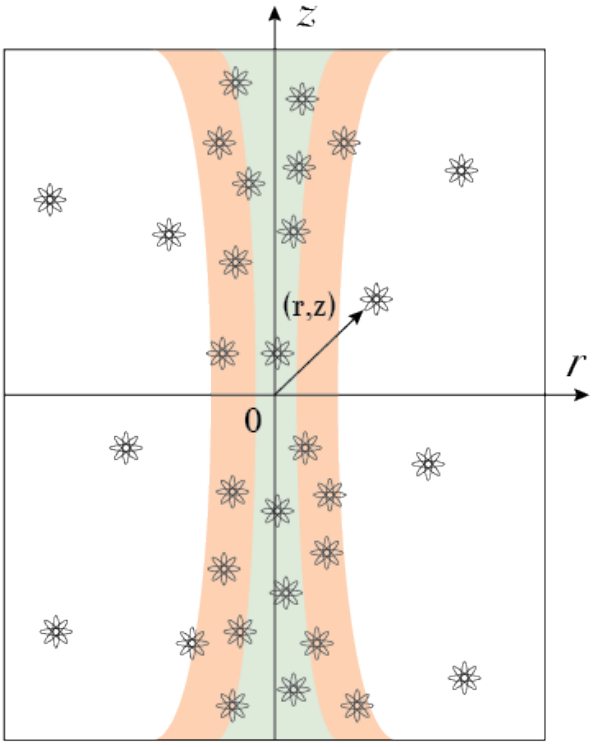

FIGURE 5.5: Experimental scheme. In *red* we represented the beams building up the FORT, in *green* the probe. As consequence of the cylindrical symmetry, we can use only two variables for describing the atomic positions: the distance r from the shared axis of the lasers and the depth z

Referring extensively to the work of Daniel Oblak [55], the potential affecting an atom shined with a Gaussian beam is given by the relation

$$V(r, z) = V_0 \frac{\omega_t^2}{\omega(z)^2} e^{-\frac{2r^2}{\omega(z)^2}}, \tag{5.10}$$

where the appendix "$_t$" refers to the trapping beam - the FORT; $\omega_t = 50\ \mu$m is the waist and $\omega(z) \equiv \omega_t \sqrt{1 + \frac{z^2}{zr_t^2}}$ the spot size. In addition, $zr_t = \pi \frac{\omega_t^2}{\lambda_t}$ defines the so-called

Raleigh-range, a parameter depending on the proper trap's wavelength $\lambda_t = 1032$ nm. The potential minimum for a linearly polarised and Far Off Resonant Trapping (FORT) beam is given by the equation [56]

$$V_0 = \frac{P}{8\pi^3 c\omega_t^2}\left(\frac{\gamma_{D1}\lambda_{D1}^3}{\Delta_{D1}} + 2\frac{\gamma_{D2}\lambda_{D2}^3}{\Delta_{D2}}\right) \simeq \frac{P\gamma_D\lambda_D^3}{8\pi^3 c\omega_t^2}\left(\frac{1}{\Delta_{D1}} + \frac{2}{\Delta_{D2}}\right). \tag{5.11}$$

Here, we have introduced the following notation:

- P is the power of the laser, in our case $P = 2.5$ W
- γ_{D1} is the *decay rate* of the $6P_{3/2}$ excited state of the Cs atoms in the trap. For such element, we have $\gamma_{D1} = 4.6$ MHz, as derived in [57]
- λ_{D1} is the $D1$-line transition wavelength coupling the $6P_{3/2}$ state to the ground level $6S_{1/2}$. According to [57], $\lambda_{D1} = 894$ nm
- Δ_{D1} is the detuning of the trapping laser:

$$\Delta_{D1} = 2\pi c\left(\frac{1}{\lambda_t} - \frac{1}{\lambda_{D1}}\right) \tag{5.12}$$

- These definitions are extended naturally to the D2-line. The practical values, taken from [57] again, are: $\gamma_{D2} = 5.2$ MHz and $\lambda_{D2} = 852$ nm.

The approximation of eq.5.11 follows from

$$\gamma_{D1}\lambda_{D1}^3 \simeq \gamma_{D2}\lambda_{D2}^3, \tag{5.13}$$

as it can be verified by plugging in the values given above.
Inserting the numbers in relation 5.11, it is possible to finally determine the potential depth for the Gaussian

$$\frac{V_0}{k_B} = 1.73 \cdot 10^{-4}\ \text{K}, \tag{5.14}$$

where k_B is the Boltzmann constant in the appropriate units.

At this point we have a well defined expression for the potential $V(r, z)$ to which our Caesium atoms are subjected. From that, it is fairly simple to obtain the atomic density $\rho(r, z)$ of the particles in the experiment. Using classical statistical mechanics, and supposing the Hamiltonian to be $H(p, r, z) = \frac{p^2}{2m} + V(r, z)$, we have that

$$\rho(r, z) = re^{\frac{V(r,z)}{k_b T}} = r\exp\left[\frac{V_0}{k_b}\frac{\omega_t^2}{T\omega(z)^2}e^{-\frac{2r^2}{\omega(z)^2}}\right]. \tag{5.15}$$

Referring to the experiment [19], we know that the temperature T can be controlled to be less than 100 μK during the whole duration of the data collection (50 μK at the loading time of the FORT, see [19]). For this reason, we will consider (for the moment) $T = 100$ μK; a higher temperature can only be deleterious for us - it pushes atoms away from the probe - and this way we are sure not to neglect some important contribution due to heating. We recall here that the factor r multiplying the exponential $e^{\frac{V(r,z)}{k_b T}}$ in eq.5.15 needs to be there, because we are using Cylindrical coordinates instead of Cartesian: $(x, y, z) \to (r\cos\theta, r\sin\theta, z)$. As immediate consequence, considering there is no θ dependence:

$$\rho(r, z) = r\rho(x, y, z). \tag{5.16}$$

Two plots of the function $\rho(r, z)$, in arbitrary units, are given in the following figure 5.6.

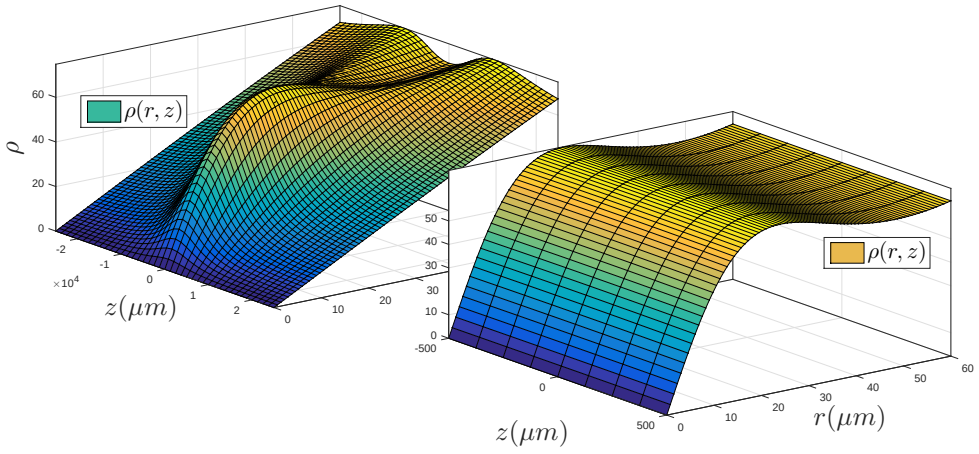

FIGURE 5.6: Distribution $\rho(r, z)$ of particles in our sample. In the left graph, we let the variable z to vary inside the big interval $[-2.5, 2.5] \cdot 10^4$ μm; in the right plot inside the smaller $[-5, 5] \cdot 10^2$ μm. The real volume occupied by the particles is one of the problematic quantities we have to deal with

Here we want to point out one of the biggest problem we had with the evaluation of the coefficients $\{\eta_i\}_{i=1}^n$. Which are the ranges $[0, L]$ and $\left[-\frac{W}{2}, \frac{W}{2}\right]$ in which r and z are allowed to vary, respectively? As it is possible to see from the previous figure 5.6, the atomic distribution $\rho(r, z)$ considerably depends upon the parameters L and W! Regarding the distance r from the main axis of the trapping beam - neglecting miss-alignment of the probe and the FORT - the answer is fair simple. The waist ω_p of the probe is given to be $\omega_p = 27$ μm, so that we can consider not detected any Caesium atom "far away" from it. For us, "far away" means further than twice the waist ω_p, where the intensity of the detecting beam is reduced more than 99.97%.

But what about W? From the left graph of figure 5.6, we can see that the FORT is not

affecting particles outside the central peak, i.e.: where $\rho(r,z)$ resembles a uniform atomic distribution. In particular, it is possible to estimate the critical point z_c from which we have an approximately linear behaviour of $\rho(r,z_c) \simeq r$. In fact, a linear behaviour of the atomic distribution in the cylindrical coordinates corresponds to a constant distribution in the Cartesian ones (see eq.5.16). It is possible to see that the value $z_c = 2.5 \cdot 10^4$ μm is appropriate for our request. This accounts to a total length of the box within which the atoms are loaded of 5 cm, that could be reasonable, as well as not. In fact, we do not have an exact idea about the dimensions of the chamber. Therefore, what we will do, is to determine the $\{\eta_i\}_{i=1}^n$ and the k-particle criteria multiple times, each one with a different value of the parameter W inside the range $(0, 2z_c]$. This way, we will be able to compare the obtained curves and determine the lowest for any k-particle entanglement criterion. Notice that, our method being based on a probabilistic procedure, the curves we obtain are necessarily affected by statistical fluctuations. We need to check that such fluctuations are less than the desired precision we want to achieve, defined by the experimental errors we have. We can reduce the theoretical fluctuations by increasing the number n of generated coefficients $\{\eta_i\}_{i=1}^n$.

For completeness, before going on with practically determining the $\{\eta_i\}_{i=1}^n$'s, we want to write down the function $\eta(r,z)$ we will use to relate the atomic coordinates to the value of the coefficient η:

$$\eta(r,z) = \frac{\omega_p^2}{\omega(z)^2} e^{-\frac{2r^2}{\omega(z)^2}}. \tag{5.17}$$

Looking at this last relation, $\omega(z)$ is, again, the spot size; but it does not have to be confused with the one of the FORT (eq.5.10), derived with the parameters ω_t and λ_t. Here we have that

$$\omega(z) = \omega_p \sqrt{1 + \frac{z^2}{z r_p^2}}, \tag{5.18}$$

where $z r_p = \pi \frac{\omega_p^2}{\lambda_p}$, $\omega_p = 27$ μm and $\lambda_p = 852$ nm are the spot size, the waist and the wavelength of the probe, respectively. Due to the arbitrariness of the function $\eta(r,z)$, it is legitimate to ask if our definition 5.17 has some sense. We believe the answer to this question is yes; in fact the coefficients $\{\eta_i\}_{i=1}^n$ have been introduced to distinguish particles interacting with the probe in different ways. The interaction is, under very general conditions, related with the intensity of this beam: $I_P(r,z)$. Therefore, up to a multiplicative constant, we decided to define $\eta(r,z)$ as

$$\eta(r,z) \propto I_p(r,z). \tag{5.19}$$

The multiplicative constant has been chosen in such a way that $\eta(r,z)$ belongs to the interval $(0,1]$.

5.3.1 Generation of the coefficients $\{\eta_i\}_{i=1}^n$

As said above, in order to determine the curves defining the minimum normalized variance $\frac{(\Delta S_x)^2}{(\Delta S_x)^2_{CSS}}$ with respect to the average spin $\frac{\langle S_z\rangle}{\langle S_z\rangle_{CSS}}$, we need to generate the coefficients $\{\eta_i\}_{i=1}^n$. This is not a trivial task, because the distribution $\rho(r,z)$ changes significantly, depending on the range $\left[-\frac{W}{2},\frac{W}{2}\right]$ in which z is allowed to vary (see Fig.5.6). In fact, for relatively small values of W, we can assume the atomic density to be independent on z,

$$\rho(r,z) = r\exp\left[\frac{V_0}{k_b}\frac{\omega_t^2}{T\omega(z)^2}e^{-\frac{2r^2}{\omega(z)^2}}\right] \simeq r\exp\left[\frac{V_0}{k_b}\frac{1}{T}e^{-\frac{2r^2}{\omega_t^2}}\right] = \rho(r); \tag{5.20}$$

while this approximation clearly does not hold for W approaching its limit z_c. In the situation described by eq.5.20, it results particularly easy to generate "virtual" particles in accordance to $\rho(r)$. Using the so-called Inverse Transform Sampling, we are in fact able to obtain the following histogram 5.7:

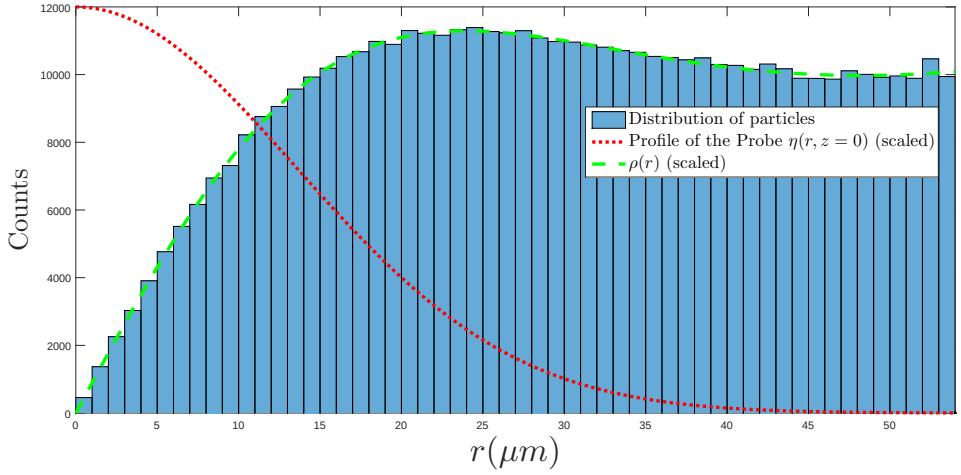

FIGURE 5.7: Histogram collecting the r coordinates of $5 \cdot 10^5$ virtual particles generated according to the approximate density function of eq.5.20. The two dashed lines represent $\rho(r)$ (in *green*), and the profile of the probe beam at $z = 0$ (in *red*), both scaled

This figure has been obtained for $n = 5\cdot 10^5$, a number sufficiently large for our purposes. The two dashed curves represent, respectively:

- (**Green**): The atomic density $\rho(r)$, scaled in order to show the agreement with the generated particle's positions
- (**Red**): The profile $\eta(r, z = 0)$ of the probe, obtained using eq.5.17

The previous histogram 5.7 collects all the radial coordinates r of the virtual particles. The other one, z, can be generated according to a uniform distribution between $\left[-\frac{W}{2}, \frac{W}{2}\right]$, being careful to choose W in a range in which the approximation 5.20 is valid. However, under some more strict conditions it is not necessary at all to give the z coordinate. In fact, if we can approximate $\rho(r,z)$ to $\rho(r)$, it is also true we can find another interval for W for which

$$\eta(r,z) = \frac{\omega_p^2}{\omega(z)^2} e^{-\frac{2r^2}{\omega(z)^2}} \simeq e^{-\frac{2r^2}{\omega_p^2}} = \eta(r) \tag{5.21}$$

is valid. Now, because the waists and the characteristic wavelengths of the probe and the FORT are very similar, it turns out that a good interval for which both approximations 5.20 and 5.21 are valid is $W \in \left[0, 10^3\right]$ μm. The validity of this choice can be understood qualitatively by looking to the next figure, in which we plot $\rho(r,z)$ and $\eta(r,z)$ in such interval.

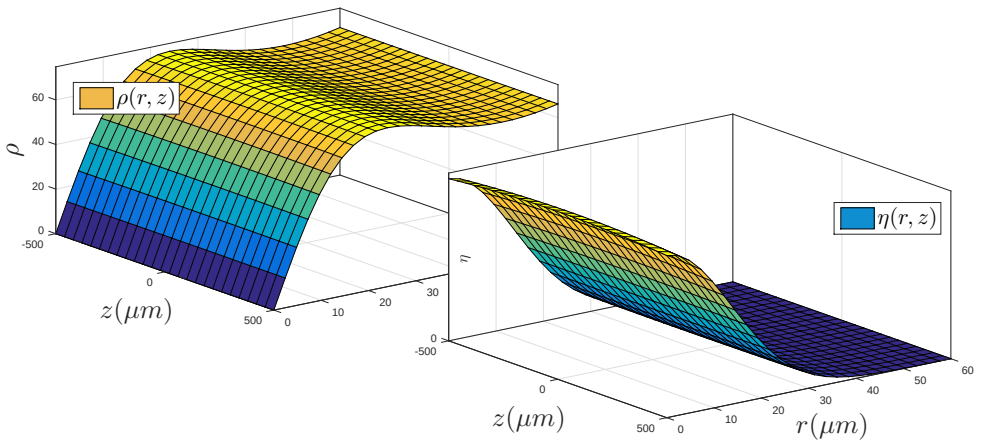

FIGURE 5.8: Profiles of the atomic density $\rho(r,z)$ (*left*) and the function $\eta(r,z)$ (*right*) for $W = 10^3$ μm. As it is possible to see, these plots are not varying significantly with the variable z, thus confirming the validity of the approximations 5.20 and 5.21 in such range

As it is possible to see, both functions are almost independent on z for $W = 10^3 \mu$m. At this point we have all we need for determining the values that the coefficients $\{\eta_i\}_{i=1}^n$ are taking whenever $W \leq 10^3$ μm. These have been put in the following histograms:

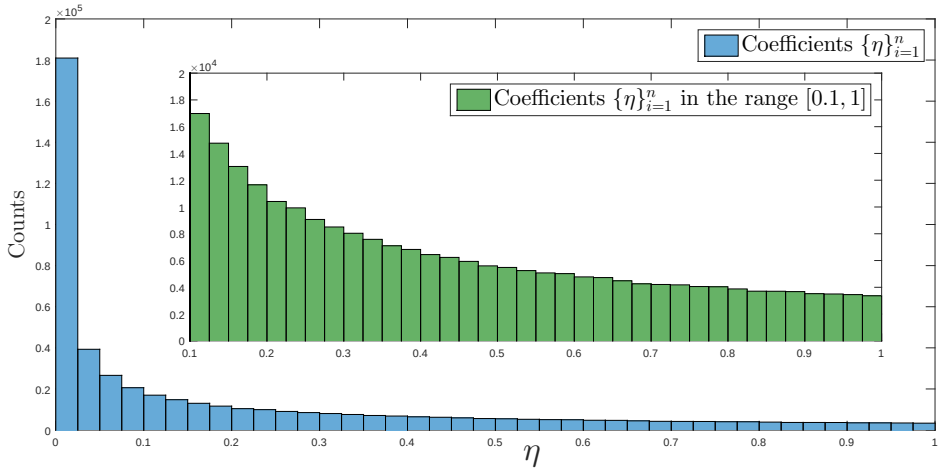

FIGURE 5.9: Histogram collecting the coefficients $\{\eta_i\}_{i=1}^{n}$, for $n = 5 \cdot 10^5$ and in the particular case in which W is small enough to use the approximations 5.20 and 5.21

It clearly shows that the majority of the $\{\eta_i\}_{i=1}^{n}$ is very small. This is, indeed, not surprising: looking at Fig.5.7 it is clear that a preponderant portion of the particles ends up to be where the probe is very weak. This is equivalent to say that all these atoms will be described by very small coefficients.

We will conclude this section with generating the particles and the related coefficient in the general case.
As we did above, the first thing to do is determine all the Cylindrical coordinates (r, z) of the atoms. This will not be as trivial as before, because now these parameters are correlated, as it is possible to see from the left plot of the density distribution $\rho(r, z)$ drawn in Fig.5.6. Using two times the technique of the Inverse Transform Sampling, however, it is possible to obtain the following three dimensional histogram. The inset we added at the bottom right is the theoretical distribution the atoms are supposed to follow. The function we draw on top of the histogram represents the (scaled) profile of the probing beam.

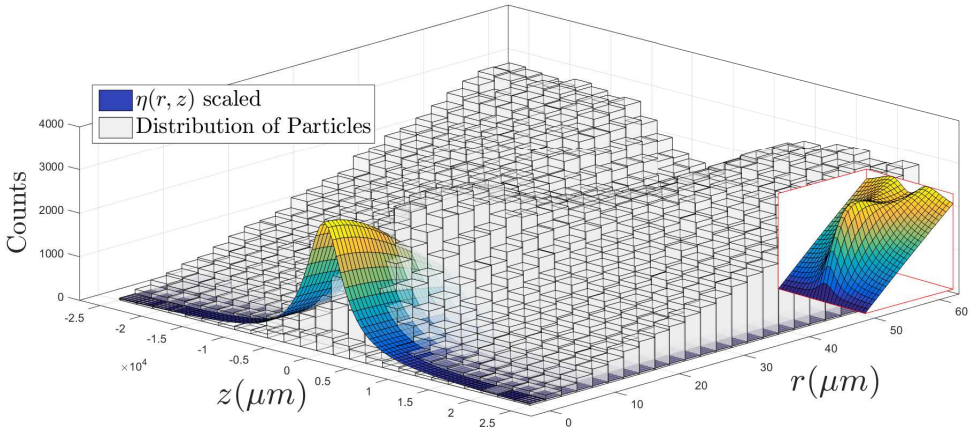

FIGURE 5.10: Histogram collecting the coordinates r and z of $n = 10^6$ virtual particles. Here $W = 5 \cdot 10^4 \mu$m, so that we needed to use the not approximate atomic density of eq.5.15. In the main plot we draw the (scaled) function $\eta(r, z)$; in the small box in the bottom right it is possible to see the theoretical distribution $\rho(r, z)$ in the interval defined by $W = 2.5 \cdot 10^4$ μm

As it is possible to see, the generated coordinates are following the theoretical curve pretty well, at least for small values of the radius r. Since the method is not particularly efficient, and we needed to take some compromises on the precision, for big values of r the simulation is not behaving perfectly. However, looking at Fig.5.10, it becomes clear that in such region the probe beam is also extremely weak (less than 1% of its maximum intensity), and therefore we don't believe it represents a problem.

Using the data collected in the last histogram 5.10, we are now able to determine the coefficients $\{\eta_i\}_{i=1}^n$. With the help of eq.5.17, it is possible to generate and subsequently collect them in the following:

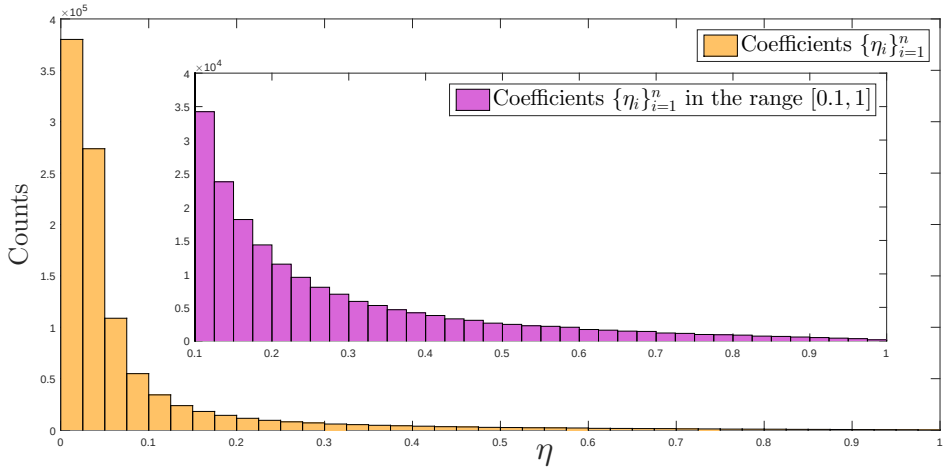

FIGURE 5.11: Histogram collecting the coefficients $\{\eta_i\}_{i=1}^n$, for $n = 10^6$ and $W = 5 \cdot 10^4 \mu$m. Given the coordinates collected in Fig.5.10, the eta_i's have been derived through eq.5.17

Comparing the two histograms 5.11 and 5.9 - that we recall are made by the coefficients $\{\eta_i\}_{i=1}^n$ in the two limiting cases $W \lesssim 10^3$ μm and $W = 5 \cdot 10^5$ μm - it becomes evident that whenever W is small enough to use approximation 5.20, we get bigger values for the η_i's. This is not surprising at all; in fact, increasing z we reduce the intensity of the probe beam, that translates in a reduction of the related coefficient.

In the following section we will use the two sets $\{\eta_i\}_{i=1}^n$ we got here, along with many others obtained with different values of W inside $[1, 50] \cdot 10^3$ μm, for determining the k-particle entanglement criteria we want. We will show that the difference between those is actually very big, resulting in a severe lowering of the criteria.

5.3.2 k-particle entanglement criteria - a first version

Let us summarize what we have done so far in this chapter, section 5.3.

1. At first, we wrote down the expression 5.10 for the potential $V(r, z)$ created by the FORT. Using this, we determined the atomic density $\rho(r, z)$ (eq.5.15), with which it is possible to generate the coordinates of the virtual particles in experiment [19]

2. Similarly, we got the equation 5.17, that gives the value of the coefficient $\eta(r, z)$ to be assigned to a particle at position (r, z)

3. Subsequently, given the fundamental instruments described in the previous points 1 and 2, we focused our attention to experiment [19], and we tried to generate the relative coefficients $\{\eta_i\}_{i=1}^n$.

4. We noticed that the profile of the atomic density $\rho(r, z)$ is changing substantially with our parameter W, that describes the length of the chamber in which the particles are loaded (see Fig.5.5). Since we do not have a precise clue about it, we decided to let W to vary inside the interval $[0, 5] \cdot 10^4$ μm

5. We designed a simplified procedure for determining, once for all, the coefficients $\{\eta_i\}_{i=1}^n$, whenever $W \leq 10^3$ μm (see Fig.5.9)

6. And we concluded the section explaining the more complicated method with which we can derive the same result, but for a generic value of W (see Fig.5.11 for the particular case $W = 5 \cdot 10^4$ μm)

At this point we are able to obtain, for all the values of the parameter W, the k-particle entanglement criteria. This way, we can determine the importance of such parameter, and subsequently find out the real lowest bounds of the variance $\frac{(\Delta S_x)^2}{(\Delta S_x)^2_{CSS}}$ with respect to the average spin $\frac{\langle S_z \rangle}{\langle S_z \rangle_{CSS}}$, for all possible k. In other words, we will draw, for many different W, similar curves to the ones represented in Fig.4.11, and we will find out which are the lowest ones. These will be taken as k-particle entanglement criteria.

But let us proceed with order, first by recalling how we derived:

- The $k = 1$ - i.e. the "real" - entanglement criterion. For this one we need to look far back to section 3.2, and in particular to Table 3.3. There resides the key to determine the most important curve, the one discriminating between a generic separable state and an entangled one. In fact, we do not need anything more; once the coefficients $\{\eta_i\}_{i=1}^n$ are known, we can directly plug them inside such Table and get the criterion.

- For $k = 2$-entanglement we will use, of course, the real Optimal limit derived in section 4.3.1, and more precisely by equations 4.118a and 4.118b.

- In conclusion, for a generic $k > 2$, we can consider what we have done in 4.4.2, and in particular the result of equations 4.146 and 4.147.

In the following figure we plotted the curves, associated to $k = 1$ (*blue*), $k = 2$ (*red*) and $k = 3$ (*green*), they represent the relative k-particle entanglement criteria for different values of W. More precisely, the area painted with the same colour associated to the k's

is the region in which the curves are varying, depending on W. As said above, the three lower coatings of such coloured regions will be taken as final k-particle entanglement criteria for this experiment (at least for the moment). It is important to note that we choose $n \geq 5 \cdot 10^5$ so that the fluctuations due to the intrinsic nature of the process can be neglected.

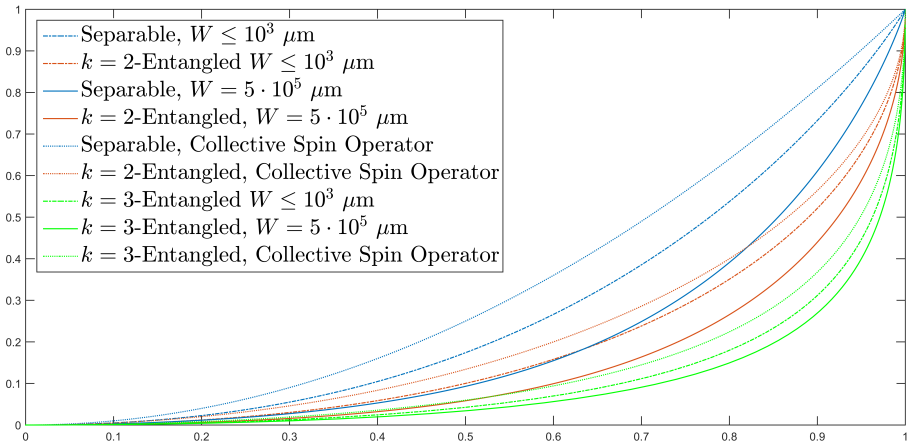

FIGURE 5.12: k-particle entanglement criteria for $k = 1$ (*blue*), $k = 2$ (*red*) and $k = 3$ (*green*), obtained with different values of W. The *dotted* curves are obtained through the collective spin operator, the *dash-dotted* in the hypothesis $W \leq 10^3$ μm and the *plain* supposing $W = 5 \cdot 10^5$ μm. The coloured regions refer to the areas in which the curves obtained using the operator $\vec{S}$ are allowed to vary. The lower coatings of these regions, that will become the new criteria for the relative k, correspond to the maximum possible value of W, $W = 5 \cdot 10^4$ μm

Notice that all the lower coatings refer to the maximum possible value of W, $W = 5 \cdot 10^4$ μm. This is something we were expecting, because it is very unlikely to get better result by letting particles to move in bigger volumes, outside the probe. The real question is: why we see such important worsening in the k-particle entanglement criteria? This is a very legitimate question, to which, unfortunately, we do not have a rigorous answer. However, we will give our guess, that we believe to be reliable. Let us recall what we did in section 2.1; there we proved that the squeezing parameter ξ^2 can take values less than one under particular circumstances. More precisely, we developed a model for which $\xi^2 \to \frac{2}{N}$, and this limit was achieved when there were many particles at the border of the probing beam and just two at the middle. As consequence, we took the qualitative conclusion that the squeezing parameter was behaving as worse as more particles were accumulating to the border, less to the centre. Regarding experiment [19], when we deal with small values of W, the FORT and the probe can decay *only* along the r direction (see Fig.5.8), being all the z's very near to the shared focus of the beams. Therefore the only way with which our criteria can get worse is to have a big

number of particles described by a great radial coordinate r, i.e.: the region in which the probe is weak. This is something that actually happens, as it is possible to understand from Fig.5.7, and in fact we obtain the first lowering of the criteria derived through the collective spin operator (the dash-dotted curves in Fig.5.12). However, when we start to consider big values of W, we let particles to accumulate in the z-region where the probing beam is mostly decayed and therefore very weak. This can be understood looking at Fig.5.10, where it is clear that where the probe is strongly decaying, there is still a substantial number of particles. This translates in a *second* lowering of the criteria, that explains the big differences between the curves relative to small and big W, as well as the difference between the dotted and the plain lines of Fig.5.12. This can be further understood comparing the two histograms 5.9 and 5.11. It is clear that the second one, referring to a $W = 5 \cdot 10^5$ μm, collects much smaller coefficients $\{\eta_i\}_{i=1}^n$ than the first. This is a clear consequence of the fact that we allow particles to accumulate far away from the focus of the beam, and translates with the lowering of the criteria.
In other words, it is better to have particles at the centre of the probing beam, where the coefficients $\{\eta_i\}_{i=1}^n$ are approaching unitary values and $\vec{S}$ tends to the collective spin operator $\vec{J}$. This is not a surprising statement, but we have shown here how dramatic can be the reduction of the entanglement criteria if the atomic distribution is particularly wide.

What we will do in the following is to introduce another mechanism that can further deteriorate our k-entanglement criteria: the miss-alignment of the probe with respect to the FORT. So far we supposed that both beams were sharing the same axis and focus. Now, if for the latter one this hypothesis is very good, because the beams pass through the same optics and share the path, for the previous one is *not*. In fact, the alignment was checked by searching the maximum response peak of the detectors: a procedure that works, but is not completely precise. What we will do in the following is to develop a new model with which it is possible to check what happens when we allow for (small) miss-alignments of the beams.
Notice that for similar reasons we can suppose that the beams are not tilted with respect to each other.

5.3.3 k-particle entanglement criteria - final version

In figure 5.12 we have determined the $k = 1, 2$ and 3 entanglement criteria for experiment [19]. There we did not account for a displacement between the main axes of the probe and the FORT; in this section we will check what happens when such displacement occurs. This will be done in two different steps; initially we will restrict ourselves

to the case in which W takes only small values, and later we will generalize to the whole domain of W. The reason for which we do not deal immediately with the general case, is that it is computationally expensive to generate the coordinates of the virtual particles whenever we cannot disregard z and consider it constant.

Let us first explain how we evaluate such displacement. Since it is relative to the two beams, and we have a Cylindrical symmetry between the x and y coordinates, we can include it in the equation for $\eta(x, y, z)$:

$$\eta(x, y, z) = \frac{\omega_p^2}{\omega(z)^2} e^{-2\frac{(x-d)^2+y^2}{\omega(z)^2}}, \tag{5.22}$$

where d represents the actual displacement, as it is possible to see in the following scheme 5.13.

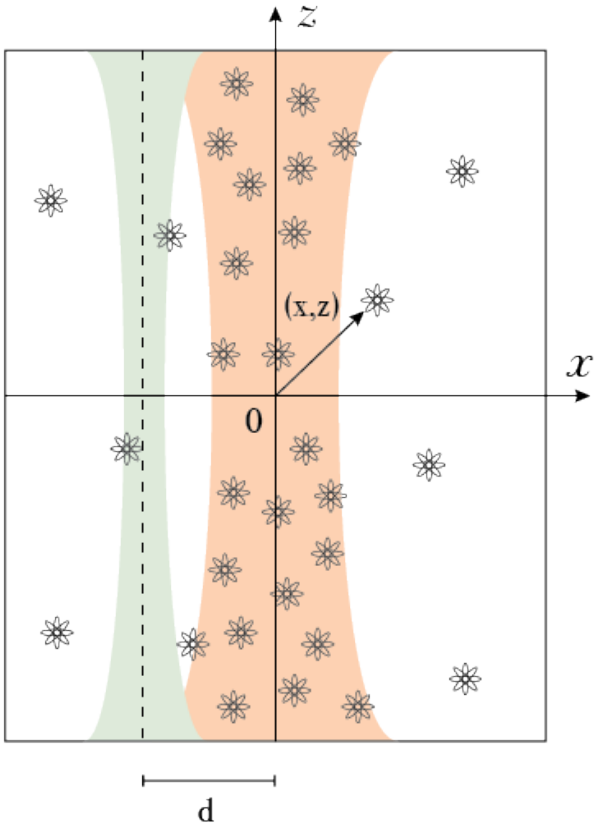

FIGURE 5.13: Schematic draw representing the setup of experiment [19] setup. Differently from Fig.5.5, here we include the possible displacement d as well. Notice now that we are not using the Cylindrical coordinates any more; because of symmetry breaking we need to use Cartesian ones. y is left implicit

Notice that, once we fix the x axis to be the one along which we shift the beams,

we loose the Cylindrical Symmetry that was so useful before. Therefore we cannot express trivially the atomic density ρ and the probe profile η as function of r any more. We need to use Cartesian coordinates. Using the method we gave above, we can proceed as follows.

First, let us suppose $W \leq 10^3$ μm, so we are allowed to use approximation 5.20, and generate the remaining z coordinate according to a uniform distribution. More in details, the relations we will use here for determining the coefficients $\{\eta_i\}_{i=1}^n$ are:

$$\rho(x,y,z) = \exp\left[\frac{V_0}{k_b}\frac{\omega_t^2}{T\omega(z)^2}e^{-2\frac{x^2+y^2}{\omega(z)^2}}\right] \simeq \exp\left[\frac{V_0}{k_b}\frac{1}{T}e^{-2\frac{x^2+y^2}{\omega_t^2}}\right] = \rho(x,y) \tag{5.23a}$$

$$\eta(x,y,z) = \frac{\omega_p^2}{\omega(z)^2}e^{-2\frac{(x-d)^2+y^2}{\omega(z)^2}}, \tag{5.23b}$$

they do not represent particular computational problems. So, for instance, the situation we refer to a displacement of 60 μm is well described by the following histogram, where we collected the (x,y) positions of the virtual particles and draw the (scaled) function $\eta(x,y,z=0)$ that associates to such coordinates (plus the z one generated randomly) the desired coefficients.

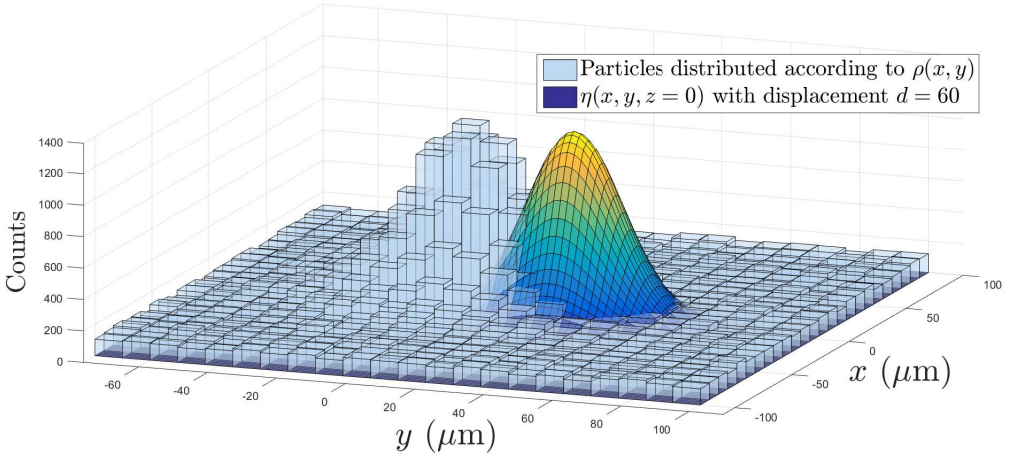

FIGURE 5.14: Histogram collecting the coordinates x and y of $n = 5 \cdot 10^5$ virtual particles. The (scaled) function $\eta(x,y,z=0)$ is also given. This figure refers to a displacement d of 60 μm

Using this method we can finally determine the k-particle entanglement criteria for different values of the displacement d - given the $\{\eta_i\}_{i=1}^n$ the procedure is exactly the one we explained in section 5.3.2. In the following figure we collected several of this curves; the *dashed* ones referring to $k = 1$, the separable case, and the *plain* to $k = 2$.

We choose W to be at the edge of our restricted interval: $W = 10^3$ μm.

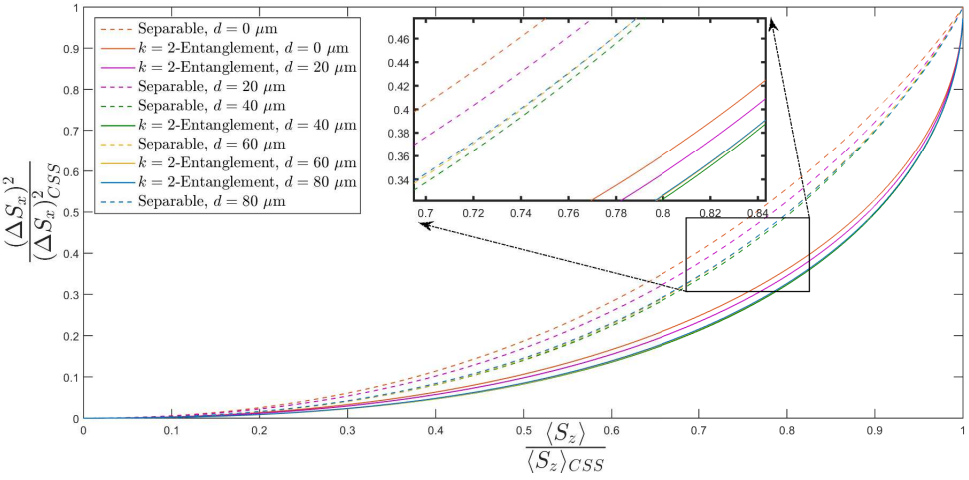

FIGURE 5.15: Several $k = 1$ and $k = 2$ entanglement criteria for different values of the displacement d. We recall this plot refers to the case in which $W = 10^3$

As it is possible to understand from this last plot, it is not true that the $k = 1$ and 2 criteria becomes worse as we are moving the probe and the FORT apart. In fact, we reach the minimum at about $d = 40$ μm, and later the curves stabilize to some bigger limit. How can we interpret this result? Accordingly to what we said before in section 5.3.2, we believe that such behaviour can be explained with a gathering of particles in a "sensible" region of the probe. When we start to shift the two beams, we start to reduce the number of particles at the middle of the probe, and to accumulate them at its sides. This results in a lowering of the k-criteria, as expressed in the Fig.5.15. However, when d increases further, the big peak of particles ends up to be where it does not count any more (the probe is too weak). The distribution of atoms that the probe actually "sees" is constant, and therefore the criteria stabilize at a particular couple of curves, slightly above the lowest ones. For supporting this hypothesis, we can draw the contour plot of the probe $\eta(x, y = 0, z)$ and the atomic density $\rho(x, y = 0, z)$ for the two displacements $d = 40$ μm and $d = 80$ μm. We chose to set $y = 0$ because our system is symmetric with respect to the (x, z) plane, and it is not necessary to explicit such variable for having a full understanding.

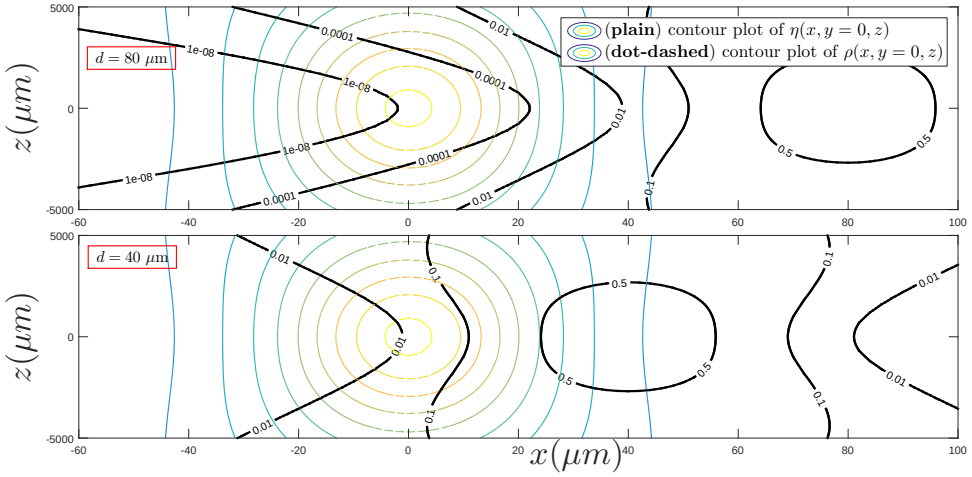

FIGURE 5.16: Contour plot of the two atomic density ρ and the function η, both at $y = 0$ because of the symmetry with respect to the (x, z) plane

As it is possible to see, for the case in which the beams are shifted of 40 μm, the virtual atoms are mainly collected where the probe is at about the ten percent of its maximum intensity. In other words, the biggest part of the atoms are at the edge of the detecting laser, and will be described by coefficients η_i approximatively equal to 0.1. On the other hand, when we move d further to 80 μm, all these particles are too far away from the probe for being detected. In this case $\eta(x, y = 0, z)$, in the region of the atomic peak, varies between 10^{-10} and 10^{-7}, that means that the particles really contributing to the k-criteria are the ones residing outside the FORT (i.e.: not trapped).

Now that we have understood how to treat the particular situation in which $W \leq 10^3$ μm, we can consider the general situation, where W can take values up to $5 \cdot 10^5$ μm. Let us first give a brief summary of what we have seen:

1. In order to determine the k-particle entanglement criteria, we have to generate virtual particles and the relative coefficients $\{\eta_i\}_{i=1}^n$

2. This is not trivial, since we have (at least) two degrees of freedom. *If* it is true that the probe and the FORT are focused at the same z-coordinate, these two degrees of freedom are the length of the loading chamber W and the displacement d of the two beams

3. In previous section 5.3.2 we saw that the first one of these parameters - W - is, indeed, important. When we consider big values for it, the criteria are getting significantly worse

4. What does "big values" for W mean? With qualitative arguments, we identified the cause of the worsening of the criteria by a gathering of atoms in regions where the probe is weak. W is "big" enough when particles are allowed to collect away from the focus

5. This conclusion is true in general. Whenever we reduce the atoms at the centre of the probe and accumulate at its border, the criteria are lowering

6. Therefore, if we fix W to be 10^3 μm, a similar argument holds for the displacement d. When we increase it, we gather particles at the edge of the probe and get worse criteria (see Fig.5.15). However, we need to be careful not to shift the beams too much, otherwise the atoms trapped in the FORT would not be detected at all. We identified the critical value of d to be around 40 μm

7. In the following, we need to check if, letting W to vary inside the interval $[1, 50] \cdot 10^3$ μm, the critical displacement remains to be $d = 40$ μm. This is the goal of the remaining part of this section

Because of the computational complexity of generating coefficients according to $\rho(x, y, z)$ and $\eta(x, y, z)$ for big W, we cannot check directly all values of d for determining the lowest criteria. Therefore, we need to have a very good idea about where we need to look at. For better understanding we draw the following picture, with the contour plots of the atomic density and the function η, both at $y = 0$.

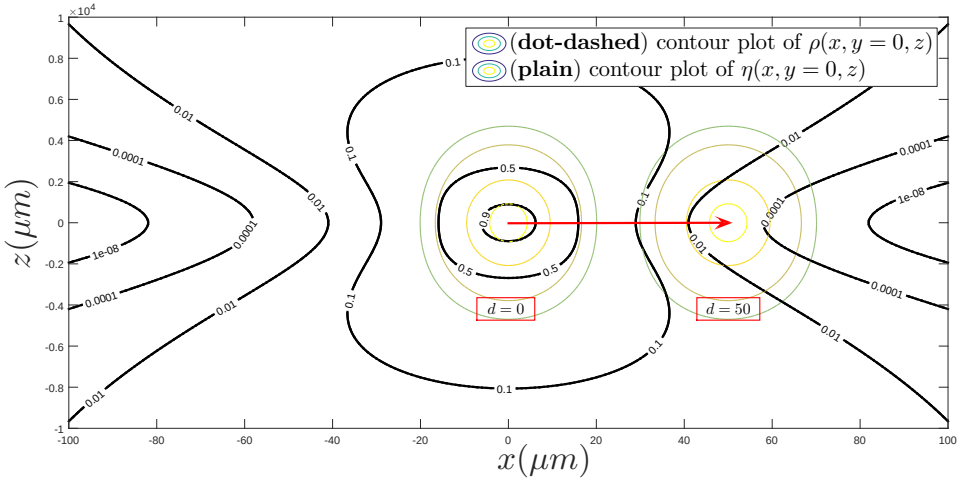

FIGURE 5.17: Contour plot of the two atomic density ρ and the function η, both at $y = 0$. We represent in the same graph the two different situations: displacement respectively null (*centre* of the figure) and 50 μm (*right* side)

This graph is very similar to the one in Fig.5.16. In fact, we are letting *only* the

variable z to be bigger. The displacement directly affects x, and therefore we believe that, for the general case, the critical value of d has to be searched in a neighbourhood of $d = 40$ μm. It *could* be not exactly 40 μm, because now we are moving along the x direction the particles that were in the z-region where the probe is decaying. However, because of similarities of the probe and FORT profiles, it is reliable to say that in the general case we have to recover a very similar result for the critical displacement d we found before in the particular case where $W = 10^3$ μm.
In fact, checking accurately in the range $d \in [35, 45]$ μm, $d = 20$ and 60 μm, we can take the conclusions:

- The lowest curves for the k-entanglement are to be searched for d between $d \in [35, 45]$ μm. In both cases $d = 20$ and 60 μm, the criteria lie above; the first one because we are too near to the focus of the probe, the second one because we are too far. Exactly as we have seen previously

- For us it is not possible to tell exactly at which value of d inside $[35, 45]$ μm resides the minimum. The statistical fluctuations due to the random nature of the virtual particle generation process are bigger than the distance between these criteria. If a better resolution is needed, it would be necessary to generate more coefficients $\{\eta_i\}_{i=1}^{n}$. However, in our case, we do not require such accuracy and limit ourselves to consider one couple of these curves to be the final 1 and 2-particle entanglement criteria. These curves can be found in the following graph 5.18

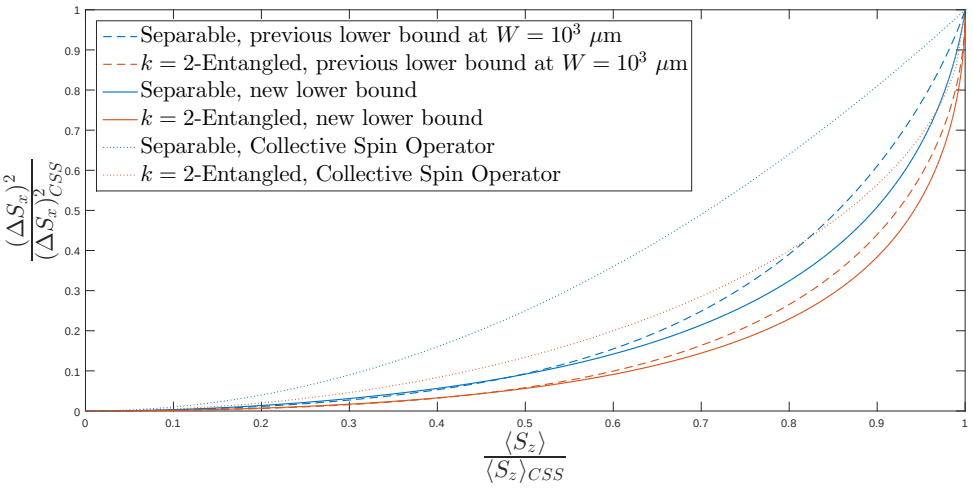

FIGURE 5.18: Curves referring to the $k = 1$ (*blue*) and $k = 2$ (*red*) Particle entanglement. The *dotted* ones refer to the collective spin operator $\vec{J}$, the *dashed* ones were derived before for $W = 10^3$ μm, and were the lowest represented in Fig.5.15 and the *plain* are the most general ones. They were derived considering $W = 5 \cdot 10^4$ μm and the displacement $d \simeq 40$ μm

Here we draw, respectively:

- *Dotted* curves: the $k = 1$ and 2-particle entanglement criteria obtained using the collective spin operator
- The *dashed* curves are the previous lower bounds, determined before for null displacement $d = 0$ μm. These have been represented above as the plain ones in Fig.5.12
- *Plain* curves: the new **general** criteria determined for $W = 5 \cdot 10^4$ μm

As we were expecting, we got a bound that is lower than before, as a consequence of the fact that now we took into account the displacement d.

5.3.3.1 Summary and comments

We believe our lowest bound for the minimum variance $\frac{(\Delta S_x)^2}{(\Delta S_x)^2_{CSS}}$ with respect to the average spin $\frac{\langle S_z \rangle}{\langle S_z \rangle_{CSS}}$ is reliable. However, in its derivation we supposed:

1. The probe and the FORT share the same z-coordinate of the focus, and are not tilted with respect to each other
2. The critical displacements d for which we obtain the lowest possible criteria for $W \leq 10^3$ μm and $W = 5 \cdot 10^5$ μm are very similar
3. The *only*, or at least *main* way for which the criteria are getting worse, is to have atomic gatherings at the edge of the probe, and few particles at the middle

During our discussion in the previous section 5.3.3, we gave qualitative arguments in favour of these hypotheses. Yet, in order to be really conclusive, we should determine the k-particle criteria scanning simultaneously the parameters d and W in the relative ranges. Moreover, we should introduce the angle θ_t, describing the tilting of the two beams, and the focus shift d_f. What we understand from this, is that the experiment itself has to be designed keeping in mind that all these parameters strongly influence the k-particle entanglement criteria. For instance, it would be very appropriate to load particles in a small box, such that W cannot be bigger than 10^3 μm. With this shrewdness only, we would avoid the bad worsening of the criteria related with big values of such parameter. Another improvement can be achieved by designing an atomic trap that collects the atoms in a smaller volume, so that the probe mainly detects particles near to its main axis. If these measures were achieved, we would obtain k-particle criteria

much nearer to the ones derived using the collective spin operator. And "nearer" means "easier to be verified". The experiment we analysed was performed some years ago, and the entanglement criteria used were the squeezing parameter ξ_R^2 and the curves obtained by Anders Sørensen in [37], all of them relative to the collective spin operator $\vec{J}$.
What we did here is to introduce some sort of procedure to evaluate the new k-particle entanglement criteria for a generic experiment in which many atoms are trapped and tested with some probe. During its derivation, we encountered some difficulties, hard to deal with "a posteriori", but potentially solvable with a better design of the experiment. In short, we showed a somehow general way to determine the k-particle entanglement criteria, and we suggested some tricks in order to make these criteria better, starting from the apparatus design.

5.4 Conclusions

Given the $k = 1$ and 2-entanglement criteria shown in Fig.5.18, we can finally determine if the atomic sample that has been tested and detected in experiment [19] was entangled or not. And, in case, how much correlated the Particle were. In the next plot, along with the lowest $k = 1$ and 2-bounds for the variance $\frac{(\Delta S_x)^2}{(\Delta S_x)^2_{CSS}}$ with respect to the average spin $\frac{\langle S_z \rangle}{\langle S_z \rangle_{CSS}}$ (the *plain* curves in Fig.5.18), we draw the experimental points of Fig.5.4.

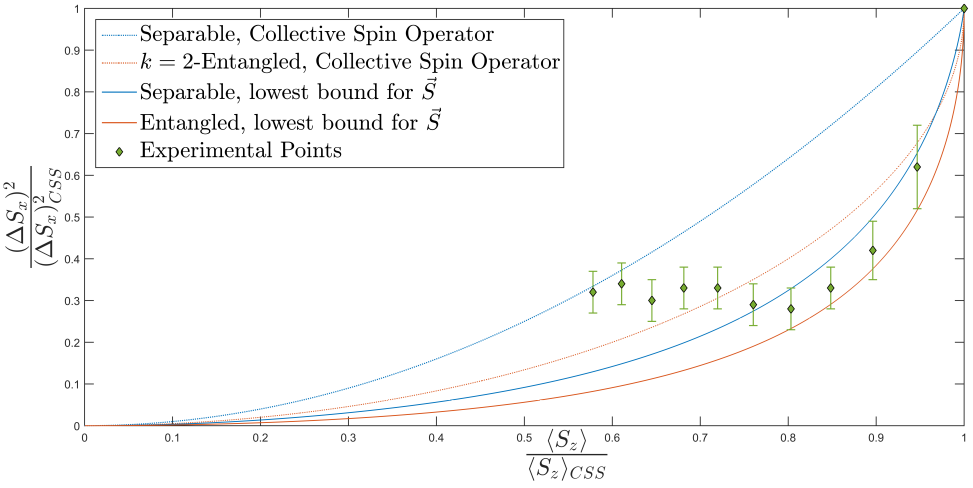

FIGURE 5.19: Experimental data obtained in the experiment, taken from [19]. The *dotted* and the *plain* curves are the $k = 1$ and $k = 2$-entanglement criteria derived using $\vec{J}$ and $\vec{S}$ respectively. More in detail, the plain ones represent the lowest possible values, derived in section 5.3.3

We see that, if majority of the points lie below the dotted curves, few can be considered not separable with our new criteria, and none with more than two particles entangled!

The conclusion taken in the article - 3.4 dB of metrologically relevant squeezing - has to be reviewed, once we look at the system with the new definition given by the operator $\vec{S}$. In fact, the criteria we derived here are much more strict than the previous ones - i.e.: the spin squeezing inequality and the lowest bounds derived in [37] - and experimental points that are lying beneath the old ones, are above the new. For a couple of atomic samples entanglement can be really proven (and still the points reside near the curve), but no state beats the 2-particle entanglement limit. Notice that we took a big number n of atoms, so that we are sure that the statistical fluctuations characterizing our theoretical curves can be neglected.
We need to accept that everything we can say about this experiment is that there are two samples that have *at least* one couple of correlated atom, but none with *at least* an entangled triplet. We cannot prove, for the worst-possible scenario described by the *plain* curves of Fig.5.19, high quality entanglement. This, despite that the procedure used, in the reality, is likely correlating most of the particles in the system at the same time.
In the next paragraphs we will try to understand why we got such horrible entanglement criteria, and an improvement will be attempted. We desire to make clear that there are two reasons for which we decided not to derive, from the beginning, the criteria we will obtain (with new constraints over our parameters) and present afterwards in Fig.5.21. The first one, is that we wanted to outline a somehow formal procedure that can be used in a general case, for which a dramatic reduction of the lower bounds for the variance is achieved. The second reason is more connected with the knowledge we have about the experiment [19]. Since we are re-analysing data taken couple of years ago, when the squeezing parameter was the inequality to be referred at, we do not have access to some experimental values important for us, but not for the authors of [19] - the length W of the chamber, for instance.

Previously we restricted T to 100 μK and W to its maximal value $5 \cdot 10^4$ μm, saying that further away the atoms were not trapped any more and the probe intensity was practically vanished. We have seen how, increasing W, all the entanglement criteria were getting worse and worse, and therefore a reduction of it can only be positive for us. In fact, what we will do now is to set it to $W = 10^4$ μm and $T = 100$ μK, in accordance with the qualitative argument given by the following picture:

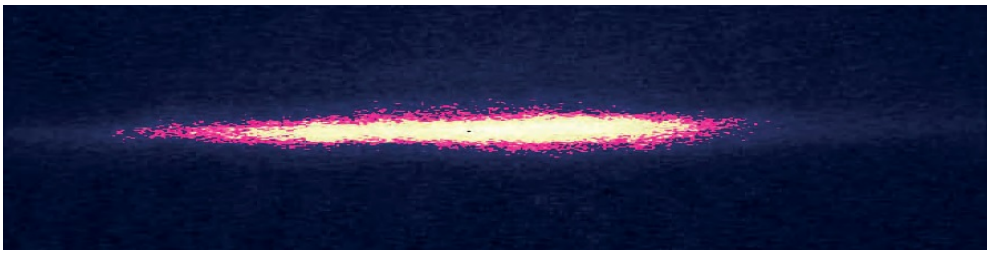

FIGURE 5.20: Image of a loaded FORT taken with a CCD camera. The image width and height correspond to 991 μm and 374 μm respectively. Picture taken from [55] for an experimental setup similar to our

This image, taken *not* for the experiment [19], but from a very similar one, can give us some clues about the atomic dispersion and the temperature in the loading chamber. In fact we can deduce that:

- The particles are not really following a thermal distribution. This is because, when loaded, they are not at the equilibrium, and the time scale for which the whole experiment run is much smaller than the one needed to the atoms to reach it. Nevertheless, at the thermal equilibrium the cloud is wider, that translates in a lowering of the coefficients $\{\eta_i\}_{i=1}^n$ and a consequent worsening of the entanglement criteria. For our purpose, we can keep consider $\rho(x, y, z)$ as in eq.5.15, being it "worse" than the real distribution, inaccessible to us

- Comparing experiment [19] and the one to which the figure 5.20 refers (see [55]), we can therefore set the maximum value of W to 10^4 μm. However, we want to make clear that this is more a (reasonable) guess, than a precise statement

- The temperature T itself, that can be estimated taking successive photos similar to 5.20, can be set to be $T = 50$ μK (overestimation). In fact, studying the spread of the cloud it is possible to have an idea about the average atomic speed, and therefore the temperature. By comparison of the two experiment, we can deduce T.

Now that we set new constraints over W and T, we will restrict the maximal displacement d that we can have as well. In fact, the idea that d could take (almost) any possible value is simply ridiculous. Our great experimental fellows are good at what they're doing, and therefore the FORT and the probe will be well aligned. How much? Overestimating again possible deleterious effects, we will set the maximal value of the displacement d as the beam's relative shift for which 90% of the maximum possible signal is achieved. In other words, we will determine $\langle S_z \rangle_{CSS}(d) = \sum_{i=1}^{n} \eta_i(d)$ for different values of d bigger or equal than zero. The one corresponding to $d = 0$ will clearly be

the maximum, and later on we will find out which is the d for which we get a reduction of the 10% in $\langle S_z \rangle_{CSS}(d = 0)$.

In conclusion, with the new constraints over W, T and d, we can give the next figure:

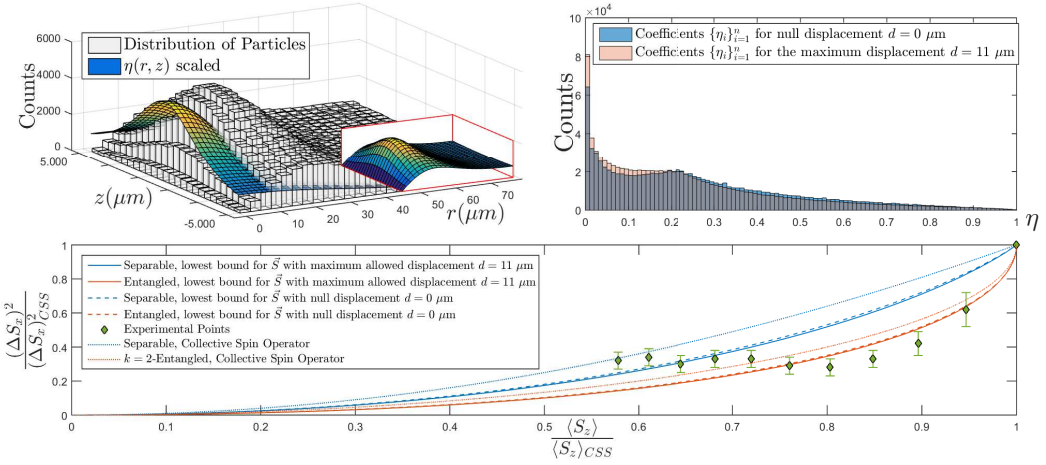

FIGURE 5.21: **Top Left**: Histogram with the generated r and z coordinates of $n = 10^6$ virtual particles. In the main plot, it is possible to see the scaled function $\eta(r, d = 0, z)$ as in eq.5.24; in the inset the theoretical distribution. **Top Right**: Histograms collecting the coefficients $\{\eta_i\}_{i=1}^n$, obtained for the virtual particles of which we were speaking above and displacement null (*blue*) and maximal (*red*). **Bottom**: Experimental data and $k = 1$ and 2 entanglement criteria (*blue* and *red* respectively). The *dotted* curves refer to the collective spin operator, the *dashed* ones to $\vec{S}$, with null displacement and the *plain* curves with the maximal $d = 11$ μm. These latter two lower bounds have been derived with $W = 10^4$ μm and $T = 50$ μK

A little procedural detail: as it is possible to see, we used the atomic distribution function ρ in Cylindrical coordinates. However, we need x for determining the coefficient η for each particle. In fact, looking at the expression for $\eta(r, x, z)$, we have:

$$\eta(r, x, z) = \frac{\omega_p^2}{\omega(z)^2} e^{-2\left(\frac{r^2+d^2-2xd}{\omega(z)^2}\right)}. \tag{5.24}$$

The coordinate x has been derived considering that the atoms are satisfying angular symmetry; we randomly generated the angles θ for all the particles and obtained x using

$$x = r \cos\theta. \tag{5.25}$$

Consider now the Fig.5.21. First, let us briefly go through, one last time, the procedure we used for the determination of the $k = 1$ and 2 entanglement criteria:

- The **top left** plot represents the histogram with the r and z coordinates of the virtual particles. These only depend on the FORT, and resemble the theoretical distribution of eq.5.15

- From the data collected in the first histogram we obtained the second figure, at the **top right**. The difference between the two set of coefficients $\{\eta_i\}_{i=1}^n$ is the displacement d used in their derivation (eq.5.24). For the *blue* ones $d = 0$ μm, while for the *red* we set the maximum allowed d, determined to be $d = 11$ μm using the procedure described above. As expected, the shift of the FORT with respect to the probe results in a lowering of the coefficients. However, because of the new constraints, such lowering is not dramatic and corresponds to a small degradation of the entanglement criteria

- Finally, at the **bottom** of Fig.5.21 we draw the $k = 1$ (*blue*) and 2 (*red*) particle entanglement criteria. In particular, the *dotted* curves are obtained with the collective spin operator, while the *dashed* and *plain* ones with $\vec{S}$. The difference between these last two is the displacement d used in their derivation. The previous refer to $d = 0$ μm, and therefore correspond to the *blue* set of coefficients $\{\eta_i\}_{i=1}^n$. The latter curves refer to maximal displacement $d = 11$ μm and are derived using the *red* set of coefficients.

Comparing the $k = 1$ and 2-particle entanglement criteria presented in the figures 5.19 and 5.21, the first thing that impress is that we "managed" to obtain much better lower bounds, so that many experimental points they were not beating the entanglement limit can now be considered correlated. In two cases we can also claim *more* than 2-particle entanglement, being the corresponding data *below* the red, plain curve. But what does exactly mean that we "managed to obtain better bounds"? The data are the same; it is our theoretical procedure that is changed. These changes, as explained before, cannot be fully justified. We needed to evaluate some parameters - the temperature T, the length W and the displacement d - of which no precise knowledge was given. Using the results of experiments similar to our and the physical intuition of the people working on those experiment (authors of [19]) we set new constraints over these cited variables and draw the better criteria of Fig.5.21. We have very good reasons to believe we overestimated the possible deleterious effect, and therefore to have obtained good criteria, but we cannot give really conclusive proves in favour of that.

Chapter 6

Conclusions

Here we will look at all the seeds we planted in the previous chapters, and harvest the fruit in terms of conclusions. In order to do this, we will give the last one of the many summaries that You, reader, probably have learned to hate with all of your heart:

- We proved, in section 2.1.2, that the squeezing parameter ξ^2 does not represent a valid entanglement criterion *if* we substitute the collective spin operator $\vec{J}$ with $\vec{S}$. In fact (eq.2.37),
$$\xi_N^2 \to \frac{2}{N} \tag{6.1}$$
for the specific model introduced there

- Trivial generalizations of the squeezing parameter as ξ_U^2 (see eq.2.66) cannot be used as useful entanglement criteria. In some extremely exotic circumstances, the particles behave such that $\xi_U^2 \to 0$, as we proved in equation 2.124. Of course this is not something that happens in realistic systems; we need to find some way to avoid these unwanted behaviours in the determination of our entanglement criteria

- Given the atomic distribution in the experimental setup, it is possible to determine, for a separable state, the minimum value that the variance $\frac{(\Delta S_x)^2}{(\Delta S_x)^2_{CSS}}$ can take with respect to the average spin $\frac{\langle S_z \rangle}{\langle S_z \rangle_{CSS}}$. In order to this limit to be realistic, we request to have a statistically relevant sample; in other words many atoms. This is the reason for which our entanglement criteria are valid for big collections of particles

- So far we are able to plot a curve that can unequivocally discern between a separable and a correlated system. It is, in fact, a sufficient criterion: experimental points located below such line need to be entangled. Moreover, if we recover the

"classical" situation $\vec{S} \to \vec{J}$, we clearly see that this criterion is completely equivalent to the spin squeezing inequality. However, whenever $\vec{S} \neq \vec{J}$, these criteria differ from one to the other (as it is clear from Fig.3.2)

- We took a step further; in Chapter 4 we considered entangled Systems, and showed that it is possible to obtain different level of multipartite correlations. For us, better quality means that there is, in the sample, at *least* some number of entangled particles. So, for instance, we draw the 2-particle sufficient criterion, stating that any System beating it contains *at least* $2+1=3$ correlated particles (see Fig.4.9). We managed to make it an optimal criterion, that essentially means that any point of the curve characterizing it resembles a real, possible state for our system

- We derived, for any integer $k > 2$, the k-particles entanglement criteria. We called these "optimal", as we did for the specific case $k = 2$, but this definition has only been used because we followed the same procedure. In fact, as explained in sections 4.4.1 and 4.4.2, these criteria exceed the real lowest bound, even if the difference reduces asymptotically to zero for $k \to \infty$. In any case, we are now able to derive a sufficient criterion for detecting k-particle entanglement in any situation

- Now that we can discern between all possible qualities of entanglement, we had the great opportunity to analyse the data taken in the experiment [19]. Under some realistic assumptions, we proved a novel multipartite entanglment criteria in terms of the squeezing parameter. To the best of our knowledge, no such criteria for detecting multipartite entanglement exist in the literature.

We conclude this work by recalling the conjecture 1 we gave. We used it in order to derive all the $k > 2$-particle entanglement criteria; proving it will be one of the big goals in the future.

We hope that what we have done here, will help others in the realization and the improvement of some experimental setups, and that the operator $\vec{S}$ we introduced is, indeed, of some interest.

Luca Dellantonio

Bibliography

[1] D. Leibfried, M. D. Barrett, T. Schaetz, J. Britton, J. Chiaverini, W. M. Itano, J. D. Jost, C. Langer, and D. J. Wineland. Toward heisenberg-limited spectroscopy with multiparticle entangled states. *Science*, 304(5676):1476–1478, 2004. doi: 10.1126/science.1097576. URL http://www.sciencemag.org/content/304/5676/1476.abstract.

[2] Lars Bojer Madsen and Klaus Mølmer. Spin squeezing and precision probing with light and samples of atoms in the gaussian description. *Phys. Rev. A*, 70:052324, Nov 2004. doi: 10.1103/PhysRevA.70.052324. URL http://link.aps.org/doi/10.1103/PhysRevA.70.052324.

[3] M. Saffman, D. Oblak, J. Appel, and E. S. Polzik. Spin squeezing of atomic ensembles by multicolor quantum nondemolition measurements. *Phys. Rev. A*, 79:023831, Feb 2009. doi: 10.1103/PhysRevA.79.023831. URL http://link.aps.org/doi/10.1103/PhysRevA.79.023831.

[4] Isabelle Bouchoule and Klaus Mølmer. Preparation of spin-squeezed atomic states by optical-phase-shift measurement. *Phys. Rev. A*, 66:043811, Oct 2002. doi: 10.1103/PhysRevA.66.043811. URL http://link.aps.org/doi/10.1103/PhysRevA.66.043811.

[5] J. Esteve, C. Gross, A. Weller, S. Giovanazzi, and M. K. Oberthaler. Squeezing and entanglement in a bose-einstein condensate. *Nature*, 455:1216–1219, Oct 2008. doi: http://dx.doi.org/10.1038/nature07332. URL http://www.nature.com/nature/journal/v455/n7217/suppinfo/nature07332_S1.html.

[6] Vittorio Giovannetti, Seth Lloyd, and Lorenzo Maccone. Quantum-enhanced measurements: Beating the standard quantum limit. *Science*, 306(5700):1330–1336, 2004. doi: 10.1126/science.1104149. URL http://www.sciencemag.org/content/306/5700/1330.abstract.

[7] Masahiro Kitagawa and Masahito Ueda. Squeezed spin states. *Phys. Rev. A*, 47: 5138–5143, Jun 1993. doi: 10.1103/PhysRevA.47.5138. URL `http://link.aps.org/doi/10.1103/PhysRevA.47.5138`.

[8] A. Sorensen, L.-M. Duan, J. I. Cirac, and P. Zoller. Many-particle entanglement with bose-einstein condensates. *Nature*, 409:63–66, Jan 2001. doi: http://dx.doi.org/10.1038/35051038.

[9] J. Hald, J. L. Sørensen, C. Schori, and E. S. Polzik. Spin squeezed atoms: A macroscopic entangled ensemble created by light. *Phys. Rev. Lett.*, 83:1319–1322, Aug 1999. doi: 10.1103/PhysRevLett.83.1319. URL `http://link.aps.org/doi/10.1103/PhysRevLett.83.1319`.

[10] A. Kuzmich, L. Mandel, and N. P. Bigelow. Generation of spin squeezing via continuous quantum nondemolition measurement. *Phys. Rev. Lett.*, 85:1594–1597, Aug 2000. doi: 10.1103/PhysRevLett.85.1594. URL `http://link.aps.org/doi/10.1103/PhysRevLett.85.1594`.

[11] T. Fernholz, H. Krauter, K. Jensen, J. F. Sherson, A. S. Sørensen, and E. S. Polzik. Spin squeezing of atomic ensembles via nuclear-electronic spin entanglement. *Phys. Rev. Lett.*, 101:073601, Aug 2008. doi: 10.1103/PhysRevLett.101.073601. URL `http://link.aps.org/doi/10.1103/PhysRevLett.101.073601`.

[12] Vivi Petersen, Lars Bojer Madsen, and Klaus Mølmer. Gaussian-state description of squeezed light. *Phys. Rev. A*, 72:053812, Nov 2005. doi: 10.1103/PhysRevA.72.053812. URL `http://link.aps.org/doi/10.1103/PhysRevA.72.053812`.

[13] C. F. Roos, M. Chwalla, K. Kim, M. Riebe, and R. Blatt. /'designer atoms/' for quantum metrology. *Nature*, 443:316–319, Sept 2006. doi: http://dx.doi.org/10.1038/nature05101.

[14] Isabelle Bouchoule and Klaus Mølmer. Spin squeezing of atoms by the dipole interaction in virtually excited rydberg states. *Phys. Rev. A*, 65:041803, Apr 2002. doi: 10.1103/PhysRevA.65.041803. URL `http://link.aps.org/doi/10.1103/PhysRevA.65.041803`.

[15] S. F. Pereira, Min Xiao, H. J. Kimble, and J. L. Hall. Generation of squeezed light by intracavity frequency doubling. *Phys. Rev. A*, 38:4931–4934, Nov 1988. doi: 10.1103/PhysRevA.38.4931. URL `http://link.aps.org/doi/10.1103/PhysRevA.38.4931`.

[16] T. Takano, M. Fuyama, R. Namiki, and Y. Takahashi. Spin squeezing of a cold atomic ensemble with the nuclear spin of one-half. *Phys. Rev. Lett.*, 102:033601,

Jan 2009. doi: 10.1103/PhysRevLett.102.033601. URL http://link.aps.org/doi/10.1103/PhysRevLett.102.033601.

[17] Patrick J. Windpassinger, Daniel Oblak, Ulrich B. Hoff, Anne Louchet, Jürgen Appel, Niels Kjærgaard, and Eugene S. Polzik. Squeezing of atomic quantum projection noise. *Journal of Modern Optics*, 56(18-19):1993–1998, 2009. doi: 10.1080/09500340903033682. URL http://dx.doi.org/10.1080/09500340903033682.

[18] D. J. Wineland, J. J. Bollinger, W. M. Itano, and D. J. Heinzen. Squeezed atomic states and projection noise in spectroscopy. *Phys. Rev. A*, 50:67–88, Jul 1994. doi: 10.1103/PhysRevA.50.67. URL http://link.aps.org/doi/10.1103/PhysRevA.50.67.

[19] J. Appel, P. J. Windpassinger, D. Oblak, U. B. Hoff, N. Kjærgaard, and E. S. Polzik. Mesoscopic atomic entanglement for precision measurements beyond the standard quantum limit. *Proceedings of the National Academy of Sciences*, 106 (27):10960–10965, 2009. doi: 10.1073/pnas.0901550106. URL http://www.pnas.org/content/106/27/10960.abstract.

[20] Rainer Blatt. Entangled states of trapped atomic ions. *Nature*, 453:1008–1015, Jun 2008. doi: http://dx.doi.org/10.1038/nature07125.

[21] Wolfgang Paul. Electromagnetic traps for charged and neutral particles. *Rev. Mod. Phys.*, 62:531–540, Jul 1990. doi: 10.1103/RevModPhys.62.531. URL http://link.aps.org/doi/10.1103/RevModPhys.62.531.

[22] Xiao-Hui Bao, Andreas Reingruber, Peter Dietrich, Jun Rui, Alexander Duck, Thorsten Strassel, Li Li, Nai-Le Liu, Bo Zhao, and Jian-Wei Pan. Efficient and long-lived quantum memory with cold atoms inside a ring cavity. *Nat Phys*, 8: 517–521, 2012. doi: http://dx.doi.org/10.1038/nphys2324.

[23] Bo Zhao, Yu-Ao Chen, Xiao-Hui Bao, Thorsten Strassel, Chih-Sung Chuu, Xian-Min Jin, Jorg Schmiedmayer, Zhen-Sheng Yuan, Shuai Chen, and Jian-Wei Pan. A millisecond quantum memory for scalable quantum networks. *Nat Phys*, 5:95–99, 2009. doi: http://dx.doi.org/10.1038/nphys1153.

[24] R. Zhao, Y. O. Dudin, S. D. Jenkins, C. J. Campbell, D. N. Matsukevich, T. A. B. Kennedy, and A. Kuzmich. Long-lived quantum memory. *Nat Phys*, 5:100–104, 2009. doi: http://dx.doi.org/10.1038/nphys1152.

[25] A. G. Radnaev, Y. O. Dudin, R. Zhao, H. H. Jen, S. D. Jenkins, A. Kuzmich, and T. A. B. Kennedy. A quantum memory with telecom-wavelength conversion. *Nat Phys*, 6:894–899, 20010. doi: http://dx.doi.org/10.1038/nphys1773.

[26] L.-M. Duan, M. D. Lukin, J. I. Cirac, and P. Zoller. Long-distance quantum communication with atomic ensembles and linear optics. *Nature*, 414:413–418, 2001. doi: http://dx.doi.org/10.1038/35106500. URL `http://www.nature.com/nature/journal/v414/n6862/suppinfo/414413a0_S1.html`.

[27] Morgan P. Hedges, Jevon J. Longdell, Yongmin Li, and Matthew J. Sellars. Efficient quantum memory for light. *Nature*, 465:1052–1056, Jun 2010. doi: http://dx.doi.org/10.1038/nature09081. URL `http://www.nature.com/nature/journal/v465/n7301/suppinfo/nature09081_S1.html`.

[28] Nicolas Sangouard, Christoph Simon, Bo Zhao, Yu-Ao Chen, Hugues de Riedmatten, Jian-Wei Pan, and Nicolas Gisin. Robust and efficient quantum repeaters with atomic ensembles and linear optics. *Phys. Rev. A*, 77:062301, Jun 2008. doi: 10.1103/PhysRevA.77.062301. URL `http://link.aps.org/doi/10.1103/PhysRevA.77.062301`.

[29] M. D. Lukin, M. Fleischhauer, R. Cote, L. M. Duan, D. Jaksch, J. I. Cirac, and P. Zoller. Dipole blockade and quantum information processing in mesoscopic atomic ensembles. *Phys. Rev. Lett.*, 87:037901, Jun 2001. doi: 10.1103/PhysRevLett.87.037901. URL `http://link.aps.org/doi/10.1103/PhysRevLett.87.037901`.

[30] T. Pellizzari, S. A. Gardiner, J. I. Cirac, and P. Zoller. Decoherence, continuous observation, and quantum computing: A cavity qed model. *Phys. Rev. Lett.*, 75:3788–3791, Nov 1995. doi: 10.1103/PhysRevLett.75.3788. URL `http://link.aps.org/doi/10.1103/PhysRevLett.75.3788`.

[31] F. Schmidt-Kaler, H. Häffner, S. Gulde, M. Riebe, G.P.T. Lancaster, T. Deuschle, C. Becher, W. Hänsel, J. Eschner, C.F. Roos, and R. Blatt. How to realize a universal quantum gate with trapped ions. *Applied Physics B*, 77(8):789–796, 2003. ISSN 0946-2171. doi: 10.1007/s00340-003-1346-9. URL `http://dx.doi.org/10.1007/s00340-003-1346-9`.

[32] A. Einstein, B. Podolsky, and N. Rosen. Can quantum-mechanical description of physical reality be considered complete? *Phys. Rev.*, 47:777–780, May 1935. doi: 10.1103/PhysRev.47.777. URL `http://link.aps.org/doi/10.1103/PhysRev.47.777`.

[33] Anton Zeilinger. Experiment and the foundations of quantum physics. *Rev. Mod. Phys.*, 71:S288–S297, Mar 1999. doi: 10.1103/RevModPhys.71.S288. URL `http://link.aps.org/doi/10.1103/RevModPhys.71.S288`.

[34] Ryszard Horodecki, Paweł Horodecki, Michał Horodecki, and Karol Horodecki. Quantum entanglement. *Rev. Mod. Phys.*, 81:865–942, Jun 2009. doi: 10.1103/RevModPhys.81.865. URL http://link.aps.org/doi/10.1103/RevModPhys.81.865.

[35] Bell John. Speakable and unspeakable in quantum mechanics. *Cambridge University*, 1987.

[36] Otfried Gühne and Géza Tóth. Entanglement detection. *Physics Reports*, 474(1–6):1 – 75, 2009. ISSN 0370-1573. doi: http://dx.doi.org/10.1016/j.physrep.2009.02.004. URL http://www.sciencedirect.com/science/article/pii/S0370157309000623.

[37] Anders S. Sørensen and Klaus Mølmer. Entanglement and extreme spin squeezing. *Phys. Rev. Lett.*, 86:4431–4434, May 2001. doi: 10.1103/PhysRevLett.86.4431. URL http://link.aps.org/doi/10.1103/PhysRevLett.86.4431.

[38] W. G. Unruh. Analysis of quantum-nondemolition measurement. *Phys. Rev. D*, 18:1764–1772, Sep 1978. doi: 10.1103/PhysRevD.18.1764. URL http://link.aps.org/doi/10.1103/PhysRevD.18.1764.

[39] P. J. Windpassinger, D. Oblak, P. G. Petrov, M. Kubasik, M. Saffman, C. L. Garrido Alzar, J. Appel, J. H. Müller, N. Kjærgaard, and E. S. Polzik. Nondestructive probing of rabi oscillations on the cesium clock transition near the standard quantum limit. *Phys. Rev. Lett.*, 100:103601, Mar 2008. doi: 10.1103/PhysRevLett.100.103601. URL http://link.aps.org/doi/10.1103/PhysRevLett.100.103601.

[40] Patrick J Windpassinger, Daniel Oblak, Ulrich Busk Hoff, Jürgen Appel, Niels Kjærgaard, and Eugene S Polzik. Inhomogeneous light shift effects on atomic quantum state evolution in non-destructive measurements. *New Journal of Physics*, 10 (5):053032, 2008. URL http://stacks.iop.org/1367-2630/10/i=5/a=053032.

[41] V. B. Braginsky and F. Ya. Khalili. Quantum nondemolition measurements: the route from toys to tools. *Rev. Mod. Phys.*, 68:1–11, Jan 1996. doi: 10.1103/RevModPhys.68.1. URL http://link.aps.org/doi/10.1103/RevModPhys.68.1.

[42] Vladimir B. Braginsky, Yuri I. Vorontsov, and Kip S. Thorne. Quantum nondemolition measurements. *Science*, 209(4456):547–557, 1980. doi: 10.1126/science.209.4456.547. URL http://www.sciencemag.org/content/209/4456/547.abstract.

[43] A. Kuzmich, N. P. Bigelow, and L. Mandel. Atomic quantum non-demolition measurements and squeezing. *EPL (Europhysics Letters)*, 42(5):481, 1998. URL http://stacks.iop.org/0295-5075/42/i=5/a=481.

[44] A. Kuzmich, L. Mandel, J. Janis, Y. E. Young, R. Ejnisman, and N. P. Bigelow. Quantum nondemolition measurements of collective atomic spin. *Phys. Rev. A*, 60: 2346–2350, Sep 1999. doi: 10.1103/PhysRevA.60.2346. URL `http://link.aps.org/doi/10.1103/PhysRevA.60.2346`.

[45] D Meiser, Jun Ye, and M J Holland. Spin squeezing in optical lattice clocks via lattice-based qnd measurements. *New Journal of Physics*, 10(7):073014, 2008. URL `http://stacks.iop.org/1367-2630/10/i=7/a=073014`.

[46] Daniel Oblak, Plamen G. Petrov, Carlos L. Garrido Alzar, Wolfgang Tittel, Anton K. Vershovski, Jens K. Mikkelsen, Jens L. Sørensen, and Eugene S. Polzik. Quantum-noise-limited interferometric measurement of atomic noise: Towards spin squeezing on the cs clock transition. *Phys. Rev. A*, 71:043807, Apr 2005. doi: 10.1103/PhysRevA.71.043807. URL `http://link.aps.org/doi/10.1103/PhysRevA.71.043807`.

[47] Poizat, J.-Ph., Roch, J.-F., and Grangier, P. Characterization of quantum nondemolition measurements in optics. *Ann. Phys. Fr.*, 19(3):265–297, 1994. doi: 10.1051/anphys:01994001903026500. URL `http://dx.doi.org/10.1051/anphys:01994001903026500`.

[48] J.-F. Roch, K. Vigneron, Ph. Grelu, A. Sinatra, J.-Ph. Poizat, and Ph. Grangier. Quantum nondemolition measurements using cold trapped atoms. *Phys. Rev. Lett.*, 78:634–637, Jan 1997. doi: 10.1103/PhysRevLett.78.634. URL `http://link.aps.org/doi/10.1103/PhysRevLett.78.634`.

[49] Kip S. Thorne, Ronald W. P. Drever, Carlton M. Caves, Mark Zimmermann, and Vernon D. Sandberg. Quantum nondemolition measurements of harmonic oscillators. *Phys. Rev. Lett.*, 40:667–671, Mar 1978. doi: 10.1103/PhysRevLett.40.667. URL `http://link.aps.org/doi/10.1103/PhysRevLett.40.667`.

[50] M. Drewsen, Ph. Laurent, A. Nadir, G. Santarelli, A. Clairon, Y. Castin, D. Grison, and C. Salomon. Investigation of sub-doppler cooling effects in a cesium magneto-optical trap. *Applied Physics B*, 59(3):283–298, 1994. ISSN 0946-2171. doi: 10.1007/BF01081396. URL `http://dx.doi.org/10.1007/BF01081396`.

[51] H.J. Metcalf and P. van der Straten. *Laser Cooling and Trapping*. Graduate Texts in Contemporary Physics. Springer New York, 2012. ISBN 9781461214700. URL `https://books.google.dk/books?id=RJXwBwAAQBAJ`.

[52] J. Ph. Poizat and P. Grangier. Experimental realization of a quantum optical tap. *Phys. Rev. Lett.*, 70:271–274, Jan 1993. doi: 10.1103/PhysRevLett.70.271. URL `http://link.aps.org/doi/10.1103/PhysRevLett.70.271`.

[53] D. Oblak, J. Appel, P. J. Windpassinger, U. B. Hoff, N. Kjærgaard, and E. S. Polzik. Echo spectroscopy of atomic dynamics in a gaussian trap via phase imprints. *The European Physical Journal D*, 50(1):67–73, 2008. ISSN 1434-6060. doi: 10.1140/epjd/e2008-00192-1. URL `http://dx.doi.org/10.1140/epjd/e2008-00192-1`.

[54] Klemens Hammerer, Anders S. Sørensen, and Eugene S. Polzik. Quantum interface between light and atomic ensembles. *Rev. Mod. Phys.*, 82:1041–1093, Apr 2010. doi: 10.1103/RevModPhys.82.1041. URL `http://link.aps.org/doi/10.1103/RevModPhys.82.1041`.

[55] Oblak Daniel. Quantum state engineering in cold caesium atoms. an entangled tale of non-destructively induced collapse and squeezing of atomic states. *Museum Tusculanum*, 2010. URL `http://quantop.nbi.ku.dk/publications/thesis/daniel_thesis.pdf`.

[56] R. Grimm, M. Weidemüller, and Y. B. Ovchinnikov. Optical Dipole Traps for Neutral Atoms. *Advances in Atomic Molecular and Optical Physics*, 42:95–170, 2000. doi: 10.1016/S1049-250X(08)60186-X.

[57] Daniel A. Steck. Caesium d line data. 2010. URL `http://steck.us/alkalidata`.

Acknowledgements

Innanzi tutto desidero spiegare perché ho deciso di dedicare la tesi ai miei genitori e a mia Nonna. Partiamo da mia madre. Sinceramente, non era affatto mia intenzione includerla, ma mi è parso un po' indelicato dedicarla a tutti tranne lei. In fondo, nonostante la demenza senile dilagante, è ed è stata una mamma decente. Urta spesso e volentieri i miei nervi, che per lei divengono estremamente fragili, ma in definitiva so che tiene alla sua più grande realizzazione (me medesimo) e farebbe di tutto per lei.
Pensando al mio papà, debbo innanzitutto dire che c'è sempre stato per me, per ogni mia esigenza. Sia per quanto riguarda l'aspetto economico - non mi è mai mancato nulla e mi sono sempre reso conto di essere un privilegiato - sia quello affettivo. Nonostante le sue piccole difficoltà a esprimersi (potremmo infatti considerarlo una specie di "carciofo emotivo"), so che ha sempre avuto piena fiducia e forse eccessivo orgoglio in me.
Infine, dedico questo lavoro a mia nonna. Di lei voglio soltanto dire che, oltre ai soliti bei concetti legati alla figura della nonna, è sempre stata uno dei modelli cui mi sono ispirato nel corso della mia vita. Dottoressa in biologia e attualmente la (forse) più vecchia biologa italiana, è stata la prima donna, oltre che la prima persona non laureata in medicina, ad aprire un laboratorio privato in Italia. Questo durante gli anni in cui, se non eri un uomo, era difficile avere un lavoro prestigioso. Dal mio punto di vista una persona orgogliosa e decisa, che ha superato ostacoli difficili da capire ai miei giovani occhi. E tuttavia una nonna affettuosa e sempre presente, che in ogni momento ha dimostrato di volermi moltissimo bene. Dal canto mio non sono stato un ottimo nipote, viste le lunghe assenze prese dall'andarla a trovare; tuttavia spero di essere riuscito a comunicarle l'importanza che ha avuto nella mia vita e la stima che nutro nei suoi confronti. Prendendo ogni tanto una deviazione, magari anche lunga, cercherò sempre di seguire le sue orme. Con questa tesi in parte spero di esserci riuscito. A mia nonna quindi, che ai miei occhi - di ieri come di oggi - è sempre stata combattente e invincibile.

Above all, I have to thank my supervisor professor Anders Sørensen, who guided me to the goals of physics and football, and my co-supervisor Sumanta Das, who followed me step after step in the realization of this work. Great help has also been given to me by professors Jürgen Appel, Jörg Müller and Eugene Polzik, they let me analyse data taken in their experiment, and advised me whenever I had questions.

For what concerns my friends, next are the person I want to remember. The order is kind of random, so do not be offended if you are not struggling for the first positions. An only exception is made, and this is Emanuele. I will put him at the place he deserves - of course the bottom - since he actually is the last wheel of the chariot.

Let us start with the academic environment. Regarding the group I have been working with, I am grateful to all the people they make it special: the Cool Physicist, the Tea Master, Sumanta, Ivan, Emil, Johan, Florentin and Johannes. Julia is not working with us, but I need to include her in this list, since she shined my days with her always present smile and my evenings with rarely refined meals. Of her, I will always remember the Ukrainian dinner, with the unforgettable traditions related. Regarding her husband - the Cool Physicist - I am not sure where to begin with. It has been a great pleasure to share with him time inside and outside the University, maybe even a honour. Person of rare kindness, he will always be one of the figures indissolubly connected with my memories of Copenhagen. His suggestions have always been intelligent and very valuable.
Sumanta has been a great co-supervisor, exceeding the part that its role was imposing to him. I made treasure of the lunch-lectures of Indian history, and I am happy I can call him a good friend.
For what concerns the Tea Master, unfortunately his name cannot be separated by a very dark episode, known as the "Profiterol Crisis". Like sometimes had happened in the history - I can recall the Missile Scare of Cuba - two opponents faced themselves for a delightful reward, and great tension was generated. Fortunately, in our case one of the two (me) is considerably open minded, so the crisis did not become a war. The Tea Master is, after all, a great person, with extremely nice t-shirts.

Non proprio nel gruppo di Ottica Quantistica, ma sempre in giro in Università, devo assolutamente citare Guido. Questo geniaccio mi ha guidato in alcuni periodi estremamente bui per quanto riguarda la mia produttività scientifica, aiutandomi a risolvere problemi a me ostici.
Altre persone in ambito accademico (e non solo) da ricordare, sono senza dubbi Artù, Bertina, Erica, Dimitris e Giulia. I primi quattro sono le vecchie rocce di Copenhagen, coloro che mi hanno accompagnato in questa avventura fin dall'inizio. Devo ringraziare in particolar modo Artù e la Bert, per l'ottimo sushi col quale mi hanno nutrito, e il supporto sempre datomi. Son lieto di dire inoltre che la fanciulla dei monti ha dimostrato eleganza e raffinatezza rare per l'ambiente da cui proviene; con lei mi son fatto tra le migliori risate di sempre. E quando era accompagnata anche da Alice, era quasi vergognoso il fracasso che facevamo in mensa, accerchiati da professoroni e silenziosissimi fisici. A proposito di Alice, è una grande. La mia stima per lei sarà sempre immensa. Un gran grazie anche a Mads, che mi ha mostrato le meraviglie della città, racchiuse nei suoi splendidi teatri.
E se ho citato quelli che mi hanno accompagnato fino alla fine di questi due anni, devo assolutamente ricordare quelli coi quali ho iniziato questa avventura: il vecchio Chief e Jacopo. Senza Marco non avrei neanche avuto il coraggio di venire a Copenhagen; sarebbe rimasto un sogno nel cassetto. Quindi a lui il mio più grande e sincero grazie.

Nulla di più, perché già sa quanto ci tenga a lui. Jacopo è stata un po' una sorpresa dalle lontane terre trentine, e con lui ho passato ottime serate, e indimenticabili notti al Drone.
Una nota a piè di pagina devo dedicarla a Giulietta, che pur non avendo nulla a che fare con Copenhagen (la papera non è neanche mai venuta a trovarmi!), ha sempre trovato il tempo per sopportarmi durante lunghe chiamate. Un momento, ho invertito i soggetti... Io la ho sempre sopportata! Ma con grande piacere.

If, from one side, Copenhagen means to me University, from the other it means Athletics. And without my Spartans, these two years would have been way worse. I shared with all of them lot of time, and I can absolutely say it was all well spent. The collective showers are one of my best memories ever! My only regret is that I never convinced the girls to join. Between the Spartans we have of course Henrik, that upgraded me technologically, followed me in Italy (two times) and with whom I discovered many big and small secrets of this city and country. I cannot think to a better guide and friend. With Jess and Michael I had one of the most important trip to Rome I ever made. Both of them are two of the most important friends I have, with which I had some of the most important moments in Copenhagen. Julie is the person on which you can count on, and is probably the strongest and more independent girl ever existed. Thomas is apparently more appreciated than me by my parents, and he will always be welcomed in my home. Romain, along with Floreal and Burubu, convinced me that French can be beautiful persons (in order to not offend anyone, I knew it before! It is just a joke we were having together). Leon is one of the persons I admire most. It is always a pleasure share time with him, being one of those rarely intelligent guys with which it is possible both to have lot of fun and be serious. I also need to cite the experience that Eduardo has of the life and that sometimes shares with me. I will remember his lectures, they - I am sure - will help me for the next part of my life. In conclusion, it is impossible to speak about Athletics without mention my multicoloured trainers, Khava and Mihn. I don't know how they are able to push me, the probably laziest person in this world, up to the limit every time. From the first to the last training I had with them, I never got bored and always enjoyed every single instant. Maybe this is a little strong statement, since the pain has many times been very intense, but nevertheless thanks for being with us!
Un commento speciale se lo merita quel mostro di Alessandro, che nonostante abbia rubato cibo mio di diritto, è stato un grande amico. Conosciuto sempre grazie allo sport, è ingiusto limitare la sua influenza a tale ambito. Mi ha infatti accompagnato in svariate disavventure che hanno senza dubbio arricchito enormemente la mia esperienza in Danimarca. Anche se sotto moltissimi aspetti lo si può considerare una specie di disastro vivente, è anche un'ottima persona e un grande atleta. Grande, non solo per i

suoi risultati. Grazie anche alla sua famiglia - Gianluca in particolare - che ho avuto il piacere di conoscere.

I also need to thank all the persons of Diakonisse Kollegium. Barbara, in particular, who brought joy in my dinners of sadness.

In conclusione, non si può non citare quelli del PARV. Due anni ci hanno separato, ma non mi sono mai sentito più vicino a tutti loro. Albert è una delle persone che più mi fa piacere ritrovare a Bolzano, non lo sostituirei con nessuno. Ogni skyppata col Valenz mi riempie di gioia, la mia stima nei suoi confronti non è mai diminuita. Bravo Luca che ha preso a chiamarmi, rimarrà sempre Luca, il nome uguale e naturale da associare al mio. Marco sospetto mi abbia sostituito con un mio sosia a Grenoble, ma gli voglio bene lo stesso. Spero si tagli la barba, ma anche se non lo dovesse fare lo perdonerò. Ultimo, e proprio ultimo, Ema, che rimane sempre uno dei migliori amici che abbia.